LBL-10978

Lawrence Berkeley Laboratory
UNIVERSITY OF CALIFORNIA

Materials & Molecular
Research Division

THE APPLICATION OF SOME HARTREE-FOCK MODEL CALCULATIONS TO THE ANALYSIS OF ATOMIC AND FREE-ION OPTICAL SPECTRA

Thomas Laine Hayhurst
(Ph.D. thesis)

May 1980

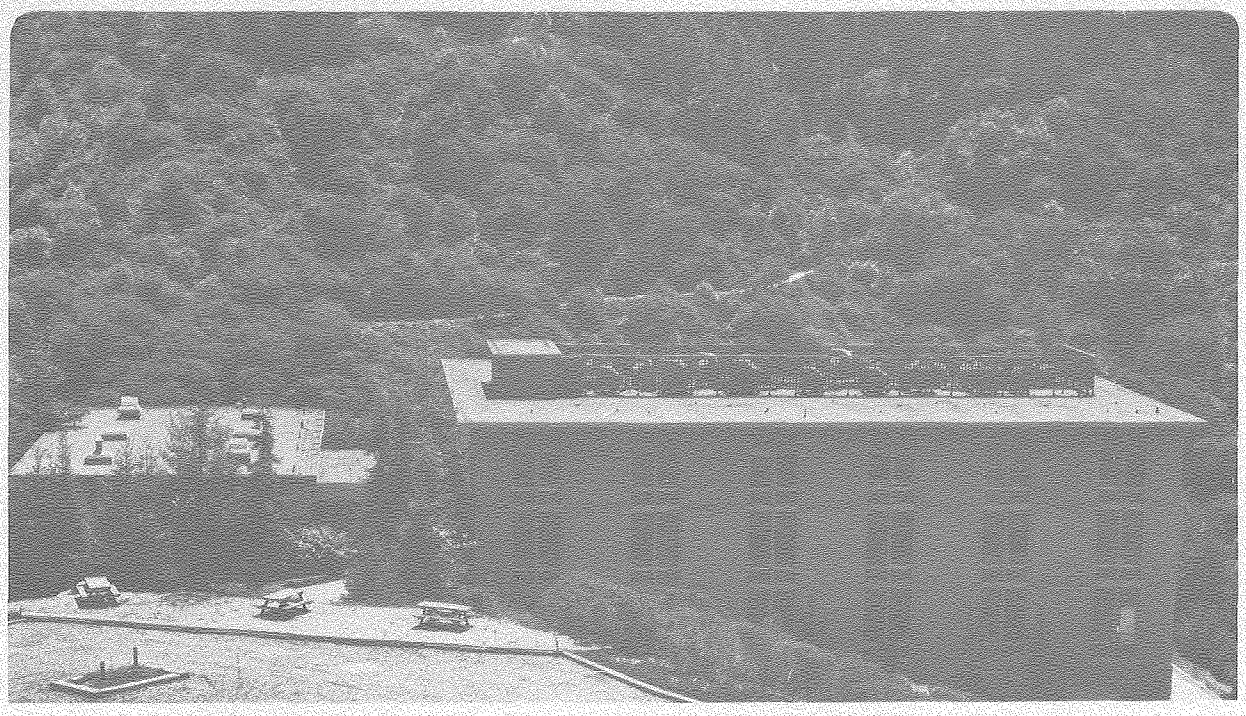

Prepared for the U.S. Department of Energy under Contract W-7405-ENG-48

DISCLAIMER

The Application of Some Hartree-Fock Model Calculations to the Analysis of Atomic and Free-Ion Optical Spectra

Thomas Laine Hayhurst

University of California, Berkeley, Ca. 94720

and

Lawrence Berkeley Laboratory, 1 Cyclotron Road, Berkeley, Ca. 94720

ABSTRACT

Techniques for applying ab-initio calculations to the analysis of atomic spectra are investigated, along with the relationship between the semi-empirical and ab-initio forms of Slater-Condon theory. Slater-Condon theory is reviewed with a focus on the essential features that lead to the effective Hamiltonians associated with the semi-empirical form of the theory. Ab-initio spectroscopic parameters are calculated from wavefunctions obtained via self-consistent field methods, while multi-configuration Hamiltonian matrices are constructed and diagonalized with computer codes written by Robert Cowan of Los Alamos Scientific Laboratory. Group theoretical analysis demonstrates that wavefunctions more general than Slater determinants (i.e. wavefunctions with radial correlations between electrons) lead to essentially the same parameterization of effective Hamiltonians. In the spirit of this analysis, a strategy is developed for adjusting ab-initio values of the spectroscopic parameters, reproducing parameters obtained by fitting the corresponding

effective Hamiltonian. Secondary parameters are used to "screen" the calculated (primary) spectroscopic parameters, their values determined by least squares. Extrapolations of the secondary parameters determined from analyzed spectra are attempted to correct calculations of atoms and ions without experimental levels. The adjustment strategy and extrapolations are tested on the K I sequence from K^{0+} through Fe^{7+}, fitting to experimental levels for V^{4+}, and Cr^{5+}; unobserved levels and spectra are predicted for several members of the sequence. A related problem is also discussed: Energy levels of the Uranium hexahalide complexes, $(UX_6)^{2-}$ for X = F, Cl, Br, and I, are fit to an effective Hamiltonian (the f^2 configuration in O_h symmetry) with corrections proposed by Brian Judd.

Sumner P. Davis
5-21-80

Acknowledgements

I would first like to express my gratitude to Bob Cowan for sending me copies of his many computer codes, and also for access to the manuscript of his forthcoming book; indirectly, I have learned much from him. I would also like to thank my research adviser, Sumner Davis, for his continued encouragement of my wide range of interests, and allowing me to pursue them at my own pace. I thank John Conway and George Shalimoff for their support of this project, and for teaching me about spectroscopy. My interest in spectroscopy of ions in crystal lattices was stimulated by Norm Edelstein, and I benefitted from his experience with parameterizing effective Hamiltonians.

In the area of non-technical support, I wish to thank Gail Bates and Sharon Coudyser for their continued faith and encouragement, and special thanks to Sharon for help with the manuscript.

This work was supported by the Division of Chemical Sciences, Office of Basic Energy Sciences, U.S. Department of Energy under Contract No. W-7405-Eng-48.

Table of Contents

List of Tables

List of Figures

I. Introduction

Since the birth of quantum mechanics, the theory of electronic structure for atoms and ions has progressed significantly in terms of the number of phenomena explained and the sophistication of calculations. The basic theory relevant to the classification of atomic states and spectral transitions was outlined by Slater[1] in 1929, and expanded in the classic text by Condon and Shortley[2] a few years later. The evolution of this theory, referred to here as Slater-Condon theory,[3] has been influenced by the parallel development of mathematical and computational tools.

Spectral Analysis

The analysis of optical spectra from atoms and ions amounts to the application of the Rydberg principle in a manner appropriate to the observed spectra. The wavelength of every spectral line is inversely proportional to the energy difference of the pair of levels involved, but even in theory, transitions between all pairs of levels are not observable. A typical emission spectrum obtained from an excited sample of atoms and a grating spectrometer motivates the need for heuristics in the analysis. Line spectra are usually contaminated with emissions from impurity atoms, and the instrument is limited to finite window of observable wavelengths. Determining the relative scheme of energy levels is complicated by superposition of impurity spectra and the absence of many of connecting transitions. Analysis of a line spectrum with no predictable patterns would be difficult and unreliable; the collection and interpretation of these patterns is Slater-Condon theory.

1.1 Slater-Condon Theory

The Slater-Condon theory of atomic structure predicts the general distribution of the low lying energy levels of an atom or ion. Orthonormal atomic wavefunctions constructed from Slater determinants, antisymmmetrized products of N 1-electron wavefunctions possessing definite rotational symmetry, are used to approximate the eigenstates of the atom or ion. Upon restriction of the atomic Hamiltonian operator to a subspace spanned by a finite set of these wavefunctions, the spectral decomposition of the resulting matrix is a variational estimate of a portion of the energy spectrum of the atom. The basis vectors can be transformed to the linear combinations of Slater determinants with definite N-electron rotational symmetry. Then the Hamiltonian matrix becomes block diagonal and the rotational degeneracy can be eliminated.

The classic version of the theory assumes the 1-electron wavefunctions are products of spin, angular, and radial functions—the eigenfunctions of a non-relativistic, rotationally invariant 1-electron Hamiltonian operator. Atomic wavefunctions are grouped according to configurations, or sets of Slater determinants constructed from a fixed set of radial wavefunctions. For an optimal choice of the radial wavefunctions, the eigenvalues and eigenvectors of the restricted Hamiltonian operator are expected to be good approximations to actual atomic energies and eigenstates. Specifying a scheme for calculating the radial wavefunctions, using them to calculate the integrals needed to construct the Hamiltonian matrix, and using the eigenvalues and eigenvectors of this matrix to obtain atomic properties is the ab-initio form of Slater-Condon theory. Assuming an optimal set radial wavefunctions

exists and parameterizing the dependence of atomic properties on them is the semi-empirical form.

Semi-empirical Slater-Condon Theory

Application of the theory to spectral analysis in its early days was largely limited to the semi-empirical form. The Hamiltonian operator is resolved into components with definite 1-electron rotational symmetry. Because the atomic wavefunctions are constructed from 1-electron central field wavefunctions, the dependence of the Hamiltonian matrix on the spin-angle wavefunctions can be separated from the radial wavefunctions. The Hamiltonian matrix becomes a superposition of matrices with coefficients that depend on integrals involving the radial wavefunctions. The semi-empirical theory treats these coefficients as free parameters, creating an effective Hamiltonian description of an N-electron system.

Analyses of spectra are accomplished by the interplay of two operations: The trial and error assignments of hypothetical energy levels according to configuration and symmetry type, and the adjustment of the free parameters until the best agreement is obtained between the eigenvalues of the Hamiltonian matrix and the experimental levels. The analysis is complete when a self-consistent agreement is reached between experimental and calculated levels, with parameter values that are acceptable on physical grounds.

The semi-empirical method of analysis has become highly developed. Its successes and limitations are presented by Edlén[7]. Although the method was prescribed by Condon and Shortley[2] in 1935, significant

advances in the analysis of complex spectra were made by applying group theory to the general problem of finding linear combinations of determinant wavefunctions with definite N-electron rotation symmetry, and to the calculation of matrix elements of tensor operators[8].

Ab-initio Slater-Condon Theory

Calculation of atomic wavefunctions and energy levels from first principles requires some method of obtaining the radial wavefunctions. Then the Hamiltonian matrix is simply diagonalized to obtain variational estimates of the energies and eigenstates. Although Hartree,[4] Fock,[5] Slater,[6] and others proposed schemes for calculating the radial wavefunctions and the integrals necessary for constructing the Hamiltonian matrix, few of these calculations were performed initially because of the labor involved.

Ab-initio calculations became feasible on a large scale with the advent of digital computers; many computer calculations began appearing in the late 1950's and early 1960's. For example, a program employing numerical integration of the self-consistent-field (SCF) equations, and the results for many atoms were published by Herman and Skillman in 1963[9]. These calculations required experience and an investment in computer time that discouraged their use by non-experts. As a result, the use of ab-initio calculations as an aid in solving experimental problems was limited to already published calculations, or collaborations between experimenters and the authors of computer codes.

With the present generation of computers, numerical integrations of the non-relativistic SCF calculations have become fairly trivial. A

sophisticated, fast, and convenient series of computer codes has been developed by Robert Cowan of Los Alamos[10,11,12]. In addition, Cowan has developed codes that construct and diagonalize the Hamiltonian matrix employing the radial integrals obtained from the the SCF codes. These codes can also calculate a theoretical spectrum arising from transitions between pairs of ab-initio energy levels[13].

Cowan's codes and the current computer technology make it possible to implement ab-initio Slater-Condon theory with a relatively small investment of time and expense. The values of the semi-empirical parameters calculated from integrals involving the radial wavefunctions, however, are found to deviate from the parameters obtained by the semi-empirical analysis of the spectra to the extent that caution must be exercised when using the calculations as a tool for analyzing spectra.

Typically, the predicted levels and spectra are qualitatively the same as the experimental observations, but the calculations are of absolute energies and cannot hope overall to be as precise as the experimental observations of relative energies, since the albeit small correlation effects are comparable to the differences between the approximate energy levels. Even within configurations, however, where observed and predicted relative energies should be of comparable precision, systematic differences are apparent[14]. This work attempts to develop a better understanding of these differences and develop a hybrid of the semi-empirical and ab-initio forms of Slater-Condon theory to make the best use of available calculations in the problem of spectral analysis.

1.2 Applications of Ab-Initio Slater-Condon Theory

Finding strategies for applying ab-initio calculations of atoms and ions to spectral analysis can be likened to developing the heuristics of semi-empirical Slater-Condon theory. Because the calculation of radial wavefunctions is so difficult without computers, a semi-empirical theory was needed to parameterize the dependence of atomic properties on them. With computers available, the ab-initio Slater-Condon theory becomes readily available to non-experts, By the same token, more sophisticated (and perhaps hypothetical) approximate atomic theories are possible[15] that account for more correlation among electrons. These calculations, however, are again beyond the reach of non-experts. This suggests that new semi-empirical theories might be developed that parameterize the discrepancies between ab-initio Slater-Condon theory and a more sophisticated approximation.

A number of interconnected problems emerge in this context. Because of the success of the semi-empirical theory, it is desirable to remain within this general framework. Then the the nature of the relationship between ab-initio and semi-empirical spectroscopic parameters, or how correlations might be included in the semi-empirical description becomes of interest. Insight into this question can help in the task of finding a new set of parameters that can be used to map the predicted spectroscopic parameters into their empirically determined values. The dependence of this mapping on the nuclear charge Z and the number of electrons N is of interest in order to extrapolate the adjustments of analyzed ions or atoms to unknown or partially analyzed cases.

Chapter II reviews the descriptive features of Slater-Condon theory

and leads naturally to Chapter III, a review of the computer calculations. Density matrices and effective operators are employed to isolate the features of Slater-Condon theory leading to the semi-empirical theory and parameterization of effective Hamiltonians. The effective operator formalism and its group theoretical analysis are developed in some detail for the discussion in Chapter IV. Chapter III discusses the SCF method for solving the configuration-averaged non-relativistic Hartree-Fock equations, Cowan's HX approximation, relativistic and correlation corrections, the construction of the Hamiltonian matrix, predicted spectra, and least squares minimization.

Chapter IV explores the possibility of wavefunctions more general than Slater determinants allowing more correlations among electrons, but leading essentially to the same semi-empirical parameterization. The parameterization of effective Hamiltonians from symmetry properties is considered, focusing on representations of symmetry groups for unperturbed Hamiltonians. The irreducible representations of these groups are examined, representations of other groups induced from them, and their branching properties under restrictions to various subgroups. These considerations are used in part to estimate the qualitative effects of additional correlations on the spectroscopic parameters examined in Chapter V.

Chapter V contains the applications of the ab-initio calculations to spectral analysis. The first section, (5.1), explains the methods used to select and adjust the spectroscopic parameters with a secondary set of free parameters to bring the ab-initio results into the best agreement with experimental levels using least squares. Methods for

agreement with experimental levels using least squares. Methods for extrapolating adjustments to other atoms and ions are considered, including isoelectronic extrapolation from formal 1/Z perturbation theory.

Section (5.2) is a study of the K I isoelectronic sequence from K^{0+} to Fe^{7+}. The adjustment and isoelectronic extrapolation strategies are combined and applied to the $3p^5 3d^2$, $3p^5 3d4f$, $3p^5 3d4s$, and the Rydberg $3p^6 n\ell$ configurations. Section (5.3) is a discussion of a modified strategy used on U^{4+}. Energy levels of the f^2 configuration in O_h symmetry are modeled and fit to data on the hexahalide complexes, $(UX_6)^{2-}$ where (X = F,Cl,Br,I), using a model proposed by Brian Judd. The results of chapter V are reviewed in the summary, chapter VI, in the context of the preceding chapters, followed by appendices containing tables of energy levels, spectra, and listings of computer programs.

II. Descriptions of N-Electron Systems and Slater-Condon Theory

A discussion of the descriptions of N-electron systems with rotational symmetry and Slater-Condon theory is presented here. Determinant wavefunctions and density matrices are discussed in section (2.1), including many density matrix expressions relevant to antisymmetrized product wavefunctions. Elements of Slater-Condon theory are reviewed in section (2.2), including atomic Hamiltonians, spherical tensor operators, effective operators, and SLJ-coupled basis vectors and their matrix elements. The parameterization of effective Hamiltonians on finite dimensional subspaces spanned by determinant wavefunctions are discussed in section (2.3); this discussion complements material in section (2.2).

Density matrices and effective operators descriptions are employed here as a framework for calculations involving determinant wavefunctions, and as a means of isolating the independent parameters associated with semi-empirical Slater-Condon theory. The effective operator methods are generalized in chapter IV to show that semi-empirical Slater-Condon theory is consistent with N-electron atomic wavefunctions constructed from 1-electron angular momentum eigenfunctions and arbitrary N-dimensional radial wavefunctions.

2.1 N-electron Wavefunctions and n-Electron Density Matrices

Ignoring corrections to the same order as hyperfine interactions and isotope shifts, an atom or ion can be described by a 2^N (or 4^N relativistic) rank spinor-valued, square-integrable (over R^{3N}), N-electron wavefunction. The i^{th} electron coordinates are denoted here by

$x_i = (\vec{r}_i, \sigma_i)$:

$$\Phi^N(\vec{r}_1, \vec{r}_2, \ldots, \vec{r}_N)_{\{\sigma\}} = \Phi^N(x_1, x_2, \ldots, x_N) \tag{2.1a}$$

$$\{\sigma\} = \{\sigma_1, \sigma_2, \ldots, \sigma_N\} \tag{2.1b}$$

$$\|\Phi^N\|^2 = \int_{(\infty)} dx_1 \ldots dx_N |\Phi^N(x_1, \ldots, x_N)|^2 < \infty \tag{2.1c}$$

$$\int_{(\infty)} dx = \sum_{\sigma=-1/2}^{+1/2} \int_{(\infty)} d^3\vec{r} \tag{2.1d}$$

Symmetry Properties

In general, an N-electron Hamiltonian is invariant with respect to permutations of the sets of electron coordinates and a group of spatial symmetry transformations. A free atom or ion is invariant with respect to simultaneous identical rotations and reflections of the electron coordinates, but permutation symmetry is perhaps the most rigorous symmetry for any N-electron system. Only wavefunctions that carry the totally antisymmetric irreducible representation of S_N, the symmetric group of order N!, can represent physical states of such a system. Nature has been kind by allowing only the one-dimensional representations of S_N for identical particles, and perhaps has been kinder still by choosing the antisymmetric rather than the symmetric representation for electrons, as this also reduces the complexity of spectra somewhat.

In any case, Slater[1] naturally used antisymmetrized products N 1-electron wavefunctions to generate N-electron wavefunctions for atoms. An arbitrary antisymmetrized N-electron product wavefunctions with

definite rotation and reflection symmetry is conceptually awkward, but 1-electron wavefunctions that carry irreducible representations of SU(2), the quantum mechanical rotation group, are well known. Slater reduced the problem to finding the irreducible representations of the rotation group that can be reduced from linear combinations of this type.

2.1.1 Determinant Wavefunctions

A determinant wavefunction is the antisymmetrized product of N 1-electron wavefunctions. Consider a set $A = \{\phi_1^A, \phi_2^A, \ldots, \phi_N^A\}$ of N linearly independent 1-electron wavefunctions, and define the matrix valued function $M(A;x_1,x_2,\ldots,x_N)$ with elements given by:

$$M(A;x_1,x_2,\ldots,x_N)_{ij} = \phi_i^A(x_j) \tag{2.2}$$

The N-electron determinant wavefunction Φ_A^N is defined:

$$\Phi_A^N(x_1,x_2,\ldots,x_N) = \det|M(A;x_1,x_2,\ldots,x_N)|/(N!)^{-1/2} \tag{2.3}$$

Uniqueness

A determinant wavefunction does not uniquely determine a set of 1-electron wavefunctions. Let A′ be the set obtained from A by a non-singular linear transformation T:

$$\phi_i^{A'}(x) = \sum_{j=1}^{N} T_{ji}\, \phi_j^A(x) \tag{2.4}$$

Since the determinant of the product of two matrices is equal to the product of their determinants, the relationship between the determinant wavefunctions Φ_A^N and $\Phi_{A'}^N$ is given by:

$$\Phi_{A'}^{N}(x_1,x_2,\cdots,x_N) = \det|T|\Phi_{A}^{N}(x_1,x_2,\cdots,x_N) \qquad (2.5)$$

In particular, a normalized determinant wavefunction constructed from an arbitrary set of N linearly independent 1-electron wavefunctions is--up to a phase factor--equal to the determinant wavefunction constructed from an orthonormal set of 1-electron wavefunctions that span the same subspace of the 1-electron Hilbert space. A given N-electron determinant wavefunction is uniquely related to an N-dimensional subspace of the 1-electron Hilbert space. This property is obvious when a density matrix description is used in place of N-electron determinant wavefunctions.

2.1.2 Matrix Elements and Density Matrices

The density matrix description was formalized by von Neumann[16] to help explain the statistical nature of quantum mechanics. Dirac[17] pioneered a density matrix description of the atom to justify theoretically the semi-classical Thomas-Fermi model, and his techniques were quickly applied to the Hartree-Fock equations for determinant wavefunctions[18]. Löwdin[19] expanded and generalized this framework for work with superpositions of Slater determinants.

Density Matrices

Table (2.1) is a list of definitions used to develop a density matrix description of the N-electron Hilbert space with a certain set of state vectors in mind. Instead of employing only reduced density matrices in this approach, an object called the n-electron transition matrix is defined. This object is unnecessary for a physical theory, as

all physical properties can be obtained from the n-electron reduced density matrices, but it is a useful component in a hybrid description involving density matrices and a specified set of N-electron wavefunctions (e.g. the Slater determinant wavefunctions). The n-electron reduced density matrices are referred to here as simply n-electron density matrices, the lower-case "n" indicating the reduced density matrix as opposed to the "N"-electron density matrix.

The n-electron transition matrices can perhaps be best described as kernels of bounded integral operators on an n-particle Hilbert space, while the n-electron density matrices comprise the convex linear hull of the non-negative definite, self-adjoint operators of trace class. Alternately, the n-electron transition matrices can be obtained by extending the set of density matrices to a vector space over the complex field.

Matrix Elements

The n-electron transition matrices allow the matrix elements of the symmetric n-electron operators to be formally expressed as:

$$\left\langle \Psi_a^N \middle| Q_n \middle| \Psi_b^N \right\rangle = \|\Psi_a^N\| \, \|\Psi_b^N\| \int dx_1 dx_1' \cdots dx_n dx_n' \; \delta(x_1 - x_1') \cdots \delta(x_n - x_n') \left[q_n \Gamma_{ba}^n \right](x_1, \ldots, x_n; x_1', \ldots, x_n') \tag{2.8a}$$

$$\int dx dx' \delta(x - x') \left[q\Gamma \right](x; x') \equiv \left\{ \begin{array}{l} \text{let } q \text{ act on } x, \text{ then set } x' = x \\ \text{and sum/integrate over } x = (\vec{r}, \sigma) \end{array} \right\} \tag{2.8b}$$

If Γ_{ba}^n is the integral operator with the corresponding n-electron transition matrix as its kernel, (2.8a) can formally be rewritten as a trace

Table (2.1)

Components of a Density Matrix—Basis Set Description

Basis Set		
$\{\Phi_i^N; i=1,2,\ldots\}$	—	any set of N-electron wavefunctions of interest

n-Electron Operators			
Q_n	=	$\sum_{i_1=1}^{N-n+1} \cdots \sum_{i_n>i_{n-1}}^{N} q_n(i_1,\ldots,i_n)$	(2.6)
$q_n(i_1,i_2,\ldots,i_n)$	—	an n-electron operator that acts on the electron coordinates with indices $(i_1,\ldots,i_n)$ and is invariant with respect to permutations of these indices	

n-Electron Kernels

n-electron transition matrices:

$$\Gamma^n_{ba}(x_1,\ldots,x_n;x'_1,\ldots,x'_n) = \binom{N}{n}\left[\|\Phi_b^N\|\,\|\Phi_a^N\|\right]^{-1}\int dy_{n+1}\cdots dy_N \left\{\Phi_b^N(x_1,\ldots,x_n,y_{n+1},\ldots,y_N)\,\Phi_a^{N*}(x'_1,\ldots,x'_n,y_{n+1},\ldots,y_N)\right\} \quad (2.7a)$$

$$\binom{N}{n} = \frac{N!}{n!(N-n)!} \quad (2.7b)$$

n-electron density matrix of Φ_a^N:

$$\Gamma^n_a(x_1,\ldots,x_n;x'_1,\ldots,x'_n) = \Gamma^n_{aa}(x_1,\ldots,x_n;x'_1,\ldots,x'_n) \quad (2.7c)$$

general n-electron density matrices:

$$\Gamma^n_\Theta(x_1,\ldots,x_n;x'_1,\ldots,x'_n) = \sum_i \Theta_i \Gamma^n_i(x_1,\ldots,x_n;x'_1,\ldots,x'_n) \quad (2.7d)$$

$$\Theta = \{\Theta_i \mid 0 \le \Theta_i \le 1;\ \textstyle\sum \Theta_i = 1\} \quad (2.7e)$$

over any complete orthonormal basis of the n-particle Hilbert space:

$$\left[\hat{\Gamma}^{n}_{ba}\Psi^{n}\right](x_1,\ldots,x_n) = \int dy_1\ldots dy_n \Gamma^{n}_{ba}(x_1,\ldots,x_n;y_1,\ldots,y_n)\Psi^{n}(y_1,\ldots,y_n) \tag{2.9a}$$

$$\left\langle \Phi^{N}_{a}\middle| Q_n \middle|\Phi^{N}_{b}\right\rangle = \|\Phi^{N}_{a}\|\,\|\Phi^{N}_{b}\|\ \underset{\sim}{\mathrm{tr}}\left[q_n\hat{\Gamma}^{n}_{ba}\right] \tag{2.9b}$$

$$= \|\Phi^{N}_{a}\|\,\|\Phi^{N}_{b}\|\ \underset{\sim}{\mathrm{tr}}\left[q_n\hat{\Gamma}^{n\dagger}_{ab}\right]$$

Expressing formally the matrix elements of n-electron operators using n-electron transition matrices is of little value unless the transition matrices can be given in more detail. This is possible for determinant wavefunctions, and proves useful for examining the symmetry properties of transition arrays of determinant wavefunctions.

2.1.3 Antisymmetrized Product Wavefunctions

Before examining in detail the components of a density matrix-determinant wavefunction description of an atom or ion, it is useful to consider antisymmetrized product wavefunctions in general. Let Φ^{V}_{a} and Φ^{C}_{b} be V- and C-electron antisymmetrized wavefunctions where C+V = N. Then the N-electron wavefunction Φ^{N}_{ab} is defined:

$$\Phi^{N}_{ab}(x_1,\ldots,x_N) = \binom{N}{V}^{1/2} A_N\left[\Phi^{V}_{a}(x_1,\ldots,x_V)\Phi^{C}_{b}(x_{V+1},\ldots,x_N)\right] \tag{2.10}$$

A_N is the projection operator for the antisymmetric representation of S_N and the binomial coefficient factor $\binom{N}{V}^{1/2}$ is convenient for normalization. Because Φ^{V}_{a} and Φ^{C}_{b} are both antisymmetric, (2.10) can be rewritten in the form of a sum over all distinct V-element ordered subsets of the index set Z(N) = {1,2,...,N}:

$$\Phi^N_{ab}(x_1,\ldots,x_N) = \binom{N}{V}^{-1/2} \sum_{I\subset Z(N)}^{V} (-1)^{S(I)} \Phi^V_a(X_I)\Phi^C_b(X_{\bar{I}}) \qquad (2.11a)$$

$$S(I) = (i_1-1) + (i_2-2) +\ldots+ (i_V-V) \qquad (2.11b)$$

$$\sum_{I\subset Z(N)}^{V} = \sum_{i_1=1}^{i_2} \sum_{i_2>i_1}^{i_3} \cdots \sum_{i_V>i_{V-1}}^{N} \qquad (2.11c)$$

X_I and $X_{\bar{I}}$ are the electron coordinates labeled by the sets $I = \{i_1,\ldots,i_n\}$ and $\bar{I} = Z(N) - I \cap Z(N)$, the complement of I in Z(N).

N-Electron Transition Matrices

Equation (2.11) can be used to obtain an expression for the N-electron transition matrix between two product wavefunctions Φ^N_{ab} and Φ^N_{cd}:

$$\Gamma^N_{abcd}(x_1,\ldots,x_N;x'_1,\ldots,x'_N) = D_{abcd} \binom{N}{V}^{-1} \qquad (2.12a)$$

$$\sum_{I\subset Z(N)}^{V} \sum_{J\subset Z(N)}^{V} (-1)^{S(I-J)} \Gamma^V_{ac}(X_I;X'_J)\Gamma^C_{bd}(X_{\bar{I}};X'_{\bar{J}})$$

$$D_{abcd} = \frac{\|\Phi^V_a\|\|\Phi^V_c\|\|\Phi^C_b\|\|\Phi^C_d\|}{\|\Phi^N_{ab}\|\|\Phi^N_{cd}\|} \qquad (2.12b)$$

$$S(I-J) = (i_1-j_1) + (i_2-j_2) +\ldots+ (i_V-j_V) \qquad (2.12c)$$

X_I, X_J, $X_{\bar{I}}$, and $X'_{\bar{J}}$ are defined as in (2.11).

The sum over the index set J, however, in (2.12) can be rewritten in form that is relative to the sum over the index set I. This is equivalent to summing over partitions of Z(N) into four disjoint subsets: $\{K,\bar{K},L,\bar{L}\}$ where $I = \{KU\bar{K}\}$ $\bar{I} = \{LU\bar{L}\}$, $J = \{\bar{K}UL\}$, and $\bar{J} = \{KU\bar{L}\}$. K

and L have o elements, $\bar{K}$ has V-o elements, while $\bar{L}$ has C-o elements; $0 \leq o \leq V$ (without loss of generality it has been assumed that $V \leq C$):

$$\Gamma^{N}_{abcd}(X_{Z(N)};X'_{Z(N)}) = D_{abcd}\binom{N}{V}^{-1}\sum_{o=0}^{V}(-1)^{o}\sum_{I\subset Z(N)}^{V} \tag{2.13}$$

$$\sum_{K\subset I}^{o}\sum_{L\subset \bar{I}}^{o}\Gamma^{V}_{ac}(X_{\bar{K}},X_{K};X'_{\bar{K}},X'_{L})\Gamma^{C}_{bd}(X_{L},X_{\bar{L}};X'_{K},X'_{\bar{L}})$$

The factor $(-1)^{o}$ is the parity of the permutation that brings the partition $\{\bar{K},K,L,\bar{L}\}$ to the form $\{\bar{K},L,K,\bar{L}\}$.

The N-electron transition matrix expression (2.13) leads to the expressions for the overlaps and norms of the product wavefunctions in terms of the n-electron transition matrices ($0 \leq n \leq V$):

$$\left\langle \Phi^{N}_{ab} \middle| \Phi^{N}_{cd} \right\rangle = \|\Phi^{V}_{a}\|\,\|\Phi^{V}_{c}\|\,\|\Phi^{C}_{b}\|\,\|\Phi^{C}_{d}\|\left\{1+\sum_{o=1}^{V}(-1)^{o}\,\mathrm{tr}\left[\hat{\Gamma}^{o}_{ac}\hat{\Gamma}^{o}_{bd}\right]\right\} \tag{2.14a}$$

$$\|\Phi^{N}_{ab}\| = \|\Phi^{V}_{a}\|\,\|\Phi^{C}_{b}\|\left\{1+\sum_{o=1}^{V}(-1)^{o}\,\mathrm{tr}\left[\hat{\Gamma}^{o}_{a}\hat{\Gamma}^{o}_{b}\right]\right\}^{1/2} \tag{2.14b}$$

n-Electron Transition Matrices

Expressions for the n-electron transition matrices between two N-electron product wavefunctions Φ^{N}_{ab} and Φ^{N}_{cd} can be obtained from (2.13) by contracting over the pairs of coordinates $\{(x_i,x'_i) \mid i=n+1,n+2,\ldots,N\}$ and multiplying by $\binom{N}{n}$. This process is somewhat awkward, however, because it involves a sum over all distributions of the index set $Z(n) = \{1,2,\ldots,n\}$ among the subsets K, $\bar{K}$, L, and $\bar{L}$. However, if the coordinates x with indices in Z(n) are summed over all distributions between Φ^{V}_{a}, Φ^{C}_{b} and similarly for the corresponding x′ coordinates between Φ^{V}_{c},

Φ_d^C, and then the remaining coordinates are summed over all possible distributions in a manner similar to (2.13), an expression for the n-electron transition matrix is emerges:

$$\Gamma^n_{abcd}(x_1,\ldots,x_n;x'_1,\ldots,x'_n) = D_{abcd} \sum_{v,v'=\max(0,n-C)}^{\min(n,V)} \sum_{e=0}^{\min(V-v_>,C-n+v_<)}$$

$$(-1)^{e+(n-v_<)(v_>-v_<)e} \begin{bmatrix} r \\ v \end{bmatrix} \begin{bmatrix} s \\ n-v \end{bmatrix} \begin{bmatrix} n \\ v' \end{bmatrix} A_n \Big(\int_{(\infty)} dZdY \qquad (2.15a)$$

$$\Gamma^r_{ac}(x_1,\ldots,x_v,Z;x'_1,\ldots,x'_{v'},Y)\Gamma^s_{bd}(x_{v+1},\ldots,x_n,Y;x'_{v'+1},\ldots,x'_n,Z)\Big) A_n^\dagger$$

$$v_< = \min(v,v'); \; v_> = \max(v,v'); \; r = v_>+e; \; s = n-v_< +e \qquad (2.15b)$$

The x and x′ coordinates are antisymmetrized with A_n and $A_n^\dagger$, and the integrations with respect to dZ and dY are over e-m and e+m dummy sets of electrcn coordinates respectively unless either e-m or e+m is zero.

Strict Orthogonality

The special case of strict or strong orthogonality[20] between the two components of an antisymmetrized product wavefunction is worth mentioning. The usual notion of orthogonality can be generalized for any pair of wavefunctions Φ_a^V and Φ_b^C by saying that Φ_a^V and Φ_b^C are orthogonal (taking for convenience $V \leq C$) if

$$\mathrm{tr}\left[\Gamma_a^V \Gamma_b^V\right] = 0 \qquad (2.16)$$

This is equivalent to the usual notion of orthogonality when C = V. The wavefunctions Φ_a^V and Φ_b^C are said to be strictly orthogonal if the (N-2)-electron wavefunction given by

$$\Phi_{ab}^{N-2}(x_1,\cdots,x_{N-2}) = \tag{2.17a}$$

$$\int_{(\infty)} dy\ \Phi_a^{V*}(x_1,\cdots,x_{V-1},y)\Phi_b^{C}(y,x_V,\cdots,x_{N-2})$$

has a norm of 0. This is equivalent to

$$\mathrm{tr}\left[\hat{\Gamma}_a^{1\dagger}\hat{\Gamma}_b^{1}\right] = 0 \tag{2.17b}$$

The probability statement implied by (2.17) is, of course, stronger than (2.16). (2.17) is equivalent to saying that the probability of finding any electron of the V electrons described by Φ_a^V and any electron of the C electrons described by Φ_b^C in the same 1-electron state or orbit is zero. Classically, this is equivalent to saying that the distribution functions describing the two systems have no overlap in phase space.

The expression for the n-electron transition matrix between the states Φ_{ab}^N and Φ_{cd}^N is much simpler, however, when the pairs of wavefunctions Φ_a^V, Φ_d^C and Φ_c^V, Φ_b^C are strictly orthogonal. (2.15) reduces to a single sum:

$$\Gamma_{abcd}^{n}(x_1,\cdots,x_n;x_1',\cdots,x_n') = D_{abcd} \sum_{v=\max(0,n-C)}^{\min(n,V)} \binom{n}{v} \tag{2.18a}$$

$$A_n\left\{\Gamma_{ac}^{v}(x_1,\cdots,x_v;x_1',\cdots,x_v')\Gamma_{bd}^{n-v}(x_{v+1},\cdots,x_n;x_{v+1}',\cdots,x_n')\right\}A_n^{\dagger}$$

For the strictly orthogonal Φ_a^V and Φ_b^C, the n-electron density matrix for Φ_{ab}^N becomes:

$$\Gamma^{n}_{abcd}(x_1,\cdots,x_n;x'_1,\cdots,x'_n) = \sum_{v=\max(0,n-C)}^{\min(n,V)} \binom{n}{v} \tag{2.18b}$$

$$A_n\left\{\Gamma^{v}_{a}(x_1,\cdots,x_v;x'_1,\cdots,x'_v)\Gamma^{n-v}_{b}(x_{v+1},\cdots,x_n;x'_{v+1},\cdots,x'_n)\right\}A^{\dagger}_n$$

2.1.4 Density Matrices and Determinant Wavefunctions

Expressions for n-electron transition matrices involving determinant wavefunctions can be obtained from the Laplace expansion of the determinant of a matrix, and contracting over the (N-n) unused coordinates. It is not always possible or desirable to assume the 1-electron wavefunctions are orthonormal, so table (2.2) contains definitions for components used in these expressions involving the overlap integrals between 1-electron wavefunctions. Table (2.3) contains the general expressions for the n-electron transition and density matrices.

Except for some notational changes, the expressions in table (2.3) are identical to those of Löwdin[19]. Equation (2.29) shows explicitly that all of the n-electron density matrices for a single Slater determinant are uniquely determined by the 1-electron density matrix. The 1-electron density matrix is the kernel of a projection operator for an N-dimensional subspace of the 1-electron Hilbert space, thus all physical properties of a determinant wavefunction can be obtained from this operator.

Orthogonalized Density Matrix Expressions

For two arbitrary sets of N 1-electron wavefunctions A and B, independent unitary linear transformations can be performed on the sets A and B so that any function of the transformed set A′ will be

Table (2.2)

1-Electron Wavefunction Expressions

Overlap Matrix Functions

overlap matrix function for Φ_A^N and Φ_B^N:

$$O(AB)_{ij} = \int_{(\infty)} dx \phi_i^{A*}(x)\phi_j^B(x) \qquad (2.19)$$

$$O(A) \equiv O(AA)$$

(N-r)-ranked submatrices of O(AB):

$$I,J = \{i_1<\ldots<i_r\},\ \{j_1<\ldots<j_r\};\ r\text{-element ordered subsets of } \{1,2,\ldots,N\} \qquad (2.20a)$$

$$O(A_{\bar{I}}B_{\bar{I}}) = \text{the sub matrix of } O(AB) \text{ obtained by deleting the rows labeled by the set I, and the columns labeled by J} \qquad (2.20b)$$

(N-r)-ranked normalized co-minors of O(AB):

$$m(A_{\bar{I}}B_{\bar{J}}) = (-1)^{S(I,J)} d(A_{\bar{I}}B_{\bar{J}})/\sqrt{d(A)d(B)} \qquad (2.21a)$$

$$d(A_{\bar{I}}B_{\bar{J}}) = \det|O(A_{\bar{I}}B_{\bar{J}})| \qquad (2.21b)$$

$$S(I,J) = i_1+\ldots+i_p+j_1+\ldots+j_p \qquad (2.21c)$$

$$m(AB) \equiv d(AB) = \det|O(AB)|$$

Primitive Kernels

d(AB) $\neq$ 0:

$$\gamma_{BA}(x;x') = \sum_{i,j=1}^{N} \phi_i^B(x)\phi_j^{A*}(x')O(AB)^{-1}_{ji} \qquad (2.22a)$$

$$\gamma_A(x;x') = \gamma_{AA}(x;x') \qquad (2.22b)$$

r-ranked subkernels:

$$\gamma_{B_J A_I}(x;x') = \sum_{\alpha=1}^{r} \phi^B_{j_\alpha}(x)\phi^{A*}_{i_\alpha}(x')m(A_{\bar{I}}B_{\bar{J}}) \qquad (2.23)$$

Table (2.3)

Density Matrix Expressions for Determinant Wavefunctions

Inner Products

overlaps:

$$\left\langle \Phi_A^N | \Phi_B^N \right\rangle = d(AB) \equiv \| \Phi_A^N \| \| \Phi_B^N \| \, \Gamma_{BA}^0 \qquad (2.24)$$

norms:

$$\left\langle \Phi_A^N | \Phi_A^N \right\rangle = \| \Phi_A^N \|^2 = d(A) \qquad (2.25)$$

n-Electron Transition Matrices

n-electron sub determinant form:

$$\Gamma_{BA}^n(x_1,\ldots,x_n;x'_1,\ldots,x'_n) = \sum_{I\subset Z(N)}^{n} \sum_{J\subset Z(N)}^{n} \Phi_{B_J}^n(x_1,\ldots,x_n) \, \Phi_{A_J}^{n*}(x'_1,\ldots,x'_n) \, m(A_{\bar{I}}B_{\bar{J}})/n! \qquad (2.26a)$$

$$\sum_{I\subset Z(N)}^{n} = \sum_{i_1=1}^{N-n+1} \sum_{i_2>i_1}^{N-n+2} \cdots \sum_{i_n>i_{n-1}}^{N} \qquad (2.26b)$$

$$A_I = \{\phi_{i_1}^A, \phi_{i_2}^A, \ldots, \phi_{i_n}^A\} \qquad (2.26c)$$

primitive kernel determinant from:

$$\Gamma_{BA}^n(x_1,\ldots,x_n;x'_1,\ldots,x'_n) = \sum_{I\subset Z(N)}^{n} \sum_{J\subset Z(N)}^{n} \det|G_{B_J A_I}(x;x')| \, m(A_{\bar{I}}B_{\bar{J}})/n! \qquad (2.27a)$$

$$[G_{B_J A_I}(x;x')]_{ij} = \gamma_{B_J A_I}(x_i;x'_j) \qquad (2.27b)$$

non-zero overlap form ($d^{AB} \neq 0$):

$$\Gamma_{BA}^n(x_1,\ldots,x_n;x'_1,\ldots,x'_n) = \det|G_{BA}(x;x')|/n! \qquad (2.28a)$$

$$[G_{BA}(x;x')]_{ij} = \gamma_{BA}(x_i;x'_j) \qquad (2.28b)$$

n-electron density matrix:

$$\Gamma_A^n(x_1,\ldots,x_n;x'_1,\ldots,x'_n) = \det|G_A(x;x')|/n! \qquad (2.29a)$$

$$[G_A(x;x')]_{ij} = \gamma_A(x_i;x'_j) \qquad (2.29b)$$

orthogonal to all but at most one of the functions of the transformed set B′. This follows from the fact that the overlap matrix O(AB) can always be written in polar form, thus there exists a unitary transformation that can be applied to the set A so that O(A′B) is Hermitian symmetric, and another unitary transformation that can be applied to both A′ and B so that O(A″B′) diagonal. Without loss of generality then, the 2N 1-electron wavefunctions of the sets A and B can be assumed to satisfy the orthogonality relations:

$$\langle \phi_i^A | \phi_j^A \rangle = \delta_{ij} \| \phi_i^A \| \tag{2.30a}$$

$$\langle \phi_i^B | \phi_j^B \rangle = \delta_{ij} \| \phi_i^B \| \tag{2.30b}$$

$$\langle \phi_i^A | \phi_j^B \rangle = \begin{cases} \delta_{ij} & i>r \\ 0 & i \leq r \end{cases} \tag{2.30c}$$

where r is a non-negative integer and (N-r) is the rank of the matrix O(AB).

The expressions for the n-electron transition matrices between two determinant wavefunctions Φ_A^N and Φ_B^N are of course simplified when the sets A and B are orthonormal with respect to each other. Unfortunately, the linear transformations required to bring two arbitrary sets of N 1-electron wavefunctions to this form is not in general uniquely or simply defined. An exceptional case occurs when the overlap matrix O(AB) is non-singular; the n-electron transition matrices are completely determined by the primitive kernel $\gamma_{BA}(x;x')$ defined by equation (2.22a) of table (2.2). In this case the orthonormalizing transformation is

generated by the matrix $O(AB)^{-1}$ applied to the set A as in equation (2.4). If A=B, O(A) is the Gram matrix, and is a positive definite Hermitian symmetric matrix for non-vanishing Φ_A^N, and the set of functions A is orthonormalized by the matrix $O(A)^{-1/2}$.

The n-electron transition matrices between Φ_A^N and Φ_B^N for sets A and B that satisfy (2.30) are conveniently expressed in terms of the r-electron transition matrices between $\Phi_{B'}^r$ and $\Phi_{A'}^r$, and the (n-r)-electron transition matrices between $\Phi_{B''}^{n-r}$ and $\Phi_{A''}^{n-r}$ where $A' = \{\phi_1^A,\ldots,\phi_r^A\}$, $B' = \{\phi_1^B,\ldots,\phi_r^B\}$, $A'' = \{\phi_{r+1}^A,\ldots,\phi_N^A\}$, and $B'' = \{\phi_{r+1}^B,\ldots,\phi_N^B\}$. This is the strict orthogonality case of the general expression for the n-electron transition matrix between N-electron wavefunctions constructed antisymmetrizing the product of a r-electron and an (N-r)-electron wavefunction, equation (2.18b).

$$\Gamma^n_{BA}(x_1,\ldots,x_n;x'_1,\ldots,x'_n) = \tag{2.31}$$

$$\binom{n}{r} A_n \left\{ \Gamma^r_{B'A'}(x_1,x_2,\ldots,x_r;x'_1,x'_2,\ldots,x'_r) \; > \; \Gamma^{n-r}_{B''A''}(x_{r+1},x_{r+2},\ldots,x_n;x'_{r+1},x'_{r+2},\ldots,x'_n) \right\} A_n$$

$\Gamma^r_{B'A'}$ and $\Gamma^{n-r}_{B''A''}$ are conveniently calculated using expressions from table (2.3).

If the sets A and B of N 1-electron wavefunctions are taken from a single set of orthonormal 1-electron wavefunctions, the orthogonality conditions (2.30) may be satisfied after one of the sets A or B is permuted so that the 1-electron wavefunctions common to A and B will have the same index. Only relative permutations need be considered, if the

identical permutation is applied to both sets, the n-electron transition matrices are unaffected. If $s(A,B)\in S_N$ is any permutation that accomplishes the desired change of relative orderings, the n-electron transition matrices are multiplied by $(-1)^{S(A,B)}$, the parity of the relative permutation. Explicit expressions for the 1 and 2-electron transition matrices become:

$$\Gamma^1_{BA}(x;x') = \delta_{B,A} \sum_{i=1}^{N} \phi_i^A(x)\phi_i^{A*}(x') + \delta_{(A-\phi_a),(B-\phi_b)} (-1)^{S(A,B)} \phi_b(x)\phi_a^*(x') \tag{2.32}$$

$$\begin{aligned}\Gamma^2_{BA}(x_1,x_2;x_1',x_2') = (-1)^{S(A,B)} \tfrac{1}{2} \Big\{ & \delta_{AB} \Big\langle \Gamma^1_A(x_1;x_1')\Gamma^1_A(x_2;x_2') - \Gamma^1_A(x_1;x_2')\Gamma^1_A(x_2;x_1') \Big\rangle \\ & + \delta_{(A-\phi_a),(B-\phi_b)} \Big\langle \phi_b(x_1)\phi_a^*(x_1')\Gamma^1_{A''}(x_2;x_2') - \phi_b(x_1)\phi_a^*(x_2')\Gamma^1_{A''}(x_2;x_1') \Big\rangle \\ & + \delta_{(A-\phi_a-\phi_c),(B-\phi_b-\phi_d)} \Big\langle \phi_b(x_1)\phi_a^*(x_1')\phi_c(x_2)\phi_d^*(x_2') - \phi_b(x_1)\phi_a^*(x_2')\phi_c(x_2)\phi_d^*(x_1') \Big\rangle \\ & + (\text{ same expression with } 1\to 2; 2\to 1) \Big\}\end{aligned} \tag{2.33}$$

2.2 Slater-Condon Theory

A method of deducing the occurrence and approximate energy intervals of groups of atomic energy levels was introduced by Slater[1] in 1929, and was expanded a few years later into a comprehensive theory of electronic structure and spectra in the classic text by Condon and Shortley[2]. Cowan[3] uses the phrase "Slater-Condon theory" to describe Slater's method of approximating groups of atomic states with linear combinations from a finite set of determinant wavefunctions. Briefly, the theory has three main features:

(1) A model N-electron atomic Hamiltonian is chosen, and the matrix representation of the Hamiltonian restricted to a subspace spanned by determinant wavefunctions is analyzed for its eigenvalues and eigenvectors.

(2) The 1-electron wavefunctions used to construct the determinant wavefunctions have definite rotation symmetry, and the determinant wavefunctions are chosen so that the subspace spanned is invariant with respect to simultaneous identical rotations of all N electrons.

(3) Because of the rotational symmetry of the atomic Hamiltonian, a major task of the theory is to reduce the subspace with respect to irreducible representations of the quantum-mechanical rotation group in order remove complexity of the Hamiltonian matrix arising from the associated degeneracies.

Several features of Slater-Condon theory are highlighted in this

section. Configurations, the subspaces of determinant wavefunctions are discussed in (2.2.1). The empirical form of Slater-Condon theory is distinguished from the ab-initio form of the theory in (2.2.2), while the atomic Hamiltonians used in the theory are discussed in (2.2.3). Spherical tensor operators and matrix elements are developed in (2.2.4), and effective operators unit tensor expansions are discussed in (2.2.5). The construction of basis vectors that carry irreducible representations of SU(2) and their matrix elements is sketched in (2.2.6), but some additional details concerning the actual construction of Hamiltonian matrices and matrix elements of other operators is presented in chapter III within the context of Cowan's computer codes.

2.2.1 Central Field Model

A common heuristic used to introduce Slater-Condon theory is the central field model. A separable N-electron Hamiltonian with a spherically symmetric local potential is used to represent the time-averaged interaction of each electron with the nucleus and the other N-1 electrons. The traditional form is non-relativistic for optical spectra analysis, as the wavefunctions of the relevant energy levels are assumed to differ significantly only in regions far from the nucleus. The central field Hamitonian takes the form (energy is measured in Rydbergs throughout this chapter):

$$H_c = \sum_{i=1}^{N} p_i^2 + U_c(r_i) \qquad (2.34)$$

The eigenfunctions of H_c are products of the eigenfunctions of the associated 1-electron Hamiltonian. The particular eigenfunctions of

interest are the the determinants comprised of N distinct 1-electron eigenfunctions

$$\phi_{n\ell m\mu}(x) = R_{n\ell}(r)Y_{\ell m}(\theta,\phi)X_{\mu}(\sigma) \tag{2.35a}$$

$$X_{\mu}(\sigma) = \delta_{\mu,\sigma} \tag{2.35b}$$

where the radial wavefunctions are labeled in analogy to the eigenfunctions of the non-relativistic hydrogen atom (this labeling, however, refers to an energy spectrum unique to the coulomb potential.[21])

The symmetry group of rotations for a non-relativistic, central-field 1-electron eigenfunction is $SU(2)xO^{+}(3)$, with representations of the form: $(u^s,u^r)\in SU(2)xO^{+}(3)\rightarrow D^{1/2}(u^s)\otimes D^{\ell}(u^r)$. This representation corresponds to independent rotations with respect to the spin and the space coordinates, and the rotations of a 1-electron central field wavefunction are given by:

$$\left[U(u^s,u^r)\phi_{n\ell m\mu}\right](x) = \sum_{\mu'=-1/2}^{1/2}\ \sum_{m'=-\ell}^{\ell} D^{1/2}_{\mu'\mu}(u^s)D^{\ell}_{m'm}(u^r)\phi_{n\ell'\mu'}(x) \tag{2.36}$$

A 1-electron central field wavefunction also has reflection symmetry with a sign of $(-1)^{\ell}$ under reflections. In contrast, relativistic 1-electron central field wavefunctions have the rotation symmetry group SU(2), corresponding to simultaneous identical rotations of the space and spin coordinates, and an even or odd reflection symmetry for a given representation $u\in SU(2)\rightarrow D^{j}(u)$.

Configurations

All central field eigenfunctions containing the same set of N 1-electron radial wavefunctions are degenerate. All determinant central field eigenfunctions constructed with the same set of radial wavefunctions are said to belong to a configuration $\underline{\Omega}$ denoted by $\underline{\Omega}=(n_1\ell_1^{u_1}, n_2\ell_2^{u_2}, \ldots, n_q\ell_q^{u_p})$, where u_i is the number of $R_{n_i\ell_i}(r)$ radial functions and p is the number of distinct radial wavefunctions in the set $\underline{\Omega}$ $(u_1+u_2+\ldots+u_q=N)$. A determinant wavefunction must be composed of N linearly independent 1-electron wavefunctions, so u_i cannot be greater than $4\ell_i+2$, the number of 1-electron eigenfunctions with a $R_{n_i\ell_i}(r)$ radial wavefunction.

The determinant wavefunctions belonging to a single configuration span the zero-order degenerate manifolds used in central field perturbation theory. A given member of a configuration $\underline{\Omega}(Z)$ corresponds to the choices for the sets $(Z_1, Z_2, \ldots, Z_q)$ of (m,μ) quantum numbers $(Z_a = \{m_\alpha, \mu_\alpha | \alpha=1,2,\ldots,w_a\})$. The number of determinants $f(\underline{\Omega})$ in a given configuration is equal to the number of possibilities for the sets $(Z_1, Z_2, \ldots, Z_q)$, given by the product of binomial coefficients:

$$f(\underline{\Omega}) = \prod_{i=1}^{q} \begin{pmatrix} 4\ell_i+2 \\ u_i \end{pmatrix} \tag{2.37}$$

The relative phases of the determinants are determined by the ordering convention for the 1-electron wavefunctions. The determinant wavefunction $\Phi^N_{\underline{\Omega}(Z)}$ obtained from $\underline{\Omega}(Z) = \{\phi_i^{W(Z)} | \; i=1,2,\ldots,N\}$, has a phase determined by the one to one correspondence of the index i to $(n\ell m_\ell \mu)$.

2.2.2 Semi-empirical and Ab-intio Theories

The semi-empirical form of Slater-Condon theory assumes that radial wavefunctions with the same "()" quantum number are orthonormal, but their specific form is arbitrary. The Hamiltonian matrix is resolved into a linear combination of Hermitian symmetric matrices with coefficients determined by integrals involving the radial wavefunctions. The Hamiltonian is resolved into a sum of spherical tensor operators, effectively separating the action of the Hamiltonian on the angle-spin coordinates from the radial coordinates of each electron.

The coefficients involving the radial wavefunctions are treated as arbitrary parameters. A set of atomic energy levels is classified according to one or more configurations if values of these parameters exist such that the eigenvalues of the Hamiltonian matrix approximate the experimental levels with reasonable accuarcy. Some restrictions are usually place on the ranges of acceptable values for the parameters as an additional test of the validity of a classification.

The ab-initio theory specifies a method for obtaining the radial wavefunctions. The Hamiltonian matrix is cast in the same form as in the semi-empirical theory, but the parameters are now calculated from the radial wavefunctions. In general, the ab-initio parameters differ significantly from the optimal values obtained in the semi-empirical theory, even when stringent criteria are applied to the ranges of acceptable values. Classification of experimental levels belonging to even a single configuration is difficult based on ab-initio predictions alone, thus susceptable to error.

For example, the discrepancy between the parameters obtained by least squares fitting to a set of observed levels and parameters calculated from Hartree-Fock radial wavefunctions is well known; the Hartree-Fock parameters for the electron-electron Coulomb interaction tend to be larger than the least squares values[22]. This discrepancy has been investigated qualitatively by formally applying second order perturbation theory to the central field model[23,24,25], and quantitatively by applying many-body perturbation techniques to zero-order self-consistent-field calculations[26,27].

A reliable ab-initio form of Slater-Condon theory is highly desirable because it is much simpler than a separate variational calculations for some of the lowest lying energy levels for each irreducible representation of the atomic symmetry group. If the successes and limitations of the semi-empirical theory are not simply fortuitous, then the significance of the semi-empirical parameters may come from the existence of a more general form of approximate atomic wavefunctions than the central field determinant wavefunctions consistent with the same parameterization. Chapter IV pursues this idea in order to gain insight into some possible strategies for analyzing atomic spectra with ab-initio predictions.

2.2.3 Atomic Hamiltonians

The parameterization of the Hamitonian matrix for a set of one or more configurations will depend on the Hamiltonian operator chosen to model the atom or ion. For the semi-empirical form of Slater-Condon theory, the Hamiltonian operator is usually obtained by selecting vari-

ous terms from the Pauli approximation[28] to the Breit equation that are deemed important to the relative level structure. The choice of only a mildly relativistic Hamiltonian, even in the case of heavy atoms, is justified by the fact that the relative energy separations are determined only by the radial wavefunctions that tend to be localized in regions far from the nucleus. Then the parameterization of the Hamiltonian matrix tends to be effectively the same for a fully relativistic central field model and the non-relativistic Pauli approximation.

The terms of the Pauli approximation to the Breit equation are given in table (2.4). The important feature of the Pauli Hamiltonian is its composition in terms of only 1 and 2-electron operators. Effective operators that act on the coordinates of 3 or more electrons are sometimes extracted from the second order perturbations of the central field,[23,24] but basically the parameterization of the Hamiltonian matrix is determined from the 1 and 2-electron transition arrays for the determinants involved.

A common approximation is the non-relativistic Hamiltonian H_e with an effective spin-orbit interaction:

$$H_e = H_o + \sum_{i=1}^{N} \xi(r_i) \vec{l}_i \cdot \vec{s}_i \qquad (2.40a)$$

$$\xi(r) = \frac{\alpha^2}{2r} \frac{dU_e(r)}{dr} \qquad (2.40b)$$

The operator $\xi(r)$ is a 1-electron radial operator characterizing the interaction of the spin magnetic moment of the electron in a central field derived from $U_e(r)$. The spin-orbit operator of H_e leads to the same parameterization of the Hamiltonian matrix as the operator H_{so} of

Table (2.4)

Atomic Hamiltonian — Pauli Approximation[28]

$$H = H_0 + H_{so} + H_{so'} + H_{ss'} + H_m + H_d + H_{oo'} \tag{2.38}$$

$$H_0 = \sum_{k=1}^{N} p_k^2 - \frac{2Z}{r_k} + \sum_{k>j=1}^{N} \frac{2}{r_{kj}} \tag{2.39a}$$

$$H_{so} = Z\alpha^2 \sum_{k=1}^{N} \vec{\ell}_k \cdot \vec{s}_k \frac{1}{r_k^3} - \alpha^2 \sum_{k\neq j=1}^{N} \frac{(\vec{r}_{kj} \times \vec{p}_k) \cdot \vec{s}_k}{r_{kj}^3} \tag{2.39b}$$

$$H_{so'} = -\alpha^2 \sum_{k\neq j=1}^{N} \frac{(\vec{r}_{kj} \times \vec{p}_k) \cdot \vec{s}_j}{r_{kj}^3} \tag{2.39c}$$

$$H_{ss'} = 2\alpha^2 \sum_{k>j=1}^{N} \left[\frac{1}{r_{kj}^3} \left\{ \vec{s}_k \cdot \vec{s}_j - 3(\vec{s}_k \cdot \vec{r}_{kj})(\vec{s}_j \cdot \vec{r}_{kj}) \right\} \right]' - \frac{16}{3} \pi\alpha^2 (\vec{s}_k \cdot \vec{s}_j) \delta(\vec{r}_{kj}) \tag{2.39d}$$

$$H_m = -\frac{\alpha^2}{4} \sum_{k=1}^{N} p_k^4 \tag{2.39e}$$

$$H_d = i \frac{Z\alpha^2}{4} \sum_{k=1}^{N} \vec{p}_k \cdot \vec{r}_k r_k^{-3} + i \frac{\alpha^2}{8} \sum_{k\neq j=1}^{N} \vec{p}_k \cdot \vec{r}_{kj} r_{kj}^{-3} \tag{2.39f}$$

$$H_{oo'} = \alpha^2 \sum_{k>j=1}^{N} \frac{1}{r_{kj}} \left\{ \vec{p}_k \cdot \vec{p}_j + \frac{\vec{r}_{kj} (\vec{r}_{kj} \cdot \vec{p}_k) \cdot \vec{p}_j}{r_{kj}^2} \right\} \tag{2.39g}$$

The term enclosed by [ ]′ is to be evaluated by integrating the desired matrix element over all space except for a sphere of radius ϵ centered about the singularity, and then taking the limit as $\epsilon \to 0$.

equation (2.39b) if H_{so} is spherically averaged over the coordinates of one of the two electrons (see section 2.3).

2.2.4 Spherical Tensor Operators and Reduced Matrix Elements

For a sufficiently well behaved n-electron operator q_n, say one with a range and a domain that are invariant under independent rotations of the n sets of electronic coordinates, an operator representation of $[0^+(3)x0^+(3)]^n = 0^+(3)x0^+(3)\ldots 0^+(3)x0^+(3)$ (n times) is generated by

$$(u_1^s,u_1^r)\ldots(u_n^s,u_n^r)\{[0^+(3)x0^+(3)]^n\rightarrow$$

$$U(u_1^s,u_1^r)\ldots U(u_n^s,u_n^r)q_n U^\dagger(u_1^s,u_1^r)\ldots U^\dagger(u_n^s,u_n^r)$$

This representation is reducible to families of operators that carry irreducible representations of $[0^+(3)x0^+(3)]^n$, thus q_n can be expressed as a sum over members of operator families:

$$q_n(1,\ldots,n) = \sum_{\kappa_1=0}^{\infty}\sum_{k_1=0}^{\infty}\cdots\sum_{\kappa_n=0}^{\infty}\sum_{k_n=0}^{\infty} q_n^{\{\kappa_1 k_1\cdots\kappa_n k_n\}}(1,\ldots,n) \qquad (2.41a)$$

$$q_n^{\{\kappa_1 k_1\cdots\kappa_n k_n\}} = \sum_{\pi_1=-\kappa_1}^{\kappa_1}\sum_{q_1=-k_1}^{k_1}\cdots\sum_{\pi_n=-\kappa_n}^{\kappa_n}\sum_{q_n=-k_n}^{k_n}\frac{1}{n!}\sum_{s\in S_n}$$

$$\left\{ c_{\pi_1 q_1\cdots\pi_n q_n}^{\kappa_1 k_1\cdots\kappa_n k_n}\, t_{\pi_1 q_1\cdots\pi_n q_n}^{\kappa_1 k_1\cdots\kappa_n k_n}(s(1),\ldots,s(n)) + \right. \qquad (2.41b)$$

$$c'^{\kappa_1 k_1\cdots\kappa_n k_n}_{\pi_1 q_1\cdots\pi_n q_n}\, t'^{\kappa_1 k_1\cdots\kappa_n k_n}_{\pi_1 q_1\cdots\pi_n q_n}(s(1),\ldots,s(n)) +$$

$$\left. c''^{\kappa_1 k_1\cdots\kappa_n k_n}_{\pi_1 q_1\cdots\pi_n q_n}\, t''^{\kappa_1 k_1\cdots\kappa_n k_n}_{\pi_1 q_1\cdots\pi_n q_n}(s(1),\ldots,s(n)) + \ldots \right\}$$

The sum over permutations $s \in S_n$ guarantees the permutation symmetry of q_n, and only a finite number of operator families $\{t^{\{\lambda k\}}_{(\pi q)}\}$, $\{t'^{\{\lambda k\}}_{(\pi q)}\}$, $\{t''^{\{\lambda k\}}_{(\pi q)}\}$, etc. can occur in the sum (for an atomic Hamiltonian, this number is less than or equal to the number of times the identity representation occurs in the reduction of $O^+(3) \subset [O^+(3) \times O^+(3)]^n$). A family of operators $\{t^{\{\lambda k\}}_{(\pi q)}\}$ transforms under rotations via

$$U(u_1^s,u_1^r)\ldots U(u_n^s,u_n^r)\, t^{\lambda_1 k_1 \ldots \lambda_n k_n}_{\pi_1 q_1 \ldots \pi_n q_n}(1,\ldots,n)\, U^\dagger(u_1^s,u_1^r)\ldots U^\dagger u_n^s,u_n^r) \;=$$

$$\sum_{\pi_1'=-\lambda_1}^{\lambda_1} \sum_{q_1'=-k_1}^{k_1} \cdots \sum_{\pi_n'=-\lambda_n}^{\lambda_n} \sum_{q_n'=-k_n}^{k_n} D^{\lambda_1}_{\pi_1'\pi_1}(u_1^s) D^{k_1}_{q_1'q_1}(u_1^r)\ldots \tag{2.41c}$$

$$D^{\lambda_1}_{\pi_n'\pi_n}(u_n^s) D^{k_n}_{q_n'q_n}(u_n^r)\, t^{\lambda_1 k_1 \ldots \lambda_n k_n}_{\pi_1' q_1' \ldots \pi_n' q_n'}(1\ldots n)$$

Examples of the resolution of the operators taken from the Pauli Hamiltonian are given by Judd[29]. The spherical symmetry of atoms implies that the spherical tensor components $Q_n^{\{\lambda k\}}$ of the atomic Hamiltonian are invariant with respect to $O^+(3) \subset [O^+(3) \times O^+(3)]^n$. The tensor operators that comprise H_e of (2.40a) take the forms Q_1^{00} (1-body scalar), Q_2^{0000} (2-body scalar), Q_1^{11} (from the spin-orbit operator), and Q_2^{0k0k} (from the $1/r_{ij}$ interaction). The resolution of the coulomb interaction between electrons, $1/r_{12}$, is given by

$$\frac{1}{r_{12}} = \sum_{k=0}^{\infty} u_k(r_1,r_2) \sum_{q=-k}^{k} (-1)^q\, C^k_q(\theta_1,\phi_1) C^k_{-q}(\theta_2,\phi_2) \tag{2.42a}$$

$$u_k(r_1,r_2) = \begin{cases} r_1^k/r_2^{k+1} & r_2 \geq r_1 \\ r_2^k/r_1^{k+1} & r_2 < r_1 \end{cases} \tag{2.42b}$$

$$C^k_q(\theta,\phi) = D^{k*}_{q0}(-\phi,\theta,0) = \left[\frac{4\pi}{(2k+1)}\right]^{1/2} Y_{kq}(\theta,\phi) \qquad (2.42c)$$

where the $D^k_{qq'}(\phi,\theta,\psi)$ is the parameterization of the representation D^k of SU(2) in terms of the Euler angles[30].

Matrix Elements and the Wigner-Eckart Theorem

The Wigner-Eckart theorem[31] describes the relationships among the matrix elements of a families of operators and groups of state vectors that all carry irreducible unitary representations of a finite or compact Lie group. For a simply reducible[32] group such as SU(2), this can be illustrated with the matrix elements the 1-electron spherical tensor operator $\{t^k_q \mid q=-k,\ldots,k\}$ between the orthonormal 1-electron wavefunctions $\{\phi_{a'j'm'} \mid m'=-j',\ldots,j'\}$ and $\{\phi_{a''j''m''} \mid m''=-j'',\ldots,j''\}$. All possible matrix elements are determined up to a constant of proportionality $\langle a'j' \| t^k \| a''j'' \rangle$:

$$\langle \phi_{a'j'm'} | t^k_q | \phi_{a''j''m''} \rangle = (-1)^{j'-m'} \begin{pmatrix} j' & k & j'' \\ -m' & q & m'' \end{pmatrix} \langle a'j' \| t^k \| a''j'' \rangle \qquad (2.43)$$

Where the 3-j symbols are related to the transformations that reduce representations of the type $D^{j_1}(u) \otimes D^{j_2}(u) \leftarrow u \in SU(2)$[29,30,32]:

$$D^{j_1}_{m'_1 m_1}(u) D^{j_2}_{m''_2 m_2}(u) = \sum_{j_3=|j_1-j_2|}^{j_1+j_2} \sum_{m_3=-j_3}^{j_3} \sum_{m'_3=-j_3}^{j_3} (2j_3+1) \begin{pmatrix} j_1 & j_2 & j_3 \\ m'_1 & m'_2 & m'_3 \end{pmatrix} \begin{pmatrix} j_1 & j_2 & j_3 \\ m_1 & m_2 & m_3 \end{pmatrix} D^{j_3 *}_{m'_3 m_3}(u) \qquad (2.44)$$

1-Electron Spherical Tensor Operators

By way of proving (2.43), the matrix element on the left-hand-side can be regarded as the trace of the operator t^k_q with one of the 1-electron operators $\tilde{\tau}_{m''m'}(a''j'';a'j')$ that carry the representation $D^{j''}(u) \otimes D^{j'}(u) \leftarrow u \in SU(2)$ (using the equivalence relationship $D^{j'*}_{m_1 m_2}(u) = D^{j'}_{-m_1 -m_2}(u)\ (-1)^{m_1 - m_2}$) where:

$$\tilde{\tau}_{m''m'}(a''j'';a'j') = (-1)^{j'+m'} \hat{\tau}_{m''-m'}(a''j'';a'j') \tag{2.45a}$$

$$\hat{\tau}_{m''m'}(a''j'';a'j') = |\phi_{a''j''m''}\rangle\langle\phi_{a'j'm'}| \tag{2.45b}$$

$$U(u)\tilde{\tau}_{m''m'}(a''j'';a'j')U^{\dagger}(u) = \sum_{m_1=-j''}^{j''} \sum_{m_2=-j'}^{j'} D^{j''}_{m_1 m''}(u)\ D^{j'}_{m_2 m'}(u)\ \tilde{\tau}_{m''m'}(a''j'';a'j') \tag{2.45c}$$

The application of (2.44) to (2.45abc) allows the operators $\hat{\tau}_{m''m'}(a''j'';a'j')$ to be related by a real orthogonal transformation to a set of 1-electron tensor operators that carry irreducible representations of SU(2):

$$\hat{\tau}_{m''m'}(a''j'';a'j') = \sum_{J=|j''-j'|}^{j''+j'} \sum_{M=-J}^{J} (-1)^{j'-m'} [J]^{1/2} \begin{pmatrix} j'' & j' & J \\ m'' & -m' & -M \end{pmatrix} (-1)^{j''-j'-M}\ \hat{w}^J_M(a''j'';a'j') \tag{2.46a}$$

$$\hat{w}^J_M(a''j'';a'j') = \sum_{m''=-j''}^{j''} \sum_{m'=-j'}^{j'} (-1)^{j'-m'} \tag{2.46b}$$

$$[J]^{1/2} \begin{pmatrix} j'' & j' & J \\ m'' & -m' & -M \end{pmatrix} (-1)^{j''-j'-M} \hat{\tau}_{m''m'}(a''j'';a'j')$$

where [x,y,...,z] is an abbreviation for [(2x+1),(2y+1),...,(2z+1)]. The adjoint 1-electron operators are given by

$$\hat{\tau}^\dagger_{m''m'}(a''j'';a'j') = \hat{\tau}_{m'm''}(a'j';a''j'') \tag{2.47a}$$

$$\hat{w}^{J\dagger}_M(a'j';a''j'') = (-1)^{j''-j'+M} \hat{w}^J_{-M}(a''j'';a'j') \tag{2.47b}$$

and in addition to (2.46ab), the relationships

$$\hat{\tau}_{m''m'}(a''j'';a'j') = \sum_{J=|j''-j'|}^{j''+j'} \sum_{M=-J}^{J} [J]^{1/2} \tag{2.48a}$$

$$(-1)^{j'-m'} \begin{pmatrix} j'' & j' & J \\ m'' & -m' & M \end{pmatrix} \hat{w}^{J\dagger}_M(a'j';a''j'')$$

$$\hat{w}^J_M(a'j';a''j'') = \sum_{m''=-j''}^{j''} \sum_{m'=-j'}^{j'} [J]^{1/2} \tag{2.48b}$$

$$(-1)^{j'-m'} \begin{pmatrix} j'' & j' & J \\ m'' & -m' & M \end{pmatrix} \hat{\tau}^\dagger_{m''m'}(a''j'';a'j')$$

are also useful. Comparing with (2.43), $(2J+1)^{1/2}$ is the reduced matrix element $\langle a'j' \| \hat{w}^J_M(a'j';a''j'') \| a''j'' \rangle$ as (2.48b) and the symmetry of the 3-j[29,30] symbols gives:

$$\langle \phi_{a'j'm'} | \hat{w}^J_M(a'j';a''j'') | \phi_{a''j''m''} \rangle = [J]^{1/2} (-1)^{j'-m'} \begin{pmatrix} j' & J & j'' \\ -m' & M & m'' \end{pmatrix} \tag{2.49}$$

The matrix element on the left-hand-side of (2.43) can now be expressed as trace involving t^k_q and the unit tensor operator $\hat{w}^J_M$. Combining equations (2.49a), and (2.46a), and exploiting the symmetry of the 3-j symbols:

$$\langle \phi_{a'j'm'} | t^k_q | \phi_{a''j''m''} \rangle = \sum_{J,M} [J]^{1/2} \qquad (2.50)$$

$$(-1)^{j'-m'} \begin{pmatrix} j' & J & j'' \\ -m' & M & m'' \end{pmatrix} \mathrm{tr}\left[t^k_q \, \hat{w}^{J\dagger}_M(a'j';a''j'') \right]$$

The trace is invariant with respect to identical rotations of both operators. The only non-vanishing contributions to (2.50) take the form (applying (2.44) for the special case of $j_3=0$):

$$\mathrm{tr}\left[t^k_q \hat{w}^{J\dagger}_M(a'j';a''j'') \right] = \delta_{J,k}\delta_{M,q} \sum_{q'=-k}^{k} \frac{\mathrm{tr}\left[t^k_{q'} \hat{w}^{k\dagger}_{q'}(a'j';a''j'') \right]}{(2k+1)} \qquad (2.51)$$

Equation (2.43) is established provided the reduced matrix element $\langle a'j' \| t^k \| a''j'' \rangle$ is identified as:

$$\langle a'j' \| t^k \| a''j'' \rangle = [k]^{1/2} \sum_{q'=-k}^{k} \frac{\mathrm{tr}\left[t^k_{q'} \hat{w}^{k\dagger}_{q'}(a'j';a''j'') \right]}{(2k+1)} \qquad (2.52)$$

The spherical unit tensor $\hat{w}^J_M$ is easily generalized to non-relativistic central field electrons with $SU(2)\times O^+(3)$ symmetry. The 1-electron transition operator $\hat{\tau}_{\mu'm'\mu''m''}(n'\ell';n''\ell'')$, obtained from a pair of N-electron central field determinant wavefunctions can be expanded in families of operators $\hat{w}^{\lambda k}_{\pi q}(n'\ell';n''\ell'')$:

$$\hat{\tau}_{\mu''m''\mu'm'}(n''\ell'';n'\ell') = |\phi_{n'\ell'm'\mu'}\rangle\langle\phi_{n''\ell''m''\mu''}| \qquad (2.53a)$$

$$\hat{\tau}_{\mu''m''\mu'm'}(n''\ell'';n'\ell') = \sum_{\lambda=0}^{1} \sum_{\pi=-\lambda}^{\lambda} \sum_{k=|\ell''-\ell'|}^{\ell''+\ell'} \sum_{q=-k}^{k} [\lambda,k]^{1/2} \tag{2.53b}$$

$$(-1)^{1/2-\mu'} \begin{pmatrix} 1/2 & \lambda & 1/2 \\ -\mu' & \pi & \mu'' \end{pmatrix} (-1)^{\ell'-m'} \begin{pmatrix} \ell' & k & \ell'' \\ -m' & q & m'' \end{pmatrix} \hat{w}^{\lambda k\dagger}_{\pi q}(n'\ell';n''\ell'')$$

The matrix elements of a 1-electron operator $t^{\lambda k}_{\pi q}$ become:

$$\langle \phi_{n'\ell'\mu'} | t^{\lambda k}_{\pi q} | \phi_{n''\ell''m''\mu''} \rangle = (-1)^{1/2-\mu'} \begin{pmatrix} 1/2 & \lambda & 1/2 \\ -\mu' & \pi & \mu'' \end{pmatrix} \tag{2.54a}$$

$$(-1)^{\ell'-m'} \begin{pmatrix} \ell' & k & \ell'' \\ -m' & q & m'' \end{pmatrix} \langle n'\ell' \| t^{\lambda k} \| n''\ell'' \rangle$$

$$\langle n'\ell' \| t^{\lambda k} \| n''\ell'' \rangle = [\lambda,k]^{1/2} \sum_{\pi=-\lambda}^{\lambda} \sum_{q=-k}^{k} \frac{\mathrm{tr}\left[t^{\lambda k}_{\pi q} \hat{w}^{\lambda k\dagger}_{\pi q}(n'\ell';n''\ell'') \right]}{(2\lambda+1)(2k+1)} \tag{2.54b}$$

The actions of the operators $\hat{w}^{\lambda k}_{\pi q}(n'\ell';n''\ell'')$ on the electronic coordinates can be factored into spin and space parts via

$$\hat{w}^{\lambda k}_{\pi q}(n'\ell';n''\ell'') = \hat{u}^{k}_{q}(n'\ell';n''\ell'')\hat{v}^{\lambda}_{\pi} \tag{2.55}$$

where $\hat{u}^{k}_{q}(n'\ell';n''\ell'')$ is an integral operator with the kernel $u_{kq}(n'\ell',n''\ell''|\ \vec{r};\vec{r}\,')$ and $\hat{v}^{\lambda}_{\pi}$ can be represented as a matrix $v_{\lambda\pi}(\sigma;\sigma')$:

$$u_{kq}(n'\ell',n''\ell''|\ \vec{r};\vec{r}\,') = \frac{\rho_{n''\ell''n'\ell'}(r;r')}{rr'} \Omega^{\ell'\ell''}_{kq}(\theta,\phi;\theta',\phi') \tag{2.56a}$$

$$\rho_{n'\ell'n''\ell''}(r;r') = rR_{n'\ell'}(r)r'R_{n''\ell''}(r') \tag{2.56b}$$

$$\Omega_{kq}^{\ell'\ell''}(\theta,\phi;\theta',\phi') = \sum_{m'=-\ell'}^{\ell'} \sum_{m''=-\ell''}^{\ell''} (-1)^{\ell'-\ell''-q} [k]^{1/2} \tag{2.56c}$$

$$\begin{pmatrix} \ell' & \ell'' & k \\ m' & m'' & -q \end{pmatrix} Y_{\ell' m'}(\theta,\phi) \; (-1)^{\ell''+m''} Y^*_{\ell''-m''}(\theta',\phi')$$

$$\Omega_{00}^{\ell\ell}(\theta,\phi;\theta',\phi') = \frac{(2\ell+1)}{4\pi} P_\ell(\hat{e}\cdot\hat{e}') \tag{2.56d}$$

$$\hat{e}\cdot\hat{e}' = \sin(\theta)\sin(\theta')\cos(\phi-\phi') + \cos(\theta)\cos(\theta') \tag{2.56e}$$

where $P_\ell(\hat{e}\cdot\hat{e}')$ is a Legendre polynomial and

$$v_{\kappa\pi}(\sigma;\sigma') = \sum_{\mu'=-1/2}^{+1/2} \sum_{\mu''=-1/2}^{+1/2} (-1)^{\pi} \begin{pmatrix} 1/2 & 1/2 & \kappa \\ \mu' & \mu'' & -\pi \end{pmatrix} \tag{2.57a}$$

$$X_{\mu'}(\sigma) X^*_{-\mu''}(\sigma') (-1)^{1/2+\mu''}$$

$$\hat{v}_0^0 = \frac{1}{\sqrt{2}} I = \frac{1}{\sqrt{2}} \begin{pmatrix} 1 & 0 \\ 0 & 1 \end{pmatrix} \tag{2.57b}$$

$$\hat{v}_1^1 = \sqrt{2}\, S_2 = \begin{pmatrix} 0 & -1 \\ 0 & 0 \end{pmatrix} \tag{2.57c}$$

$$\hat{v}_0^1 = \sqrt{2}\, S_0 = \begin{pmatrix} 1 & 0 \\ 0 & -1 \end{pmatrix} \tag{2.57d}$$

$$\hat{v}_{-1}^1 = \sqrt{2}\, S_{-1} = \begin{pmatrix} 0 & 0 \\ 1 & 0 \end{pmatrix} \tag{2.57e}$$

S_q is a spherical tensor component of the spin angular momentum operator $\vec{S}$. The identification of the $\hat{v}_\pi^\kappa$ operators with the identity and spin angular momentum operators for a single electron reveals that

the operators $\hat{\tau}_{m''\mu''\mu'm'}(n''\ell'';n'\ell')$ and $\hat{w}^{\langle k}_{mq}(n''\ell'';n'\ell')$ have inversion symmetry given by $(-1)^{\ell''+\ell'}$.

n-Electron Spherical Tensor operators

Equation (2.43) is easily generalized to n-electron operators. A matrix element of a tensor operator $t^{J_1\cdots J_n}_{M_1\cdots M_n}$ is expressable in terms of a trace with 1-electron operators $\hat{\tau}_{m''m'}(n'\ell';n''\ell'')$:

$$\left\langle \phi_{a'_1 j'_1 m'_1}\cdots\phi_{a'_n j'_n m'_n} \middle| t^{J_1\cdots J_n}_{M_1\cdots M_n} \middle| \phi_{a''_1 j''_1 m''_1}\cdots\phi_{a''_n j''_n m''_n}\right\rangle =$$

$$\underset{\sim}{\mathrm{tr}}\left[\hat{\tau}^{n\dagger}_{(m')(m'')}(\{a'j'\};\{a''j''\})\, t^{J_1\cdots J_n}_{M_1\cdots M_n}\right] \tag{2.58a}$$

$$= \langle\{a'j'\}\|t^{\{J\}}\|\{a''j''\}\rangle \prod_{i=1}^{n}(-1)^{j'_i-m'_i}\begin{pmatrix} j'_i & J_i & j''_i \\ -m'_i & M_i & m''_i\end{pmatrix}[J_i]^{1/2}$$

$$\langle\{a'j'\}\|t^{\{J\}}\|\{a''j''\}\rangle = [J_1,\ldots,J_n]^{1/2}\sum_{M_1=-J_1}^{J_1}\cdots\sum_{M_n=-J_n}^{J_n} \frac{\underset{\sim}{\mathrm{tr}}\left[\hat{w}^{J_1\cdots J_n\dagger}_{M_1\cdots M_n}(\{a'j'\};\{a''j''\})\, t^{J_1\cdots J_n}_{M_1\cdots M_n}\right]}{[J_1,\ldots,J_n]} \tag{2.58b}$$

$$\hat{\tau}^{n\dagger}_{(m')(m'')}(\{a'j'\};\{a''j''\}) = \prod_{i=1}^{n}\hat{\tau}_{m''_i m'_i}(a''_i j''_i;a'_i j'_i) \tag{2.58c}$$

$$\hat{w}^{J_1\cdots J_n\dagger}_{M_1\cdots M_n}(\{a'j'\};\{a''j''\}) = \prod_{i=1}^{n}\hat{w}^{J_i\dagger}_{M_i}(a'_i j'_i;a''_i j''_i) \tag{2.58d}$$

Matrix elements of n-electron tensor operators $t^{\{\lambda q\}}_{(\pi q)}$ between products of 1-electron central field wavefunctions can be expressed similarly:

$$\left\langle \phi_{n'_1 \ell'_1 \mu'_1} \cdots \phi_{n'_p \ell'_p m'_p \mu'_p} \left| t^{\lambda_1 k_1 \cdots \lambda_p k_p}_{\pi_1 q_1 \cdots \pi_p q_p} \right| \phi_{n''_1 \ell''_1 m''_1 \mu''_1} \cdots \phi_{n''_p \ell''_p m''_p \mu''_p} \right\rangle = \tag{2.59a}$$

$$\langle \{n' \ell'\} \| t^{\{\lambda k\}} \| \{n'' \ell''\} \rangle \prod_{i=1}^{p} (-1)^{\ell'_i - m'_i + 1/2 - \mu'_i} \begin{pmatrix} 1/2 & \lambda & 1/2 \\ -\mu'_i & \pi & \mu''_i \end{pmatrix} \begin{pmatrix} \ell'_i & k & \ell''_i \\ -m'_i & q & m''_i \end{pmatrix}$$

$$\langle \{n' \ell'\} \| t^{\{\lambda k\}} \| \{n'' \ell''\} \rangle = \tag{2.59b}$$

$$\sum_{\pi_1 q_1} \cdots \sum_{\pi_p q_p} \mathrm{tr} \left[t^{\{\lambda k\}}_{\{\pi q\}} \prod_{i=1}^{p} \frac{\hat{w}^{\lambda_i k_i \dagger}_{\pi_i q_i} (n'_i \ell'_i ; n''_i \ell''_i)}{\sqrt{(2k_i+1)(2\lambda_i+1)}} \right]$$

If the operator $t^{\{\lambda k\}}_{(\pi q)}$ posesses a definite inversion symmetry with respect to the i^{th} electron's coordinates, it must be $(-1)^{\ell''_i + \ell'_i}$ or the matrix element vanishes.

2.2.5 Unit Tensors, Effective Operators, and Tensor Algebra

The application of the Wigner-Eckart theorem to the matrix elements of a family of operators $\{t^{\{\lambda k\}}_{(\pi q)}\}$ as in (2.59ab) demonstrates that the matrix elements of any equivalent family of operators $\{t'^{\{\lambda k\}}_{(\pi q)}\}$ (one that carries the same irreducible representation of $[O^+(3) \times O^+(3)]^n$) are simply related by the ratios of the reduced matrix elements. This suggests that the matrix elements of n-body spherical tensor operators between atomic wavefunctions can be reduced to calculating matrix elements for certain "unit" tensor families of operators and reduced matrix elements as needed. Equivalently, on a given manifold spanned by products of 1-

electron central field wavefunctions, the n-body spherical tensor operators can be replaced by effective operators—sums over unit tensors multiplied by parameterized reduced matrix elements.

Integral Operator Expansions

For the purpose of calculating matrix elements of n-electron operators on the subspace X, the linear span of all N-electron determinant wavefunctions constructed from a set $S = \{\phi_\alpha(x) \mid \alpha=1,\ldots,d\}$ of orthonormal 1-electron wavfunctions, the n-electron operators can be expanded in terms of 1-electron integral operators $\{\hat{\tau}_{\alpha\beta} \mid \alpha,\beta=1,\ldots,d\}$:

$$Q_n = \sum_{\alpha_1\ldots\alpha_n=1}^{d} \sum_{\beta_1\ldots\beta_n=1}^{d} m(q_n)_{ab} \sum_{1=i_1<\ldots<i_n}^{N} \hat{\tau}^n_{ab}(i_1,\ldots,i_n) \quad (2.60a)$$

$$m(q_n)_{ab} = \langle\phi_{\alpha_1}\ldots\phi_{\alpha_n}|q_n|\phi_{\beta_1}\ldots\phi_{\beta_n}\rangle \quad (2.60b)$$

$$\hat{\tau}^n_{ab}(1,\ldots,n) = \hat{\tau}_{\alpha_1\beta_1}(1)\ldots\hat{\tau}_{\alpha_n\beta_n}(n) \quad (2.60c)$$

$\hat{\tau}_{\alpha\beta}(i)$ is the integral operator with the kernel

$$\tau_{\alpha\beta}(x_i;x_i') = \phi_\alpha(x_i)\phi^*_\beta(x_i') \quad (2.60d)$$

i.e.

$$\left[\hat{\tau}^n_{ab}(1,\ldots,n)\Psi^N\right](x_1,\ldots,x_N) = \phi_{\alpha_1}(x_1)\ldots\phi_{\alpha_n}(x_n) \quad (2.60e)$$
$$\int dx_1'\ldots dx_n'\phi^*_{\beta_1}(x_1')\ldots\phi^*_{\beta_n}(x_n')\Psi^N(x_1',\ldots,x_n',x_{n+1},\ldots,x_N)$$

On the linear span of all possible product wavefunctions constructed from S, the operators $\hat{\tau}^n_{ab}$ are an orthonormal basis for all n-body operators that map this linear span into itself. The scalar

product is the trace over all n-particle product wavefunctions constructed from S,

$$\underset{\sim}{\mathrm{tr}}\left[\hat{\tau}^{n\dagger}_{a'b'}\hat{\tau}^{n}_{ab}\right] = \delta_{\alpha'_1\alpha_1}\delta_{\beta'_1\beta_1}\cdots\delta_{\alpha'_n\alpha_n}\delta_{\beta'_n\beta_n} \equiv \delta_{ab} \tag{2.61}$$

and an operator q_n becomes:

$$q_n = \sum_{\alpha_1\cdots\alpha_n}^{d}\sum_{\beta_1\cdots\beta_n}^{d} \underset{\sim}{\mathrm{tr}}\left[\hat{\tau}^{n\dagger}_{ab}q_n\right]\hat{\tau}^{n}_{ab} \tag{2.62}$$

On an N-particle space however, the n-body operators for n<N are linear combinations of the N-particle operators. For example

$$\hat{\tau}^{n}_{ab}(1,\ldots,n) = \hat{\tau}^{n}_{ab}(1,\ldots,n)\hat{I}^{N-n}(n+1,\ldots,N) \tag{2.63}$$

$$= \sum_{1=\gamma_{n+1}\cdots\gamma_N}^{d} \hat{\tau}^{N}_{\{a,\gamma_{n+1},\ldots,\gamma_N\}\{b,\gamma_{n+1},\ldots,\gamma_N\}}$$

where

$$\hat{I}^{N-n}(n+1,\ldots,N) = \hat{I}(n+1)\ldots\hat{I}(N) \tag{2.64a}$$

and the 1-particle identity operator $\hat{I}(i)$ is an integral operator with the kernel:

$$I(x_i;x'_i) = \sum_{\alpha=1}^{d} \tau_{\alpha\alpha}(x_i;x'_i) \equiv \delta_S(x_i-x'_i) \tag{2.64b}$$

The n-body operators of interest are invariant with respect to permutations of the particle coordinates. A symmetric n-body operator Q_n acting on the N-particle subspace can be expressed in terms of the symmetric n-body operators E^n_{ab}:

$$Q_n = \frac{1}{n!}\sum_{\alpha_1\cdots\alpha_n=1}^{d}\sum_{\beta_1\cdots\beta_n=1}^{d} m(q_n)_{ab}\,E^{n}_{ab} \tag{2.65a}$$

$$E^n_{ab} = \sum_{1=i_1<\ldots<i_n}^{N} \hat{e}^n_{ab}(i_1,\ldots,i_n) \tag{2.65b}$$

$$\hat{e}^n_{ab}(i_1,\ldots,i_n) = \sum_{s\in S_n} \hat{\tau}^n_{ab}(i_{s(1)},\ldots,i_{s(n)}) \tag{2.65c}$$

The factor $\frac{1}{n!}$ compensates for overcounting, and the sum over $s\in S_n$ indicates the symmetrization with respect to to all permutations of the arguments.

The operators E^n_{ab}, even for n=N, are not linearly independent. To examine some of their properties, first notice that the 1-electron operators $E_{\alpha\beta} \equiv E^1_{ab}$, a = {α} and b = {β}, have the commutation relations

$$[E_{\alpha\beta}, E_{\alpha'\beta'}] = \delta_{\beta\alpha'}E_{\alpha\beta'} - \delta_{\beta'\alpha}E_{\alpha'\beta} \tag{2.66}$$

The $E_{\alpha\beta}$'s are therefore a representation of the Lie algebra of the unitary group U(d) corresponding to unitary transformations of the set S. The number operator $\hat{N}$ defined by

$$\hat{N} = \sum_{i=1}^{N} \hat{I}(i) = \sum_{\alpha=1}^{d} E_{\alpha\alpha} \tag{2.67}$$

is a scalar invariant with respect to unitary transformations of the set S and commutes with all the $E_{\alpha\beta}$'s.

The operators E^n_{ab} are expressable as polynomials in the $E_{\alpha\beta}$'s. This can be seen from the recursive relationship

$$E^n_{\{a,\alpha_n\}\{b,\beta_n\}} = E^{n-1}_{ab}E_{\alpha_n\beta_n} - \sum_{i=1}^{n-1} \delta_{\alpha_n\beta_i} E^{n-1}_{a\{b-\beta_i+\beta_n\}} \tag{2.68}$$

where $\{b-\beta_i+\beta_n\}$ indicates the subset of S obtained by replacing β_i with β_n in the set b. For example, when n=2:

$$E^2_{\{\alpha_1\alpha_2\}\{\beta_1\beta_2\}} = E_{\alpha_1\beta_1}E_{\alpha_2\beta_2} - \delta_{\alpha_2\beta_1}E_{\alpha_1\beta_2} \tag{2.69}$$

Equation (2.68) also implies the contraction property

$$\sum_{\alpha=1}^{d} E^n_{\{a,\alpha\}\{b,\alpha\}} = (N-n+1)E^{n-1}_{ab} \tag{2.70}$$

Restricted Operators

The properties exhibited in equations (2.66) through (2.70) are independent of the permutation symmetry of the space acted on by the n-body operators. Additional properties result from the specialization to the antisymmetric case, as an n-electron operator has non-vanishing matrix elements only between determinant wavefunctions that differ by n or less 1-electron wavefunctions. To be explicit, if $a(\subseteq A(\subseteq S$, $b(\subseteq B(\subseteq S$, and $\{b-a\cap b\}\cap A = \emptyset$, then apart from a factor ± 1, E^n_{ab} transforms Φ^N_A into Φ^N_B. A permutation applied to either of the sets a or b of an operator E^n_{ab} is equivalent to a permutation applied to Φ^N_A or Φ^N_B respectively.

The n-electron operators restricted to a subspace spanned by all determinant wavefunctions constructed from the set S can be expressed in the form (a "~" is used here to indicate that and operator has been restricted to a subspace of antisymmetrized N-electron wavefunctions):

$$\tilde{Q}_n = \frac{1}{n!} \sum_{1=\alpha_1\ldots\alpha_n}^{d} \sum_{1=\beta_1\ldots\beta_n}^{d} m(q_n)_{ab}\ \tilde{E}^n_{ab} \tag{2.71a}$$

$$= \sum_{1=\alpha_1<\ldots<\alpha_n}^{d} \sum_{1=\beta_1<\ldots<\beta_n}^{d} \tilde{m}(q_n)_{ab}\ \tilde{E}^n_{ab} \tag{2.71b}$$

$$\tilde{m}(q_n)_{ab} = \left\langle \Phi_a^n \middle| q_n \middle| \Phi_b^n \right\rangle = \mathrm{tr}\left[\Gamma_{ab}^{n\dagger} q_n\right] \tag{2.71c}$$

This representation of the n-electron operator Q_n is the projection of Q_n onto a space of operators that map the subspace X into itself. However, if a density matrix description of the basis vectors is used, the representation of q_n in the form of (2.71) is implicit in the calculation of matrix elements. In addition to the commutation relations (2.66) the restricted 1-electron operators, $\{\tilde{E}_{\alpha\beta} \mid \alpha,\beta=1,\ldots,d\}$, also satisfy

$$\tilde{E}_{\alpha\beta}\tilde{E}_{\alpha'\beta'} = -\tilde{E}_{\alpha\beta'}\tilde{E}_{\alpha'\beta} + \delta_{\alpha'\beta}\tilde{E}_{\alpha\beta'} + \delta_{\alpha\beta'}\tilde{E}_{\alpha'\beta} \tag{2.72}$$

reflecting the projection of the generators onto the antisymmetric subspace carrying the representation of the Lie algebra.

Configurations

In general, atomic wavefunctions are not all possible determinants constructed from a single set S, but are grouped into configurations. A configuration $\underline{Q} = \{w_1, w_2, \ldots, w_p\}$ consists of all determinant wavefuntions constructed by selecting w_i elements ($w_i > 0$) from each of the sets $S_i = \{\phi_{i\alpha} \mid \alpha=1,\ldots,d_i\}$ of orthonormal 1-electron wavefunctions where ($i=1,2,\ldots,p$) and ($w_1+\ldots+w_p = N$). The operators $\tilde{E}_{ab}^n$ factor into components corresponding to each set S_i, and the operator expansion (2.71) is revised to include all partitions of n consistent with $\underline{Q}$:

$$\tilde{Q}_n = \sum_{0\le\nu_i\le w_i}^{\nu_1+\ldots+\nu_p=n} \sum_{1=\alpha_{1,1}<\ldots<\alpha_{n,1}}^{d} \sum_{1=\beta_{1,1}<\ldots<\beta_{n,1}}^{d} \ldots \tag{2.73}$$

$$\sum_{1=\alpha_{1,p}<\ldots<\alpha_{n,p}}^{d} \sum_{1=\beta_{1,p}<\ldots<\beta_{n,p}}^{d} \tilde{m}(q^n)_{ab} \left[\prod_{i=1}^{p} \tilde{E}_{a_i b_i}^{\nu_i} \right]$$

Restricted to a single configuration, the number operators $\tilde{N}_i$ replace $\tilde{N}$ where each $\tilde{N}_i$ has the eigenvalue w_i. Inter-configuration operators do not factor in the form of (2.73), and must be treated as special cases.

Unit Tensor Expansions

The integral operator expansions are easily adapted to spherical tensor operators. An operator $o_n^{\{J\}}$, constructed from a family of operators that carries the irreducible representation $D^{J_1} \otimes D^{J_2} \otimes \ldots D^{J_n}$ of $[SU(2)]^n$, where

$$o_n^{\{J\}} = \sum_{M_1=-J_1}^{J_1} \ldots \sum_{M_n=-J_n}^{J_n} c_{M_1\ldots M_n}^{J_1\ldots J_n} t_{M_1\ldots M_n}^{J_1\ldots J_n} \tag{2.74a}$$

has a spherical unit tensor expansion

$$o_n^{\{J\}} = [J_1,\ldots,J_n]^{-1/2} \sum_{\{a'j'\}}^{S} \sum_{\{a''j''\}}^{S} \langle \{a'j'\} \| t^{\{J\}} \| \{a''j''\} \rangle \tag{2.74b}$$

$$\sum_{M_1=-J_1}^{J_1} \ldots \sum_{M_n=-J_n}^{J_n} c_{M_1\ldots M_n}^{J_1\ldots J_n} \hat{w}_{M_1\ldots M_n}^{J_1\ldots J_n}(\{a'j'\};\{a''j''\})$$

where the sums $\sum_{\{a'j'\}}^{S} \sum_{\{a''j''\}}^{S}$ are over sets of 1-electron wavefunctions $S_{a'} = \{\phi_{a'j'm'} \mid m' = -j', \ldots, j'\}$ etc. needed to span the subspace X. Note that $o_n^{\{J\}}$ is not necessarily invariant under permutations of the

electronic coordinates.

If $o_n^{\{J\}}$ has rotational or point group symmetry, the sum over the operators $\hat{w}_{(M)}^{\{J\}}$ takes the form

$$\sum_{M_1=-J_1}^{J_1} \cdots \sum_{M_n=-J_n}^{J_n} c_{(M)}^{\{J\}} \hat{w}_{(M)}^{\{J\}}(\{a'j'\};\{a''j''\}) = \sum_{\bar{M}=-\bar{J}}^{\bar{J}} B_{\bar{M}}^{\bar{J}} \sum_{(m') \subset \{j'\}} \tag{2.75}$$

$$\sum_{(m'') \subset \{j''\}} \langle C(\theta)\{j';j''\}\bar{J}\bar{M}|\{j'\}(m')\{j''\}(m'')\rangle \hat{\tau}^n_{(m')(m'')}(\{a'j'\};\{a''j''\})$$

where $\hat{\tau}^n_{(m')(m'')}(\{a'j'\};\{a''j''\})$ is the n-electron analog of (2.45a):

$$\hat{\tau}^n_{(m')(m'')}(\{a'j'\};\{a''j''\}) = \prod_{i=1}^{n} \hat{\tau}_{m'_i-m''_i}(a'_i j'_i;a''_i j''_i)(-1)^{j''_i+m''_i} \tag{2.76}$$

and $\bar{J} = 0$ in case of rotational symmetry. The coefficients $\langle C(\theta)\{j';j''\}\bar{J}\bar{M}|\{j'\}(m')\{j''\}(m'')\rangle$ are the matrix elements of a unitary transformation C that reduces the representation $D^{\{j';j''\}} = D^{j'_1} \otimes D^{j''_1} \otimes \cdots \otimes D^{j'_n} \otimes D^{j''_n}$ of $[SU(2)]^{2n}$ carried by the $\hat{\tau}^n_{(m')(m'')}(\{a'j'\};\{a''j''\})$ operators to block diagonal form with blocks of irreducible representations $D^{\bar{J}}$. The transformation C will generally require a parameter or parameters θ to distinguish between multiple occurrences of an irreducible representations $D^{\bar{J}}$ in the reduction of $D^{\{j';j''\}}$.

If n>1, there can be several possible reductions of the representation $D^{\{j';j''\}}$ of $[SU(2)]^{2n}$ into irreducible representations $D^{\bar{J}}$. As a result there are several possibilities for the decomposition of the n-electron operators $\hat{\tau}^n_{(m')(m'')}(\{a'j'\};\{a''j''\})$ into irreducible operator representations of SU(2). For example the two decompositions:

$$\hat{\tau}^{n}_{(m')(m'')}(\{a'j'\};\{a''j''\}) \quad = \tag{2.77a}$$

$$\sum_{\bar{J},\bar{M}}^{C} \sum_{\theta}^{C} \langle C(\theta)\{j';j''\}\bar{J}\bar{M}|\{j'\}(m')\{j''\}(m'')\rangle \hat{w}^{C(\theta)\bar{J}}_{\bar{M}}(\{a'j'\};\{a''j''\})$$

$$\hat{\tau}^{n}_{(m')(m'')}(\{a'j'\};\{a''j''\}) \quad = \tag{2.77b}$$

$$\sum_{\bar{J},\bar{M}}^{C'} \sum_{\theta'}^{C'} \langle C'(\theta')\{j';j''\}\bar{J}\bar{M}|\{j'\}(m')\{j''\}(m'')\rangle \hat{w}^{C'(\theta')\bar{J}}_{\bar{M}}(\{a'j'\};\{a''j''\})$$

where C and C′ are two possible unitary transformations or coupling schemes that accomplish the reduction of $D^{\{j';j''\}}$. The two schemes are related by the recoupling unitary transformation:

$$\hat{w}^{C'(\theta')\bar{J}}_{\bar{M}}(\{a'j'\};\{a''j''\}) \quad = \tag{2.78}$$

$$\sum_{\theta}^{C} \langle C(\theta)\{j';j''\}\bar{J}|C'(\theta')\{j';j''\}\bar{J}\rangle \; \hat{w}^{C(\theta)\bar{J}}_{\bar{M}}(\{a'j'\};\{a''j''\})$$

Relationships of this type simplify expressions for the n-electron operators (2.71ab) given in spherical tensor form.

1-Electron Effective Operators

Consider first the effective 1-electron spherical tensor operators. A general 1-electron tensor operator $q^{\{0<k\}}_{1}$ can be expanded:

$$q_1^{\{\lambda k\}} = \sum_{n'\ell'}^{S} \sum_{n''\ell''}^{S} [\lambda,k]^{-1/2} \langle n'\ell' \| t^{\lambda k} \| n''\ell'' \rangle \qquad (2.79a)$$

$$\sum_{\pi=-\lambda}^{\lambda} \sum_{q=-k}^{k} c_{\pi q}^{\lambda k} \hat{W}_{\pi q}^{\lambda k}(n'\ell';n''\ell'')$$

(2.79a) is the spherical tensor analog of (2.62). The spherical tensor analog of (2.65a) is

$$Q_1^{\{\lambda k\}} = \sum_{n'\ell'}^{S} \sum_{n''\ell''}^{S} [\lambda,k]^{-1/2} \langle n'\ell' \| t^{\lambda k} \| n''\ell'' \rangle \qquad (2.79b)$$

$$\sum_{\pi=-\lambda}^{\lambda} \sum_{q=-k}^{k} c_{\pi q}^{\lambda k} W_{\pi q}^{\lambda k}(n'\ell';n''\ell'')$$

$W_{\pi q}^{\lambda k}$ corresponds to $\hat{W}_{\pi q}^{\lambda k}$ in (2.53b) if $\hat{t}_{\mu''m''\mu'm'}$ is replaced with with $E_{\mu''m''\mu'm'}$.

Examples of operators $Q_1^{\{\lambda k\}}$ are the angular momentum operators $\vec{L} = \sum_{i=1}^{N} \vec{\ell}_i$ and $\vec{S} = \sum_{i=1}^{N} \vec{s}_i$:

$$(\vec{L})_q = \sum_{n\ell}^{\Omega} L(n\ell)_q = \sum_{n\ell}^{\Omega} \langle \ell \| \vec{\ell} \| \ell \rangle \frac{U_q^1(n\ell)}{\sqrt{6}} \qquad (2.80a)$$

$$\langle \ell \| \vec{\ell} \| \ell \rangle = \sqrt{(2\ell+1)\ell(\ell+1)} \qquad (2.80b)$$

$$(\vec{S})_q = \sum_{n\ell}^{\Omega} S(n\ell)_q = \sum_{n\ell}^{\Omega} \langle 1/2 \| \vec{s} \| 1/2 \rangle \frac{V_\pi^1(n\ell)}{\sqrt{3(2\ell+1)}} \qquad (2.81a)$$

$$\langle 1/2 \| \vec{s} \| 1/2 \rangle = \sqrt{3/2} \qquad (2.81b)$$

where $V_\pi^\lambda(n\ell)U_q^k(n\ell) \equiv W_{\pi q}^{\lambda k}(n\ell) \equiv W_{\pi q}^{\lambda k}(n\ell;n\ell)$, and $\vec{L}$ and $\vec{S}$ are given in spherical tensor components.

The operators $\{W^{\lambda k}_{\mu q}(n\ell) \mid \mu=-\lambda,\ldots,\lambda;\ q=-k,\ldots,k\}$, for a given subshell $(n\ell)$, are equivalent to Racah's unit tensors[8]. If $\ell>0$, two rotationally invariant operators can be constructed from this set. The first, $W^{00}_{00}(n\ell;n\ell)$ is invariant with respect to $O^+(3)\times O^+(3)$, and is related to the number operator $\hat{N}(n\ell)$:

$$\hat{N}(n\ell) = \sqrt{(4\ell+2)}\ W^{00}_{00}(n\ell) \tag{2.82}$$

The other operator is invariant under $O^+(3) \subset O^+(3)\times O^+(3)$:

$$W^{(11)0}(n\ell) = \sum_{q=-1}^{1} (-1)^q\ 3^{-1/2}\ W^{11}_{-qq}(n\ell) \tag{2.83}$$

$W^{(11)0}(n\ell)$ is used to construct the effective spin-orbit operator for a given configuration $\underline{Q}$:

$$\sum_{i=1}^{N} \xi(r_i)\vec{\ell}_i\cdot\vec{s}_i \rightarrow \sum_{n\ell}^{Q} \zeta_{n\ell}\ \frac{1}{3}\ \langle\ell\|\vec{\ell}\|\ell\rangle\langle 1/2\|\vec{s}\|\ 1/2\rangle\ \tilde{W}^{(11)0}(n\ell) \tag{2.84}$$

$$\zeta_{n\ell} = \int_0^\infty dr\ r^2 R^2_{n1}(r)\xi(r) \tag{2.85}$$

2-Electron Spherical Tensor Operators

Consider now a general 2-electron spherical tensor operator:

$$\left\{\lambda_1 k_1 \lambda_2 k_2\right\}_{q_2} = \sum_{\mu=-\bar{\lambda}}^{\bar{\lambda}} \sum_{q=-\bar{k}}^{\bar{k}} B^{\bar{\lambda}\bar{k}}_{\mu q} \tag{2.86a}$$

$$\frac{1}{2}\left\{ t_{\mu q}(\lambda_1 k_1 \lambda_2 k_2)\bar{\lambda}\bar{k} + (-1)^{\lambda_1+\lambda_2-\bar{\lambda}+k_1+k_2-\bar{k}}\ u_{\mu q}(\lambda_2 k_2 \lambda_1 k_1)\bar{\lambda}\bar{k} \right\}$$

where

$$t^{(\kappa_1 k_1 \kappa_2 k_2)\overline{\kappa k}}_{\pi q} = \sum_{\pi_1=-\kappa_1}^{\kappa_1} \sum_{\pi_2=-\kappa_2}^{\kappa_2} \sum_{q_1=-k_1}^{k_1} \sum_{q_1=-k_1}^{k_1} [\kappa_1,k_1,\kappa_2,k_2]^{1/2}$$

$$(-1)^{\kappa_1-\kappa_2+\pi} (-1)^{k_1-k_2+q} \begin{pmatrix} \kappa_1 & \kappa_2 & \overline{\kappa} \\ \pi_1 & \pi_2 & -\pi \end{pmatrix} \begin{pmatrix} k_1 & k_2 & \overline{k} \\ q_1 & q_2 & -q \end{pmatrix} t^{\kappa_1 k_1 \kappa_2 k_2}_{\pi_1 q_1 \pi_2 q_2} \qquad (2.86b)$$

$q_2^{\{\kappa_1 k_1 \kappa_2 k_2\}}$ is symmetric with respect to interchanges of the electron coordinates as long as

$$u^{\kappa_2 k_2 \kappa_1 k_1}_{\pi_2 q_2 \pi_1 q_1}(1,2) \equiv t^{\kappa_1 k_1 \kappa_2 k_2}_{\pi_1 q_1 \pi_2 q_2}(2,1) \qquad (2.86c)$$

Adapting (2.74ab) to non-relativistic, central-field 1-electron wavefunctions, and for convenience, ordering the sums over sets $S_{n\ell}$ etc. of 1-electron wavefunctions leads to the equation (2.87). The coupled 2-electron spherical tensor operators $\hat{w}^{(\kappa_1 k_1 \kappa_2 k_2)\overline{\kappa k}}_{\pi q}$ are obtained by substituting $\hat{w}^{\kappa_1 k_1 \kappa_2 k_2}_{\pi_1 q_1 \pi_2 q_2}$ for $t^{\kappa_1 k_1 \kappa_2 k_2}_{\pi_1 q_1 \pi_2 q_2}$ in equation (2.86b).

An expression for the effective operator $\tilde{Q}_2^{\{\kappa_1 k_1 \kappa_2 k_2\}}$ generated from $q_2^{\{\kappa_1 k_1 \kappa_2 k_2\}}$ is obtained by recoupling the operators $\hat{w}^{(\kappa_1 k_1 \kappa_2 k_2)\overline{\kappa k}}_{\pi q}$. Then the symmetry properties of the $E^2_{(m'\mu')(m''\mu'')}$ operators with respect to permutations of the 1-electron quantum numbers can be exploited. For example, the alternate coupling scheme, C_{12}, with coefficients of the form

$$\langle C_{12}(\tilde{\kappa}_1\tilde{k}_1\tilde{\kappa}_2\tilde{k}_2)\bar{\kappa}\pi\bar{k}q \,|\, s_1'\mu_1'\phi_1'm_1's_2'\mu_2'\phi_2'm_2'q \,|\, s_1''\mu_1''\phi_1''m_1''s_2''\mu_2''\phi_2''m_2''\rangle = \tag{2.88}$$

$$\langle C^{\kappa}_{12}(\tilde{\kappa}_1\tilde{\kappa}_2)\bar{\kappa}\pi \,|\, s_1'\mu_1's_2'\mu_2's_1''\mu_1''s_2''\mu_2''\rangle \langle C^{k}_{12}(\tilde{k}_1\tilde{k}_2)\bar{k}q \,|\, \phi_1'm_1'\phi_2'm_2'\phi_1''m_1''\phi_2''m_2''\rangle$$

couples ϕ_1', ϕ_1'' to $\tilde{k}_1$, ϕ_2', ϕ_2'' to $\tilde{k}_2$, and $\tilde{k}_1$, $\tilde{k}_2$ to $\bar{k}$, while the parallel scheme is used to couple the spins to $\bar{\kappa}$. The C_{12} coupling scheme is parameterized by the intermediate angular momenta $\theta = (\tilde{\kappa}_1\tilde{k}_1\tilde{\kappa}_2\tilde{k}_2)$ and a typical recoupling takes the form:

$$\frac{\hat{w}^{(\kappa_1 k_1 \kappa_2 k_2)\bar{\kappa}\bar{k}}_{\pi q}(n_1'\phi_1'n_2'\phi_2';n_2''\phi_2''n_1''\phi_1'')}{\sqrt{[\kappa_1,k_1,\kappa_2,k_2]}} = \sum_{\tilde{\kappa}_1\tilde{k}_1\tilde{\kappa}_2\tilde{k}_2=\theta} [\tilde{\kappa}_1,\tilde{k}_1,\tilde{\kappa}_2,\tilde{k}_2]^{1/2}$$

$$(-1)^{\phi_1''-\phi_2''+\tilde{k}_2-k_2+\tilde{\kappa}_2-\kappa_2} \begin{Bmatrix} 1/2 & 1/2 & \kappa_1 \\ 1/2 & 1/2 & \kappa_2 \\ \tilde{\kappa}_1 & \tilde{\kappa}_2 & \bar{\kappa} \end{Bmatrix} \begin{Bmatrix} \phi_1' & \phi_2'' & k_1 \\ \phi_1'' & \phi_2' & k_2 \\ \tilde{k}_1 & \tilde{k}_2 & \bar{k} \end{Bmatrix} \tag{2.89}$$

$$\hat{w}^{C_{12}(\theta)\bar{\kappa}\bar{k}}_{\pi q}(n_1'\phi_1'n_2'\phi_2';n_2''\phi_2''n_1''\phi_1'')$$

where the recoupling coefficients are expressed in terms of the 9-j symbols[29] and phase factors are added as needed (cf. the SL coupling case, equation (2.94) below). The operators $\tilde{W}^{C_{12}(\theta)\bar{\kappa}\bar{k}}_{\pi q}$ are defined by replacing the $\tau^{n}_{(m'\mu')(m''\mu'')}$'s with the $E^{2}_{(m'\mu')(m''\mu'')}$'s in the transformation that yields the $\hat{w}^{C_{12}(\theta)\bar{\kappa}\bar{k}}_{\pi q}$'s, and satisfy the relationships

$$\tilde{W}^{C_{12}(\theta)\bar{\kappa}\bar{k}}_{\pi q}(n_2'\phi_2'n_1'\phi_1';n_1''\phi_1''n_2''\phi_2'') = -\tilde{W}^{C_{12}(\theta)\bar{\kappa}\bar{k}}_{\pi q}(n_1'\phi_1'n_2'\phi_2';n_2''\phi_2''n_1''\phi_1'') \tag{2.90}$$

Effective Operator Expansion of $q_2^{\{\lambda_1 k_1 \lambda_2 k_2\}}$

$$
\begin{aligned}
q_2^{\{\lambda_1 k_1 \lambda_2 k_2\}} = {} & D[\lambda_1, k_1, \lambda_2, k_2]^{-1/2} \sum_{\pi q} B_{\pi q}^{\overline{\lambda k}} \Bigg\{ \frac{1}{2} \sum_{(n_1' \emptyset_1') < (n_2' \emptyset_2')}^{\Omega} \sum_{(n_1'' \emptyset_1'') < (n_2'' \emptyset_2'')}^{\Omega} \\
& \langle n_1' \emptyset_1' n_2' \emptyset_2' \| t^{\lambda_1 k_1 \lambda_2 k_2} \| n_1'' \emptyset_1'' n_2'' \emptyset_2'' \rangle \cdot \\
& \Big[\hat{w}_{\pi q}^{(\lambda_1 k_1 \lambda_2 k_2)\overline{\lambda k}} (n_1' \emptyset_1' n_2' \emptyset_2'; n_1'' \emptyset_1'' n_2'' \emptyset_2'') + (-1)^{F_{12}} \hat{w}_{\pi q}^{(\lambda_2 k_2 \lambda_1 k_1)\overline{\lambda k}} (n_2' \emptyset_2' n_1' \emptyset_1'; n_2'' \emptyset_2'' n_1'' \emptyset_1'') \Big] \\
& + \langle n_2' \emptyset_2' n_1' \emptyset_1' \| t^{\lambda_1 k_1 \lambda_2 k_2} \| n_2'' \emptyset_2'' n_1'' \emptyset_1'' \rangle \cdot \\
& \Big[\hat{w}_{\pi q}^{(\lambda_1 k_1 \lambda_2 k_2)\overline{\lambda k}} (n_2' \emptyset_2' n_1' \emptyset_1'; n_2'' \emptyset_2'' n_1'' \emptyset_1'') + (-1)^{F_{12}} \hat{w}_{\pi q}^{(\lambda_2 k_2 \lambda_1 k_1)\overline{\lambda k}} (n_1' \emptyset_1' n_2' \emptyset_2'; n_1'' \emptyset_1'' n_2'' \emptyset_2'') \Big] \\
& + \langle n_1' \emptyset_1' n_2' \emptyset_2' \| t^{\lambda_1 k_1 \lambda_2 k_2} \| n_2'' \emptyset_2'' n_1'' \emptyset_1'' \rangle \cdot \\
& \Big[\hat{w}_{\pi q}^{(\lambda_1 k_1 \lambda_2 k_2)\overline{\lambda k}} (n_1' \emptyset_1' n_2' \emptyset_2'; n_2'' \emptyset_2'' n_1'' \emptyset_1'') + (-1)^{F_{12}} \hat{w}_{\pi q}^{(\lambda_2 k_2 \lambda_1 k_1)\overline{\lambda k}} (n_2' \emptyset_2' n_1' \emptyset_1'; n_1'' \emptyset_1'' n_2'' \emptyset_2'') \Big] \\
& + \langle n_2' \emptyset_2' n_1' \emptyset_1' \| t^{\lambda_1 k_1 \lambda_2 k_2} \| n_1'' \emptyset_1'' n_2'' \emptyset_2'' \rangle \cdot \\
& \Big[\hat{w}_{\pi q}^{(\lambda_1 k_1 \lambda_2 k_2)\overline{\lambda k}} (n_2' \emptyset_2' n_1' \emptyset_1'; n_1'' \emptyset_1'' n_2'' \emptyset_2'') + (-1)^{F_{12}} \hat{w}_{\pi q}^{(\lambda_2 k_2 \lambda_1 k_1)\overline{\lambda k}} (n_1' \emptyset_1' n_2' \emptyset_2'; n_2'' \emptyset_2'' n_1'' \emptyset_1'') \Big] \\
& + \sum_{(n' \emptyset')}^{\Omega} \sum_{(n'' \emptyset'')}^{\Omega} \langle n' \emptyset' n' \emptyset' \| t^{\lambda_1 k_1 \lambda_2 k_2} \| n'' \emptyset'' n'' \emptyset'' \rangle \cdot \\
& \Big[\hat{w}_{\pi q}^{(\lambda_1 k_1 \lambda_2 k_2)\overline{\lambda k}} (n' \emptyset' n' \emptyset'; n'' \emptyset'' n'' \emptyset'') + (-1)^{F_{12}} \hat{w}_{\pi q}^{(\lambda_2 k_2 \lambda_1 k_1)\overline{\lambda k}} (n' \emptyset' n' \emptyset'; n'' \emptyset'' n'' \emptyset'') \Big] \Bigg\}
\end{aligned}
$$

$$
(-1)^{F_{12}} = (-1)^{\lambda_1 + \lambda_2 - \overline{\lambda} + k_1 + k_2 - \overline{k}}
$$

Equation (2.87)

because of the antisymmetry of the operators $E^2_{(m'\mu')(m''\mu'')}$ with respect to permutations of the 1-electron quantum numbers, and the factorization of $E^2_{(m'\mu')(m''\mu'')}$ given by (2.69) is transformed to ($\theta = \{\kappa_1 k_1 \kappa_2 k_2\}$)

$$\tilde{W}^{C_{12}(\theta)\overline{\kappa k}}_{\pi q}(n'_1\ell'_1 n'_2\ell'_2;n''_1\ell''_1 n''_2\ell''_2) = \left[\tilde{W}^{\kappa_1 k_1}(n'_1\ell'_1;n''_1\ell''_1)\tilde{W}^{\kappa_2 k_2}(n'_2\ell'_2;n''_2\ell''_2)\right]^{\overline{\kappa k}}_{\pi q}$$

$$- \delta_{(n'_2\ell'_2),(n''_1\ell''_1)}\,(-1)^{\overline{\kappa}+\ell'_1-\ell''_2+\overline{k}} \tag{2.91}$$

$$\begin{Bmatrix} 1/2 & \kappa_1 & 1/2 \\ \kappa_2 & 1/2 & \overline{\kappa} \end{Bmatrix} \begin{Bmatrix} \ell'_1 & k_1 & \ell'_2 \\ k_2 & \ell''_2 & \overline{k} \end{Bmatrix} \tilde{W}^{\overline{\kappa k}}_{\pi q}(n'_1\ell'_1;n''_2\ell''_2)$$

where $(\;)^{\overline{\kappa k}}_{\pi q}$ indicates the coupling of (2.86b). The expression for the effective 2-electron operator $\tilde{Q}_2^{\{\kappa_1 k_1 \kappa_2 k_2\}}$ restricted to a single configuration, is given by equation (2.92), the spherical tensor analog of (2.71a).

Applications

The effective operator expansions of operators $\tilde{Q}_1^{\{\kappa k\}}$ and $\tilde{Q}_2^{\{\kappa_1 k_1 \kappa_2 k_2\}}$ have useful applications. For example, effective operator expansions can be used to find particular types of contributions of the Pauli Hamiltonian (table 2.4) when restricted to a single configuration. An overall constant energy can be found by inspection when the Pauli Hamiltonianis expanded in components $\tilde{Q}_2^{\{\kappa_1 k_1 \kappa_2 k_2\}}$. The operators $\tilde{W}^{00}(n\ell;n\ell)$ are equivalent to $u_{n\ell}/\sqrt{(4\ell+2)}$, so collecting all terms composed only of operators of this type gives a contribution proportional

Effective Operator Expansion of $\tilde{Q}_2^{\{\kappa_1 k_1 \kappa_2 k_2\}}$

$$\tilde{Q}_2^{\{\kappa_1 k_1 \kappa_2 k_2\}} = \sum_{\tilde{\kappa}_1 \tilde{k}_1 \tilde{\kappa}_2 \tilde{k}_2} \Bigg\{ \frac{1}{2} \sum_{(n'\ell')\neq(n''\ell'')}^{\Omega} \Big[\langle n'1'n''\ell'' \| t^{\kappa_1 k_1 \kappa_2 k_2} \| n'\ell' n''\ell'' \rangle$$

$$\cdot \frac{\delta_{\tilde{\kappa}_1 \kappa_1} \delta_{\tilde{k}_1 k_1} \delta_{\tilde{\kappa}_2 \kappa_2} \delta_{\tilde{k}_2 k_2}}{\sqrt{[\kappa_1, k_1, \kappa_2, k_2]}} + [\tilde{\kappa}_1, \tilde{k}_1, \tilde{\kappa}_2, \tilde{k}_2]^{1/2} \begin{Bmatrix} 1/2 & 1/2 & \kappa_1 \\ 1/2 & 1/2 & \kappa_2 \\ \tilde{\kappa}_1 & \tilde{\kappa}_2 & \bar{\kappa} \end{Bmatrix} \begin{Bmatrix} \ell' & \ell'' & k_1 \\ \ell' & \ell'' & k_2 \\ \tilde{k}_1 & \tilde{k}_2 & \bar{k} \end{Bmatrix}$$

$$\cdot (-1)^{\ell'-\ell''+\tilde{k}_2-k_2+\tilde{\kappa}_2-\kappa_2} \langle n'\ell' n''\ell'' \| t^{\kappa_1 k_1 \kappa_2 k_2} \| n''\ell'' n'\ell' \rangle \Big]$$

$$\left[\tilde{W}^{\tilde{\kappa}_1 \tilde{k}_1}(n'\ell') \tilde{W}^{\tilde{\kappa}_2 \tilde{k}_2}(n''\ell'') \right]^{\overline{\kappa k}}_{\overline{m}q}$$

$$+ \sum_{(n\ell)}^{\Omega} \langle n\ell n\ell \| t^{\kappa_1 k_1 \kappa_2 k_2} \| n\ell n\ell \rangle \Big[\Big[\tilde{W}^{\tilde{\kappa}_1 \tilde{k}_1}(n\ell) \tilde{W}^{\tilde{\kappa}_2 \tilde{k}_2}(n\ell) \Big]^{\overline{\kappa k}}_{\overline{m}q}$$

$$+ (-1)^{\overline{\kappa}+\overline{k}} \begin{Bmatrix} 1/2 & \kappa_1 & 1/2 \\ \kappa_2 & 1/2 & \bar{\kappa} \end{Bmatrix} \begin{Bmatrix} \ell & k_1 & \ell \\ k_2 & \ell & \bar{k} \end{Bmatrix} \tilde{W}^{\overline{\kappa k}}_{\overline{m}q}(n\ell) \Big] \Bigg\}$$

Equation (2.92)

to the identity matrix.

Contributions the restricted Pauli Hamiltonian in the form of the spin-orbit operator, (2.83), are also of interest for constructing the effective Hamiltonian given by (2.40a). This was accomplished by Blume and Watson[33] for a configuration with a single unfilled subshell ($n\ell$), by first resolving the Pauli Hamiltonian into components of the form of

$q_2^{\{\kappa_1 k_1 \kappa_2 k_2\}}$ and then inspecting the matrix elements with determinant wavefunctions for all contributions proportional to $\xi_{n\ell}\vec{\ell}\cdot\vec{s}$.

Alternately, the component operators can be expanded in the form of $\tilde{Q}_2^{\{\kappa_1 k_1 \kappa_2 k_2\}}$. Then, using (2.91) all terms proportional to $\tilde{W}^{(11)0}(n\ell;n\ell)$ or $\tilde{W}^{00}(n'\ell';n'\ell')$. $\tilde{W}^{(11)0}(n\ell;n\ell)$ can be found. The terms of this type have matrix elements proportional to those of $\xi_{n\ell}\cdot\tilde{W}^{(11)0}(n\ell;n\ell)$. In this way, an expression for $\xi_{n\ell}$ can be obtained involving integrals over radial wavefunctions, without an explict operator $\xi(r)$, or assuming a configuration with only a single unfilled subshell.

SL Coupling

Another recoupling of the 2-electron tensor operators, connected with the 2-electron SL basis functions, is related to the C_{12} scheme via

$$\frac{\tilde{W}_{\pi q}^{C_{12}\{\kappa_1 k_1 \kappa_2 k_2\}\overline{\kappa k}}(n_1'\ell_1' n_2'\ell_2';n_1''\ell_1'' n_2''\ell_2'')}{\sqrt{[\kappa_1,k_1,\kappa_2,k_2]}} = \sum_{S'L'S''L''} [S',L',S'',L'']^{1/2} \quad (2.93a)$$

$$\begin{pmatrix} 1/2 & 1/2 & \kappa_1 \\ 1/2 & 1/2 & \kappa_2 \\ S' & S'' & \overline{\kappa} \end{pmatrix} \begin{pmatrix} \ell_1' & \ell_1'' & k_1 \\ \ell_2' & \ell_2'' & k_2 \\ L' & L'' & \overline{k} \end{pmatrix} \tilde{W}_{\pi q}^{C_{SL}(S'L'S''L'')\overline{\kappa k}}(n_1'\ell_1' n_2'\ell_2';n_1''\ell_1'' n_2''\ell_2'')$$

and the inverse transformation

$$\frac{\tilde{W}^{C_{SL}(S'L'S''L'')\bar{\kappa}\bar{k}}_{\pi q}(n'_1\ell'_1 n'_2\ell'_2;n''_1\ell''_1 n''_2\ell''_2)}{\sqrt{[S',L',S'',L'']}} = \sum_{\kappa_1 k_1 \kappa_2 k_2} [\kappa_1,k_1,\kappa_2,k_2]^{1/2} \quad (2.93b)$$

$$\left\langle \begin{matrix} 1/2 & 1/2 & \kappa_1 \\ 1/2 & 1/2 & \kappa_2 \\ S' & S'' & \bar{\kappa} \end{matrix} \middle| \begin{matrix} \ell'_1 & \ell''_1 & k_1 \\ \ell'_2 & \ell''_2 & k_2 \\ L' & L'' & \bar{k} \end{matrix} \right\rangle \tilde{W}^{C_{12}(\kappa_1 k_1 \kappa_2 k_2)\bar{\kappa}\bar{k}}_{\pi q}(n'_1\ell'_1 n'_2\ell'_2;n''_1\ell''_1 n''_2\ell''_2)$$

The alternate coupling scheme, C_{SL}, is parameterized by the intermediate angular momenta (S′L′S″L″), and factorizes like the C_{12} scheme into pairs of coefficients $\langle C_L(L'L'')\bar{k}q \mid \ell'_1 m'_1 \ldots \ell''_2 m''_2\rangle$ and $\langle C_S(S'S'')\bar{\kappa}\pi \mid s'_1\mu'_1 \ldots s''_2\mu''_2\rangle$. C_{SL} couples ℓ'_1, ℓ'_2 to L′, ℓ''_1, ℓ''_2 to L″, and L′, and L″ to $\bar{k}$, while the parallel scheme is used to couple the spins to $\bar{\kappa}$.

If $(\ell''_1 m''_1 s''_1 \mu''_1)$ and $(\ell''_2 m''_2 s''_2 \mu''_2)$ are exchanged in the C_{SL} scheme, a new scheme, $C^{e''}_{SL}$, results. From the properties of the 3-j or vector coupling coefficients,[29,30] this $C^{e''}_{SL}$ is related to by a change in phase:

$$\langle C^{e''}_L(L'L'')\bar{k}q \mid \ell'_1 m'_1 \ell'_2 m'_2 \ell''_1 m''_1 \ell''_2 m''_2\rangle = \langle C_L(L'L'')\bar{k}q \mid \ell'_1 m'_1 \ell'_2 m'_2 \ell''_2 m''_2 \ell''_1 m''_1\rangle$$

$$= (-1)^{\ell''_1+\ell''_2-L''} \langle C_L(L'L'')\bar{k}q \mid \ell'_1 m'_1 \ell'_2 m'_2 \ell''_1 m''_1 \ell''_2 m''_2\rangle \quad (2.94)$$

A similar relation applies to the spins, so that

$$\hat{w}_{\pi q}^{C_{SL}^{e''}(\Theta)\overline{\times k}}(n_1'\ell_1'n_2'\ell_2';n_2''\ell_2''n_1''\ell_1'') = \tag{2.95}$$

$$-(-1)^{\ell_1''+\ell_2''-L''-S''}\hat{w}_{\pi q}^{C_{SL}(\Theta)\overline{\times k}}(n_1'\ell_1'n_2'\ell_2';n_2''\ell_2''n_1''\ell_1'')$$

As in the C_{12} coupling case, the $\tilde{W}_{\pi q}^{C_{SL}(\Theta)\overline{\times k}}$ operators are related to the $\tilde{E}^n_{(m'\mu')(m''\mu'')}$'s by the same linear transformation that connects the $\hat{w}_{\pi q}^{C_{SL}(\Theta)\overline{\times k}}$'s and the $\hat{\tau}^n_{(m'\mu')(m''\mu'')}$'s, so the antisymmetry of the $\tilde{E}^n_{(m'\mu')(m''\mu'')}$'s with respect to permutations of the 1-electron quantum numbers implies:

$$\tilde{W}_{\pi q}^{C_{SL}(\Theta)\overline{\times k}}(n_1'\ell_1'n_2'\ell_2';n_2''\ell_2''n_1''\ell_1'') = -\tilde{W}_{\pi q}^{C_{SL}(\Theta)\overline{\times k}}(n_1'\ell_1'n_2'\ell_2';n_1''\ell_1''n_2''\ell_2'') \tag{2.96}$$

Combined with (2.95), (2.96) implies that if $(n_1''\ell_1'') = (n_2''\ell_2'')$, then $S''+L''$ must be even or the operator vanishes, and similarly, $S'+L'$ must be even if $(n_1'\ell_1') = (n_2'\ell_2')$.

The SL-coupled 2-electron spherical tensor operators are symmetrized integral operators with kernels that can be expressed in terms of 2-electron wavefunctions:

$$\tilde{W}_{\pi q}^{C_{SL}(S'L'S''L'')\overline{\times k}}(n_1'\ell_1'n_2'\ell_2';n_1''\ell_1''n_2''\ell_2'') = \tag{2.98a}$$

$$\sum_{1=i_1<i_2}^{N}\int dx_{i_1}'\,dx_{i_2}'\,K_{\pi q}^{C_{SL}(S'L'S''L'')\overline{\times k}}(x_{i_1},x_{i_2};x_{i_1}',x_{i_2}')$$

$$K_{\pi q}^{C_{SL}(S'L'S''L'')\overline{\kappa k}}(x_1,x_2;x_1',x_2') = \sum_{M_{L'}=-L'}^{L'}\sum_{M_{L''}=-L''}^{L''}\sum_{M_{S'}=-S'}^{S'}\sum_{M_{S''}=-S''}^{S''}$$

$$(-1)^{S'-M_{S'}}\begin{pmatrix} S' & \overline{\kappa} & S'' \\ -M_{S'} & \pi & M_{S''}\end{pmatrix}(-1)^{L'-M_{L'}}\begin{pmatrix} L' & \overline{k} & L'' \\ -M_{L'} & \pi & M_{L''}\end{pmatrix} \tag{2.98b}$$

$$\Phi^2_{\{n'\ell'\}}(S'L'M_{S'}M_{L'};x_1,x_2)\Phi^{2*}_{\{n''\ell''\}}(S''L''M_{S''}M_{L''};x_1',x_2')$$

If the coefficients $B^{\overline{\kappa k}}_{\pi q}$ take the form

$$B^{\overline{\kappa k}}_{\pi q} = (-1)^{\overline{\kappa}-\overline{k}+\overline{M}}\,[\overline{J}]^{1/2}\begin{pmatrix}\overline{\kappa} & \overline{k} & \overline{J} \\ \pi & q & -\overline{M}\end{pmatrix}B^{\overline{J}}_{\overline{M}} \tag{2.99}$$

then the sum over the SL-coupled spherical tensor effective operators becomes

$$\sum_{\pi q} B^{\overline{\kappa k}}_{\pi q}\,\tilde{W}^{C_{SL}(\Theta)\overline{\kappa k}}_{\pi q}(n_1'\ell_1'n_2'\ell_2';n_1''\ell_1''n_2''\ell_2'') = \tag{2.100}$$

$$\sum_{\overline{M}=-\overline{J}}^{\overline{J}} B^{\overline{J}}_{\overline{M}}\,\tilde{W}^{C_{SL}(\Theta\overline{\kappa k})\overline{J}}_{\overline{M}}(n_1'\ell_1'n_2'\ell_2';n_1''\ell_1''n_2''\ell_2'')$$

and the operators $\tilde{W}^{C_{SL}(\Theta\overline{\kappa k})\overline{J}}_{\overline{M}}$ can be expressed by recoupling

$$\tilde{W}_{\bar{M}}^{C_{SL}(\Theta\bar{\kappa}\bar{k})\bar{J}}(n'_1\ell'_1 n'_2\ell'_2;n''_1\ell''_1 n''_2\ell''_2) = \tag{2.101}$$

$$\sum_{J'J''}[\bar{\kappa}\bar{k}J'J'']^{1/2}\begin{Bmatrix} S' & S'' & \bar{\kappa} \\ L' & L'' & \bar{k} \\ J' & J'' & \bar{J} \end{Bmatrix}\tilde{W}_{\bar{M}}^{C_{SLJ}(\Theta J'J'')\bar{J}}(n'_1\ell'_1 n'_2\ell'_2;n''_1\ell''_1 n''_2\ell''_2)$$

where $\tilde{W}_{\bar{M}}^{C_{SLJ}(\Theta J'J'')\bar{J}}$ is an integral operator related to the 2-electron SLJ-coupled wavefunctions in the same manner as in (2.98). In the special case where $\bar{J} = 0$:

$$\sqrt{(2J+1)}\;\tilde{W}^{C_{SLJ}(S'L'JS''L''J)0}(n'_1\ell'_1 n'_2\ell'_2;n''_1\ell''_1 n''_2\ell''_2) = \tag{2.102a}$$

$$\sum_{1=i_1<i_2}^{N}\int dx'_{i_1}dx'_{i_2}\;K^{C_{SLJ}(S'L'JS''L''J)0}(x_{i_1},x_{i_2};x'_{i_1},x'_{i_2})$$

$$K^{C_{SLJ}(S'L'JS''L''J)0}(x_1,x_2;x'_1,x'_2) = \sum_{M=-J}^{J} \tag{2.102b}$$

$$\Phi^2_{\{n'\ell'\}}(S'L'JM;x_1,x_2)\Phi^{2*}_{\{n''\ell''\}}(S''L''JM;x'_1,x'_2)$$

2.2.6 SLJ-Coupled Basis Vectors

Although the N-electron determinant wavefunctions employed in Slater-Condon theory are constructed from 1-electron wavefunctions that carry irreducible representations of $SU(2)\times O^+(3)$, in general, a subspace spanned by one or more configurations cannot be invariant with respect to the independent rotations of the spin and space coordinates of all N

SL-Coupled Operator Expansion of $1/r_{12}$

$$\frac{1}{r_{12}} = \sum_{k=0}^{\infty} \Bigg\{ \sum_{\overline{SL}} \sum_{(n_1'\ell_1')<(n_2'\ell_2')} \sum_{(n_1''\ell_1'')<(n_2''\ell_2'')}$$

$$\Bigg[(-1)^{\ell_1''+\ell_2'+\overline{L}+k} \begin{Bmatrix} \ell_1' & \ell_1'' & k \\ \ell_2'' & \ell_2' & \overline{L} \end{Bmatrix} \langle n_1'\ell_1' \| C^k \| n_1''\ell_1'' \rangle \langle n_2'\ell_2' \| C^k \| n_2''\ell_2'' \rangle$$

$$R^k(n_1'\ell_1' n_2'\ell_2'; n_1''\ell_1'' n_2''\ell_2'')$$

$$+ (-1)^{\ell_1''+\ell_2'+\overline{S}+k} \begin{Bmatrix} \ell_1' & \ell_2'' & k \\ \ell_1'' & \ell_2' & \overline{L} \end{Bmatrix} \langle n_1'\ell_1' \| C^k \| n_2''\ell_2'' \rangle \langle n_2'\ell_2' \| C^k \| n_1''\ell_1'' \rangle \Bigg]$$

$$R^k(n_1'\ell_1' n_2'\ell_2'; n_2''\ell_2'' n_1''\ell_1'')$$

$$[\overline{S},\overline{L}]^{1/2} \; \tilde{W}^{C_{SL}(\overline{SLSL})00}(n_1'\ell_1' n_2'\ell_2'; n_1''\ell_1'' n_2''\ell_2'')$$

$$+ \sum_{(n'\ell')\neq(n''\ell'')} (-1)^{\ell'+\ell''+k+\overline{L}} \langle n'\ell' \| C^k \| n''\ell'' \rangle^2 \; R^k(n'\ell' n'\ell'; n''\ell'' n''\ell'')$$

$$\sum_{\overline{SL}} [\overline{S},\overline{L}]^{1/2} \; \frac{1+(-1)^{\overline{S}+\overline{L}}}{2} \begin{Bmatrix} \ell' & \ell'' & k \\ \ell'' & \ell' & \overline{L} \end{Bmatrix} \tilde{W}^{C_{SL}(\overline{SLSL})00}(n'\ell' n'\ell'; n''\ell'' n''\ell'') \Bigg\}$$

$$R^k(n_1'\ell_1' n_2'\ell_2'; n_1''\ell_1'' n_2''\ell_2'') =$$

$$\int_0^{\infty} dr r^2 \int_0^{\infty} ds s^2 \; R_{n_1'\ell_1'}(r) R_{n_1''\ell_1''}(r) R_{n_2'\ell_2'}(s) R_{n_2''\ell_2''}(s) u_k(r;s)$$

Equation (2.97)

An example of the LS recoupling scheme: The effective operator expansion of $1/r_{12}$ in SL-coupled spherical unit tensors.

electrons because of the antisymmetry requirement. Atomic Hamiltonians are invariant with respect to identical rotations applied to all electronic coordinates, although many components of an atomic Hamiltonian are spin independent. For this reason it is convenient to transform the N-electron central field determinant wavefunctions into a set of basis vectors that carry irreducible representations D^J of $SU(2) \subset [SU(2)\times O^+(3)]$, making the Hamiltonian matrix block diagonal, and removing of the (2J+1)-dimensional degeneracy associated with each D^J.

The effective operators $L(n\ell)_q$, $S(n\ell)_q$, and $J(n\ell)_q = L(n\ell)_q + S(n\ell)_q$ defined through (2.81) and (2.82) commute with permutations of electrons, commute with their equivalents for any $(n'\ell') \neq (n\ell)$, and are a representation of the Lie algebra for the simultaneous rotations of all 1-electron wavefunctions $\{\phi_{n\ell m\mu} \mid \mu=\pm 1/2 ; m=-\ell,\ldots,\ell\}$ on any subspace spanned by products of 1-electron wavefunctions of this type. The existence of these operators implies that the determinant basis vectors of a configuration $\underline{Q} = \{w_1,\ldots,w_p\}$ can be transformed to a set of antisymmetrized products of wavefunctions $\Phi^{w_1}_{n_1\ell_1}\left[\alpha_1 S_1 L_1 M_L^1 M_S^1\right]$, $\ldots$, $\Phi^{w_p}_{n_p\ell_p}\left[\alpha_p S_p L_p M_L^p M_S^p\right]$ that carry irreducible representations $D^{S_1} \otimes D^{L_1} \otimes \ldots \otimes D^{S_p} \otimes D^{L_p}$ of $[SU(2)\times O^+(3)]^p$, where the α_i's are indices used to distinguish among any identical representations $D^{S_i} \otimes D^{L_i}$ that may occur.

These antisymmetrized product wavefunctions can be reduced by any coupling scheme to irreducible representations D^J under the restriction $SU(2) \subset [SU(2)\times O^+(3)]^p$. A common choice is successively couple the S's and the L's in the form S_1, S_2 to $\tilde{S}_2$, then $\tilde{S}_2$, S_3 to $\tilde{S}_3$, and so on until

$\tilde{S}_{p-1}$, S_p are coupled to $\tilde{S}_p$, while a parallel coupling scheme is used on the L's to couple to $\tilde{L}_p$. Then $\tilde{S}_p$ and $\tilde{L}_p$ are coupled to J. This reduction, SLJ coupling, is often used when Hamiltonian matrices are explicitly constructed and diagonalized. The difficult part of this scheme is the construction of the antisymmetrized wavefunctions $\Psi^{uu}\left(\alpha SLM_S M_L\right)$, because the individual rotations of electrons described by one of these wavefunctions do not commute with permutations. A coupling scheme or pairwise reduction of representations of $[SU(2)xO^+(3)]^{uu}$ of uu-products of $(n\ell)$ electrons cannot guarantee the resulting wavefunctions are antisymmetric.

Fractional Parentage

Racah[8] found an iterative solution to the problem of constructing the wavefunctions $\Psi^{uu}_{n\ell}\left(\alpha SLM_S M_L\right)$, using an earlier concept of fractional parentage. The solutions took the form

$$\Psi^{uu}\left(\alpha SLM_S M_L\right) = \sum_{\overline{\alpha SL}} \left(\ell^{u-1}\overline{\alpha(LS}\right\}\ell^{u}\alpha SL\right) \Psi^{uu}\left(\ell^{u-1}\overline{\alpha SL},\ell;\alpha SLM_S M_L\right) \qquad (2.103a)$$

$$\Psi^{uu}\left(\ell^{u-1}\overline{\alpha SL},\ell;\alpha SLM_S M_L|x_1,\ldots x_{uu}\right) \equiv \qquad (2.103b)$$

$$\sum_{\mu m \bar{M}_S \bar{M}_L} [S,L]^{1/2} (-1)^{\bar{S}-1/2+M_S+\bar{L}-\ell+M_L} \begin{pmatrix} \bar{S} & 1/2 & S \\ M_{\bar{S}} & \mu & M_S \end{pmatrix} \begin{pmatrix} \bar{L} & \ell & L \\ M_{\bar{L}} & m & -M_L \end{pmatrix}$$

$$\Psi^{u-1}\left(\overline{\alpha SLM_{\bar{S}}M_{\bar{L}}}|x_1,\ldots,x_{u-1}\right)\phi_{n\ell m_\mu}(x_u)$$

where $\left(\ell^{u-1}\overline{\alpha LS}\right\}\ell^{u}\alpha SL\right)$ is a coefficient of fractional parentage, or cfp. Standard conventions have been adopted for phases and the selection of states $(\ell^{u}\alpha SL)$ when several states with the same SL occur[34]. These

choices can be related to a chain of irreducible representations carried on the supspace of u-electron determinant wavefunctions constructed from the $\{\phi_{n\ell m\mu}\}$ wavefunctions[8,29]. The chain of subgroups begins with the antisymmetric representation of the unitary group U(u) induced from the representation $D^{1/2} \otimes D^{\ell}$ carried by each electron and ends with representations $D^{S} \otimes D^{L}$

The matrix elements of the 1-electron spherical unit tensors $W^{(k)}_{mq}(n\ell)$ (the standard cfp's are real) are given by:

$$\left\langle \ell^{u} \alpha' S' L' M_{S'} M_{L'} \left| W^{(k)}_{mq}(n\ell) \right| \ell^{u} \alpha'' S'' L'' M_{S''} M_{L''} \right\rangle =$$

$$(-1)^{S'-M_{S'}} \begin{pmatrix} S' & k & S'' \\ -M_{S'} & m & M_{S''} \end{pmatrix} (-1)^{L'-M_{L'}} \begin{pmatrix} L' & k & L'' \\ -M_{L'} & q & M_{L''} \end{pmatrix} \qquad (2.104a)$$

$$\left\langle \ell^{u} \alpha' S' L' \| W^{(k)}(n\ell) \| \ell^{u} \alpha'' S'' L'' \right\rangle$$

$$\left\langle \ell^{u} \alpha' S' L' \| W^{(k)}(n\ell) \| \ell^{u} \alpha'' S'' L'' \right\rangle = u(-1)^{\ell+L'+k} [k, k, L', L'', S', S'']^{1/2}$$

$$\sum_{\overline{\alpha SL}} (-1)^{\overline{L}+\overline{S}+S'+3/2} \begin{Bmatrix} 1/2 & 1/2 & k \\ S' & S'' & \overline{S} \end{Bmatrix} \begin{Bmatrix} \ell & \ell & k \\ L' & L'' & \overline{L} \end{Bmatrix} \qquad (2.104b)$$

$$(\ell^{u-1} \overline{\alpha SL}\, \ell \,\|\, \ell^{u} \alpha' S' L') \; (\ell^{u-1} \overline{\alpha SL}\, \ell \,\|\, \ell^{u} \alpha'' S'' L'')$$

Standard cfps, $(\ell^{u}\alpha(SL)$ states, and the reduced matrix elements of the unit tensor operators $U^{k}(n\ell) \equiv \sqrt{2}\, W^{0k}(n\ell)$ and $V^{k1}(n\ell) \equiv \sqrt{(2\ell+1)}\, W^{10}(n\ell)$ have been tabulated by Nielsen and Koster[34]. With this information, the matrix elements of a 2-electron unit tensor can be calculated via

$$\left\langle \Phi^{uu}\left[\alpha' S' L' M_{S'} M_{L'}\right] \middle| W^{(\kappa_1 k_1 \kappa_2 k_2)\overline{\kappa} k}_{\pi q}(n\ell n\ell; n\ell n\ell) \middle| \Phi^{uu}\left[\alpha'' S'' L'' M_{S''} M_{L''}\right] \right\rangle =$$

$$(-1)^{S'-M_{S'}} \begin{pmatrix} S' & \kappa & S'' \\ M_{S'} & -\pi & M_{S''} \end{pmatrix} (-1)^{L'-M_{L'}} \begin{pmatrix} L' & k & L'' \\ M_{L'} & -q & M_{L''} \end{pmatrix} \qquad (2.105a)$$

$$\left\langle \Phi^{uu}\alpha' S' L' \| W^{(\kappa_1 k_1 \kappa_2 k_2)\overline{\kappa} k}(n\ell n\ell; n\ell n\ell) \| \Phi^{uu}\alpha'' S'' L'' \right\rangle$$

$$\left\langle \Phi^{uu}\alpha' S' L' \| \left[\tilde{W}^{\kappa_1 k_1}(n\ell) \tilde{W}^{\kappa_2 k_2}(n\ell)\right]^{\overline{\kappa} k} \| \Phi^{uu}\alpha'' S'' L'' \right\rangle =$$

$$[\overline{\kappa}, \overline{k}]^{1/2} (-1)^{S'+\overline{\kappa}+S''+L'+\overline{k}+L''} \sum_{\alpha SL} \begin{pmatrix} & & \\ \kappa_2 & \overline{\kappa} & \kappa_2 \\ S' & S & S'' \end{pmatrix}_{<} \begin{pmatrix} & & \\ k_2 & \overline{k} & k_1 \\ L' & L & L'' \end{pmatrix}_{>} \qquad (2.105b)$$

$$\left\langle \Phi^{uu}\alpha' S' L' \| W^{\kappa k}(n\ell) \| \Phi^{uu}\alpha SL \right\rangle \left\langle \Phi^{uu}\alpha SL \| W^{\kappa k}(n\ell) \| \Phi^{uu}\alpha'' S'' L'' \right\rangle$$

With (2.91), effective operator expansions, and the above expressions for reduced matrix elements, all matrix elements of the 1- and 2-electron operators can be calculated between $(\Phi^{uu}\alpha SL)$ wavefunctions. With suitable recouplings, all intra-configuration matrix elements can be calculated with these expressions, and with these same principles, the inter-configuration matrix elements as well. Calculation of matrix elements by these techniques are discussed in detail by Cowan,[3] and a few more comments on this subject are made in chapter III.

2.3 Parameterization of Effective Hamiltonians

Consider a subspace X of the N-electron Hilbert space spanned by the set of orthonormal N-electron wavefunctions $\underline{\Omega} = \{\Phi_a^N \mid a=1,\ldots,f\}$. Since X has dimension f, upon restriction to X, an operator Q with a

domain $D(Q) \supseteq X$ will have an $f^x f$ matrix representation $M(Q)$ given by:

$$M(Q)_{ab} = \left\langle \Phi_a^N \middle| Q \middle| \Phi_b^N \right\rangle \tag{2.106}$$

Equivalently, the operator Q can be replaced on the N-electron Hilbert space by the effective operator (a "~" is used here to denote the restriction of an operator to X):

$$\tilde{Q} = \sum_{a,b=1}^{f} M(Q)_{ab} \hat{\Gamma}_{ab}^N \tag{2.107a}$$

Following equation (2.9),

$$\hat{\Gamma}_{ab}^N = \left| \Phi_a^N \right\rangle \left\langle \Phi_b^N \right| \tag{2.107b}$$

The matrix elements $M(Q)_{ab}$ are also given by:

$$M(Q)_{ab} = \mathrm{tr}\left[\hat{\Gamma}_{ab}^{N\dagger} Q \right] \tag{2.107c}$$

In principle, there are f^2 linearly independent equivalent operators on X, but if the operators considered have any additional symmetry properties, this number is reduced (e.g. Q self-adjoint, $Q^\dagger = Q$, Q can have only $f(f-1)$ linearly independent components). This section discusses the relationship of the independent components of an effective operator to its symmetry properties, particularly in the case of the N-electron Hamiltonian.

2.3.1 Effective Hamiltonians

The symmetry properties of H, the Hamiltonian for an N-electron system, and the structure of the subspace X determine the possible set of linearly independent operators that can be used to represent $\tilde{H}$. If H

has a group of invariant symmetry transformations G, then assume X carries or is minimally extended to carry a unitary representation of G. The representation of G carried by X is a subset of the unitary transformations on the basis vectors $\underline{\Omega}$; an irreducible representation of the f-dimensional unitary group U(f). The operators Γ^{N}_{ab} are the representation of the Lie Algebra for U(f) on X, and as such carry the reducible representation $U(f) \otimes U(f)^{*}$.[29,35,36,37]

The operators Γ^{N}_{ab} can be transformed into families of operators that carry irreducible representations U(f) via the vector coupling matrix that reduces the representation $U(f) \otimes U(f)^{*}$. The symmetry transformations of G on X are a subgroup of U(f), so on restriction to this subgroup, irreducible representations of U(f) become reducible into irreducible representations of G. Since H is invariant under the transformations of G, $\tilde{H}$ is a linear combination of the operators that carry identity representations of G.

For a suitable choice for X, the number of independent components of the effective Hamiltonian operator $\tilde{H}$ is often less than the number of distinct eigenvalues of the matrix M(H). In this case, $\tilde{H}$ can be considered a vector in the space spanned by its component operators, and its coefficients treated as free parameters (within constraints such as Hermiticity of M(H) and physical considerations). The optimal set of parameters give the best agreement between a set of observed energy levels and the eigenvalues of M(H). This parameterization is implied when "effective Hamiltonian" is referred to here in the context of a semi-empirical theory.

2.3.2 Unitary Decomposition of the n-Electron Operators

A major simplification in the parameterization of effective operators on X occurs if X is spanned by determinant wavefunctions. For simplicity, let $\underline{\Omega}$ be the set of all N-electron determinant wavefunctions constructed from $S = \{\phi_\alpha \mid \alpha=1,\ldots,d\}$, a set of orthonormal 1-electron wavefunctions; $\underline{\Omega} = \{\Phi_A^N \mid A \subseteq S\}$, and X has dimension $f = \binom{d}{N}$. S is chosen so that one or more irreducible representations of the symmetry group G of the Hamiltonian are carried by subsets of S. The transformations of the group G can regarded as subgroup of U(d), the set of unitary transformations on S. In the case of atoms, G = SU(2) and the wavefunctions of S carry representations of $SU(2)\times O^+(3)$.

The first step toward finding the linearly independent operators on X is the reduction of representations of U(f) carried by the operators upon restriction to U(d). The N-electron determinants $\underline{\Omega}$ carry the irreducible representation $[1^N]$ of U(d),[35,36,37] where $[1^N]$ is an abbreviation for the set of non-negative integers $[\lambda_1 \geq \ldots \lambda_d \geq 0]$ that specify a Weyl[36] tableau representation of U(d). The set of all linear operators acting on the basis set W carries the representation $[1^N]\otimes[1^N]^*$ of U(d), which is equivalent to $[1^N]\otimes[1^{d-N}]\otimes[1^d]^*$ and can be reduced to the direct sum of irreducible representations:

$$[1^N]\otimes[1^{d-N}]\otimes[1^d]^* \sim \left\{ [0] + \sum_{k=1}^{\min(N,d-N)} [2^k 1^{d-2k}] \right\} \otimes [1^d]^* \quad (2.108a)$$

Each representation on the right-hand-side of (2.108a) is irreducible and occurs only once. The reduction is perhaps simpler with the restriction $SU(d) \subseteq U(d)$: $[r^d]$ for any integer r becomes the identity ([0])

representation (if $r<0$, $[r^d] \equiv [|r|^d]^*$)[37].

Because Hamiltonian operators generally act on the coordinates of only one or two electrons, it is convenient to expand them in operators $\tilde{E}^n_{ab}$, n=1,2, as in (2.65). These n-body operators can also be reduced according to their transformation properties under U(d)[38]. It is clear from (2.70) that the operators $\tilde{E}^n_{ab}$ are contractions of the operators $\{\hat{\Gamma}^N_{AB} \mid A,B \subseteq S\}$ that span the space of all operators on X, and this relationship also implies that the operators $\tilde{E}^n_{ab}$ carry the representation $[1^n]\otimes[1^n]^*$ of SU(d). This representation is equivalent to $[1^n]\otimes[1^{d-n}]$ and reduces to a direct sum of irreducible representations

$$[1^n]\otimes[1^{d-n}] \sim [0] + \sum_{k=1}^{\min(n,d-n)} [2^k,1^{d-2k}] \qquad (2.108b)$$

Again, each irreducible representation in the sum occurs only once, but the reductions for the n-,(d-n)-body operators are identical. The dimension of a representation $[\lambda]$ of U(d) or SU(d)[29,37] is

$$\dim([\lambda_1\cdots\lambda_d]) = \prod_{1=i<j}^{d} \frac{j-i+\lambda_i-\lambda_j}{j-i} \qquad (2.109)$$

but the number of independent components an n-body operators is related to the number of identity representations contained in the reduction of SU(d) restricted to the symmmetry group of the operator involved (e.g. $O^+(3)$ or some point symmetry group).

In the common situation where $n \leq \min(N,d-N)$, the n-electron operators that carry various irreducible representations of SU(d) can be recognized by their trace properties. It follows from the contraction property, (2.70), that the traceless n-electron operators[20], (i.e. Q_n

such that

$$\sum_{\alpha_i,\beta_j=1}^{d} \delta_{\alpha_i\beta_j}\, m(q_n)\{\alpha_1\cdots\alpha_n\}\{\beta_1\cdots\beta_n\} = 0; \quad i,j=1,2,\ldots,n \qquad (2.110)$$

and $m(q_n)_{ab}$ as in(2.60b)) must carry the representation $[2^n 1^{d-2n}]$ of SU(d). For example, when n=1:

$$\tilde{Q}_1^{[21^{d-2}]} = \sum_{\alpha\beta} \left\{ \tilde{m}(q_1)_{\alpha\beta} - \delta_{\alpha\beta}\, \bar{m}(q_1) \right\} \tilde{E}_{\alpha\beta} \qquad (2.111a)$$

$$\tilde{Q}_1^{[0]} = \bar{m}(q_1)\, \tilde{N} \qquad (2.111b)$$

$$\bar{m}(q_1) = \frac{1}{d} \sum_{\alpha=1}^{d} m(q_1)_{\alpha\alpha} \qquad (2.111c)$$

Configurations

Wavefunctions belonging to a configuration carry the antisymmetrized irreducible representation $\{[1^{u_1}],[1^{u_2}],\ldots,[1^{u_p}]\}$ of the direct product of unitary groups $U(d_1)\times U(d_2)\times\ldots\times U(d_p)$. The direct product representation can of course be regarded as a subgroup of $U(d_1+d_2+\ldots+d_p)$. The operators $\tilde{E}^n_{ab}$ factor into components corresponding to each representation of $U(d_i)$ as expressed by equation (2.63), and the n-electron operators can be resolved with respect to irreducible representations of the unitary groups $U(d_i)$. Within a configuration, this can sometimes be accomplished by resolving the matrices $\tilde{m}(q^n)_{ab}$ into components that are traceless or proportional to the traces with respect to pairs of indices corresponding to the same set S_i.

Inter-configuration operators can be resolved by considering situa-

tions such as $(u_i, u_j) \rightarrow (u_i-1, u_j+1)$ as a new configuration carrying a representation of $U(d_i+d_j) \times \prod_{k\neq i,j} \times U(d_k)$, merging the sets S_i and S_j. However, not all operator representations of $U(d_i+d_j)$ will occur, because of the restriction on the number of elements allowed from S_i and S_j used to construct the determinant wavefunctions. Usually inter-configuration operators are resolved into 2-electron operators E^2_{ab} with no common indices that can be contracted, and as such are linearly independent of all the intra-configuration operators.

2.3.3 Subgroup Decomposition of the n-Electron Operators

A method for resolving the n-electron operators into linearly independent components is to consider the reductions into irreducible representations of the operators on restriction of U(d) to its various subgroups. Judd[29] has studied the properties of the operators under various symmetries, and in a second-quantized creation and destruction operator formalism[39,40]. There are two basic choices for the chains of subgroups: $SU(4\ell+2) \supset SU(2)\times SU(2\ell+1) \supset SU(2)\times O^+(2\ell+1) \supset SU(2)\times O^+(3)$ and $SU(4\ell+2) \supset Sp(4\ell+2) \supset SU(2)\times O^+(2\ell+1) \supset SU(2)\times O^+(3)$, where $Sp(4\ell+2)$ is the symplectic group of $4\ell+2$ dimensions generated by the unit tensors $W^{\lambda k}(n\ell)$ for $\lambda+k$ odd. For f electrons ($\ell = 3$), an additional link in the chain can be added with the group G(2); $O^+(7) \supset G(2) \supset O^+(3)$.

The representations of $SU(2)\times O^+(3)$ carried by the 1-electron tensors $\{W^{\lambda k}(n\ell) \mid \lambda = 0,1;\ k=0,1,\ldots,2\ell\}$ are self-evident, but their relationships to the other groups are not. $W^{00}(n\ell)$ becomes the identity representation and the others carry the representation $[21^{4\ell}]$ of

$SU(4\ell+2)$. $[21^{4\ell}]$ branches to the irreducible representations $(20\ldots0)$ and $(110\ldots0)$ of $Sp(4\ell+2)$ (the representations of $Sp(2\nu)$ are given by ν non-negative integers $(\sigma_1,\ldots,\sigma_\nu)$), carried by the tensors $W^{\lambda k}(n\ell)$ with $\lambda+k$ odd and even respectively[36]. Then the tensors with k even (and a fixed projection μ for $\lambda=1$) carry the representation $(20^{\ell-1})$ of $O^+(2\ell+1)$ while the the tensors with k odd carry the representation $(110^{\ell-2})$[29,40]. If $\ell = 3$, the unit tensors with $\{k = 2,4,6\}$, $\{k = 1,5\}$, and $\{k=3\}$, carry the respective representations (20), (11), and (10) of G(2).

The reduction of the 2-electron unit tensors into chains of subgroup representations is considerably more complex. The tensors $\{W^{C_{SL}(S'L'S''L'')}\}$, $S'+L'$ and $S''+L''$ even, must carry the operator representations of $SU(4\ell+2)$ on the antisymmetric subspace of ω, $(n\ell)$-electrons when $2 \leq \omega \leq 4\ell$. These operators can be coupled, recoupled, and expanded via:

$$\frac{\tilde{W}^{C_{SL}(S'L'S''L'')\overline{\lambda k}}_{\mu q}(n\ell n\ell;n\ell n\ell)}{\sqrt{[S',L',S'',L'']}} = \sum_{\lambda_1 k_1 \lambda_2 k_2} [\lambda_1,k_1,\lambda_2,k_2]^{1/2} \begin{pmatrix} 1/2 & 1/2 & \lambda_1 \\ 1/2 & 1/2 & \lambda_2 \\ S' & S'' & \overline{\lambda} \end{pmatrix} \begin{pmatrix} \ell & \ell & k_1 \\ \ell & \ell & k_2 \\ L' & L'' & \overline{k} \end{pmatrix} \left[\left(\tilde{W}^{\lambda_1 k_1}(n\ell) \tilde{W}^{\lambda_2 k_2}(n\ell) \right)^{\overline{\lambda k}}_{\mu q} \right.$$

$$\left. + (-1)^{\overline{\lambda}+\overline{k}} \begin{pmatrix} 1/2 & \lambda_1 & 1/2 \\ \lambda_2 & 1/2 & \overline{\lambda} \end{pmatrix} \begin{pmatrix} \ell & k_1 & \ell \\ k_2 & \ell & \overline{k} \end{pmatrix} \tilde{W}^{\overline{\lambda k}}_{\mu q}(n\ell) \right] \qquad (2.112)$$

Linear combinations of the $W^{C_{SL}(S'L'S''L'')\overline{\lambda k}}$ unit tensors can be used to find tensor operators that carry the irreducible representations of SU(4ℓ+2). For example, the trace over all 2-electron operators $\tilde{E}^2_{ab}$, equivalent to

$$\sum_{\overline{SL}} [\overline{S},\overline{L}]^{1/2} \frac{1+(-1)^{\overline{S+L}}}{2} \tilde{W}^{C_{SL}(\overline{SLSL})00}(n\ell n\ell;n\ell n\ell) = \frac{u(u-1)}{2} - \sum_{\lambda=0}^{1} \sum_{k=0}^{2\ell} \left[\sum_{\pi=-\lambda}^{\lambda} \sum_{q=-k}^{k} (-1)^{\pi+q} \tilde{W}^{\lambda k}_{\pi q}(n\ell) \tilde{W}^{\lambda k}_{-\pi-q}(n\ell) - \frac{u}{4\ell+2} \right]$$

must correspond to the identity representation [0]. The reduction of the effective Coulomb operator, $\frac{1}{r_{12}}$, has been carried out by Racah[8] and also presented by Judd[29].

III. Computer Calculations

This chapter is a review of the ab-initio calculations performed by Cowan's computer codes, and least squares fitting the eigenvalues of a parmeterized matrix to a set of experimental energy levels. Section (3.1) reviews the self consistent field calculations controlled by the codes RCN and HF(mod7), while section (3.2) briefly reviews the construction of the Hamiltonian matrix and ancillary calculations involving the eigenvectors (gyromagnetic ratios, line strengths, lifetimes, etc.) performed by the computer code RCG. Detailed accounts of these calculations are given elsewhere,[3,10-13,43-45] so only a brief outline is given here with a few additional comments. Section (3.3) is the review of least squares minimization.

3.1 SCF Calculations

Most schemes for obtaining radial wavefunctions for the ab-initio form of Slater-Condon theory involve the solution of a set of coupled integro-differential equations by an iterative procedure known as the self consistent field or SCF method. These equations are arrived at by assuming that a matrix element or linear combination of matrix elements of the atomic Hamiltonian operator between central field determinant wavefunctions is stationary with respect to variations of the radial wavefunctions.

Usually, a set of radial wavefunctions is found for each configuration. For a single configuration consisting only of closed subshells ($w_i = 4\ell_i+2$; $i=1,\ldots,q$), there is only one determinant wavefunction in the configuration, so equations for the radial wavefunctions can be

found by variation of average energy (the diagonal matrix element) of this state. For an arbitrary configuration, Slater[41] purposed that the average energy of configuration

$$E_{av} = \frac{1}{f_W} \sum_{Z \in W} \left\langle \Phi_{W(Z)} \middle| H \middle| \Phi_{W(Z)} \right\rangle \tag{3.1}$$

should be stationary with respect to variation of any of the radial wavefunctions, as a zero order Hamiltonian used in a Slater-Condon theory perturbation scheme will be degenerate with respect to all the determinant states belonging to the same configuration.

For the non-relativistic Hamiltonian

$$H = \sum_{i=1}^{N} \left[p_i^2 - \frac{2Z}{r_i} \right] + \sum_{i>j=1}^{N} \frac{2}{r_{ij}} \tag{3.2}$$

the average energy of configuration becomes (a spin-orbit interaction of the type $\xi(r)\vec{l}\cdot\vec{s}$ does not contribute):

$$E_{av} = \sum_{i=1}^{q} w_i I(i) + \sum_{i=1}^{q} \frac{w_i(w_i-1)}{2} \left[F^0(i;i) - \frac{2\ell_i+1}{4\ell_i+1} \sum_{k>0} \begin{pmatrix} \ell_i & k & \ell_i \\ 0 & 0 & 0 \end{pmatrix}^2 F^k(i;i) \right]$$

$$+ \sum_{1=i<j}^{q} w_i w_j \left[F^0(i;j) - \frac{1}{2} \sum_{k>0} \begin{pmatrix} \ell_j & k & \ell_j \\ 0 & 0 & 0 \end{pmatrix}^2 G^k(i;j) \right] \tag{3.3a}$$

Where

$$I(i) = \int_0^\infty dr P_i(r) \left[-\frac{d^2}{dr^2} + \frac{\ell_i(\ell_i+1)}{r^2} - \frac{2Z}{r} \right] P_i(r) \tag{3.3b}$$

$$F^k(i;j) = R^k(i,j;i,j) \tag{3.3c}$$

$$G^k(i;j) = R^k(i,j;j,i) \tag{3.3d}$$

$$R^k(a,c;b,d) = \int_0^\infty dr \int_0^\infty ds P_a(r) P_c(s) U_k(r;s) P_b(r) P_d(s) \tag{3.3e}$$

and

$$U_k(r;s) = \begin{cases} \dfrac{r^k}{s^{k+1}} & r<s \\ \dfrac{s^k}{r^{k+1}} & r \geq s \end{cases} \tag{3.3f}$$

3.1.1 Hartree-Fock Equations for the Average Energy of Configuration

Requiring the quantity

$$E_{av} - \sum_{i=1}^{q} w_i \epsilon_i \int_0^\infty dr |P_i(r)|^2 + \sum_{i \neq j}^{q} w_i w_j \epsilon_{ij} \int_0^\infty dr P_i(r) P_j(r)$$

to be stationary with respect to variations of the radial wavefunctions leads to the configuration average Hartree-Fock or HF equations given in table (3.1). The ϵ_i's and the ϵ_{ij}'s are Lagrange multipliers ($\epsilon_{ij} = \epsilon_{ji}$ and $\epsilon_{ij} = 0$ if $\phi_i \neq \phi_j$) used to preserve the orthonormality of the radial wavefunctions. These equations are solved numerically by HF(mod7), a modified version of a Froese-Fischer[42,43] code. Griffin[44] explains in detail the method of solution and the numerical procedures used by the computer code, so only a few highlights are given here.

SCF Procedure

The first step in the solving these equations is the selection of some initial estimates for the radial wavefunctions (screened hydrogenic, solutions to some central potential model, etc.). Then these

Table (3.1)

Configuration Averaged Hartree-Fock Equations

$$\left\{-\frac{d^2}{dr^2}+\frac{\ell_i(\ell_i+1)}{r^2}-\frac{2(Z-Y_i(r))}{r}-\varepsilon_i\right\}P_i(r) = + \frac{2}{r}X_i(r) - \sum_{j\neq i} w_j \varepsilon_{ij} P_j(r) \tag{3.4a}$$

$$P_i(0) = 0 \; ; \qquad \lim_{r\to\infty} P_i(r) = 0 \tag{3.4b}$$

$$X_i(r) = \sum_{j\neq i} w_j \, 1/2 \sum_{k=0} \begin{pmatrix} \ell_i & k & \ell_j \\ 0 & 0 & 0 \end{pmatrix}^2 Y^k(i,j;r) \tag{3.5a}$$

$$Y_i(r) = Y(r) - y_i(r) \tag{3.5b}$$

$$Y(r) = \sum_{j=1}^{q} w_j Y^0(j,j;r) \tag{3.5c}$$

$$y_i(r) \quad Y^0(i,i;r) + (w_i-1)\frac{2\ell_i+1}{4\ell_i+1}$$

$$= \sum_{k>0} \begin{pmatrix} \ell_i & k & \ell_i \\ 0 & 0 & 0 \end{pmatrix}^2 Y^k(i,i;r) \tag{3.5d}$$

$$Y^k(i,j;r) = \int_0^\infty ds \; P_i(s) r U_k(r;s) P_j(s) \tag{3.5e}$$

ε_i, ε_{ij} — Lagrange multipliers (see text)

estimates are used to calculate $Y^i(r)$ and $X^i(r)$, the potential and exchange functions, and the off diagonal energy parameters or ε_{ij}'s. The ε_{ij}'s satisfy

$$\epsilon_{ij} = \epsilon_{ji} = \delta_{\ell_i \ell_j} \frac{1}{w_j - w_i} \left\langle \int_0^\infty dr \, \frac{2}{r}\left[Y_i(r) - Y_j(r)\right] P_i(r) P_j(r) \right.$$

$$\left. + \int_0^\infty dr \left[X_i(r) P_{j(r)} - X_j(r) P_{i(r)}\right] \right\rangle \qquad (3.6)$$

$$= \delta_{\ell_i \ell_j} \frac{1}{w_j - w_i} \sum_{k=0}^{\infty} \begin{pmatrix} \ell_i & k & \ell_i \\ 0 & 0 & 0 \end{pmatrix}^2 \frac{1}{2}\left[\delta_{k0} - \frac{1}{4\ell+2}\right]$$

$$\left([4\ell+2 - w_i] R^k(ij;ii) - [4\ell+2 - w_j] R^k(ij;jj) \right)$$

where $\ell = \ell_i = \ell_j$, and can be computed with this expression if $w_i \neq w_j$. If $w_i = w_j$, then the average energy is invariant with respect to any real orthogonal transformation applied to $P_i(r)$ and $P_j(r)$. In this case, any solution of the configuration average HF equations that has linearly independent radial functions with the same "ℓ" and occupation number can be arbitrarily orthogonalized. The off-diagonal energy parameters can be estimated with a trial and error procedure, or eliminated if the SCF technique used to solve the equations leads to linearly independent radial wavefunctions.

The next step is to integrate the resulting differential equations to obtain a new or output set of radial wavefuntions. These functions are then used to compute potential, exchange, and ϵ_{ij} terms for the next iteration or potential cycle. For the remainder of the procedure, the previous steps are repeated until the output radial wavefunctions are equal to the input radial wavefunctions to within the desired accuracy.

In practice, the convergence is expedited by taking the input radial wavefunctions for the $(m+1)^{st}$ cycle as linear combinations of the

input and output radial wavefunctions from the m^{th} cycle:

$$P^{m+1}_{n_i \ell_i}(\text{input}) = c_i P^{m}_{n_i \ell_i}(\text{input}) + (1-c_i) P^{m}_{n_i \ell_i}(\text{output}) \qquad (3.7)$$

The acceleration factors, $\{c_i \mid i=1,\ldots,p;\ 0 \le c_i < 1\}$, can be adjusted during the course of the SCF cycles to speed convergence, and are sometimes essential in obtaining any convergence at all.

Numerical Integration of the Radial Wavefunctions

For each potential cycle of the SCF calculation, the output $P_i(r)$'s are solutions of inhomogeneous differential equations of the form:

$$\left[-\frac{d^2}{dr^2} + f_i(r) - \epsilon_i \right] P_i(r) = g_i(r) \qquad (3.8a)$$

with the boundary conditions:

$$P_i(0) = 0\ ; \quad \lim_{r\to\infty} P_i(r) = 0\ ; \quad \|P_i\| = 1 \qquad (3.8b)$$

The ϵ_i's must be chosen so that the $P_i(r)$'s are normalized, and have $n_i - \ell_i - 1$ nodes.

The radial wavefunctions are represented as values at points on a numerical grid. Since the functions oscillate more rapidly near the origin, the density of grid points must be greater as $r\to 0$. In HF, this is accomplished by making the change of variable

$$t = \ln(Zr) \qquad (3.9a)$$

$$\bar{P}_i(t) = r(t)^{-1/2} P_i(r(t)) \qquad (3.9b)$$

with the corresponding changes are made in configuration average HF equations The $\overline{P}_i(t)'s$ are represented on a numerical grid of typically 600 equally spaced points.

With an asymptotic form for $P_i(r)$ as $r\rightarrow 0$ and an estimate for ϵ_i, the differential equation for a given $P_i(r)$ can be accurately integrated outward to the matching radius, the point where the curvature of $P_i(r)$ changes sign (somewhere after its last node). The asymptotic forms of all the $P_i(r)'s$ at small r are determined by the $\epsilon_i's$ and the initial "slope" parameters

$$a_0^i = \lim_{r\rightarrow 0} r^{\ell_i+1} P_i(r) \qquad i=1,2,\ldots,q \tag{3.10}$$

with the convention that the $a_0^{i\prime}s$ are always chosen to be positive. Cowan's codes obtain the matching radii as well as initial estimates of the $P_i(r)'s$, the $\epsilon_i's$, and the $a_0^{i\prime}s$ for the first cycle of the SCF procedure from an approximation to the configuration average HF equations that leads to homogenous differential equations (see the HX approximation below—in this case each matching radius corresponds to a classical turning point in a potential well).

Similarly, the asymptotic form for a given radial wavefunction as $r\rightarrow\infty$ allows (3.8) to be integrated inward to the matching radius, the point where the outward integration is ended. The large r dependence of the $P_i(r)'s$ is a function of the $\epsilon_i's$ and another set of scale factors analgous to the $a_0^{i\prime}s$, which can be simply chosen to make the radial wavefunctions continuous at the matching radius. The precise asymptotic forms of the radial wavefunctions are difficult to obtain because of the

presence of the exchange and ε_{ij} terms in (3.4), so these are neglected and essentially the WKB solutions for the homgeneous differential equations are used in the large r region. This results in some errors, mainly to the wavefunctions localized nearest the nucleus, as the exchange and off diagonal terms cause some very small amplitude oscilaations in the tail region of these wavefunctions. Since the relative energies of the low lying atomic levels are most sensitive to the radial wavefunctions with the greatest radial extent, this source of error is tolerated.

Then the ε_i's and the a_0^i's are adjusted and the integrations repeated until the outward $P_i(r)$'s have n_i-l_i-1 nodes, the derivatives of the radial wavefunctions are continuous at the matching radii, and the $P_{i(r)}$'s are normalized to unity. In practice, linear combinations of the homogenous and inhomogenous integrals are used to obtain continuity of the derivatives at the matching radius, so that two numerical integrations of each radial wavefunction are made and only the ε_i's are adjusted until the conditions (3.8b) are obtained. The entire numerical integration procedure has been explained in detail by Griffin[44], including variations for cases where convergence of the SCF calculation is difficult to obtain (e.g. configurations with excited d and f electrons[45]).

3.1.2 HX Approximation to the E_{av} Hartree-Fock Equations

Cowan has developed an approximation to the configuration average HF equations resulting in homogenous differential equations for the radial wavefunctions. This is equivalent to replacing the off-diagonal

and exchange terms with a local potential in (3.4), although the local potential term used is functionally dependent on the radial wavefunctions. Cowan's potential is a semi-empirical improvement over a similar approximation proposed by Slater[46].

Slater replaced the exchange terms by a local potential, expressed in terms of the spherically averaged electron number density, $\rho(r)$:

$$V_s(r) = \alpha \frac{3}{2} \left[24 \frac{\rho(r)}{\pi} \right]^{1/3} \tag{3.11a}$$

$$\rho(r) = \sum_{i=1}^{q} w_i \rho_i(r) = \sum_{i=1}^{q} w_i P_i^2(r) \tag{3.11b}$$

$V_s(r)$ has the same functional dependence on the number density $\rho(r)$ as the exchange contribution per electron to the average energy of a zero temperature free electron gas. The radial wavefunctions are found by solving the equations:

$$\left\{ -\frac{d^2}{dr^2} + \frac{\ell_i(l_i+1)}{r^2} - V^i(r) \right\} P_i(r) = \epsilon_i P_i(r) \tag{3.12a}$$

Where

$$V^i(r) = \frac{2[Z - Y(r)]}{r} - V_s(r) \tag{3.12b}$$

Slater chose $\alpha = 1$, but if the radial wavefunctions are chosen by variation of the average energy of configuration with the exchange terms approximated by the volume integral of $\rho(r)V_s(r)$, $\alpha = 1$ is replaced by $\alpha = 2/3$. In this approximation, all the electrons have the same central potential, so the P_i's are automatically orthogonal and no off diagonal Lagrange multipliers are required.

The radial wavefunctions obtained by Slater's approximation or HFS method are significantly different from the HF radial wavefunctions because of the asymptotic behavior of the exchange potential. Cowan modified and adjusted the exchange potential to find an approximation in better agreement with the HF results, and arrived at a new local potential:

$$V^i(r) = -2\frac{[Z-Y(r)-y^i(r)]}{r} + V_x^i(r) \qquad (3.13a)$$

Where

$$V_x^i(r) = -k_1 f(r)\left[\frac{\rho'}{\rho'+k_2/(n_i-l_i)}\right]\left(\frac{\rho'}{\rho}\right)\left[\frac{24}{\pi}\rho\right)\Big]^{1/3} \qquad (3.13b)$$

$$\rho' = \rho'(r) = \rho(r) - [\min(2,w_i)]\rho_i(r) \qquad (3.13c)$$

$$\rho_i(r) = \frac{P_i^2(r)}{4\pi r^2} \qquad (3.13d)$$

and f(r) is a factor that improves the orthogonality of radial wavefunctions with the same "ℓ" but different "n" values. Usually, f(r) = 1, but in some cases f(r) slightly increases the value of the potential in for $\ell_i>1$ where $\ell_{i-1} = \ell_i$ or $\ell_{i-2} = \ell_i$ and $w_i = 1$:

$$f(r) = \begin{cases} 1 & ; \quad r \geq r_0 \\ 1+k_3(1-r/r_0) & ; \quad r<r_0 \end{cases} \qquad (3.13e)$$

The point r_0 is the location of the m^{th} node of $P_i(r)$; where m is the number of subshells with $\ell = \ell_i$ and $n<n_i$. $k_1 = .65$, $k_2 = .70$, and $k_3 = .50$ are Cowan's[12] choices for the three empirically adjustable

parameters.

Numerical Solution of the HX Equations

The SCF calculation of the radial wavefunctions via the HX approximation is performed by the computer code RCN. RCN evolved from a code implementing the HFS method written by Hermann and Skillman.[9] The radial wavefunctions are represented on a numerical grid of 640 points that are equally spaced values of the radius for blocks of 40 points. The step size of each block increases so that the density of points increases with decreasing r. The differential equations for each potential cycle are integrated out from the origin and in from the large r region to a matching radius that occurs near $V^i(r) = \epsilon_i$.

The local potential approximation (3.12a) in place of (3.4) has some advantages with respect to the numerical SCF prodedure: The differential equations are homogeneous, so only the ϵ_i's are adjusted until the $P_i(r)$'s have the correct number of nodes and continuous first derivatives at the matching radius. Only one numerical integration of each radial wavefunction is required instead of a homogeneous and an inhomogeneous integral. This makes convergence of the SCF process much easier to obtain.

3.1.3 Relativistic and Correlation Corrections

Cowan has introduced approximate corrections to the configuration averaged energy and the radial wavefunctions due to relativistic and correlation effects. As in the spirit of the HX approximation itself, these corrections are perhaps best justified by the improvements they

make in the agreement between the results of the HF and HX calculations with experiment, rather than on rigorous theoretical grounds.

The relativity corrections[3,11] are derived from the 1-body terms in the Pauli reduction of the Breit Hamiltonian[28]. If the radial wavefunction equations satisfy the local potential equation (3.12), the relativistic mass-velocity and Darwin terms can be evaluated via:

$$E_m^i = \int_0^\infty dr P_i(r) \left[\epsilon_i - V^i(r)\right]^2 P_i(r) \tag{3.14}$$

$$E_d^i = -\delta_{\ell_i 0} \frac{\alpha^2}{4} \int_0^\infty dr P_i(r) \left[1 + \frac{\alpha^2}{4}\left[\epsilon_i - V^i(r)\right]\right]^{-1} \cdot \left[\frac{dV^i(r)}{dr}\right]\left[\frac{d}{dr} - \frac{1}{r}\right] P_i(r) \tag{3.15}$$

These corrections are normally added to the configuration average energy by the computer codes ($V^i(r)$ is taken as the local potential of the HX approximation for both the HX and HF calculations). If the radial wavefunctions are determined variationally with these terms included in the configuration average energy, the quantities between the pair of $P_i(r)$'s appear as operators in the radial wave equation for $P_i(r)$ in either the HF or HX equations. As an option, Cowan incorporates these changes in the radial wavefunction equations in his codes for both the HX (HXR) or HF (HFR) methods.

The correlation correction to the average energy of configuration is rather roughly defined as the difference between the HF average energy and the experimentally determined average energy after relativistic effects have been added to the HF average energy. Empirically it is

determined that for heavy atoms the average correlation energy $\bar{e}_c$ is roughly -.08 Ry per electron[47].

A number of perturbative calculations of the average correlation energy per electron of a zero temperature free electron gas have been made[48] for both high and low density limits. The correlation energy is usually parameterized by r_s, the radius of a sphere with volume equal to the average volume per electron:

$$r_s = \left[\frac{3}{4\pi\rho}\right]^{1/3} \tag{3.16}$$

The average result of calculations of the correlation energy per electron of a free electron gas in the low density limit takes the form $\bar{e}_c(r_s) = (1.142r_s)^{-1}$. Cowan used an approximate interpolation formula between the high and low density limits of the form

$$e_c(r_s) = -\left[4(r_s+9)^{1/2} + \frac{3}{4}(1.142r_s)\right]^{-1} \tag{3.17}$$

and computed the correlation energy via

$$E_c = \sum_{i=1}^{q} w_i E_c^i = 4\pi\int_0^\infty \rho^i(r)\bar{e}_c(r_s^i(r))dr \tag{3.18a}$$

where

$$r_s^i(r) = \left[\frac{4\pi}{|\rho(r)-\rho^i(r)|}\right]^{1/3} \tag{3.18b}$$

However this method tends to overestimate the correlation energy of the atom, presumably because it tends to count the contribution from a strongly correlated pair of electrons twice. In an effort to avoid poor counting statistics of an atom of relatively few electrons as opposed to

an infinite number of electrons in a free electron gas, the correlation energy is also computed by summing over the increments of in the correlation energy as electrons are added to the atom in order from the most tightly bound to the least tightly bound. This alternative correlation energy is computed via

$$E_c = \sum_{i=1}^{q} \sum_{\beta=1}^{w_i} \int_0^{\infty} P_i^2(r) e_c(r_s^{i\beta}(r)) \qquad (3.19a)$$

where

$$r_s^{i\beta}(r) = \left\{ \frac{1}{3r^2} \sum_{j=1}^{i} (w_j - \beta) P_j^2(r) \right\}^{1/3} \qquad (3.19b)$$

This correction improves the theoretical ionization energies computed for various neutral atoms by differencing the average energies of configuration,[10] but there is little or no evidence for its usefulness with respect to higher stages of ionization. Any user of Cowan's computer codes should be aware that the correlation correction is automatically added to the configuration average energies, because the outputted values of various quantities may not be appropriate for any purpose other than the ab-initio predictions of the optical spectrum of an atom or ion.

3.1.4 Output Parameters

The programs RCN and HF produce absolute configuration average energies, the Slater integrals F^k and G^k needed for signle configration energy matrix calculations, and estimates of the spin orbit parameters $\zeta_{n\ell}$. The program RCN merely calculates the HX approximation to $\zeta_{n\ell}$,

$$\xi_{n\ell}^{HX} = \frac{\alpha^2}{2} \int_0^\infty dr P_{n\ell}^2(r) \frac{1}{r} \frac{\partial V^{n\ell}(r)}{\partial r} \qquad (3.20)$$

while the program HF estimates the spin-orbit coupling parameter from the M^k integrals as described by Blume and Watson[33]. Additional radial integrals are needed for the Hamiltonian matrix of several interacting configurations, and for calculating the spectra from the resulting energy levels.

The program RCN2 takes radial wavefunctions calculated by either RCN or HF (interpolating the logrithmic grid used by HF to the block linear grid of RCN) and calculates the Slater integrals R^k between configurations of the same parity. In general, only the core wavefunctions are assumed identical for all configurations and the spin-orbit interaction between configurations is ignored, introducing a small error that Cowan argues is within the overall accuracy of the approximation[3]. However, the program RCN2 can be used to calculate overlap integrals between any pair of radial wavefunctions, and the R^k integral with any four radial wavefunctions, so this assumptions can be tested if desired.

In addition, RCN2 calculates the reduced matrix elements of the electric dipole operator between pairs of configurations of opposite parity that differ in one radial wavefunction (using the same orthogonality assumptions as for the configuration interaction). As an option, the electric quadrapole reduced matrix elements can also be calculated, supplying all the information needed to calculate electric dipole, magnetic dipole, and electric quadrupole transition probabilities.

3.2 Hamiltonian Matrix and Eigenvector Calculations

Hamiltonian matrices are constructed in a straight-forward fashion by Cowan's RCG(mods 5,6,7) computer codes based on Racah's[8] techniques. The Hamiltonian matrix is diagonalized giving the eigenvalues, eigenvectors, and gyromagnetic ratios in the intemediate coupling scheme. If the appropriate reduced matrix elements are supplied, the spontaneous emission rates and line strength factors for electric dipole, magnetic dipole, and electric quadrapole radiation are calculated, as well as estimates for the lifetimes. The algorithms used are very well documented[3,13], so only brief comments are given here.

3.2.1 Construction of the Hamiltonian Matrix

As described in section (2.2.6), Racah[8] was able to systematically attack the problem of constructing Hamiltonian matrices for complex configurations by finding a basis set for $(n\ell)^w$ configurations by group $\supset$ subgroup chains of representations ending in irreducible representations $D^S \otimes D^L$ of SU(2)xSU(2), and by using recoupling or "tensor algebra" techniques. Basis vectors for N-electron configurations with more than one subshell become antisymmetrized products of $(n\ell^w)$ basis states, $\Psi\left(n\ell^w \alpha(SLM_S M_L)\right)$, and the resulting direct product representations of SU(2)xSU(2) are reduced by successive SL coupling to irreducible $D^S \otimes D^L$ representations, and finally to representations D^J of $SU(2) \subset SU(2)xSU(2)$.

The program RCG represents all configurations of a given parity as q-tuples of the form $(\ell_1^{w_1}, \ldots, \ell_2^{w_2})$ and calculates the matrix elements for the Hamiltonian (2.40). The matrix elements are calculated with the

effective operator techniques described in chapter II; the cfps appropriate to each configuration are supplied and all unit tensor reduced matrix elements and recoupling coefficients are calculated as needed. Considerable recoupling of the SLJ basis vectors must be done for the intra-configuration matrix elements if there are several unfilled shells[13], and the details of the procedure used by RCG are discussed in chapter twelve of Cowan's text[3]. Inter-configuration matrix elements can be more complicated, and Cowan has grouped them into eleven classes including expansions with the coefficients of fractional grandparents (uncoupling of 2-electron states from the $\emptyset^{uu}$(SL states) described in detail in chapter thirteen.

Although the SLJ coupling sheme is used to construct the Hamiltonian matrix, transformations to the jj and other schemes are calculated and the eigenvectors given in these basis if desired. Because of these transformations, Cowan's code constructs the states (LS)J rather than (SL)J. The net result is a phase change:

$$\left\langle L'S'J' \middle| Q \middle| L''S''J'' \right\rangle = \tag{3.21}$$

$$(-1)^{S'+L'+S''+L''-J'-J''} \left\langle S'L'J' \middle| Q \middle| S''L''J'' \right\rangle$$

This convention has no physical consequences for the energy levels or transition probabilities, but is of interest if the matrix elements were used to construct a Hamiltonian matrix with lower symmetry (e.g. a crystal field problem).

3.2.2 Calculations of Spectra

If the SCF calculations are made for an atom or ion with configurations of both parities, the program RCN2 that prepares input data for RCG calculates the reduced matrix elements of the $\vec{r}$ operator between the appropriate radial wavefunctions. As an option, the reduced matrix elements of the electric quadrapole operator are also calculated, so that transition probabilities for electric dipole, magnetic dipole, and electric quadrapole can be calculated by RCG. The transition probabilities peraunit time for spontaneous emission by electric and magnetic multipole radiation are given by[49]:

$$a_{E\lambda} = \frac{\alpha^{2\lambda+1}\sigma^{2\lambda+1}\pi 2^{\lambda+1}[(\lambda+1)!]^2(2\lambda+1)}{[(2\lambda+1)!]^2\lambda(\lambda+1)} \left|\left\langle \Psi_f \middle| P^\lambda_m \middle| \Psi_i \right\rangle\right|^2 \qquad (3.21a)$$

$$P^\lambda_m = \sum_{i=1}^{N} r_i^\lambda C^\lambda_m(\hat{e}_i) \qquad (3.21b)$$

$$a_{M\lambda} = \frac{\alpha^{2\lambda+3}\sigma^{2\lambda+1}\pi 2^{\lambda-1}[(\lambda+1)!]^2(2\lambda+1)}{[(2\lambda+1)!]^2\lambda(\lambda+1)} \left|\left\langle \Psi_f \middle| M^\lambda_m \middle| \Psi_i \right\rangle\right|^2 \qquad (3.22a)$$

$$M^\lambda_m = \sum_{i=1}^{N} \sqrt{\lambda(2\lambda-1)}\, r_i^\lambda \left\{ C^{\lambda-1}(\hat{e}_i) \left[\frac{2}{\lambda+1} \vec{l}_i + 2\vec{s}_i \right] \right\}^\lambda_m \qquad (2.22b)$$

where σ is the reciprocal wavelength in Rydbergs, the unit of time is the orbital period of the Bohr atom electron $h/\alpha^2 mc^2$, and Ψ_f, Ψ_i are the final and initial states.

The initial and final states are members of J-manifolds, $\Psi_f = \Psi(\gamma_f J_f M_f)$ and $\Psi_i = \Psi(\gamma_i J_i M_i)$, so the Wigner Eckart theorem imlies a relationship between the transition probabilities for all components:

$$\left\langle \gamma_f J_f M_f \left| Q_m^\lambda \right| \gamma_i J_i M_i \right\rangle = \begin{pmatrix} J_f & \lambda & J_i \\ -M_f & m & M_i \end{pmatrix}^2 \left| \left\langle \gamma_f J_f \| Q^\lambda \| \gamma_i J_i \right\rangle \right|^2 \qquad (3.23)$$

(Q^λ is any multipole operator). Symmetries also dictate selection rules: $M_f - M_i = m$; J_f, J_i, and λ must satisfy the triangle condition; J_f and J_i cannot both be zero; and the product of parities of the initial and final states must equal the parity of the multipole operator.

If the light is observed from an isotropic source, the individual Zeeman components ($M_i \rightarrow M_f$) are not resolved, and all states of a given energy are equally populated. The probability of observing a line associated with a transition between the pair of J-manifolds from such a source is proportional to an average over the initial states and a sum over the final states and components of the multipole operator:

$$A(\gamma_i J_i \rightarrow \gamma_f J_f)_{Q\lambda} = g_{J_i}^{-1} S_{Q\lambda}(\gamma_i J_i, \gamma_f J_f) \qquad (3.24a)$$

$$g_J = 2J+1 \qquad (3.24b)$$

$$S_{Q\lambda}(\gamma_i J_i, \gamma_f J_f) = \left| \left\langle \gamma_f J_f \| Q^\lambda \| \gamma_i J_i \right\rangle \right|^2 \qquad (3.24c)$$

$S_{Q\lambda}(\gamma_i J_i, \gamma_f J_f)$ is the line strength factor for the Q^λ multipole transition between the $(\gamma_f J_f)$ and $(\gamma_i J_i)$ J-manifolds, and is symmtric with respect to interchange of $(\gamma_i J_i)$ and $(\gamma_f J_f)$. The observed rate of spontaneously emitted radiation for a given line and an isotropic source is proportional to the weighted transition probability gA,

$$gA = g_{J_i} A(\gamma_i J_i \rightarrow \gamma_f J_f) = g_{J_f} A(\gamma_f J_f \rightarrow \gamma_i J_i) \qquad (3.25)$$

and is also symmetrical with respect to interchange of the initial and final J-manifolds. A quantity proportional to the induced emission or absorption transitional probability is the weighted oscillator strength gf,

$$gf \equiv g_{J_i} f(\gamma_i J_i \rightarrow \gamma_j J_f) = \frac{\alpha}{2\pi} \sigma^{-2} g_{J_f} A(\gamma_f J_f \rightarrow \gamma_i J_i) \qquad (3.26)$$

where the oscillator strength is taken as positive for absorption and negative for emission.

The code RCG calculates the electric dipole gA and gf for each transition in an array of configurations of both parities. The key quantity is $S_{E1}(\gamma_f J_f, \gamma_i J_i)$, the line strength, or its aquare root, $\langle \gamma_f J_f \| P^1 \| \gamma_i J_i \rangle$. The details of how the code RCG calculates this reduced matrix element in the SL basis set are given in chapter fourteen of Cowan's text,[3] and when the Hamiltonian matrix is diagonalized, the line strength factors are transformed to the eigenvector (intermediate coupling) basis. An estimate of the lifetime of a given state is obtained from the reciprocal sum of all the transition probabilties to lower-lying levels in the transition array.

Gyromagnetic Ratios

If the light source is placed in a strong magnetic field, the individual Zeeman components of a line can be resolved. For a weak uniform magnetic field, the change in the energy of a given (γJ)-level is given by

$$\Delta E_{mag} = \langle \gamma J | \alpha(\vec{L} + g_s \vec{S}) \cdot \vec{B} | \gamma J \rangle \qquad (3.27a)$$

$$= \frac{\langle \gamma J \| (\vec{L}+g_s\vec{S}) \| \gamma J\rangle}{\langle \gamma J \| \vec{J} \| \gamma J\rangle} \langle \gamma JM | \vec{J} | \gamma JM\rangle = g_{\gamma J} M\alpha(B \qquad (3.27b)$$

where $\vec{B}$ (in Bohr magnetons) has been taken along the z axis, $g_{\gamma J}$ is the gyromagnetic ratio, and g_s is the spin gyromagnetic ratio ($g_s \cong 2.0023$).

In SL coupling g_{SLJ} is given simply:

$$g_{SLJ} = 1 + (g_s-1) \frac{J(J+1) + S(S+1) - L(L+1)}{2J(J+1)} \qquad (3.28)$$

The magnetic field operator is diagonal to first order in the (αSLJ) basis (off diagonal elements with states of $J' = J\pm 1$ are not considered), so the gyromagnetic ratio in the intermediate coupling basis is given simply by

$$g_{\gamma J} = \sum_{\alpha SLJ} \left| \left\langle \gamma J \middle| \alpha SLJ \right\rangle \right|^2 g_{SLJ} \qquad (3.29)$$

so the gyromagnetic ratios for the eigenvectors of the Hamiltonian matrix are easily calculated by RCG.

so the gyromagnetic ratio in the intermediate coupling basis is given simply by

$$g_{\gamma J} = \sum_{\alpha SLJ} \left| \left\langle \gamma J \middle| \alpha SLJ \right\rangle \right|^2 g_{SLJ} \qquad (3.29)$$

The gyromagnetic ratios for the eigenvectors of the Hamiltonian matrix are easily calculated by RCG.

3.3 Least Squares Fitting

The method of least squares is commonly used to estimate parameters of a theoretical model from experimental data. In this work the spectroscopic parameters of the semi-empirical Slater-Condon theory and the

parameters of isoelectronic sequence polynomials are determined by least squares. The method is briefly outlined in this section to define the quantities used to characterize the least squares fits presented here.

3.3.1 Statistical Model

The paradigm for the least squares analysis is one or more experiments with outcomes that are predictable, in principle up to random fluctuations[50,51]. A set of experimental quantities, $x = \{e_1, e_2, \cdots, e_N\}$, are determined to precisions represented by the error estimates $\{\sigma_1, \sigma_2, \cdots, \sigma_N\}$. The experimental quantities are assumed to represent a random sample from a multivariate normal distribution for N independent random variables centered about the theoretical quantities $\{t_1, t_2, \cdots, t_N\}$.

In general the theoretical values are known only as functions of a set of parameters $\{p_1 p_2, \cdots, p_m\}$, and the point $\bar{p} = \{\bar{p}_1, \bar{p}_2, \cdots, \bar{p}_m\}$ in parameter space corresponding to the ideal theoretical quantities, $\{\bar{t}_1, \bar{t}_2, \cdots, \bar{t}_N\}$, must be found from the experimental data. The parameterization of the theoretical quantities often includes the measuring process of the experiment, as well as the fundamental nature of the system under examination.

Maximum Likelihood Estimates

A common method of estimating the parameters of a statistical model is the maximum likelihood method. Given the above assumptions about the experimental data, the probability of having obtained the experimental quantities $x = \{e_1, e_2, \cdots, e_N\}$ for a specified set of parameters p is

given by the likelihood function $L(x;p)$:

$$L(x;p) = \left[\prod_{k=1}^{N} \frac{1}{\sqrt{2\pi}\sigma_k}\right] \exp\left\{ -\tfrac{1}{2} \sum_{k=1}^{N} \frac{(e_k - t(p)_k)^2}{\sigma_k^2} \right\} \tag{3.30}$$

The maximum likelihood estimates for the parameters $\{\bar{p}_1, \bar{p}_2, \ldots, \bar{p}_m\}$ are obtained by maximizing the likelihood function $L(x;p)$ with respect to the parameters p. This is equivalent to minimizing the sum of squares $X^2(p)$:

$$X^2(p) = \sum_{k=1}^{N} \frac{(e_k - t_k)^2}{\sigma_k^2} \tag{3.31}$$

where the random variable $X^2(\bar{p})$ has a probability density given by the chi-square density function for N degrees of freedom:

$$P(X^2;N) = \frac{X^{N/2-1}}{\Gamma(N/2)\,2^{N/2}} \exp\left\{ -X^2/2 \right\} \tag{3.32}$$

The maximum likelihood parameters $\hat{p} = \{\hat{p}_1, \hat{p}_2, \ldots, \hat{p}_m\}$ are obtained by solving the equations

$$d_i(x;\hat{p}) = 0 \tag{3.33a}$$

where

$$d_i(x;p) = \sum_{k=1}^{N} \frac{e_k - t_k(p)}{\sigma_k^2} \frac{\partial t_k(p)}{\partial p_i} \qquad i=1,2,\ldots,m \tag{3.33b}$$

Statistical Parameters

The random variables $\{d_i(x;\bar{p}) \mid i=1,2,\ldots,m\}$, are normally distributed with means of 0 and covariances given by

$$\sigma^2_{d_i d_j} = C_{ij} = \sum_{k=1}^{N} \frac{1}{\sigma_k^2} \frac{\partial t_k}{\partial p_i} \frac{\partial t_k}{\partial p_j}\Big|_{p=\bar{p}} \qquad i,j=1,2,..,m \qquad (3.34)$$

If the theoretical quantities are linear functions of the parameters, the deviations of the least squares parameters from the "true" parameters (i.e. the quantities $\{\hat{p}_i - \bar{p}_i \mid i=1,2,\ldots,m\}$ are linearly related to the random variables $\{d_i(x;\bar{p}) \mid i=1,2,\ldots,m\}$), the least squares parameters can be shown to be unbiased estimates for the parameters $\bar{p}$. The covariance matrix for the least squares estimates is the inverse of the covariance matrix for the $d_i(x;\bar{p})$:

$$\sigma^2_{\hat{p}_i \hat{p}_j} = C^{-1}_{ij} \qquad i,j=1,2,\ldots,m \qquad (3.35)$$

If the theoretical quantities are non-linear functions of the parameters, the least squares estimates for the parameters often have the same properties. For experimental data that are sufficiently precise, a random sample $x = \{e_1, e_2, \ldots, e_N\}$ will with high probability be very close to the theoretical quantities $\{\bar{t}_1, \bar{t}_2, \ldots, \bar{t}_N\}$ (i.e. $|e_k - \bar{t}_k| = \sigma_k$). Barring any pathological behavior of the theoretical quantities as functions of the parameters p, the least squares estimates should fall within a neighborhood of the parameters $\bar{p}$ such that the theoretical quantities can be approximated as linear functions of the parameters p. In this case the matrices C_{ij} and C^{-1}_{ij} are obtained by evaluating the right-hand-side of equation (3.34) at the point $\hat{p}$.

The residual sum of squares $X^2(\hat{p})$ is a statistic, distributed according to a chi-square probability density with N-m degrees of freedom. Thus $X^2(\hat{p})$ is a useful test of the hypothesis that the experimental data $\{e_1, e_2, \ldots, e_N\}$ were obtained from the model defined by equation

(3.30). Also, the reduced chi-square, $X^2(\hat{p})/(N-m)$, can be used to test the relative likelihood of two or more models. The relative probability of obtaining the set of experimental data from one model and not another can be expressed in terms of the ratio of the reduced chi-squares for the two models. Finally, if the precisions of the experimental data represented by the error estimates $\{\sigma_1,\sigma_2,\ldots,\sigma_N\}$ are only relative error estimates, then the reduced chi-square $X^2(\hat{p})/(N-m)$ is an unbiased estimate of the ratio of the absolute error estimates to the relative error estimates. The expression on the right-hand-side of (3.34) must be multiplied by this factor to obtain the best estimates for the matrices C and C^{-1}.

3.3.2 Spectroscopic Parameter Fitting

For the case of fitting the spectroscopic parameters associated with the semi-empirical form of Slater-Condon theory, the experimental quantities are the energy levels of an atom and ion, and the theoretical quantities are the eigenvalues of a Hamiltonian matrix for the configurations of interest. If the Zeeman splittings of the spectra determining the experimental energy levels have been observed, then it is possible to fit the experimental gyromagnetic ratios. The gyromagnetic ratios are more sensitive to the choice of eigenvectors than the eigenvalues, but their partial derivatives with repect to the parameters are more complicated and take longer to compute, thus they are generally not used in the fitting procedure.

The Hamiltonian Matrix

The Hamiltonian is a linear combination of the spectroscopic parameters times their respective real symmetric coefficient matrices. In general H is block diagonal due to the symmetry of the physical situation (i.e. H is a direct sum of submatrices corresponding to irreducible representations of SU(2) or some point group), so H takes the form:

$$H = \sum_{s=1}^{K} \sum_{i=1}^{m} p_i M(s;i) \tag{3.36}$$

K is the number of block diagonal submatrices of H, and the coefficient matrices M(s;i) can be of higher symmetry than H, sometimes having only a small percentage of non-vanishing elements.

Using symmetry of the N-electron system, the Hamiltonian matrix is reduced so that there only accidental degeneracies can occur in the eigenvalue spectrum of any submatrix. The eigenvalues of H are holomorphic functions of the parameters with exceptional points corresponding to accidental degeneracies[52]. If the eigenvalues and eigenvectors are dentoted by $\{\lambda(s;p)_j, \Phi(s;p)_j \mid j=1,2,\ldots,R_s\}$ with the ordering convention $\{\lambda(s;p)_1 \leq \lambda(s;p)_2 \leq \cdots \leq \lambda(s;p)_{R_s}\}$, the eigenvalues can be linearly approximated in the region of the point p^0 (assuming p^0 is not an exceptional point) by

$$\lambda(s;p)_j = \lambda(s;p^0)_j + \sum_{i=1}^{m} \frac{\partial\lambda(s;p^0)}{\partial p_i} (p_i - p_i^0) \tag{3.37a}$$

$$\frac{\partial\lambda(s;p^0)_j}{\partial p_i} = \left\langle \Phi(s;p^0)_j \middle| M(s;i) \middle| \Phi(s;p^0)_j \right\rangle \tag{3.37b}$$

the eigenvectors by

$$\Phi(s;p)_j = \Phi(s;p^0)_j + \sum_{i=1}^{m} \frac{\partial\Phi(s;p^0)_j}{\partial p_i}(p_i - p_i^0) \qquad (3.38a)$$

$$\frac{\partial\Phi(s;p^0)_j}{\partial p_i} = \sum_{k\neq j}^{R_s} \frac{\left\langle \Phi(s;p^0)_k \middle| M(s;i) \middle| \Phi(s;p^0)_j \right\rangle}{\lambda(s;p^0)_k - \lambda(s;p^0)_j} \Phi(s;p^0)_k \qquad (3.38b)$$

and the gyromagnetic ratios by

$$g(s;p)_j = \left\langle \Phi(s;p^0)_j \middle| G(s) \middle| \Phi(s;p^0)_j \right\rangle + 2 \sum_{i=1}^{m} \sum_{k\neq j} \qquad (3.39)$$

$$\frac{\left\langle \Phi(s;p^0)_j \middle| M(s;i) \middle| \Phi(s(k);p^0)_k \right\rangle \left\langle \Phi(s;p^0)_k \middle| G(s) \middle| \Phi(s;p^0)_j \right\rangle}{\lambda(s;p^0)_k - \lambda(s;p^0)_j} (p_i - p_i^0)$$

G(s), the gyromagnetic ratio matrix, and the matrices M(s;i) have been taken as real symmetric.

Minimizing Chi-Square

The chi-square to be minimized is in the form of (3.31); the theoretical quantities are eigenvalues of the Hamiltonian matrix and gyromagnetic ratios:

$$X^2(p) = \sum_{k=1}^{N_1} \frac{1}{\sigma_k^2} \left[E_k - \lambda(s(k);p)_{i(k)} \right]^2 \qquad (3.40)$$

$$+ \sum_{k=1}^{N_2} \frac{1}{\sigma'^2_k} \left[g'_k - g(s(k);p)_{i(k)} \right]^2$$

The E_k's are the experimental energies, the g_k's are the experimental g values, and s(k), i(k) indicate the assignment of the experimental

quantities to the symmetry submatrix and eigenvalue or eigenvector.

Using the linear approximations to the eigenvalues and g factors, the minimum can be found iteratively by solving for the minimum of $X^2(\Delta p)$ $\Delta p = (D_1^I, \ldots, D_m^I)$ where

$$D_j^I = p_j - p_j^{I-1} \tag{3.41a}$$

$$p_j^I = p_j^{I-1} + D_j^I \tag{3.41b}$$

and then diagonalizing the matrix for the new set of parameters p^I until convergence is reached. This algorithm is used in this work via the computer program THI written by Melhorn[53], modified slightly for present purposes. Modifications include a means of defining a new set of parameters by linear transformation, and the assignment of experimental levels to eigenvalues.

If all energy levels are corresponding to the eigenvalues of a given Hamiltonian matrix, the experimental and calculated values can be matched by relative energy ordering. The starting values of the parameters, p^0, must be close to the desired set, however, as many local minima can exist for chi-square. This problem is compounded when the experimental levels are incomplete. Two or more eigenvalues can change their relative energy orderings with each iteration, but may retain an approximate symmetry or eigenvector charactieristic of some coupling scheme.

If the Hamiltonian matrix is nearly diagonal in SL coupling, for example, it is desirable to assign energies on the basis of the largest eigenvector component, when relative intensities of the spectral lines

might indicate such a preference (see chapter sixteen of Cowan's text[3]). In addition to assignments based on energy ordering, the program THI was modified to assign selected experimental levels by largest eigenvector component if the absolute magnitude of the component is greater than a predetermined value. Remaining experimental energies are assigned on the basis of minimum residuals subject to a requirement that the eigenvectors have a specific component greater than some minimum value.

3.3.3 Isoelectronic Polynomial Fitting

A number empirical formulas are used to characterize the behavior of atomic properties as functions of the nuclear charge Z, with N, the number of electrons, fixed. For example, configuration average term energies have been fit to polynomials of the form[54,55]

$$E_{av}(Z) = \sum_{p=0}^{P} a_p (Z-s)^{2-p} \qquad (3.42)$$

with relativistic corrections[55]

$$\Delta_r(Z) = A(Z-s')^4 + B(Z-s')^6 + C(Z-s')^8 \qquad (3.43)$$

including term splittings and shifts of the average energy.

Since many atomic properties can be interpolated and extrapolated by such polynomials, the program SPCFT was written to fit an arbitrary polynomial of the form

$$a_1(Z-D_1)^{P_1} + a_2(Z-D_2)^{P_2} + \ldots$$

Because negative powers are desirable, SPCFT was constructed around a least squares minimization package VARPRO[56] that allows fitting on both

linear and non-linear parameters. SPCFT computes the all the statistical parameters mentioned above and is used here whenever a polynomial fit is needed for extrapolation or interpolation; a copy of the program can be obtained from the author.

IV. Effective Hamiltonians from Symmetry Considerations

Portions of the energy spectrum of an N-electron system such as an atom or molecule are often related to a set of semi-empirical parameters by an effective Hamiltonian description of the system. From Slater-Condon theory, an atomic effective Hamiltonians is obtained by first restricting the Hamiltonian operator to a finite dimensional subspace of the N-electron Hilbert space. Then a matrix representation of the Hamiltonian operator on the subspace is found using a basis set of Slater determinants constructed from 1-electron central field wavefunctions. To compute the Hamiltonian matrix, the integrals over angle and sums over spin coordinates are done explicitly, while integrals over the radial coordinates are treated parametrically.

Although the spin and angle dependence of the N-electron wavefunctions in terms of 1-electron angular momentum eigenfunctions is essential to the Slater-Condon parameterization, a basis set of antisymmetrized products of 1-electron central field wavefunctions is not. In general, effective Hamiltonians descriptions are useful when portions of the spectrum of a Hamiltonian operator can be well approximated by restricting it to finite dimensional subspaces spanned by wavefunctions with certain symmetry properties. The optimal set of trial wavefunctions can be chosen variationally, via the min-max principle, but an effective Hamiltonian emerges if the choice is treated empirically: The action of the Hamiltonian operator with respect to the unspecified portions of the trial wavefunctions is parameterized, with parameters chosen to give the best agreement between eigenvalues and a set of experimental energy levels.

This chapter discusses a paradigm for effective Hamiltonian descriptions of systems of N identical particles based on symmetry considerations. Trial wavefunctions are not specifically assumed to be linear combinations of products of 1-particle wavefunctions, but are allowed stronger correlations among coordinates unrelated to the specified symmetry properties. Section (4.1) outlines how effective Hamiltonians are obtained, while sections (4.2) and (4.3) discuss the structure and representation theory of the relevant symmetry groups. Section (4.4) compares this approach with independent particle models, paying particular attention to the relevance to atomic structure.

4.1 Origins of Effective Hamiltonians

Let $H = H_0 + H_1$ be the Hamiltonian for N identical particles, where H_0 is an unperturbed Hamiltonian and H_1 is a perturbation. H_0 is invariant with respect to permutations of the particles, and G; a finite or compact Lie group of symmetry transformations on the generalized coordinates of any individual particle. Then F_N, the covering group of all symmetry transformations of H_0, is either finite or a product (direct, semi-direct, etc.) of a finite and a compact Lie group. The representation theory of F_N, of its subgroups, and of induced representations of other groups provides the framework for parameterizing effective Hamiltonians.

H_1 must be invariant with respect to permutations of the particles, and, if an effective Hamiltonian description is to be used, H_1 must have lower symmetry than H_0. Typically G_H, the symmetry group of H (and therefore H_1), is G or one of its subgroups (identical transformations

applied to all particles). If H_1 must also be reasonably well behaved if it is to be restricted to a finite dimensional subspace that carries a representation of F_N (e.g. $f \in F_N \rightarrow U(f)$ a unitary operator representation of F_N, and $f \in F_N \rightarrow U(f)H_1U^{\dagger}(f)$ is well defined). Then H_1 can be expressed as a linear combination of elements from a vector space of operators that carries a (reducible) representation of F_N.

Except for accidental degeneracies, the spectral projections of H_0 generate subspaces that carry irreducible representations of F_N. Assuming that G is compact implies these representations are finite and are a subset of the the unitary transformations that map a given subspace into itself. A set of basis vectors can be found to span the subspace and carry the representation of F_N as one link in a chain of subgroups beginning with the unitary transformations on the set of basis vectors (i.e. the unitary transformations that map the subspace into itself and ending with G_H, the symmetry group of the Hamiltonian. All operators that map the subspace into itself are linear combinations of the generators of the unitary transformations on the basis vectors, and can be resolved according to irreducible representations of the same chain of subgroups. The operators that are invariant representations of G_H are possible components of the effective Hamiltonian.

Of course, not all possible components of an effective Hamiltonian are required, as in Slater-Condon theory (section (2.3)), only the components related to the 1- and 2-electron operators are needed. If $G_c \subseteq F_N$ is a link in the chain of subgroups, H_1 and the basis vectors can be reduced according to irreducible representations of G_c. The matrix elements of the restricted Hamiltonian can be written in the form:

$$\left\langle \Phi^{X'}_{x'} \middle| H \middle| \Psi^{X''}_{x''} \right\rangle = \frac{1}{2} \sum_{Q^X, x} q^X_x \left\langle \Phi^{X'}_{x'} \middle| Q^X_x \middle| \Psi^{X''}_{x''} \right\rangle + \overline{q}^{\overline{X}}_x \left\langle \Phi^{X'}_{x'} \middle| \overline{Q}^{\overline{X}}_x \middle| \Psi^{X''}_{x''} \right\rangle \qquad (4.1a)$$

$D^X(f)$ is an irreducible representation of G_c,

$$\sum_x \overline{q}^{\overline{X}}_x \overline{Q}^{\overline{X}}_x = \sum_x q^{X*}_x Q^{X\dagger}_x \qquad (4.1b)$$

and $D^{\overline{X}}$ is equivalent to D^{X*} (H is expressed as explicitly self-adjoint). The coefficients q_x must make the linear combination a scalar under the subgroup G_H; there can be as many distinct operators Q^X for a given X as there are scalar representations in this reduction.

The Wigner-Eckart theorem applies at any level of the chain, so the matrix elements $\left\langle \Phi^{X'}_{x'} \middle| Q^X_x \middle| \Psi^{X''}_{x''} \right\rangle$ for any choice of $\{x', x, x''\}$ are determined up to one or more reduced matrix elements:

$$\left\langle \Phi^{X'}_{x'} \middle| Q^X_x \middle| \Psi^{X''}_{x''} \right\rangle = \sum_{\alpha=1}^{C^{X'}_{XX''}} \left\langle X'(X,X'';\alpha),x' \middle| X,x;X'',x'' \right\rangle \frac{\left\langle \Phi^{X'} \| Q^X \| \Psi^{X''} \right\rangle_\alpha}{\sqrt{d_{X'}}} \qquad (4.2a)$$

$d_{X'}$ is the dimension of the representation $D^{X'}$ and

$$\left\langle \Phi^{X'} \| Q^X \| \Psi^{X''} \right\rangle_\alpha = \sum_{x',x,x''} \left\langle X'(X,X'';\alpha),x' \middle| X,x;X'',x'' \right\rangle^* \frac{\left\langle \Phi^{X'}_{x'} \middle| Q^X_x \middle| \Psi^{X''}_{x''} \right\rangle}{\sqrt{d_{X'}}} \qquad (4.2b)$$

The Clebsch-Gordon or CG coefficient, $C^{X'}_{XX''}$, is the number of times the irreducible representation $D^{X'}$ occurs in the reduction of $D^X \otimes D^{X''}$, and $\left\langle X'(X,X'';\alpha),x' \middle| X,x;X'',x'' \right\rangle$ is a coefficient of the unitary transformation that explicitly displays the reduction. The reduced matrix elements provide a natural parameterization for an effective Hamiltonian, subject to whatever constraints are necessary to insure Hermiticity of the

matrix. The effective Hamiltonian must also be physically reasonable (e.g. Slater-Condon theory: reasonable values for the radial integrals).

Effective Hamiltonians can be constructed without an explicit H_0 or H_1, only the algebraic properties of F_N and the detailed symmetry properties of H_1 are essential to the parameterization: The number and types of irreducible representations of a subgroup G_c are determined by the representation of F_N carried by the subspace. The construction of an effective Hamiltonian might be difficult at an arbitrary level in the chain of subgroups because the coupling coefficients to reduce the Kronecker product representations of the group are needed. For this reason, construction is usually done at the level where a detailed knowledge of the representation theory is available (e.g. SU(2) or one of its point subgroups).

The assumption that G is a compact Lie group allows much to be said about the algebraic structure of F_N, and useful information can be obtained from such general knowledge. The basic structure of an effective Hamiltonian is determined from the CG coefficients and branching properties of F_N and the other links in the chain of subgroups. The number of independent component operators available for the effective Hamiltonian are determined by these factors. In the next two sections, conjugate classes, unitary irreducible representations, simple characters, etc. are related to their counterparts of G and the symmetric (permutation) groups.

4.2 The Structure of F_N

The relationship of the structure of F_N to the structure of G and the symmetric groups is discussed in this section. Some of the properties of an abstract group F_N are revealed in (4.2.1), while the conjugate classes of F_N are related to the conjugate classes of G and the symmetric groups in (4.2.2). This relationship is needed for the discussion of the simple characters, CG coefficients, and branching properties of F_N in section (4.3).

4.2.1 Multiplication Table of F_N

F_N has two major subgroups: the permutation group S_N, and the group $G_N = GxGx...xG$ (N times). However, the unitary operators representing elements of S_N and G_N acting on N-particle wavefunctions do not in general commute. If the elements of F_N, $\{(s;\gamma) \mid s \in S_N, \gamma \in G_N\}$, correspond to the sequential application of a permutation s followed by a transformation γ to a set of coordinates $(x_1, x_2, \cdots, x_N)$, then the natural law of composition becomes (cf. eq. (4.12) below):

$$(s;\gamma)\cdot(s';\gamma') = (ss';\gamma\gamma'_s) \tag{4.3a}$$

$$(s;\gamma) = (I;\gamma)\cdot(s;I) = (s;I)\cdot(I;\gamma_{\bar{s}}) \tag{4.3b}$$

$$(s;\gamma)^{-1} = (\bar{s};\gamma_{\bar{s}}^{-1}) \tag{4.3c}$$

Where

$$\bar{s}s = I \tag{4.3d}$$

$$\gamma = \{g_1, g_2, \cdots, g_N\} \tag{4.3e}$$

$$\gamma\cdot\gamma' = \{g_1g'_1, g_2g'_2, \cdots, g_Ng'_N\} \tag{4.3f}$$

$$\gamma_s = \{g_{\bar{s}(1)}, g_{\bar{s}(2)}, \cdots, g_{\bar{s}(N)}\} \tag{4.3g}$$

(for notational convenience a $(\bar{\cdot})$ over a permutation denotes its inverse). It is clear from the multiplication law of the group elements, (4.3a), that F_N is a semi-direct product of G_N with S_N. As a result, G_N is a normal subgroup of F_N and the structure of F_N is rather intimately related to the structure of S_N.

4.2.2 Conjugate Classes of F_N

Just as an element s of S_N can be resolved into a product of commuting cyclic permutations, an element $(s;\gamma)$ of F_N has a similar resolution:

$$(s;\gamma) = \prod_i (\nu_i;\varepsilon_i) \tag{4.4a}$$

A typical $(\nu;\varepsilon)\in F_N$ in this resolution consists of a cyclic permutation of length o

$$\nu \equiv (v_1 v_2 \cdots v_o) \tag{4.4b}$$

$$\nu^n(k) = \begin{cases} v_{q(i;n,o)} & k=v_i\in\nu \\ k & k\notin\nu \end{cases} \quad k=1,\ldots,N \tag{4.4c}$$

$$q(i;n,o) = 1 + (i+n-1)_{\text{modulo}(o)} \tag{4.4d}$$

with the convention $v_1 \le v_i$, $i=1,2,\ldots,o$, and a corresponding element ε of G_N:

$$\varepsilon = \{c_1,c_2,\ldots,c_N\} \tag{4.4e}$$

$$c_i = \begin{cases} g_i\in\gamma & i\in\nu \\ I & i\notin\nu \end{cases} \tag{4.4f}$$

Conjugation of $(\nu;\xi)$ with an arbitrary element $(t;\tilde{\gamma})$ of F_N takes the form

$$(t;\tilde{\gamma})\cdot(\nu;\xi)\cdot(\bar{t};\tilde{\gamma}_{\bar{t}}^{-1}) = (I;\tilde{\gamma})\cdot(t;I)\cdot(\nu;\xi)\cdot(\bar{t};I)\cdot(I;\tilde{\gamma}^{-1}) \qquad (4.5a)$$

equivalent to conjugation with the permutation $(t;I)$ followed by conjugation with $(I;\tilde{\gamma})$. Conjugation of $(\nu;\xi)$ with $(t;I)$ results in:

$$(t;I)\cdot(\nu;\xi)\cdot(\bar{t};I) = (\nu_t;\xi_t) \qquad (4.5b)$$

$$\nu_t = t\nu\bar{t} = \left[(v_t)_1\cdots(v_t)_o\right] \qquad (4.5c)$$

$$(v_t)_i = t\left[v_{q(i;p,o)}\right] \qquad (4.5d)$$

$$t(v_p) \leq t(v_i) \qquad i=1,2,\ldots,o \qquad (4.5e)$$

An element $(\nu_t;\xi_t)$ conjugate to $(\nu;\xi)$ for a given $t\in S_N$ consists of a cyclic permutation conjugate to ν, and an element of G_N corresponding to a cyclic permutation of a fixed subset of G indexed by the cycle of permuted particles. To be more explicit, let ϕ be the o-element ordered subset of G defined as a function of $(\nu;\xi)$:

$$\phi = \phi(\nu;\xi) = \{c_{v_1},c_{v_2},\ldots,c_{v_o}\} \qquad (4.6)$$

Then $\phi^t = \phi(\nu_t;\xi_t)$, $t\in S_N$, is a cyclic permutation of ϕ, as

$$\phi^t = \phi(\nu_t;\xi_t) = \{c_{\bar{t}[(v_t)_1]},c_{\bar{t}[(v_t)_2]},\ldots,c_{\bar{t}[(v_t)_o]}\} \qquad (4.7a)$$

$$c_{\bar{t}[(v_t)_i]} = c_{q(i;n,o)} \qquad (4.7b)$$

and in particular, if $t = \nabla^n$, $\nu = \nabla^n \vee \nabla^n$, and

$$\phi(\nu;\varepsilon_{\nabla^n}) = \{c_{q(1;n,o)},\cdots,c_{q(o;n,o)}\} \tag{4.7c}$$

Conjugation of $(\nu;\varepsilon)$ with an element $(I;\tilde{\gamma})$ of F_N results in

$$(\nu;\tilde{\varepsilon}) = (I;\tilde{\gamma})\cdot(\nu;\varepsilon)\cdot(I;\tilde{\gamma}^{-1}) = (\nu;\tilde{\gamma}\varepsilon\tilde{\gamma}^{-1}_{\nu}) \tag{4.8a}$$

Then

$$\tilde{\phi} = \phi(\nu;\tilde{\gamma}\varepsilon\tilde{\gamma}^{-1}_{\nu}) = \{\tilde{g}_{v_1}c_{v_1}\tilde{g}^{-1}_{v_o},\tilde{g}_{v_2}c_{v_2}\tilde{g}^{-1}_{v_1},,\cdots,\tilde{g}_{v_o}c_{v_o}\tilde{g}^{-1}_{v_{o-1}}\} \tag{4.8b}$$

Notice that $\tilde{\phi}$ can also be any cyclic permutation of ϕ (e.g. let $\tilde{\gamma} = \varepsilon_{\nabla^n}\varepsilon_{\nabla^{n-1}}\cdots\varepsilon_{\nabla})$.

Cycle Products

The conjugate elements $(\nu;\varepsilon)$ and $(\nu;\tilde{\varepsilon})$ are related to a conjugate class of G by their cycle products $\pi,\tilde{\pi}\in G$, where

$$\pi = \pi(\nu;\varepsilon) = c_{v_o}c_{v_{o-1}}\cdots c_{v_1} \tag{4.9a}$$

$$\tilde{\pi} = \pi(\nu;\tilde{\varepsilon}) = \tilde{g}_{v_o}\pi\tilde{g}^{-1}_{v_o} \tag{4.9b}$$

The cycle products of any two conjugate cycle elements are in the same conjugate class of G, and conversely, if two cycle elements of F_N of the same length have cycle products in the same conjugate class of G, they are conjugate elements of F_N. This follows from the property that an equality between the two products of group elements

$$g'_1g'_2\cdots g'_n = g_1g_2\cdots g_n \tag{4.10a}$$

has a general relationship between individual elements of the form

$$g_i' = h_{i-1} g_i h_i^{-1} \tag{4.10b}$$

where

$$h_i = (g_1' \cdots g_i')^{-1} g_1 \cdots g_i \qquad i=1,\ldots,n \tag{4.10c}$$

$$h_0 = h_n = I \tag{4.10d}$$

The cycle product is the link between the conjugate classes of F_N and the conjugate classes of G and S_N. The conjugate classes of F_N are related to the conjugate classes of G and S_N as follows:

> Let $s \in S_N$ have a cycle resolution $s = \nu_1 \nu_2 \cdots \nu_m$. Then $(s;\gamma) \in F_N$ can be characterized by the pairs $\{(\nu_i, \pi_i) \mid i=1,\ldots,m\}$, $\pi_i = \pi(\nu_i;\gamma)$. If $(\tilde{s},\tilde{\gamma})$ is also an element of F_N characterized by the pairs $\{(\tilde{\nu}_i, \tilde{\pi}_i) \mid i=1,\ldots,m\}$, $(s;\gamma)$ and $(\tilde{s};\tilde{\gamma})$ are conjugate elements of F_N, if and only if there exists a one to one correspondence between the pairs $\{\nu,\pi\}$ and the pairs $\{\tilde{\nu},\tilde{\pi}\}$ such that each corresponding $\nu,\tilde{\nu}$ and $\pi,\tilde{\pi}$ are conjugate elements of S_N and G respectively. It follows that a conjugate class of F_N is characterized by a permutation cycle structure $\{\alpha_1,\ldots,\alpha_N\}$ (α_i is the number of cycles of length i and $1\alpha_1 + 2\alpha_2 + \cdots N\alpha_N = N$), with a corresponding conjugate class K of G for each cycle $\{K_1^1,\ldots, K_{\alpha_1}^1, K_1^2,\ldots, K_{\alpha_2}^2, \ldots, K_{\alpha_N}^N\}$.

4.3 Representation Theory of F_N

Unitary matrix irreducible representations of F_N can be found by the following method:

(1) An induced unitary operator representation of F_N is obtained by allowing the permutation operators to act on an orthonormal set of N-particle wavefunctions that carry an irreducible representation of G_N. The resulting unitary operator representation of F_N is carried on a finite dimensional space.

(2) An orthonormal basis for this space can be used to generate a unitary matrix representation of F_N.

(3) A finite dimensional unitary representation of F_N can be completely reduced to a direct sum of irreducible representations.

4.3.1 Induced Representations of F_N

Let the N-electron wavefunctions $\{\Psi^N_{R\beta}(x_1,\ldots,x_N) \mid \beta \in B^R\}$, $B^R = \{(b_1,\ldots,b_N) \mid 1 \le b_1 \le d_{r_1}, \ldots, 1 \le b_N \le d_{r_N}\}$, carry the irreducible representation $\gamma \in G_N \rightarrow D^R(\gamma) = D^{r_1}(g_1) \otimes \ldots \otimes D^{r_N}(g_N)$; $g \in G \rightarrow D^r(g)$ is a unitary matrix irreducible representation of G, $R = \{r_1,\ldots,r_N\}$, and d_r is the dimension of D^r. The action of the unitary operator representation of F_N on these wavefunctions is defined by:

$$\left[U(s;\gamma)\Psi^N_{R\beta}\right](x_1,\ldots,x_N) = \sum_{\beta'\in B^R} D^R_{\beta'\beta}(\gamma_s^-)\Psi^N_{R\beta'}(x_{s(1)},\ldots,x_{s(N)})$$

$$= \sum_{\beta'\in B^R} D^{R_s}_{\beta'_s\beta_s}(\gamma)\Psi^N_{sR_s\beta'_s}(x_1,\ldots,x_N) \qquad (4.12a)$$

Where

$$\sum_{\beta\in B^R} \equiv \sum_{b_1=1}^{d_{r_1}} \cdots \sum_{b_N=1}^{d_{r_N}} \qquad (4.12b)$$

$$R_s = (r_{s^-(1)},\ldots,r_{s^-(N)}) \qquad (4.12c)$$

$$\beta_s = (b_{s^-(1)},\ldots,b_{s^-(N)}) \qquad (4.12d)$$

so that

$$D^R_{\beta'\beta}(\gamma) = D^{R_s}_{\beta'_s\beta_s}(\gamma_s) \qquad (4.12e)$$

The functions $\{\Psi^N_{sR_s\beta_s} \equiv \left[U(s;I)\Psi^N_{R\beta}\right] \mid s\in S_N,\ \beta\in B^R\}$ span the carrier space of the induced representation of F_N, but generally are not all linearly independent. The carrier space of the induced representation is, however, composed of orthogonal subspaces that carry inequivalent irreducible representations of G_N, corresponding to the distinct permutations of $R = \{r_1,\ldots,r_N\}$.

Representations D^{Ω} of F_N

It suffices to consider representations of F_N induced from representations $\gamma\in G_N \rightarrow D^{\Omega}(\gamma)$ of G_N, where $\Omega = \{r_1^{u_1},\ldots,r_p^{u_p}\}$ ($r_i^{u_i}$ indicates D^{r_i} occurs u_i times); $u_1+\ldots+u_p = N$. If $S_N^{\Omega} \subset S_N$ is the subgroup

of all permutations within the subsets of elements $W_1 = \{1,2,\ldots,w_1\}$, $W_2 = \{w_1+1,\ldots,w_1+w_2\}$, $\ldots$, $W_p = \{N-w_p+1,\ldots,N\}$ (i.e. $S_N^{\underline{\Omega}}$ is isomorphic with $S_{w_1} x \ldots x S_{w_p}$), then the left cosets $C_{\underline{\emptyset}}^{\underline{\Omega}} = \{\underline{\emptyset} w \mid w \in S_N^{\underline{\Omega}}\}$ of $S_N^{\underline{\Omega}}$ generated by the permutations $L^{\underline{\Omega}} = \{\underline{\emptyset} \in S_N \mid \underline{\emptyset}(k) < \underline{\emptyset}(j)$ if $k < j$ and $k,j \in W_i$ for some $i=1,2,\ldots,p\}$ in turn generate orthogonal subspaces that carry inequivalent representations $D^{\underline{\Omega}_{\underline{\emptyset}}}$ of G_N spanned by the vectors $K_{\underline{\emptyset}}^{\underline{\Omega}} = \{\Psi^N_{\underline{\emptyset} w \underline{\Omega}_{\underline{\emptyset}} \beta} \equiv U(\underline{\emptyset} w; I)\Psi^N_{\underline{\Omega}\beta_{\bar{w}}} \mid w \in S_N^{\underline{\Omega}},\ \beta \in B^{\underline{\Omega}}\}$ (note: $\underline{\Omega}_{\underline{\emptyset} w} = \underline{\Omega}_{\underline{\emptyset}}$). Under the action of the unitary operator representation of F_N, these vectors transform:

$$U(s;\gamma)\Psi^N_{\underline{\emptyset}' w' \underline{\Omega}_{\underline{\emptyset}'} \beta'} = \sum_{\underline{\emptyset} \in L^{\underline{\Omega}}} \sum_{w \in S_N^{\underline{\Omega}}} \sum_{\beta \in B^{\underline{\Omega}}} \delta_{\underline{\emptyset} w, s \underline{\emptyset}' w'} D^{\underline{\Omega}}_{\beta \beta'_{w\bar{w}'}}(\gamma_{\bar{\emptyset}})\Psi^N_{\underline{\emptyset} w \underline{\Omega}_{\underline{\emptyset}} \beta} \quad (4.13a)$$

$$= \sum_{\underline{\emptyset} \in L^{\underline{\Omega}}} \sum_{w \in S_N^{\underline{\Omega}}} \sum_{\beta \in B^{\underline{\Omega}}} \delta_{\underline{\emptyset} w, s \underline{\emptyset}'} D^{\underline{\Omega}_{\underline{\emptyset}}}_{\beta_{\underline{\emptyset}} \beta'_{\underline{\emptyset} w}}(\gamma)\Psi^N_{\underline{\emptyset}(ww')\underline{\Omega}_{\underline{\emptyset}} \beta} \quad (4.13b)$$

From equation (4.13b) it appears, perhaps, that the induced carrier space of F_N carries a reducible representation of $G_N x S_N^{\underline{\Omega}}$ as a subgroup of F_N. In fact, (4.13b) has the correct form for an element of the direct product representation of $G_N x S_N^{\underline{\Omega}}$ if $\underline{\emptyset}' = \underline{\emptyset}$, $\underline{\emptyset} s \bar{\underline{\emptyset}} = w$, and $\beta'_w = \beta'$.

Each linear span of vectors $K_{\underline{\emptyset}}^{\underline{\Omega}}$ is in turn a direct sum of orthogonal subspaces $J^{\underline{\Omega}}_{\beta\underline{\emptyset}}$, spanned by the vectors $V^{\underline{\Omega}}_{\underline{\emptyset}\beta} = \{\Psi^N_{\underline{\emptyset} w \underline{\Omega}_{\underline{\emptyset}} \beta} \mid w \in S_N^{\underline{\Omega}}\}$ for each pair $(\underline{\emptyset},\beta)$. Any subspace $J^{\underline{\Omega}}_{\beta\underline{\emptyset}}$ is mapped by a unitary transformation (permutation) into any other subspace $J^{\underline{\Omega}}_{\underline{\emptyset}'\beta'}$. Thus any orthonormal basis constructed from the subset $V^{\underline{\Omega}}_{I\tilde{\beta}}$ spanning $J^{\underline{\Omega}}_{I\tilde{\beta}}$, where $\tilde{\beta}$ is any fixed element of $B^{\underline{\Omega}}$, generates an orthonormal basis for the entire carrier space of the induced representation of F_N. The inner product between

any pair of vectors in the set $\{\Psi_{\emptyset w \underline{\Omega}_\emptyset \beta} \mid \emptyset \leftarrow L^{\underline{\Omega}}, w \leftarrow S_N^{\underline{\Omega}}, \beta \leftarrow B^{\underline{\Omega}}\}$ can be expressed:

$$\left\langle \Psi^N_{\emptyset' w' \underline{\Omega}_{\emptyset'} \beta'} \middle| \Psi^N_{\emptyset w \underline{\Omega}_\emptyset \beta} \right\rangle = \delta_{\beta\beta'} \delta_{\emptyset\emptyset'} \left\langle \Psi^N_{Iw' \underline{\Omega}_\emptyset \tilde{\beta}} \middle| \Psi^N_{Iw \underline{\Omega}_\emptyset \tilde{\beta}} \right\rangle \qquad (4.14)$$

Generators and Subgroups

The operator representations of some of the projections from the group ring of G_N can be employed to investigate the carrier space of the induced representation of F_N. Let the operators $\{E^R_{\beta\beta'} \mid \beta, \beta' \leftarrow B^R\}$ be defined:

$$E^R_{\beta\beta'} = d_{r_1} \cdots d_{r_N} \int_{G_N} d^N y \; D^R_{\beta'\beta}(y^{-1}) \; U(I;y) \qquad (4.15)$$

The integral

$$\int_{G_N} d^N y = \int_{G_N} dg_1 dg_2 \cdots dg_N = 1$$

represents the multiple integration with respect to the normalized left invariant Haar measure over the group G[57,58].

The translation invariance of the Haar measure[57,58], combined with the orthogonality of the matrix elements of unitary irreducible representations expressed by

$$\int_{G_N} d^N y \; D^{R'*}_{\beta_1\beta_1'}(y) D^R_{\beta_2\beta_2'}(y) = \frac{\delta_{RR'} \delta_{\beta_1\beta_1'} \delta_{\beta_2\beta_2'}}{d_{r_1} \cdots d_{r_N}}$$

give these operators the properties:

$$E^{R\dagger}_{\beta\beta'} = E^R_{\beta\beta'} \qquad (4.16a)$$

$$U(s;\gamma)E^{R}_{\beta\beta'} = \sum_{\beta''\in B^R} D^{R_s}_{\beta''_s\beta_s}(\gamma)E^{R_s}_{\beta''_s\beta'_s}U(s;I) \qquad (4.16b)$$

$$E^{R_1}_{\beta_1\beta'_1}E^{R_2}_{\beta_2\beta'_2} = \delta_{R_1R_2}\delta_{\beta'_1\beta_2}E^{R_1}_{\beta_1\beta'_2} \qquad (4.16c)$$

$$E^{R_1}_{\beta_1\beta'_1}\Psi_{R_2\beta_2}(x_1,\ldots,x_N) = \delta_{R_1R_2}\delta_{\beta'_1\beta_2}\Psi_{R_1\beta_1}(x_1,\ldots,x_N) \qquad (4.16d)$$

The operators, $\{E^{R}_{\beta\beta'},\ \beta,\beta'\in B^R\}$ for fixed R, are also a representation of the Lie algebra for the set of all unitary transformations on the set of N-particle wavefunctions $\{\Psi_{R\beta}\mid \beta\in B^R\}$, that carry $\gamma\in G_N\to D^R(\gamma)$ (i.e. $\gamma\in G_N\to D^R(\gamma)$ $D^R(\gamma)\subset U(d_R)$, $d_R = d_{r_1}\ldots d_{r_N}$). The representation D^R is a link in a number of possible chains of subgroups headed by $U(d_R)$.

A representation of $SU(d_{r_1})xSU(d_{r_2})x\ldots xSU(d_{r_N})$ is generated by the operators $\{e^{(r_i)}_{b''b'}(i;R)\mid b'',b' = 1,2,\ldots,d_{r_i}\}$ defined by

$$e^{(r_i)}_{b''b'}(i;R) = \sum_{\beta'',\beta'\in B^R}\delta_{b'_ib'}\,\delta_{b''_ib''}\prod_{j\neq i}\delta_{b'_jb''_j}\,E^{R}_{\beta''\beta'} \qquad (4.17)$$

A representation D^r is a subgroup of $SU(d_r)$, generated by some subset of the operators $\{e^{r}_{b''b'}\}$. If the representations $\{D^{r_i}\mid i=1,\ldots,N\}$ are faithful representations of the group G, there is a chain of subgroups $U(d_R)\supset SU(d_{r_1})x\ldots xSU(d_{r_N})\supset G_N\supset G$.

Another chain of subgroups appropriate to the irreducible representations of $S_N xG\subset F_N$ is generated by the operators $\{E^{r}_{b''b'}\mid b'',b' = 1,2,\ldots,d_r\}$, defined by

$$E^{r}_{b''b'} = \sum_{\emptyset \in L^{\Omega}} \sum_{i=1}^{N} \delta_{r,r_i} e^{(r_i)}_{b''b'}(i;\underline{\Omega}_{\emptyset}) \qquad (4.18)$$

These operators commute with permutations of the particles and generate a representation of $SU(d_{r_1}) \times \ldots \times SU(d_{r_p})$ on the induced carrier space of F_N.

Representations of S^{Ω}_N

Another subgroup of $U(d_R)$, induced from a representation D^R of G_N, is the set of permutations the vectors $\{\Psi_{R\beta} \mid \beta \in B^R\}$, distinct from the subgroup of permutations of the particles that leaves R invariant. This relationship is a key to the representation structure of F_N.

If $\tilde{\beta} = \{b_1 = \ldots = b_{u_1} = \tilde{b}_1,\ b_{u_1+1} = \ldots = b_{u_2} = \tilde{b}_2,\ \ldots,\ b_{N-u_p+1} = \ldots = b_N = \tilde{b}_p\}$, the vectors $V^{\Omega}_{I\tilde{\beta}} = \{\Psi_{Iw\underline{\Omega}\tilde{\beta}} \mid w \in S^{\Omega}_N\}$ carry a representation of S^{Ω}_N under $w \in S^{\Omega}_N \rightarrow U(w;I)$. An equivalent representation of S^{Ω}_N is carried by the vectors $V^{\Omega}_{\emptyset\beta}$ for each $\emptyset \in L^{\Omega}$, $\beta \in B^{\Omega}$, with the equivalence mapping:

$$\Psi_{I\underline{\Omega}\tilde{\beta}} \rightarrow \Psi_{\emptyset w\underline{\Omega}_{\emptyset}\beta} = U(\emptyset;I)E^{\Omega}_{\beta\tilde{\beta}}\Psi_{Iw\underline{\Omega}\tilde{\beta}} \qquad (4.19a)$$

$$U(w;I) \rightarrow \left[U(\emptyset;I)E^{\Omega}_{\beta\tilde{\beta}}\right]U(w;I)\left[U(\emptyset;I)E^{\Omega}_{\beta\tilde{\beta}}\right]^{\dagger} \qquad (4.19b)$$

$$= E^{\Omega_{\emptyset}}_{\beta_{\emptyset}\tilde{\beta}_{\emptyset}} U(\emptyset w \emptyset^{-1};I) E^{\Omega_{\emptyset}}_{\tilde{\beta}_{\emptyset}\beta_{\emptyset}}$$

The unitary operators $\{P^{\Omega}(w) \mid w \in S^{\Omega}_N\}$, defined by

$$P^{\Omega}(w) = \sum_{\emptyset \in L^{\Omega}} \sum_{\beta \in B^{\Omega}} E^{\Omega_{\emptyset}}_{\beta_{\emptyset}\tilde{\beta}_{\emptyset}} U(\emptyset w \emptyset^{-1};I) E^{\Omega_{\emptyset}}_{\tilde{\beta}_{\emptyset}\beta_{\emptyset}} \qquad (4.20a)$$

are a representation of S_N^{Ω}, and from (4.6d)

$$P^{\Omega}(w')\Psi_{\emptyset w \underline{\Omega}_{\emptyset}\beta} = \Psi_{\emptyset w' w \underline{\Omega}_{\emptyset}\beta} \tag{4.20b}$$

implying that

$$P^{\Omega}(w)U(I,\gamma) = U(I;\gamma)P^{\Omega}(w) \tag{4.20c}$$

For completeness, note that the unitary operators, $\{\Gamma^{\Omega}(w) \mid w \in S_N^{\Omega}\}$, defined by

$$\Gamma^{\Omega}(w) = \sum_{\emptyset \in L^{\Omega}} \sum_{\beta \in B^{\Omega}} E^{\Omega_{\emptyset}}_{\beta_{\emptyset} w \beta_{\emptyset}} \tag{4.21}$$

commute with the operators $\{P^{\Omega}(w) \mid w \in S_N^{\Omega}\}$, and are also a representation of S_N^{Ω}. These operators permute the vectors $\{\Psi_{\emptyset w_o \underline{\Omega}_{\emptyset}\beta} \mid \beta \in B^{\Omega}\}$ for fixed $\emptyset, w_o$. Also, the combined operators $\{\Pi^{\Omega}(w) \mid w \in S_N^{\Omega}\}$,

$$\Pi^{\Omega}(w) = \Gamma^{\Omega}(w)P^{\Omega}(w) = P^{\Omega}(w)\Gamma^{\Omega}(w) \tag{4.22}$$

are direct sums operators $\{U(\emptyset w \emptyset^{-1};I) \mid w \in S_N^{\Omega}\}$ restricted to the subspaces $J^{\Omega}_{\beta\emptyset}$.

The commutation relation (4.20c) indicates that a set of N-particle wavefunctions can be found that carries an irreducible representation $D^{\Omega} \otimes D^{\wedge}$ of $G_N \times S_N^{\Omega}$ under $\gamma \in G_N, w \in S_N^{\Omega} \rightarrow U(I;\gamma)P^{\Omega}(w)$. If G, the symmetry group of a single particle, is the rotation group, the symmetry group S_N^{Ω} applies to the radial coordinates: The operators $\{P^{\Omega}(w) \mid w \in S_N^{\Omega}\}$ permute the radial coordinates of the particles that carry the same representation of the rotation group. In general, the N-particle wavefunctions have one or more degrees of freedom associated with each particle that

are independent of symmetry operations of G, and the operators $\{P^{\Omega}(w) \mid w \in S_N^{\Omega}\}$ permute the coordinates associated with the additional degrees of freedom among groups of corresponding to the same irreducible representation of G.

The irreducible matrix representations of S_N^{Ω} are Kronecker products of the irreducible matrix representations of S_{u_1}, S_{u_2}, ..., S_{u_p}. An irreducible representation of S_u is described by a Young diagram, or equivalently a set of integers $[\lambda] = [\lambda_1 \geq \cdots \geq \lambda_u \geq 0]$; $\lambda_1 + \cdots + \lambda_u = u$. The basis vectors of of an irreducible representation of S_u are labeled by the standard Young tableaux depicted in figure (4.1a). A standard Young tableau is simply the Young diagram filled with the integers $\{1,2,\ldots,u\}$ in increasing order from left to right in each row and top to bottom in each column. The standard tableaux graphically denote the decomposition of an irreducible representation of S_u into irreducible representations of its subgroups via the chain $S_u \subset S_{u-1} \subset \cdots \subset S_1$. Removing the boxes containing the integers u, u-1, ..., u-q+1, from a standard tableau of S_u leaves a standard tableau of S_{u-q}.

An irreducible representation D^{Λ} of S_N^{Ω} is labeled by p Young diagrams or the p sets of integers $\Lambda = \{[\lambda]^i \mid i=1,\ldots,p\}$ where $[\lambda]^i = \{\lambda_1^i \geq \lambda_2^i \geq \cdots \geq \lambda_{u_i}^i \geq 0;\ \lambda_1^i + \cdots + \lambda_{u_i}^i = u_i\}$. The basis vectors of D^{Λ} are p-tuples of standard Young tableaux as indicated in figure (4.1b). A standard p-tuple p from the set Y^{Ω} consists of p Young diagrams where the i^{th} diagram is filled with the integers W_i, ordered by increasing values with respect to rows and columns.

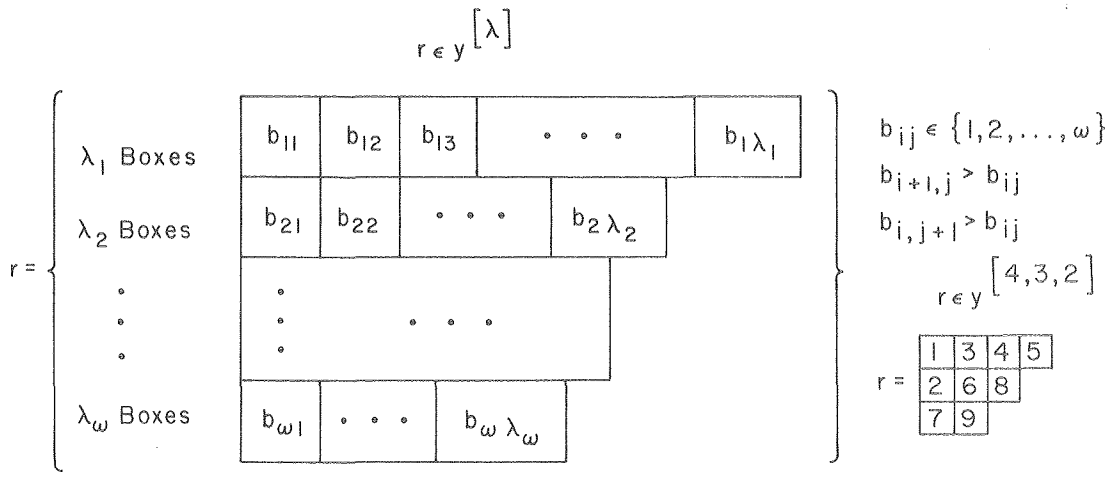

Figure (4.1a)

Young tableau describing a basis vector of an irreducible representation $D^{[\lambda]}$ of S_ω.

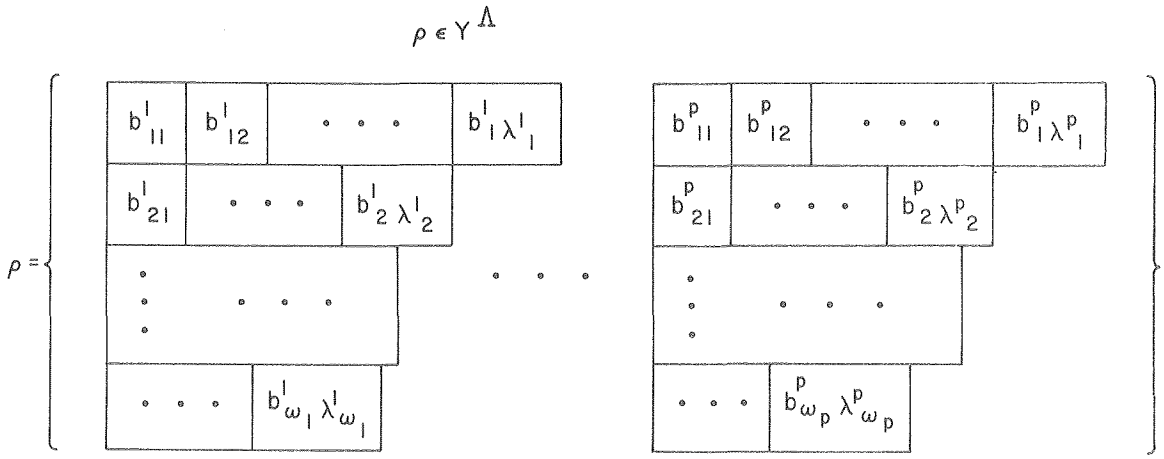

$b^k_{ij} \in W_k = \{\sigma_k + 1, \sigma_k + 2, \ldots, \sigma_k + \omega_k\}$

$\sigma_k = \omega_1 + \omega_2 + \ldots + \omega_{k-1}$

XBL 805-899

Figure (4.1b)

p-Tuple of Young tableaux describing a basis vector of the irreducible representation D^{Λ} of S_N^Q.

4.3.2 Unitary Irreducible Representations of F_N

With the above considerations about the reduction of the induced representation of F_N in terms of representation of $G_N \times S_N^{\Omega}$, a general statement about unitary representations of F_N can now be made:

Let $\{\Phi^{(\Omega,\Lambda)}_{\beta\rho} \mid \beta \in B^{\Omega},\ \rho \in Y^{\Lambda}\}$ be an orthonormal set of N-particle wavefunctions that carries the unitary irreducible representations $D^{\Lambda} \otimes D^{\Omega}$ of $S_N^{\Omega} \times G_N$ and under the actions of the operator representations $\gamma \in G_N \rightarrow U(I;\gamma)$, $w \in S_N^{\Omega} \rightarrow P^{\Omega}(w)$:

$$P^{\Omega}(w)U(I;\gamma)\Phi^{(\Omega,\Lambda)}_{\beta'\rho'}(x_1,\ldots,x_N) = \sum_{\rho \in Y^{\Lambda}} \sum_{\beta \in B^{\Omega}} D^{\Lambda}_{\rho\rho'}(w) D^{\Omega}_{\beta\beta'}(\gamma) \Phi^{(\Omega,\Lambda)}_{\beta\rho}(x_1,\ldots,x_N) \tag{4.23}$$

with $U(I;\gamma)$ and $P^{\Omega}(w)$ defined as above: Then the set of N-particle wavefunctions $\{\Phi^{(\Omega,\Lambda)}_{\phi\beta\rho} = U(\phi;I)\Phi^{(\Omega,\Lambda)}_{\beta\rho} \mid \phi \in L^{\Omega},\ \beta \in B^{\Omega},\ \rho \in Y^{\Lambda}\}$ carry an induced unitary representation of F_N given by

$$U(s;\gamma)\Phi^{(\Omega,\Lambda)}_{\phi'\beta'\rho'}(x_1,\ldots,x_N) = \sum_{\phi \in L^{\Omega}} \sum_{w \in S_N^{\Omega}} \delta_{\phi w, s\phi'} \tag{4.24a}$$

$$\sum_{\beta \in B^{\Omega}} \sum_{\rho \in Y^{\Lambda}} D^{\Omega_\phi}_{\beta_\phi \beta'_{s\phi'}}(\gamma)\ D^{\Lambda}_{\rho\rho'}(w) \Phi^{(\Omega,\Lambda)}_{\phi\beta\rho}(x_1,\ldots,x_N)$$

and the matrices for this representation are given by

$$\left\langle \Phi^{(\Omega,\Lambda)}_{\phi\beta\rho} \mid U(s;\gamma) \mid \Phi^{(\Omega,\Lambda)}_{\phi'\beta'\rho'} \right\rangle = D^{(\Omega,\Lambda)}_{\phi\beta\rho\phi'\beta'\rho'}(s;\gamma) = \tag{4.24b}$$

$$\Delta(\bar{\phi}s\phi';S_N^{\Omega})\ D^{\Omega_\phi}_{\beta_\phi \beta'_{s\phi'}}(\gamma)\ D^{\Lambda}_{\rho\rho'}(\bar{\phi}s\phi')$$

where

$$\Delta(w;S_N^{\underline{\Omega}}) = \begin{cases} 1 & w\in S_N^{\underline{\Omega}} \\ 0 & w\notin S_N^{\underline{\Omega}} \end{cases} \qquad (4.24c)$$

Irreducibilty of $D^{(\underline{\Omega},\Lambda)}$

It is straight forward to show that the unitary representations of F_N defined by (4.24) are also irreducible. From the orthogonality relation (4.6) it follows that

$$\int_{G_N} d^N y \; D^{(\underline{\Omega}_a,\Lambda_a)*}_{\phi_a\beta_a p_a \phi'_a\beta'_a p'_a}(s;y)\; D^{(\underline{\Omega}_b,\Lambda_b)}_{\phi_b\beta_b p_b \phi'_b\beta'_b p'_b}(s;y) =$$

$$\frac{\delta_{\beta_a\beta_b}\delta_{(\beta'_a)s\phi'_a(\beta'_b)s\phi'_b}\delta_{\underline{\Omega}_a\underline{\Omega}_b}\delta_{\phi_a\phi_b}}{d_{\underline{\Omega}_a}} D^{\Lambda_a *}_{\rho_a\rho'_a}(\bar{\phi}_a s\phi'_a)\; D^{\Lambda_b}_{\rho_b\rho'_b}(\bar{\phi}_a s\phi'_b) \qquad (4.26a)$$

$$\Delta(\bar{\phi}_a s\phi'_a;S_N^{\underline{\Omega}_a})\,\Delta(\bar{\phi}_a s\phi'_b;S_N^{\underline{\Omega}_a})$$

but

$$\Delta(\bar{\phi}_a s\phi'_a;S_N^{\underline{\Omega}_a})\,\Delta(\bar{\phi}_a s\phi'_b;S_N^{\underline{\Omega}_a}) = \Delta(\bar{\phi}_a s\phi'_a;S_N^{\underline{\Omega}_a})\,\Delta(\bar{\phi}'_a\phi'_b;S_N^{\underline{\Omega}_a}) \qquad (4.26b)$$

since $(\bar{\phi}_a s\phi'_a)\in S_N^{\underline{\Omega}_a}$ implies that $\overline{(\bar{\phi}_a s\phi'_a)} = (\bar{\phi}'_a \bar{s}\phi_a)\in S_N^{\underline{\Omega}_a}$. Thus (4.26a) is non-vanishing only if $\phi'_b = \phi'_a w$, $w\in S_N^{\underline{\Omega}_a}$. However, each $\phi\in L^{\underline{\Omega}}$ generates distinct left coset of $S_N^{\underline{\Omega}_a}$, so this can only be true if $\phi'_b = \phi'_a$ and $w = I$. Then from the orthogonality of the unitary matrix elements of D^{Λ}:

$$\frac{1}{N!}\sum_{s\in S_N}\int_{G_N} d^N y\; D^{(\underline{\Omega}_a,\Lambda_a)*}_{\emptyset_a\beta_a p_a \emptyset'_a\beta'_a p'_a}(s;y)\; D^{(\underline{\Omega}_b,\Lambda_b)}_{\emptyset_b\beta_b p_b \emptyset'_b\beta'_b p'_b}(s;y) \;=\; (4.26c)$$

$$\frac{\delta_{\beta_a\beta_b}\delta_{\beta'_a\beta'_b}\delta_{\underline{\Omega}_a\underline{\Omega}_b}\delta_{\emptyset_a\emptyset_b}\delta_{\emptyset'_a\emptyset'_b}\delta_{\Lambda_a\Lambda_b}\delta_{\rho_a\rho_b}\delta_{\rho'_a\rho'_b}}{d_{\underline{\Omega}_a} d_{\Lambda_a}}$$

In the case of a finite or compact Lie group, the orthogonality (4.26c) of the matrix representations is equivalent to irreducibilty.

4.3.3 The Characters of F_N

The character of the irreducible representation $D^{(\underline{\Omega},\Lambda)}$ is calculated by summing the diagonal matrix elements given by (4.24b):

$$X^{(\Lambda;\underline{\Omega})}(s;y) \;=\; \sum_{\emptyset\in L^{\underline{\Omega}}}\sum_{\beta\in B^{\underline{\Omega}}}\sum_{p\in Y^{\Lambda}} \Delta(\bar{\emptyset}s\emptyset;S_N^{\underline{\Omega}})\; D^{\underline{\Omega}\emptyset}_{\beta\emptyset\,\beta\emptyset}(y) D^{\Lambda}_{pp}(\bar{\emptyset}s\emptyset) \qquad (4.27)$$

$$= \sum_{\emptyset\in L^{\underline{\Omega}}}\sum_{w\in S_N^{\underline{\Omega}}} \delta_{(\bar{\emptyset}s\emptyset),w} \sum_{\beta\in B^{\underline{\Omega}}}\sum_{p\in Y^{\Lambda}} D^{\underline{\Omega}}_{\beta\beta_w}(y_{\bar{\emptyset}}) D^{\Lambda}_{pp}(w)$$

The content of this expression becomes clearer if $w\in S_N^{\underline{\Omega}}$ is resolved into cycle elements. The cycle structure of any $w\in S_N^{\underline{\Omega}}$ is comensurate with $\underline{\Omega} = \{\omega_1,\ldots,\omega_p\}$, so a given $w\in S_N^{\underline{\Omega}}$ can be expressed in the form:

$$w \;=\; \prod_{i=1}^{p}\prod_{j=1}^{n(i)} \nu^{ij} \qquad (4.28a)$$

$$\nu^{ij} \;=\; \left\{ v_1^{ij} v_2^{ij} \ldots v_{o_{ij}}^{ij} \right\} \subset W_i \qquad (4.28b)$$

Combining with (4.27) leads to:

$$\sum_{\beta\in B^{\Omega}} \sum_{\rho\in Y^{\Lambda}} D^{\Omega}_{\beta\beta_w}(\gamma_{\phi}) D^{\Lambda}_{\rho\rho'}(w) = \sum_{\beta\in B^{\Omega}} \prod_{i=1}^{p} X^{[\lambda]^i}(\psi^{i1}\cdots\psi^{in(i)}) \tag{4.29}$$

$$\prod_{j=1}^{n(i)} \left[D^{r_i}_{b_{v_1} b_{v_o}}(g_{\phi(v_1)}) D^{r_i}_{b_{v_2} b_{v_1}}(g_{\phi(v_2)}) \cdots D^{r_i}_{b_{v_o} b_{v_{o-1}}}(g_{\phi(v_o)}) \right]_{(v_1\cdots v_o)=\psi^{ij}}$$

The sum over any cycle of elements $\{b_{v_1},\ldots,b_{v_o}\}$ is a character of a cycle product:

$$X^r(c_{v_o}\cdots c_{v_1}) = \sum_{b_{v_1}\cdots b_{v_o}=1}^{d_r} D^r_{b_{v_1} b_{v_o}}(c_{v_1})\cdots D^r_{b_{v_o} b_{v_{o-1}}}(c_{v_o}) \tag{4.30}$$

The character of $f\in F_N \rightarrow D^{(\Omega,\Lambda)}(f)$ becomes

$$X^{(\Omega,\Lambda)}(s;\gamma) = \sum_{\phi\in L^{\Omega}} \sum_{w\in S_N^{\Omega}} \delta_{(w,\phi s\phi)} \tag{4.31}$$

$$\prod_{i=1}^{p} X^{[\lambda]^i}(\psi^{i1}\cdots\psi^{in(i)}) \prod_{j=1}^{n(i)} X^{r_i}(\pi^{ij})$$

where $\pi^{ij} = \pi(\psi^{ij};\gamma_{\phi})$.

A nonvanishing term in the double sum on the right-hand-side of (4.31) means that $\phi w\phi = s$, or equivalently that each $\psi^{ij} = \tilde{\psi}^k_{\phi}$, where $\tilde{\psi}^k$ is a cyclic permutation of s. It follows that $\pi(\psi^{ij};\gamma_{\phi^{-1}})$ and $\pi(\tilde{\psi}^k;\gamma)$ are conjugate elements of G, and that $X^{(\Omega,\Lambda)}(s;\gamma)$ is a function of only the cycle structure $\{\alpha\} = \{\alpha_1,\alpha_2,\ldots,\alpha_N\}$ of s, and the cycle products $\{\pi\} = \{\pi^i_j \mid j=1,2,\ldots,\alpha_i;\ i=1,2,\ldots,N\}$. The permutations $\phi\in L^{\Omega}$ map the sets of integers W_i into all possible u_1-, u_2-, ..., u_p-element, ordered, disjoint subsets of $\{1,2,\ldots,N\}$. Effectively, (4.30) is a sum over all distinct distributions of the cycle pairs of $(s;\gamma)$, $\{(\psi,\tilde{\pi})\}$, in

to p groups with the cycle lengths commensurate with $\{w_1,w_2,\ldots,w_p\}$. Expressed in terms $\{\alpha\}$, $\{\pi\}$, $X^{(\Omega,\Lambda)}(s;\gamma)$ becomes

$$X^{(\Omega,\Lambda)}(\{\alpha;\pi\}) = \sum_{(\beta)_1 \geq 0}^{\alpha_1} \cdots \sum_{(\beta)_N \geq 0}^{\alpha_N} \prod_{i=1}^{p} \delta_{(\beta_1^i+2\beta_2^i+\ldots+N\beta_N^i),w_i}$$

$$\prod_{j=1}^{N} \frac{\alpha_j!}{\beta_j^1!\cdots\beta_j^p!} X^{[\lambda]^i}(\beta_1^i,\ldots,\beta_N^i)\, Y^{\Omega}(\{\beta\},\{\alpha;\pi\}) \tag{4.32a}$$

$$Y^{\Omega}(\{\beta\},\{\alpha;\pi\}) = \prod_{j=1}^{N} \frac{1}{\alpha_j!} \sum_{t\in S_{\alpha_j}} \prod_{k=1}^{\alpha_j} X^{r[k;(\beta)_j]}(\pi^j_{t(k)}) \tag{4.32b}$$

$$X^{r[k;(\beta)_j]} = \begin{cases} X^{r_1} & 1 \leq k \leq \beta_j^1 \\ X^{r_2} & 1+\beta_j^1 \leq k \leq \beta_j^1+\beta_j^2 \\ \vdots & \vdots \\ X^{r_p} & \alpha_j-\beta_j^p+1 \leq k \leq \alpha_j \end{cases} \tag{4.32c}$$

$$\sum_{(\beta)_j \geq 0}^{\alpha_j} \equiv \sum_{\beta_j^1 \geq 0} \cdots \sum_{\beta_j^p \geq 0} \delta_{(\beta_j^1+\cdots+\beta_j^p),\alpha_j} \tag{4.32d}$$

and from the translation invariance of the Haar measure and the orthonormality of the characters of a finite or compact Lie group, the functions $Y^{\Omega}(\{\beta\},\{\alpha;\pi\})$ have orthogonality properties:

$$\int_{G_N} d^N y \; Y^{\Omega}(\{\beta\},\{\alpha;\pi\}) Y^{\Omega'}(\{\beta'\},\{\alpha;\pi\}) \quad = \tag{4.33a}$$

$$\prod_{j=1}^{N} \frac{\beta_j^1! \ldots \beta_N^p!}{\alpha_j!} \delta_{\{\beta'\}\{\beta\}} \delta_{\Omega'\Omega}$$

In addition, some other relations useful in determining the CG coefficients of F_N are given by:

$$\prod_{j=1}^{N} \frac{\alpha_j!}{\beta_j^1! \ldots \beta_N^p!} \int_{G_N} d^N y \; \left| Y^{\Omega}(\{\beta\},\{\alpha;\pi\}) \right|^2 X^r(\pi_k^j) \quad = \quad \frac{1}{\alpha_j} \sum_{i=1}^{p} C_{rr_i}^{r_i} \beta_j^i \tag{4.33b}$$

$$\prod_{j=1}^{N} \frac{\alpha_j!}{\beta_j^1! \ldots \beta_N^p!} \int_{G_N} d^N y \; \left| Y^{\Omega}(\{\beta\},\{\alpha;\pi\}) \right|^2 X^r(\pi_k^j) X^{r'}(\pi_{k'}^j) \quad = \tag{4.33c}$$

$$\frac{1}{\alpha_j(\alpha_j-1)} \left[\sum_{i=1}^{p} C_{rr_i}^{r_i} C_{r'r_i}^{r_i} \beta_j^i(\beta_j^i-1) + \sum_{i \neq i'=1}^{p} (C_{rr_i}^{r_i} C_{r'r_{i'}}^{r_{i'}} + C_{rr_i}^{r_{i'}} C_{r'r_{i'}}^{r_i}) \beta_j^i \beta_j^{i'} \right]$$

$C_{rr'}^{r''}$ is a CG coefficient for the group G, and $k \neq k'$ in (4.33c).

Subgroup Branching

The expression for the character $X^{(\Omega,\Lambda)}$ given by (4.32) is especially suited to the branching of F_N under the restriction to the subgroup G_N. In this case the permutation s = I, so $\alpha_1 = N$, $\alpha_2 = \ldots = \alpha_N = 0$, and $X^{(\Omega,\Lambda)}$ reduces to

$$X^{(\Omega,\Lambda)}(\{\alpha_1=N\};y) \quad = \quad d_\Lambda \sum_{\emptyset \leftarrow L^\Omega} X^{\Omega_\emptyset}(y) \tag{4.34}$$

reflecting the decomposition of the carrier space into a direct sum of subspaces that carry the representations $D^{\Omega_\emptyset}$ of G_N.

Representations of F_N must decompose into irreducible representations of $S_N \times G$ upon restriction to this subgroup. To exhibit this decomposition of of F_N, The function $Y^{\Omega}(\{\beta\},\{\alpha;\pi\})$ can be rewritten as

$$Y^{\Omega}(\{\beta\},\{\alpha;\pi\}) = \left[\prod_{i=1}^{p} \sum_{[\mu]^i}^{S_{w_i}} X^{[\mu]^i}(\beta_1^i,\ldots,\beta_N^i)\right] Z^{\Omega}(\{[\mu]\},\{\alpha;\pi\}) \qquad (4.35a)$$

$$Z^{\Omega}(\{[\mu]\},\{\alpha;\pi\}) = \sum_{(\beta)_1 \geq 0}^{\alpha_1} \cdots \sum_{(\beta)_N \geq 0}^{\alpha_N} \prod_{i=1}^{p} \delta_{(\beta_1^i+2\beta_2^i+\ldots+N\beta_N^i),w_i} \qquad (4.35b)$$

$$\prod_{i=1}^{p} \frac{O(\{\beta\}^i)}{w_i!} X^{[\mu]^i}(\{\beta\}^i)\ Y^{\Omega}(\{\beta\},\{\alpha;\pi\})$$

using the completeness of the simple characters in the space of class valued functions of the symmetric groups[36], i.e.

$$\delta_{\{\beta'\}\{\beta\}} = \sum_{[\lambda]}^{S_w} X^{[\lambda]}(\{\beta'\}) X^{[\lambda]}(\{\beta\}) \frac{O(\{\beta\})}{w!} \qquad (4.35c)$$

and $O(\{\beta\})$ is the number of group elements in the conjugate class $\{\beta\}$.

The products of characters of the symmetric groups S_{w_i} reduce to the Clebsch-Gordon series

$$X^{[\lambda]^i}(\{\beta\}^i) X^{[\mu]^i}(\{\beta\}^i) = \sum_{[\nu]^i} C^{[\nu]^i}_{[\lambda]^i[\mu]^i} X^{[\nu]^i}(\{\beta\}^i) \qquad (4.36)$$

The expression (4.35a) contains a multiple sum of terms of this type, as

$$\prod_{i=1}^{p} X^{[\lambda]^i}(\beta_1^i,\ldots,\beta_N^i)\ Y^{\Omega}(\{\beta\},\{\alpha;\pi\}) = \qquad (4.37)$$

$$\sum_{[\nu]^1} C^{[\nu]^1}_{[\lambda]^1[\mu]^1} \cdots \sum_{[\nu]^p} C^{[\nu]^p}_{[\lambda]^p[\mu]^p} \prod_{i=1}^{p} X^{[\nu]^i}(\beta_1^i,\ldots,\beta_N^i)$$

The sum over products of simple characters of $S_{w_1}, \ldots, S_{w_p}$,

$$\chi^{\wedge}(\{\alpha\}) = \sum_{(\beta)_1 \geq 0}^{\alpha_1} \cdots \sum_{(\beta)_N \geq 0}^{\alpha_N} \prod_{i=1}^{p} \delta_{(\beta_1^i + 2\beta_2^i + \ldots + N\beta_N^i), w_i} \tag{4.38}$$

$$\prod_{j=1}^{N} \frac{\alpha_j!}{\beta_j^1! \ldots \beta_j^p!} \prod_{i=1}^{p} \chi^{[\nu]^i}(\beta_1^i, \ldots, \beta_N^i)$$

is a compound character of S_N, the character of the outer product representation[36] obtained from $D^{[\nu]^1}, \ldots, D^{[\nu]^p}$. An outer product representation is completely reducible into irreducible representations of S_N; the rules for the reduction are given graphically using Young diagrams by Hammermesh[36].

If the reduction of an outer product representation contains the symmetric representation of S_N ($D^{[N]}$), the component representations must all be symmetric ($[\nu]^i = [w_i]$), and if it contains the antisymmetric representation ($D^{[1^N]}$), the component representations must all be antisymmetric ($[\nu]^i = [1^{w_i}]$). This places a constraint on the Kronecker product representations $D^{[\lambda]^i} \otimes D^{[\mu]^i}$. In the symmetric case, $[\lambda]^i$ must equal $[\mu]^i$, while in the antisymmetric case, $D^{[\lambda]^i}$ and $D^{[\mu]^i}$ must be conjugate representations (the Young diagram of one representation is the transpose of the other).

Upon restriction of F_N to $S_N \times G$, $Z^{\Omega}(\{[\mu]\},\{\alpha;\pi\})$ has a clearer interpretation. $Z^{\Omega}(\{[\mu]\},\{\alpha;\pi\})$ is the product of characters of the representations $D^{r_i} \otimes \ldots \otimes D^{r_i}$ (w_i times) projected on the permutation symmetry $[\mu]^i$. Equivalently, $Z^{\Omega}(\{[\mu]\},\{\alpha;\pi\})$ is the character of the

direct product representations of $[\mu]^i$ of $SU(d_{r_i})$ for i=1,...,p, restricted to the subgroup representation of G as discussed in (4.3.1). In particular, if D^{r_i} is a 1-dimensional representation of G, the representation of $SU(d_{r_i})$ is $[\omega_1]$, and $[\lambda]^i$ must be $[\omega_1]$ or $[1^{\omega_1}]$ if the representation of $S_N \times G$ is to contain a symmetric or antisymmetric representation of S_N respectively.

1-Particle Operators

Although an evaluation of (4.32) in the general case is formidable, the characters of the representations carried on the vector spaces of the 1- or 2-particle operators are simple and of practical interest. The irreducible representations of F_N carried by operators on the N-particle Hilbert space must contain identity representations of S_N on restriction of F_N to this subgroup. This limits the possible choices for Λ in (Ω,Λ). For example, a non-trivial 1-particle operator implies $\Omega = \{r, I^{N-1}\}$, where I is the identity representation and $r \neq I$ is an arbitrary representation of G (if r = I, the operator is a multiple of the identity). This implies $\Lambda = \{[1],[N-1]\}$, and

$$X^{(r)}(\{\alpha;\pi\}) = (1-\delta_{\alpha_1 0}) \sum_{k=1}^{\alpha_1} X^r(\pi_k^1) \tag{4.39a}$$

$$= \left[X^{[N]}(\{\alpha\}) + X^{[N-1,1]}(\{\alpha\})\right] \frac{(1-\delta_{\alpha_1 0})}{\alpha_1} \sum_{k=1}^{\alpha_1} X^r(\pi_k^1)$$

The forms relevant to both subgroup branchings, $F_N \supset G_N$ and $F_N \supset S_N \times G$, are given. The permutation invariant representation in the branching to $S_N \times G$ has the character of $D^{[N]} \otimes D^r$:

$$X^{(r)}(\{\alpha;\pi\}) \rightarrow X^{[N]}(\{\alpha\})X^{r}(g) \tag{4.39b}$$

To find the number of times the representation $D^{(\Omega,\Lambda')}$ occurs in the reduction of $D^{(r)}\otimes D^{(\Omega,\Lambda)}$ for a general (Ω,Λ), notice that (4.33a) implies

$$\sum_{k=1}^{\alpha_1} X^{r}(\pi_k^1)Y^{\Omega}(\{\beta\},\{\alpha;\pi\}) = \tag{4.40a}$$

$$Y^{\Omega}(\{\beta\},\{\alpha;\pi\}) \sum_{i=1}^{p} C_{rr_i}^{r_i}\beta_i + Y^{\Omega'}(\{\beta\},\{\alpha;\pi\})\ldots$$

i. e. the product can be expanded in the orthogonal set of functions $\{Y^{\Omega}(\{\beta\},\{\alpha;\pi\}), Y^{\Omega'}(\{\beta\},\{\alpha;\pi\}), \ldots\}$ with the original component multiplied by a coefficient dependent on the CG coefficients for the group G. The CG coefficients for F_N become

$$C_{(r)(\Omega,\Lambda)}^{(\Omega,\Lambda')} = \frac{1}{u_1!}\sum_{\{\beta\}^1}^{S_{u_1}}\cdots\frac{1}{u_p!}\sum_{\{\beta\}^p}^{S_{u_p}}\left[\sum_{j=1}^{p} C_{rr_j}^{r_j}\beta_1^j\right] \tag{4.40b}$$

$$\prod_{i=1}^{p} O(\{\beta\}^i)\; X^{[\lambda]^i}(\{\beta\}^i)X^{[\lambda']^i}(\{\beta\}^i)$$

$$\sum_{\{\beta\}^i}^{S_{u_i}} \equiv \sum_{\beta_1^i \geq 0}\cdots\sum_{\beta_N^i \geq 0}\delta_{(\beta_1^i+2\beta_2^i+\cdots+N\beta_N^i),u_i} \tag{4.40c}$$

$$C^{(\underline{\Omega},\Lambda')}_{(r)(\underline{\Omega},\Lambda)} = \sum_{j=1}^{p} C^{r_j}_{rr_j} \left\{ \delta_{\Lambda\Lambda'} \left[1 + \sum_{k=2}^{u_j} (1-\delta_{\lambda^j_k \lambda^j_{k-1}}) \right] \right. \tag{4.40d}$$

$$\left. + \delta_{\{\Lambda-[\lambda]^j\}\{\Lambda'-[\lambda]^j\}} \sum_{k\neq n=1}^{u_j} \left[\prod_{m\neq k,n} \delta_{(\lambda')^j_m,\lambda^j_m} \right] \delta_{(\lambda')^j_k,\lambda^j_k-1} \delta_{(\lambda')^j_n,\lambda^j_n+1} \right\}$$

where the last step follows from $\beta_1 = X^{[u]}(\{\beta\}) + X^{[u-1,1]}(\{\beta\})$ and the CG coefficients for the symmetric groups[36]. For simply reducible groups, the CG coefficients are either 0 or 1, and $C^{(\underline{\Omega},\Lambda)}_{(r)(\underline{\Omega},\Lambda)} \leq p$.

2-Particle Operators

The vector space of 2-particle operators can carry three possible non-trivial representations of F_N:

(1) $\underline{\Omega} = \{r^2, I^{N-2}\}$ $(r\neq I)$, $\Lambda = \{[2],[N-2]\}$:

$$X^{(r^2)}(\{\alpha;\pi\}) = (1-\delta_{\alpha_1 0})(1-\delta_{\alpha_1 1}) \sum_{j>k=1}^{\alpha_1} X^r(\pi^1_k) X^r(\pi^1_j) \tag{4.41a}$$

$$+ (1-\delta_{\alpha_2 0}) \sum_{k=1}^{\alpha_2} X^r(\pi^2_k)$$

with an alternate form

$$X^{(r^2)}(\{\alpha;\pi\}) = \left[X^{[N-2,1^2]}(\{\alpha\}) + X^{[N-2,2]}(\{\alpha\}) + 2X^{[N-1,1]}(\{\alpha\}) + X^{[N]}(\{\alpha\})\right] \frac{(1-\delta_{\alpha_1 0})(1-\delta_{\alpha_1 1})}{\alpha_1(\alpha_1-1)} \sum_{j>k=1}^{\alpha_1} X^r(\pi_k^1)X^r(\pi_j^1) \qquad (4.41b)$$

$$+ \left[X^{[N-2,2]}(\{\alpha\}) - X^{[N-2,1^2]}(\{\alpha\}) + X^{[N]}(\{\alpha\})\right] \frac{(1-\delta_{\alpha_2 0})}{2\alpha_2} \sum_{k=1}^{\alpha_2} X^r(\pi_k^2)$$

The permutation invariant representation of $S_N \times G$ is

$$X^{(r^2)}(\{\alpha;\pi\}) \rightarrow X^{[N]}(\{\alpha\}) \frac{1}{2}\left[\left[X^r(g)\right]^2 + X^r(g^2)\right] \qquad (4.41c)$$

the symmetrized portion of $D^r \otimes D^r$. The carrier space of this representation also carries an induced representation [2] of $SU(d_r)$; the symmetrized $D^r \otimes D^r$ can be regarded as a subgroup representation.

(2) $\Omega = \{r^2, I^{N-2}\}$, $\Lambda = \{[1^2],[N-2]\}$ $(r \neq I,\ d_r \geq 2)$:

$$X^{(r^2,[1^2])}(\{\alpha;\pi\}) = (1-\delta_{\alpha_1 0})(1-\delta_{\alpha_1 1}) \sum_{j>k=1}^{\alpha_1} X^r(\pi_k^1)X^r(\pi_j^1) - (1-\delta_{\alpha_2 0}) \sum_{k=1}^{\alpha_2} X^r(\pi_k^2) \qquad (4.42a)$$

with the same alternate form as (4.39b) except the α_2 term has the opposite sign. The permutation invariant representation of $S_N \times G$ is

$$X^{(r^2,[1^2])}(\{\alpha;\pi\}) \rightarrow X^{[N]}(\{\alpha\}) \frac{1}{2}\left[\left[X^r(g)\right]^2 - X^r(g^2)\right] \qquad (4.42b)$$

the antisymmetrized portion of $D^r \otimes D^r$. This representation can be regarded as a subgroup of the representation $[1^2]$ of $SU(d_r)$.

(3) $\Omega = \{r,r',I^{N-2}\}$ $(r\neq r'\ r\neq I,\ r'\neq I)$, $\Lambda = \{[1],[1],[N-2]\}$:

$$X^{(r,r')}(\{\alpha;\varpi\}) = (1-\delta_{\alpha_1 0})(1-\delta_{\alpha_1 1}) \tag{4.43a}$$

$$\sum_{j>k=1}^{\alpha_1} \left[X^r(\varpi_k^1)X^{r'}(\varpi_j^1) + X^r(\varpi_j^1)X^{r'}(\varpi_k^1)\right]$$

with the alternate form

$$X^{(r,r')}(\{\alpha;\varpi\}) = \left[X^{[N-2,1^2]}(\{\alpha\}) + X^{[N-2,2]}(\{\alpha\}) + \right.$$

$$\left. 2X^{[N-1,1]}(\{\alpha\}) + X^{[N]}(\{\alpha\})\right] \frac{(1-\delta_{\alpha_1 0})(1-\delta_{\alpha_1,1})}{\alpha_1(\alpha_1-1)} \tag{4.43b}$$

$$\sum_{j>k=1}^{\alpha_1} \left[X^r(\varpi_k^1)X^{r'}(\varpi_j^1) + X^r(\varpi_j^1)X^{r'}(\varpi_k^1)\right]$$

The permutation invariant representation of $S_N{}^{x}G$ is

$$X^{(r,r')}(\{\alpha;\varpi\}) \rightarrow X^{[N]}(\{\alpha\})X^r(g)X^{r'}(g) \tag{4.43c}$$

the character of $D^r \otimes D^{r'}$. This representation can be regarded as a subgroup representation of $SU(d_r)^{x}SU(d_{r'})$.

The CG coefficients $C^{(\Omega,\Lambda')}_{(\Omega'',\Lambda'')(\Omega,\Lambda)}$, where $D^{(\Omega'',\Lambda'')}$ is an irreducible representation carried by a 2-particle tensor operator, are obtained with the use of (4.33b) and (4.33c), analagous to (4.40).

$$C^{(\Omega,\Lambda')}_{(r^2)(\Omega,\Lambda)} = \frac{1}{w_1!}\sum_{\{\beta\}^1}^{S_{w_1}} \cdots \frac{1}{w_p!}\sum_{\{\beta\}^p}^{S_{w_p}} \prod_{i=1}^{p} O(\{\beta\}^i) X^{[\lambda]^i}(\{\beta\}^i) X^{[\lambda']^i}(\{\beta\}^i)$$

$$\frac{1}{2}\sum_{i=1}^{p}\left[(C^{r_i}_{rr_i})^2 \beta_1^i(\beta_j^i-1) + 2C^{r_i}_{rr_i}\beta_2^i\right] + \sum_{i\neq j=1}^{p} C^{r_i}_{rr_i} C^{r_j}_{rr_j}\beta_1^i\beta_1^j \qquad (4.44a)$$

$$C^{(\Omega,\Lambda')}_{(r^2,[1^2])(\Omega,\Lambda)} = \frac{1}{w_1!}\sum_{\{\beta\}^1}^{S_{w_1}} \cdots \frac{1}{w_p!}\sum_{\{\beta\}^p}^{S_{w_p}} \prod_{i=1}^{p} O(\{\beta\}^i) X^{[\lambda]^i}(\{\beta\}^i) X^{[\lambda']^i}(\{\beta\}^i)$$

$$\frac{1}{2}\sum_{i=1}^{p}\left[(C^{r_i}_{rr_i})^2\beta_1^i(\beta_j^i-1) - 2C^{r_i}_{rr_i}\beta_2^i\right] + \sum_{i\neq j=1}^{p} C^{r_i}_{rr_i} C^{r_j}_{rr_j})\beta_1^i\beta_1^j \qquad (4.44b)$$

$$C^{(\Omega,\Lambda')}_{(rr')(\Omega,\Lambda)} = \frac{1}{w_1!}\sum_{\{\beta\}^1}^{S_{w_1}} \cdots \frac{1}{w_p!}\sum_{\{\beta\}^p}^{S_{w_p}} \prod_{i=1}^{p} O(\{\beta\}^i) X^{[\lambda]^i}(\{\beta\}^i) X^{[\lambda']^i}(\{\beta\}^i)$$

$$\sum_{i=1}^{p} C^{r_i}_{rr_i} C^{r_i}_{r'r_i}\beta_1^i(\beta_j^i-1) + \sum_{i\neq j=1}^{p} C^{r_i}_{rr_i} C^{r_j}_{r'r_j})\beta_1^i\beta_1^j \qquad (4.44c)$$

Evaluation of sums of the type

$$c_{nm} = \frac{1}{w!}\sum_{\{\beta\}}^{S_w} O(\{\beta\}) X^{[\lambda]}(\{\beta\}) X^{[\lambda']}(\{\beta\}) \frac{(\beta_1-n+1)!(\beta_2-m+1)!2^m}{(\beta_1-n)!(\beta_2-m)!} \qquad (4.45a)$$

have been discussed by Hammermesh[36], and the results can be stated graphically with Young diagrams. The factors c_{nm} can also be solved for iteratively using the completeness of the simple characters, equation (4.40), and

$$c_{0,1} = \frac{1}{w!} \sum_{\{\beta\}}^{S_w} \theta(\{\beta\}) \chi^{[\lambda]}(\{\beta\}) \chi^{[\lambda']}(\{\beta\}) 2\beta_2 \qquad (4.45b)$$

$$= \delta_{[\lambda][\lambda']} \left[\sum_{k=1}^{w} \theta(\lambda_i - 2 - \lambda_{i+1}) - \delta_{\lambda_i \lambda_{i+1}} \sum_{k=1}^{w} \theta(\lambda_{i+1} - 1 - \lambda_{i+2}) \right]$$

$$+ \sum_{k \neq n=1}^{w} \prod_{m \neq k,1} \delta_{\lambda_m \lambda'_m} \delta_{\lambda'_k \lambda_k - 2} \delta_{\lambda'_n \lambda_n + 2}$$

$$\theta(x) = \begin{cases} 1 & x \geq 0 \\ 0 & x < 0 \end{cases}; \qquad \lambda_i \equiv 0, \quad i > w \qquad (4.45c)$$

4.4 Comparisons with Independent Particle Models

The structure and representation theory of F_N determines the properties of possible effective Hamiltonians on subspaces that carry representations $D^{(\Omega,\Lambda)}$. Physical wavefunctions must be symmetric or antisymmetric with respect to permutations of the particles, so effective Hamiltonians are restricted to the portion of the carrier space of $D^{(\Omega,\Lambda)}$ that also carries representations of $S_N \times G$ with the appropriate symmetry. The antisymmetric subspaces are considered in (4.4.1) and compared with configurations of Slater determinants, the 1- and 2-electron operators are discussed in (4.4.2), and some general observations about atomic structure are made in (4.4.3).

4.4.1 N-Electron Wavefunctions

The subspace of the carrier space of a representation $D^{(\Omega,\Lambda)}$ that carries the antisymmetric representation of S_N also carries an induced representation $[\tilde{\lambda}]^1 \otimes \ldots \otimes [\tilde{\lambda}]^p$ of $SU(d_{r_1}) \times \ldots \times SU(d_{r_p})$ (the partitions of $w_1, w_2, \ldots, w_p$ conjugate to $[\lambda]^1, \ldots, [\lambda]^p$), as was noted in the

discussion of the subgroup branching $F_N \supset S_N \times G$. In the case of non-relativistic atomic Hamiltonians, the group G is $SU(2) \times O^+(3)$ with representations $D^{1/2} \otimes D^{\ell}$, and the N-electron wavefunctions can be constructed in the following fashion:

An antisymmetric wavefunction results from a marriage of a set of radial wavefunctions $\{P^{\Lambda}_{\rho}(r_1,\ldots,r_N) \mid \rho \in Y^{\Lambda}\}$ that carry the irreducible representation D^{Λ} of S_N^{Ω}, and a set of spin-angle wavefunctions $\{A^{(\Omega,\Lambda)}_{\tilde{\rho}\tau}(\hat{e}_1\sigma_1,\ldots,\hat{e}_N\sigma_N) \mid \tilde{\rho} \in Y^{\tilde{\Lambda}},\ \tau \in W^{\tilde{\Lambda}}\}$, that carry representations of $S_N^{\Omega} \times SU(4\ell_1+2) \times \ldots \times SU(4\ell_p+2)$, denoted by the partitions $[\tilde{\Lambda}] = \{[\tilde{\lambda}]^1, \ldots, [\tilde{\lambda}]^p\}$ of the integers $\{u_1,\ldots,u_p\}$. The spin-angle functions are product functions $\{A^{[\tilde{\lambda}]^i}_{\tilde{r}_i \tilde{t}_i}\}$ that carry the representations $[\tilde{\lambda}]^i$ of $S_{u_i} \times SU(4\ell_i+2)$, constructed from 1-electron spin-angle wavefunctions $\{Y_{\ell_i m}(\theta,\phi)X_{\mu}(\sigma) \mid -\ell_i \le m \le \ell_i;\ \mu = +-\tfrac{1}{2}\}$. The basis vectors of representations $[\tilde{\lambda}]$ of $SU(4\ell+2)$ can be represented by Weyl tableaux $t \in W^{[\tilde{\lambda}]}$, Young diagrams of the pattern $[\tilde{\lambda}]$ filled with ordered pairs (m,μ) as pictured in figure (4.2)[36,59]. The functions $\{A_{\rho'\tau}\}$ are labeled by p-tuples of Weyl and Young tableaus.

Products of the radial and spin-angle functions are antisymmetrized. This is equivalent to constructing the representation $[1^{u_1}] \times \ldots [1^{u_p}] \times [\tilde{\lambda}]^1 \times \ldots \times [\tilde{\lambda}]^p$ of $S_N^{\Omega} \times SU(4\ell_1+2) \times \ldots \times SU(4\ell_p+2)$ and then antisymmetrizing with respect to the permutations $\ell \in L^{\Omega}$:

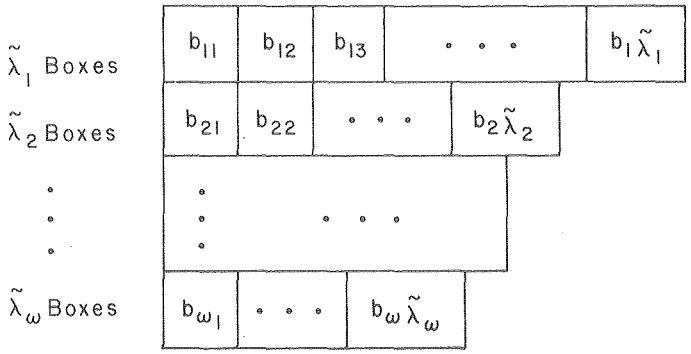

XBL 805-898

Figure (4.2)

Weyl tableau describing a basis vector of the irreducible representation $D^{\tilde{\Lambda}}$ of S_N^Ω; the representation carried by the wavefunctions $\{A_{\tilde{\rho}\tilde{\tau}}^{(\Omega,\Lambda)}(\hat{e}_1\sigma_1,\ldots,\hat{e}_N\sigma_N) \mid \tilde{\rho} \vdash Y^{\tilde{\Lambda}},\ \tilde{\tau} \vdash W^{\tilde{\Lambda}}\}$.

$$\Psi^{\{[1^{w_i}]\}}_{\Lambda\tau}(x_1,\ldots,x_N) = d_\Lambda^{-1/2} \sum_{p\in Y^\Lambda} P^\Lambda_p(r_1,\ldots,r_N) A^{(\Omega,\Lambda)}_{p\tau}(\hat{e}_1\sigma_1,\ldots,\hat{e}_N\sigma_N) \tag{4.46a}$$

$$\Phi^N_{\Lambda\tau}(x_1,\ldots,x_N) = \left[\frac{w_1!\cdots w_p!}{N!}\right]^{1/2} \sum_{\phi\in L^\Omega} (-1)^\phi \Psi^{\{[1^{w_i}]\}}_{\Lambda\tau}(x_{\phi(1)},\ldots,x_{\phi(N)}) \tag{4.46b}$$

In principle these wavefunctions can be transformed from the Weyl basis of $SU(4\ell_1+2)\times\ldots\times SU(4\ell_p+2)$ into an SLJ basis by finding subgroup representations of the same chains as discussed in chapter II. In practice, however, this can be difficult because the coefficients of fractional parentage for general representations $[\lambda]$ of $SU(4\ell+2)$ are largely unknown.

Slater Determinants

A fairly simple relationship exists between basis vectors constructed by the above method and the Slater determinants of a given configuration. The radial wavefunctions $\{P^\Lambda_p \mid p\in Y^\Lambda\}$ can be constructed from products of 1-electron radial wavefunctions in the same manner as the spin-angle wavefunctions were constructed. The functions $\{P^\Lambda_p \mid p\in Y^\Lambda\}$ become products of functions $\{P^{[\lambda]^i}_{r_i} \mid r_i\in y^{[\lambda]^i}\}$ constructed from ℓ_i-type 1-electron radial wavefunctions $\{R_{n\ell_i}, R_{n'\ell_i},\ldots,R_{n''\ell_i}\}$. In many cases there are only N distinct 1-electron wavefunctions that can be constructed with a specified set of (m,μ) values from the 1-electron

radial and spin-angle wavefunctions available to a configuration. In such a situation, only one linearly independent N-electron wavefunction can be constructed by any method, essentially a Slater determinant.

For simplicity, consider a configuration $\hat{\omega}$ of ω ϕ-electrons of the form $\{n_1\phi^{w_1}, n_2\phi^{w_2}, \ldots, n_q\phi^{w_q}\}$. The spin-angle wavefunctions $A_{\tilde{r}t}^{[\tilde{\lambda}]}$ can be constructed for any representations $[\tilde{\lambda}]$ of $S_\omega \times SU(4\phi+2)$ as long as $\tilde{\lambda}_k = 0$ if $k > 4\phi+2$. The basis functions must be antisymmetric with respect to subsets of coordinates with as many members as there are boxes in each column of a Young diagram[36]; any wavefunction constructed from a set of $4\phi+2$ 1-particle functions cannot be antisymmetric with respect to more than $4\phi+2$ coordinates.

The products of ω radial wavefunctions $\{R_{n_1\phi}, \ldots, R_{n_q\phi}\}$ carry a representation of $S_\omega \times SU(q)$ under permutations of the radial coordinates and unitary transformations on the set of radial wavefunctions. The representation reduces into irreducible representations $[\lambda]$, but because $[\lambda]$ must be conjugate to a representation $[\tilde{\lambda}]$, carried by the spin-angle functions, $\lambda_k \leq 4\phi+2$. Also $\lambda_k = 0$ if $k > q$, because there are only q-radial wavefunctions, thus the possible Young diagrams are limited to rows no longer than $4\phi+2$, and columns no longer than q. In addition, the number of each type of radial wavefunction $n_i\phi$ is fixed at w_i, and if $w_1 \geq w_2 \geq \cdots \geq w_q$, the number of columns of length q must be $\geq w_q$.

Unless $w_1 = w_2 = \cdots = w_{q-1} = 4\phi+2$, there is more than one possible representation $[\lambda]$ that meets these constraints. In general, the 1-electron radial and spin-angle wavefunctions $\hat{\omega}$ can carry several representations $D^{(\phi^\omega;[\lambda])}$ of F_ω that reduce to antisymmetric

representations under $F_{\omega} \supset S_{\omega} \times SU(2) \times O^{+}(3)$. The simplest example is a 2-electron configuration $\{n\ell, n'\ell\}$ with $n \neq n'$, so the radial functions can be symmetric [2] or antisymmetric $[1^2]$. There are two irreducible representations of F_2 that can be constructed; the representations $D^{(r^2)}$ and $D^{(r^2,[1^2])}$, with the characters given by (4.41a) and (4.42a) respectively. The 2-electron configuration $n\ell^2$ carries only the representation $D^{(r^2)}$.

The extension to a general configuration is made by constructing the radial functions $\{P^{\Lambda}_{p} \mid p \in \Upsilon^{\Lambda}\}$ from products $P^{[\lambda]^1}_{r_1} \ldots P^{[\lambda]^p}_{r_p}$. However, the Weyl tableau basis vectors, $\{\Phi^{N}_{\Lambda\tau} \mid \tau \in W^{\tilde{\Lambda}}\}$, are generally not identical to single Slater determinants. Consider the determinants of the configuration $\hat{\omega}$ as antisymmetrized products of w_i-electron subshell wavefunctions with radial dependence given by $R_{n_i\ell}(r_1) \ldots R_{n_i\ell}(r_{w_i})$. The determinants of the configuration $\hat{\omega}$ carry a representation $[1^{w_1}] \times \ldots \times [1^{w_q}]$ of $[SU(4\ell+2)]^q = SU(4\ell+2) \times \ldots SU(4\ell+2)$ (q times).

Since ℓ is the same for all subshells, the reduction $SU(4\ell+2) \subset SU(4\ell+2)^q$ can be made, and the resulting sum of irreducible representations is block diagonalized with the basis $\{\Phi^{N}_{\Lambda\tau} \mid \tau \in W^{\tilde{\Lambda}}\}$. Except in the case $w_i = 4\ell_i+2$, $i \neq q$, the representation of $[SU(4\ell+2)]^q$ reduces to several irreducible representations of $SU(4\ell+2)$ and the Slater determinants are generally linear combinations of Weyl tableau basis vectors. In the exceptional case, however, the representation of $[SU(4\ell+2)]^q$ is composed of at most one non-trivial (identity) representation of $SU(4\ell_i+2)$ and the Weyl tableau basis vectors are identical to Slater

determinants.

4.4.2 n-Electron Operators

On a linear span of Slater determinants that is closed under rotations, the n-electron operators can be expanded as integral operators with kernels constructed from 1-electron wavefunctions. The set of 1-electron wavefunctions is composed of subsets that carry irreducible representations $D^{1/2} \times D^{\ell}$ of $SU(2) \times O^{+}(3)$, and each subset can be induced to carry a representation of $SU(4\ell+2)$. The set of all symmetric integral operators that maps a configuration with p-subshells into itself carries a representation $[1^{w_1}] \otimes [1^{w_1}]^* \otimes \ldots \otimes [1^{w_p}] \otimes [1^{w_p}]^*$ of $SU(4\ell_1+2) \times \ldots \times SU(4\ell_p+2)$, reducible to a direct sum of irreducible representations given by (2.108a). Thus this vector space of operators carries p-fold direct products of irreducible representations of various links in the chain of subgroups $SU(4\ell_i+2) \supset Sp(4\ell_i+2) \supset O^{+}(3) \times O^{+}(2\ell_i+1) \supset O^{+}(3) \times O^{+}(3)$, and ℓ_i for each $n_i \ell_i$ subshell.

Within a configuration where the number of each type of 1-electron wavefunction is conserved, the restricted n-electron operators carry representations $[1^{\nu_1}] \otimes [1^{\nu_1}]^* \otimes \ldots \otimes [1^{\nu_p}] \otimes [1^{\nu_p}]^*$ of $SU(4\ell_1+2) \times \ldots \times SU(4\ell_p+2)$, $\nu_1 + \ldots + \nu_p = n$, and the possible representations of this type are limited, since usually, n=1,2. Each representation $[1^{\nu_i}] \otimes [1^{\nu_i}]^*$ is reduced to a direct sum of irreducible representations of $SU(4\ell_i+2)$ given by (2.108b), and the basis of each irreducible representation can be chosen to display the reduction via the same chain of subgroups headed by $SU(4\ell_i+2)$ and terminated with $O^{+}(3) \times O^{+}(3)$. Only the scalar representations of the tail subgroup $O^{+}(3) \times O^{+}(3)$ are

important for the effective Hamiltonians.

If a configuration has only one unfilled subshell for each ℓ (i.e. $w_i=4\ell_i+2$ except for perhaps one $n\ell$-subshell of each ℓ-type), it can be considered the antisymmetric subspace of the carrier space of a single irreducible representation $D^{(\Omega,\Lambda)}$ of F_N. The algebraic properties of the operators that map this subspace into itself are identical whether or not the radial dependence of the wavefunctions spanning this subspace is given explicitly by 1-electron radial wavefunctions. This suggests that for configurations of this type at least, that the parameterization of effective Hamiltonians is essentially the same if the radial dependence is given by products of 1-electron radial wavefunctions or more general radial wavefunctions, i.e. arbitrary functions of the radial coordinates, and the parameters are not limited to linear combinations of integrals involving 1-electron radial wavefunctions.

To explore this idea further, consider the restriction to the antisymmetric subspace of the carrier space of $D^{(\Omega,\Lambda)}$. This subspace carries the irreducible representation $\tilde{\Lambda}$ of $SU(4\ell_1+2)\times \ldots SU(4\ell_p+2)$ when spanned by the Weyl tableau basis vectors, $\{\Phi^N_{\tilde{\Lambda}\tau}\}$, defined by (2.46ab). The operators that map this subspace into itself are invariant with respect to permutations and are characterized by the representation $([\tilde{\lambda}]^1\otimes[\tilde{\lambda}]^{1*})\times \ldots \times([\tilde{\lambda}]^p\otimes[\tilde{\lambda}]^{p*})$. Again, each representation $[\tilde{\lambda}]^i\otimes[\tilde{\lambda}]^{i*}$ reduces to a direct sum of irreducible representations of $SU(4\ell_i+2)$, and the same chain of subgroups and their representations occurs as for the linear span of Slater determinants.

Also, by construction, the relationship of this symmetry adapted

basis set of operators to the physical transformations on the subspace (e.g. rotations) is the same in either case. This can be seen by comparing the actions of the generators (4.18) with those generators (2.66) on their respective subspaces. Of course the restrictions of 1- and 2-electron operators to subspaces spanned by configurations of Slater determinants and carrier spaces of representations of F_N need to be examined in greater detail, but it is evident that semi-empirical theories can legitimately account for correlations beyond the independent particle models from which they are derived. Some of the subtleties of the algebraic properties of the restricted operators can be illustrated with the 1-electron operators.

Consider the 1-electron operators on a carrier space of an irreducible representation of F_N. These operators carry representations $D^{(\mathcal{K}xk)}$ of F_N induced from $(D^{\mathcal{K}}xD^{k})x(D^{0}xD^{0})x\ \ldots x(D^{0}xD^{0})$ of $[O^{+}(3)xO^{+}(3)]^{N}$. From (4.40d),

$$C^{(\Omega,\Lambda)}_{(\mathcal{K}xk)(\Omega,\Lambda)} = \sum_{i=1}^{p} C^{\mathcal{K}xk,\ 1/2x\phi_i}_{(\Omega,\Lambda)} \left[1 + \sum_{k=1}^{u_1} (1-\delta_{\lambda_k^i,\lambda_{k-1}^i})\right] \qquad (4.47)$$

and there are $m_i\ (\mathcal{K}xk)$ linearly independent operator representations for each $2\phi_i \geq k$, $\mathcal{K} \leq 1$, where m_i is the number of distinct $\lambda_k^{i\prime}s$ in the partition $[\lambda]^i$. Each of these operator representations maps the carrier space of $D^{(\Omega,\Lambda)}$ into itself, but not all of these representations are diagonal with respect to permutation symmetry of the particles. Thus, although a 1-electron operator can be resolved into tensor components for the group F_N, not all irreducible representations of the type carried by 1-particle operators can correspond to physical operations.

On the other hand, consider the restriction of the 1-particle operators to the smaller subspace (of the carrier space of the representation of F_N) with antisymmetric permutation symmetry. Now the 1-electron operators can be expressed as linear combinations of the generators $\{E^{r}_{b''b'}\}$ (4.18) with $r=(\frac{1}{2}x\emptyset_i)$. The generators carry the representation $D^{[N]}x\,[(D^{\frac{1}{2}}xD^{\emptyset_i})\otimes(D^{\frac{1}{2}*}xD^{\emptyset_i*})]$ of $S_N xO^+(3)xO^+(3)$ $(\subset F_N$, and the representation $[(D^{\frac{1}{2}}xD^{\emptyset_i})\otimes(D^{\frac{1}{2}*}xD^{\emptyset_i*})]$ reduces to the direct sum of irreducible representations $\{D^{[N]}x\,D^{\chi}xD^{k}\,|\,,\ \chi=0,1;\ k=0,1,\ldots,2\emptyset_i\}$. Now suppose this subspace is spanned by a basis set of Slater determinants. For a given $\emptyset_i=\emptyset$, the reduction of the generators $\{\}$ to irreducible representations of $O^+(3)xO^+(3)$ and their actions on the basis vectors can be expressed in the form:

$$E^{(s\times\emptyset)}_{\mu m\mu' m'} = \sum_{\chi,k,\pi,q} c^{\chi k}_{\pi q}\left[W^{\chi k}_{\pi q}(n\emptyset) + W^{\chi k}_{\pi q}(n'\emptyset) + \ldots + W^{\chi k}_{\pi q}(n''\emptyset)\right] \quad (4.48)$$

The coefficients $\{c^{\chi k}_{\pi q}\}$ are the same as in (2.53b) and the operators $\{W^{\chi k}_{\pi q}(n\emptyset)\}$ are as in (2.79b). Since the operators $\{W^{\chi k}(n\emptyset)\}$ vanish for non-zero (χ,k) if $(n\emptyset)$ is a filled subshell, the analysis of the 1-electron operators agrees with the analysis in section (2.3) when there is only one unfilled subshell of a given $\emptyset$-type. When there is more than one unfilled subshell of $\emptyset$-electrons, however, it is obvious that the situation becomes more complicated, as the correspondence given by (4.48) is no longer one to one.

4.4.3 Energy Spectrum of Atomic Hamiltonian Operators

An interesting observation can now be made about the low-lying bound states of the non-relativistic atomic Hamiltonian, H_0, given by

(2.39a). If the electron-electron Coulomb term is expanded in the usual Legendre polynomial expansion with only the lowest order term retained, the resulting operator H_o fits the symmetry prescription for F_N with the $G = O^+(3)xO^+(3)$:

$$H_o = \sum_{k=1}^{N} \left(p_k^2 - \frac{2Z}{r_k} \right) + \sum_{k>j=1}^{N} \frac{2}{r_>(r_k, r_j)} \tag{4.49}$$

Adding this largest contribution to the electron-electron potential energy to the N-electron hydrogenic central field Hamiltonian breaks some configuration degeneracy and results in new degenerate subspaces characterized by irreducible representations of the semi-direct product of S_N and $[SU(2)xO^+(3)]^N$. The configuration character of the energy spectrum is nearly preserved, however, (at least for configurations with only one unfilled subshell of a given ℓ), and it is plausible that the remainder of the electron-electron interaction is a small enough perturbation so that many of the lowest eigenenergies of H_0 can be identified with central field configurations.

Another interesting observation is that the $1/r_{12}$ potential is bounded between two potentials with complete rotational symmetry, i.e.

$$\frac{1}{r_1+r_2} \leq \frac{1}{r_{12}} \leq \frac{1}{|r_1-r_2|} \tag{4.50}$$

With considerations given to domain questions for Hamiltonian operators with these inter-electron potentials, rigorous statements might be made about the bound states of H_o[52]. For example, the ground state energy of H_0 should lie between ground state energies of the Hamiltonians with the corresponding smaller and larger electron-electron potentials. Although these bounds might be poor numerically, especially for the heavier

atoms, they could support the shell model of the atom and the periodic table of the elements from first principles, without resorting to Slater determinants.

V. Applications to Spectral Analyses

The usefulness of any mathematical model lies in how the model compares with nature. If a model deviates from nature in a well known or predictable manner, it can be modified to account for this, thereby increasing its usefulness. Such modifications have been attempted for independent particle models of free atoms and ions. For example, the relationship of the single configuration Hartree-Fock (HF) model to the fully correlated, "true" atomic eigenfunctions and eigenenergies has been discussed by several authors[15,60]. In particular, the variation-perturbation approach to the corrections to HF theory has been studied extensively by Sinanoglu[60,61]. Explicit calculations of higher order corrections to the HF approximation are complicated, but their forms have been used in developing semi-empirical methods[23-25], the approach taken here.

Section (5.1) begins with some conjectures about "accurate" approximate atomic wavefunctions that differ from say, HF wavefunctions, but are basically consistent with semi-empirical Slater-Condon theory. The qualitative effects of the differences on the estimates of atomic energy levels are discussed and suggestions for adjusting ab-initio spectroscopic parameters are presented. Combined with a study of the calculated (via the HXR approximation) and observed energy levels of the K I ions, these ideas are used to develop a strategy for adjusting the ab-initio spectroscopic parameters of V^{4+} and Cr^{5+} ions in section (5.2). These adjustments are then extrapolated to Ti^{3+}, Mn^{6+}, and Fe^{7+}. Section (5.3) describes a variation on the analysis problem; the energy levels of an ion in a crystal lattice at a site with a local symmetry.

5.1 Parameter Strategies

A single configuration Slater-Condon effective Hamiltonian (H_e of (2.40), restricted to a single configuration) can, in principle, be statistically fit to experimental energy levels. The number of free parameters does not exceed the number of levels, but single configuration effective Hamiltonians are not always good descriptions and must be amended to include configuration interaction. Regardless of how configuration interaction is introduced into the effective Hamiltonian, the number of free parameters will increase relative to the number of energy levels. Also, in the early course of analyzing a spectrum, only a few experimental levels for a given configuration might be known, which in turn may be derived from only a few of the parameters. These factors contribute to the usual situation where the effective Hamiltonian has more independent free parameters than experimental data associated with it.

Generally, the number of parameters is reduced by adding constraints. One method used to reduce the number of degrees of freedom is to assume that empirically determined parameters such as $F^k(n\ell n'\ell')$ and $G^k(n\ell n'\ell')$ are proportional to their counterparts computed from hydrogenic radial wavefunctions. With increased availability of ab-initio calculations, however, the integrals computed from the ab-initio radial wavefunctions have replaced the hydrogenic ones. Scaling the ab-initio parameters is perhaps the simplest way of using theoretical calculations in the analysis of spectra, (aside from the initial estimates). Cowan[14] distinguishes five classes of parameters and routinely scales them to obtain better agreement with the observed energy levels.

Perhaps the best justification of the scaling of predicted parameters is its simplicity. This technique is likely to be successful in many cases because only a few parameters are dominant in determining the eigenvalues of the effective Hamiltonian matrix. Some ideas about the validity of linear constraints derived from ab-initio parameters are discussed in this section, and extrapolation of corrections to ab-initio parameters along an isoelectronic series is also discussed.

5.1.1 Conceptual Strategies

A scenario for describing atoms and ions with considerable inter-electron correlation that is basically consistent with semi-empirical Slater-Condon theory is presented in this section. The emphasis is on radial correlations, as developed in chapter IV, but an argument consistent with the semi-empirical parameterization is made in favor of more general correlations among electrons localized near the nucleus. In addition, correlations described by explicit configuration interaction are considered, but the actual magnitudes of these parameters in the context of the more general atomic wavefunctions differ from the Hartree-Fock estimates.

Radial Correlations

The qualitative effects of allowing an atomic wavefunction to have radial correlations can be investigated with a simplified version of Sinanoglu's analysis of the corrections to a single determinant Hartree-Fock atomic wavefunction. For simplicity, consider a single configuration $\underline{Q} = \{n_1\phi_1^{u_1},\ldots,n_p\phi_p^{u_p}\}$ with p distinct ϕ's ($\phi_i \neq \phi_j$; $i>j=1,2,\ldots,p$). A Slater determinant belonging to this configuration

can be written in the form

$$\Phi^N_{\underline{Q}\gamma}(x_1,x_2,\ldots,x_N) = \tag{5.1a}$$

$$\sqrt{N!}A_N\left\langle \prod_{i=1}^{p}\prod_{\alpha=1}^{w_i} Y_{\phi_i m_{i\alpha}}(\theta_{\nu(i,\alpha)},\phi_{\nu(i,\alpha)})\chi_{\mu_{i\alpha}}(\sigma_{\nu(i,\alpha)})\,\frac{P^0_{\underline{Q}}(r_1,\ldots,r_N)}{r_1\cdots r_N}\right\rangle$$

$$\nu(i,\alpha) = \alpha + \sum_{k=1}^{i-1} w_k \tag{5.1b}$$

$$P^0_{\underline{Q}}(r_1,\ldots,r_N) = \prod_{i=1}^{p}\prod_{\alpha=1}^{w_i} P_i(r_{\nu(i,\alpha)}) \tag{5.1c}$$

where A_N is the antisymmetrization projection operator, $\gamma = \{m_{i\alpha}\mu_{i\alpha} \mid i=1,\ldots,p;\ \alpha=1,\ldots,w_i\}$ denotes a determinant belonging to the configuration, and $P_i(r) \equiv P_{n_i\phi_i}(r)$. The average energy of configuration can be written in the form

$$E^{HF}_{av} = \int_0^\infty dr_1\cdots dr_N P^0_{\underline{Q}}(r_1,\ldots,r_N)H_{av}(r_1,\ldots,r_N)P^0_{\underline{Q}}(r_1,\ldots,r_N) \tag{5.2a}$$

where

$$H_{av}(r_1,\ldots,r_N) = \sum_{i=1}^{p}\sum_{\alpha=1}^{w_i}\left[-d^2/dr^2_{\nu(i,\alpha)} + \frac{\ell_i(\ell_i+1)}{r^2_{\nu(i,\alpha)}} + V_c(r_{\nu(i,\alpha)})\right] + V_C(r_1,\ldots,r_N) \tag{5.2b}$$

$V_c(r)$ is a central potential (e.g. $-2Z/r$) and V_C is the configuration averaged Coulomb potential:

$$V_C(r_1,\ldots,r_N) = \sum_{i=1}^{p} \sum_{\alpha>\beta=1}^{w_i} V_C^{ii}(r_{\nu(i,\alpha)},r_{\nu(i,\beta)}) + \tag{5.2c}$$

$$\sum_{i>j=1}^{p} \sum_{\alpha=1}^{w_i} \sum_{\beta=1}^{w_j} V_C^{ij}(r_{\nu(i,\alpha)},r_{\nu(j,\beta)})$$

$$V_C^{ii}(r';r'') = 2\left[U_0(r';r'') - \frac{2\phi_i+1}{4\phi_i+1} \sum_{k>0} \begin{vmatrix} \phi_i & k & \phi_i \\ 0 & 0 & 0 \end{vmatrix}^2 U_k(r';r'')\right] \tag{5.2d}$$

$$V_C^{ij}(r';r'') = 2\left[U_0(r';r'') - \frac{1}{2} \sum_{k=0} \begin{vmatrix} \phi_i & k & \phi_j \\ 0 & 0 & 0 \end{vmatrix}^2 U_k(r';r'')\tau_{r'r''}\right] \tag{5.2e}$$

The operator $\tau_{r'r''}$ transposes the coordinates r';r'' of the function on the right, and $U_k(r',r'')$ is given by equation (3.3f).

Including radial correlations in the atomic wavefunction for a configuration of this type is equivalent to replacing the radial wavefunction P_Q^0 with a radial wavefunction that satisfies

$$H_{av}(r_1,\ldots,r_N)P_Q(r_1,\ldots,r_N) = E_{av}P_Q(r_1,\ldots,r_N) \tag{5.3}$$

with suitable boundary conditions on P_Q and the additional constraint that $P_Q(r_1,\ldots,r_N)$ be invariant with respect to permutations of the subsets of coordinates $W_1 = \{1,2,\ldots,w_1\}$, $W_2 = \{w_1+1,\ldots,w_1+w_2\}$, ..., $W_p = \{N-w_p+1,\ldots,N\}$. If equation (5.3) is solved perturbatively, an independent particle (i.e. separable) zero-order Hamiltonian, H_{av}^0, is chosen so that P_Q^0 is an eigenstate with the eigenvalue E_Q^0. The first order correction to the wavefunction satisfies:

$$\left[H_{av}^0 - E_Q^0\right]P_Q^1 = -\left[H_{av}^1 - E_{av}^1\right]P_Q^0 \tag{5.4a}$$

$$H_{av} - H_{av}^{0} = H_{av}^{1} \tag{5.4b}$$

$$E_{av}^{1} = E_{av} - E_{\underline{Q}}^{0} \tag{5.4c}$$

$$H_{av}^{0} = \sum_{i=1}^{p} \sum_{\alpha=1}^{w_i} h_i(r_{\backslash(i,\alpha)}) \tag{5.4d}$$

$$E_{\underline{Q}}^{0} = \sum_{i=1}^{p} w_i \epsilon_i \tag{5.4e}$$

$$\left(h_i(r) - \epsilon_i\right) P_i(r) = 0 \tag{5.4f}$$

Equation (5.4) is ideally suited to Sinanoglu's method for finding the first order corrections to Hartree-Fock wavefunction for a configuration consisting of a single determinant (MET)[61]. The solution to (5.4) can be written in the form

$$P_{\underline{Q}}^{1}(r_1,\ldots,r_N) = A(r_1,\ldots,r_N) P_{\underline{Q}}^{0}(r_1,\ldots,r_N) \tag{5.5a}$$

$$A(r_1,\ldots,r_N) = \sum_{i=1}^{p} (1-\delta_{w_i 1}) \sum_{\alpha>\beta=1}^{w_i} \frac{a_{ii}(r_{\backslash(i,\alpha)}, r_{\backslash(i,\beta)})}{P_i(r_{\backslash(i,\alpha)}) P_i(r_{\backslash(i,\beta)})}$$

$$+ \sum_{i>j=1}^{p} \sum_{\alpha=1}^{w_i} \sum_{\beta=1}^{w_j} \frac{a_{ij}(r_{\backslash(i,\alpha)}, r_{\backslash(j,\beta)})}{P_i(r_{\backslash(i,\alpha)}) P_j(r_{\backslash(j,\beta)})} \tag{5.5b}$$

where $a_{ii}(r',r'')$ and $a_{ij}(r',r'')$ satisfy

$$\left(h_i(r') - \epsilon_i + h_i(r'') - \epsilon_i\right) a_{ii}(r',r'') = \tag{5.6a}$$

$$-\left(V_C^i(r',r'') - v_{ii}(r') - v_{ii}(r'') - \epsilon_C^{ii}\right) P_i(r) P_i(r)$$

$$\left[h_i(r') - \epsilon_i + h_j(r'') - \epsilon_j\right] a_{ij}(r',r'') = \tag{5.6b}$$

$$-\left[V_C^{ij}(r',r'') - v_{ij}(r') - v_{ji}(r'') - \epsilon_C^{ij}\right] P_i(r')P_j(r'')$$

$$\epsilon_C^{ii} = F^0(i,i) - \frac{2\ell_i+1}{4\ell_i+1} \sum_{k>0} \begin{pmatrix} \ell_i & k & \ell_i \\ 0 & 0 & 0 \end{pmatrix}^2 F^k(i,i) \tag{5.6c}$$

$$\epsilon_C^{ij} = F^0(i,j) - \frac{1}{2} \sum_{k=0} \begin{pmatrix} \ell_i & k & \ell_j \\ 0 & 0 & 0 \end{pmatrix}^2 G_k(i,j) \tag{5.6d}$$

and the operators v_{ij} satisfy (5.4b) and

$$\int_0^\infty dr'dr''P_i(r')P_j(r'')\left[V_C^{ij}(r',r'') - v_{ij}(r') - \right. \tag{5.6e}$$

$$\left. v_{ji}(r'') - \epsilon_C^{ij}\right] P_i(r')P_j(r'') = 0$$

Equation (5.4) separates into a set of $p(p+1)/2$ equations for the pair functions $\{a_{ij}(r',r'') \mid i \leq j = 1,\ldots,p\}$, where the single subshell pair functions $\{a_{ii}(r',r'')\}$ must be symmetric with respect to an interchange of their arguments. Because of the assumption that the configuration $\underline{0}$ has no two subshells with the same ℓ quantum number, there are no permutation symmetry restrictions on the pair functions $\{a_{ij}(r',r'')\}$. However, the pair functions must satisfy the formal orthogonality conditions,

$$\int_0^\infty dr'dr'' \; a_{ij}(r',r'')P_i(r')P_j(r'') = 0 \tag{5.7a}$$

but because the expectation value of H_{av} is stationary with respect to variations of the functions $P_{n\ell}(r)$, Brillouin's[62] theorem leads to the

condition of strong orthogonality:

$$\int_0^\infty dr'dr'' \; a_{ij}(r';r'')P_i(r') \equiv 0 \qquad (5.7b)$$

$$\int_0^\infty dr'dr'' \; a_{ij}(r';r'')P_j(r'') \equiv 0 \qquad (5.7c)$$

The stronger orthogonality conditions, (5.7bc), greatly simplify the corrections to the radially correlated configuration average energy. The second order correction to the energy is obtained by making the substitutions:

$$\bar{F}^k(i,j) = F^k(i,j) + 4\int_0^\infty dr'dr'' \; a_{ij}(r';r'')U_k(r';r'')P_i(r')P_j(r'') \qquad (5.8a)$$

$$\bar{G}^k(i,j) = G^k(i,j) + 4\int_0^\infty dr'dr'' \; a_{ij}(r';r'')U_k(r';r'')P_j(r')P_i(r'') \qquad (5.8b)$$

($\bar{p}$ denotes the adjusted value of the ab-initio parameter p). The third order corrections are also easily obtained, and include 1-body terms as well as the 2-body terms.

Internal Correlations

Radially correlated atomic wavefunctions cannot hope to account for all the discrepancies between Slater-Condon theory and experimental observations. Parameterization of effective Hamiltonians is preserved nearly intact with this generalization, so predictions of ratios of relative energy separations for levels within a multiplet are unchanged from Slater-Condon theory, but are often at variance with experimental observations. These deviations are usually explained by configuration

interaction (CI), but in many cases a very large number of configurations are required to correct the discrepancies in an ab-initio calculation[15,63].

An effective Hamiltonian, however, can reproduce a set of experimental levels manifesting such discrepancies quite well by adding only a few interacting configurations, a few semi-empirical parameters[23-25], or both. Apparently, a large number of configurations are needed as corrections to the core (closed subshell) portion of the wavefunction[25,26]. If trial wavefunctions were used consisting of antisymmetrized products of a fully correlated, rotationally invariant ionic core wavefunction, and Slater determinants describing only the outer (open subshell) valence electrons, many configurations needed for an accurate CI calculation might already be included.

The choice of a rotationally invariant, closed shell core wavefunction is suggested by large ionization energies of atoms and ions with this ground state configuration, which indicates tight binding and a small ionic radius. Some theoretical support of this conjecture has recently been presented for a non-relativistic Shroedinger atomic model[64]. The charge density has been shown to have the assymptotic property

$$\rho(r) \leq kr^{2\beta}e^{-2\alpha r}; \quad r \geq Z/\epsilon \tag{5.9a}$$

$$\beta = (Z-N)/\alpha - 1; \quad \alpha = \sqrt{2\epsilon} \tag{5.9b}$$

where ϵ is the ionization energy of the state of interest and the upper bound is rigorous for some positive k. If a valence wavefunction mainly

represents electrons in high angular momentum states, it will have small amplitude at small radii because of the centerfugal potential. In this case, an antisymmetrized product wavefunction should be a good approximation to the true wavefunction. "Internally" correlated wavefunctions take the form

$$\Phi_y^N(x_1,\ldots,x_N) = \binom{N}{V}^{1/2} A_N \left[\Phi_y^V(x_1,\ldots,x_V)\Phi_0^C(x_{V+1},\ldots,x_N)\right] \qquad (5.10)$$

as given by equation (2.10). Φ_y^V is a V-electron Slater determinant wavefunction, and Φ_0^C is a C-electron core wavefunction.

Average energies calculated with wavefunctions given by (5.8) differ in form as well as in value from their simple determinant counterparts. This difference is reflected in the n-electron density matrices, which can be obtained from equation (2.15). A wavefunction Φ_y^V is not in general strictly orthogonal to Φ_0^C, so the 1- and 2-electron density matrices have corrections arising from the overlap of the core and valence wavefunctions. Assuming normalized component wavefunctions, corrections to the 1-electron transition matrices are given by (5.11a), and corrections to the 2-electron transition matrices are given by (5.11b):

$$\Gamma^1_{y0y'0}(x;x') = \|\Phi_y^N\|^{-2}\|\Phi_{y'}^N\|^{-2}\Big\{\Gamma^1_{yy'}(x;x') + \Gamma^1_{00}(x;x')$$

$$+ \int dy\left[\Gamma^1_{yy'}(x;y)\Gamma^1_{00}(y;x') + \Gamma^1_{00}(x;y)\Gamma^1_{yy'}(y;x')\right] \qquad (5.11a)$$

$$- \int dydz\left[\Gamma^2_{00}(x,z;x',y)\Gamma^1_{yy'}(y;z) + \Gamma^2_{yy'}(x,z;x',y)\Gamma^1_{00}(y;z)\right] + \ldots\Big\}$$

where each expression is the beginning of a series of overlap corrections with the number of contracted coordinates taken as the expansion parameter. If there is only a single valence electron, then (5.11a) and (5.11b) are exact if the terms with valence n-electron transition matrices with n>1 are omitted.

$$\Gamma^2_{y0y'0}(x_1,x_2;x'_1,x'_2) = \|\Phi^N_y\|^{-2}\|\Phi^N_{y'}\|^{-2}A_2\Big\{ \Gamma^2_{yy'}(x_1,x_2;x'_1,x'_2)$$

$$+ 2\Gamma^1_{yy'}(x_1;x'_1)\Gamma^1_{00}(x_2;x'_2) + \Gamma^2_{00}(x_1,x_2;x'_1,x'_2)$$

$$-2\int dz\Big[\Gamma^2_{yy'}(x_1,z;x'_1x'_2)\Gamma^1_{00}(x_2;z) + \Gamma^2_{yy'}(x_1x_2;x'_1z)\Gamma^1_{00}(z;x'_2)$$

$$-2\int dy\Big[\Gamma^1_{yy'}(x_1;y)\Gamma^2_{00}(x_2,y;x'_1x'_2) + \Gamma^1_{yy'}(y;x'_1)\Gamma^2_{00}(x_1x_2;x'_2y)\Big]$$

$$-3\int dydz\Big[\Gamma^3_{yy'}(x_1,x_2,z;x'_1x'_2,y)\Gamma^1_{00}(y;z) + \Gamma^1_{yy'}(y;z)\Gamma^3_{00}(x_1x_2,z;x'_1x'_2,y)\Big]$$

$$+\int dydz\Big[\Gamma^2_{yy'}(x_1,x_2;y,z)\Gamma^2_{00}(y,z;x'_1x'_2) + \Gamma^2_{yy'}(y,z;x'_1,x'_2)\Gamma^2_{00}(x_1x_2;y,z)\Big]$$

$$-8\int dydz\Big[\Gamma^2_{00}(x_1,z;x'_1,y)\Gamma^2_{yy'}(x_2,y;x'_2,z)\Big] + \ldots \Big\}_{>A_2^\dagger}$$

Equation (5.11b)

The major effect of assuming a correlated core wavefunction is a change in the configuration average energy, but terms of the form

$$\int dydz\ \Gamma^3_{yy'}(x_1,x_2,z;x'_1,x'_2,y)\Gamma^1_0(y;z)$$

contribute corrections to the $\bar{F}^k$ and $\bar{G}^k$ parameters, while terms of the form

$$\int dydz\ \Gamma^2_{yy'}(x_1,x_2,;y,z)\Gamma^1_0(y,z;x'_1,x'_2)$$

can contribute to the empirical configuration interaction parameters[23-26].

Core Polarization

It is difficult to make any specific observations about the effects of including internal correlations; perturbation calculations have shown there can be many nearly canceling terms in the sum over corrections due to correlations of the core electrons[26,27]. In cases where there is little overlap between the core and valence wavefunctions, a core polarization model can describe the correction to the average energy. This technique has been used mainly with excited single valence electrons in non-penetrating orbits[7,28,65-67]. Considering only the dipole polarizability, the change in energy due to polarization of the core by a highly excited valence electron is given by

$$\Delta E_p = \alpha\left\langle r^{-4}\right\rangle_{n\ell} \tag{5.12}$$

where $\left\langle r^{-4}\right\rangle_{n\ell}$ indicates the average of r^{-4} over the valence $(n\ell)$ electron charge density.

The relative energies of a Rydberg series calculated via the Hartree-Fock approximation should be fairly accurate up to the order of the dipole polarization. This suggests that the polarizability might be used as a free parameter in an adjustment scheme for the configuration average energies. More generally, the polarizability of an internally correlated core wavefunction could be parameterized and interpreted as the dipole polarizability of the parent ion in its ground state that has

been allowed to relax in the averaged field of the valence electrons.

External Correlations

In some cases, effective Hamiltonians must explicitly include more than a single configuration. The additional configurations required in a given situation will depend on the correlations absorbed into the single configuration wavefunctions. Large numbers of configurations corresponding to a given type of promotion (e.g. $(n_1\ell_1, n_2\ell_2) \rightarrow (n_1'\ell_1', n_2'\ell_2')$ for many n_1', n_2') are often needed in an ab-initio calculation to get an accurate approximation of a given atomic state belonging to zero-order configuration. Many of configurations with important contributions can have average energies that lie above the ionization energy, making an accurate ab-initio calculation even more difficult.

If configuration interaction is considered in light of radially and internally correlated single configuration wavefunctions, large numbers of configurations should not be necessary. With the addition of radial correlations, all generalized configurations (in the sense of chapter IV) i.e. all zero-order atomic states that carry the same irreducible representation of the semi-direct product of S_N and $[SU(2)\times O^+(3)]^N$ are already included. With many other zero-order configurations included via core correlations, quite accurate atomic wavefunctions could, in principle, be obtained by superposition of only a few generalized configurations.

5.1.2 Adjustment Strategies

A combination of the ideas discussed in (5.1.1) and the empirical results of atomic spectroscopy as presented by Edlén[7] suggests methods of adjusting ab-initio parameters using least squares minimization and linear constraints. The principle parameters are considered in turn, roughly in order of importance: E_{av}; the Slater Integrals F^k, G^k, and R^k; and the spin-orbit parameters $\zeta_{n\ell}$. The empirical parameters α, β, γ, etc. are considered here as fine adjustments to the effective Hamiltonian that can be determined by least squares optimization when all possible levels have been assigned.

Configuration Average Energies

The bulk of the detailed correlation effects described in (5.1.1) will contribute large unknown shifts to the configuration average energies. The effective Hamiltonian approach describes only relative energies, so the configuration average energies basically must be treated as free parameters. An exception is a group of highly excited Rydberg configurations, where the core polarization model is applicable. Then, the ab-initio average energies can be adjusted via a two parameter fit

$$\overline{E}_{av}^{n\ell} = E_{av}^{n\ell} + \alpha\langle r^{-4}\rangle_{n\ell} + E_0^{nl} \qquad (5.13)$$

where E_0^{nl} is a constant correction needed because of the sensitivity of the core polarization correction to the ionization energy. The corrections to the configuration average energies can also, of course, be extrapolated along isoelectronic sequences (see section (5.1.3) below).

Slater Integrals

The Slater integrals $F^k(n\ell n'\ell')$ and $G^k(n\ell n'\ell')$ are the most commonly constrained parameters. Typically, the adjusted parameters are taken in the form

$$\bar{R}^k(abcd) = \Theta_{abcd} R^k(abcd) \tag{5.14a}$$

so that the ratios of the adjusted and ab-initio parameters are the same, i.e.

$$\frac{\bar{R}^{k+2}(abcd)}{\bar{R}^k(abcd)} = \frac{R^{k+2}(abcd)}{R^k(abcd)} \tag{5.14b}$$

The dominant corrections to the parameters representing Slater integrals involving only unfilled subshells, both within and between configurations, probably take the form of (5.8). In this context, a simple argument can be made for linear constraints, (5.14a).

An integral $R^k(abcd)$ is determined mainly by contributions from regions near $r'=r''$, because the functions $U_k(r',r'')$ are peaked about $r'=r''$, with the sharpness increasing with increasing k. If $U_k(r',r'')$ is rewritten in the form

$$U_k(r',r'') = \tilde{U}_k(r,x) = \frac{2}{r}\frac{(1-|x|)^k}{(1+|x|)^{k+1}} \tag{5.15a}$$

$$r = \frac{r'+r''}{2} \; ; \quad x = \frac{r'-r''}{r'+r''} \tag{5.15b}$$

then the integral takes the form

$$R^k(abcd) = 2\int_{-1}^{1} dx \int_0^\infty dr\, r\tilde{U}_k(r,x) p_{ac}(r[1+x]) p_{bd}(r[1-x]) \tag{5.16a}$$

$$p_{ac}(r) = P_a(r)P_c(r) \; ; \; p_{bd}(r) = P_b(r)P_d(r) \qquad (5.16b)$$

If the radial wavefunctions are slowly varying at large radii, (5.16a) can be expanded

$$R^k(abcd) = 8I_k \left[\int_0^\infty dr p_{ac}(r)p_{bd}(r) + \right.$$

$$\langle x^2 \rangle_k \int_0^\infty dr r^2 \left[p''_{ac}(r)p_{bd}(r) + p''_{bd}(r)p_{ac}(r) \right. \qquad (5.16c)$$

$$\left. \left. - 2p'_{ac}(r)p'_{bd}(r) \right] + \ldots + O\left[\langle x^4 \rangle_k \right] \right]$$

$$I_k = \int_0^1 dx \frac{(1-x)^k}{(1+x)^{k+1}} \qquad (5.16d)$$

$$\langle x^n \rangle_k = \frac{1}{I_k} \int_0^1 dx x^n \frac{(1-x)^k}{(1+x)^{k+1}} \qquad (5.16e)$$

The ratios between Slater integrals are roughly determined by the integrals I_k:

$$\frac{\bar{R}^{k+2}(abcd)}{\bar{R}^k(abcd)} \simeq \frac{I_{k+2}}{I_k} \qquad (5.17)$$

The integrals I_k for $0 \leq k \leq 6$, their ratios, $\langle x^2 \rangle_k$, and $\langle x^4 \rangle_k$ are given in table (5.1). If the corrections to the Slater parameters (5.8ab) are fairly small (say about 20%), then a fairly small error is introduced by adjusting them with the constraint (5.14). Also, if the dominant corrections are in the form of (5.8) and the functions $\{a_{ij}(r';r'')\}$ are much like $\{P_i(r)P_j(r)\}$ for $r'=r''=r$, then a linear constraint is an even better approximation.

Table (5.1)
Integrals of $(1-|x|)^k/(1+|x|)^{k+1}$

k	I_k	$\langle x^2 \rangle$	$\langle x^4 \rangle$	I_k/I_0	I_k/I_1	I_k/I_2	I_k/I_3	I_k/I_4	
0	.6931	.2787	.1584	1.0					
1	.3069	.1116	.0380	.4427	1.0				
2	.1931	.0565	.0123	.2787	.6924	1.0			
3	.1402	.0340	.0064	.2022	.4569	.7528	1.0		
4	.1098	.0216	.0022	.1584	.3579	.5686	.7833	1.0	
5	.0902	.0150	.0011	.1301	.2939	.4669	.6433	.8213	1.0
6	.0765	.0110	.0064	.1103	.2492	.3960	.5456	.6965	.8480

Spin-Orbit Parameters

The spin-orbit parameters are generally less important than the other parameters in the lighter atoms, and corrections to the ab-initio estimates can probably be ignored if sufficient data does not exist to determine them by least squares minimization. In the heavier atoms, the spin-orbit parametersfficult to predict accurately, and final values must be determined empirically. In the case of a Rydberg series (nℓ), however, empirical observations lead to a natural constraint for the $\xi_{n\ell}$'s. The empirical formula for $\xi_{n\ell}$ is given by[7]

$$\xi_{n\ell} = \frac{R\alpha^2(Z-s)^4}{(n^*)^3(\ell+\frac{1}{2})(\ell+1)} \qquad (5.18a)$$

where n* is the effective quantum number. An ab-initio estimate for $\xi_{n\ell}$ will be correct to order Z^4, so a constraint for all spin-orbit parameters of a series is given by

$$\bar{\xi}_{n\ell} = \left[\frac{Z-\bar{s}}{Z-s}\right]^4 \xi_{n\ell} \qquad (5.18b)$$

This idea tends to support the use of an overall scale factor with groups of spin-orbit parameters. The success of the expression (5.18a) is due to the sensitivity of $\xi_{n\ell}$ to small r, while the ab-initio estimates may not be correctly "screened" at small r.

5.1.3 Extrapolations

The behavior of the energy spectrum of atomic Hamiltonians as a function of nuclear charge Z with the number of electrons N fixed has been well-studied theoretically and empirically[7,55,68-71]. If a scale transformation is made on the non-relativistic atomic Hamiltonian so that $r \rightarrow r/Z$, then

$$H \rightarrow Z^2\left[H_0 + Z^{-1}V_C\right] \tag{5.19a}$$

$$H_0 = \sum_{i=1}^{N} p_i^2 - \frac{2}{r_i} \tag{5.19b}$$

$$V_C = \sum_{1=i<j}^{N} \frac{2}{r_{ij}} \tag{5.19c}$$

leading to a new eigenvalue equation

$$\left[H_0 + Z^{-1}V_C\right]\bar{\Phi}^N = \left[E/Z^2\right]\bar{\Phi}^N \tag{5.19d}$$

This form naturally suggests treating V_C as a perturbation with the perturbation parameter Z^{-1}.

The non-relativistic energies and eigenfunctions take the form

$$E = \sum_{n=0}^{\infty} Z^{2-n}E_n \tag{5.20a}$$

$$\Psi^N = \sum_{n=0}^{\infty} Z^{-n} \Phi_n^N \qquad (5.20b)$$

The zero-order eigenfunctions are Slater determinants of hydgrogenic 1-electron eigenfunctions, so that all determinants with the same set of principle (n) quantum numbers are degenerate. All degenerate configurations with the same inversion symmetry belong to a complex. A complex[70] is treated with first order degenerate perturbation theory, hence in the limit of large Z, the configurations of a complex have a limiting configuration interaction. Configurations of a complex are also considered likely candidates for multiple configuration effective Hamiltonians, especially when the differences between their average energies are not too large.

If the interelectron Coulomb potential is replaced with any approximation as in the case of the Hartree-Fock model, the 1/Z perturbation expansion can still be made. This implies that the difference in energy between such a model and the exact non-relativistic energy is a polynomial in Z of the form

$$E - E^{HF} = Z\,\Delta E_1 + \Delta E_0 + Z^{-1}\,\Delta E_1 + \cdots \qquad (5.21a)$$

and the parameters $\bar{F}^k$, $\bar{G}^k$, and $\bar{R}^k$ representing the coulomb interaction differ from the Hartree-Fock values by a polynomial

$$\bar{R}^k - R^k = R_0^k + Z^{-1}R_1^k + \cdots \qquad (5.21b)$$

Edlén[7] has successfully fit empirically determined values of F^k and G^k along isoelectronic sequences with formulae of the form

$$\overline{F}^k(ab) = Az + B + \frac{C}{z+D} \qquad (5.22)$$

where $z = Z-N+1$.

The relativistic version of the 1/Z perturbation theory is considerably more complex[70,71]. Many of the contributions to the Z dependence of the atomic energy levels are simply first order perturbations of the Pauli atomic Hamiltonian, table (2.4). As discussed in chapter III, some of these corrections can be incorporated into the configuration average energy calculated with any given independent particle model. If this is the case, and extrapolations are made for only a few values of Z in the early stages of ionization, the non-relativistic formula shoud be adequate. This is the view taken here.

For a fixed Z and N, methods can also be considered for obtaining corrections to some of the parameters from the adjustments made to others. One example applies to the configuration average energies of a Rydberg series. For an unperturbed Rydberg series, the average energies can often be fit very well to the Rydberg formula[7],

$$T_n = E_I - E_n = \frac{(Z-N+1)^2}{n^{*2}} \qquad (5.23a)$$

with

$$n^* = n - \alpha - \beta T_n \qquad (5.23b)$$

The adjustable parameters are the ionization energy E_I, α, and β. With a perturbed series, an effective Hamiltonian can be used that explicitly includes the major part of the configuration interaction, so that average energies for some members of the series can be adjusted to "unper-

turbed" values. The adjusted average energies can then be fit to the Rydberg formula and used to predict new average energies for the rest of the series.

A brief comment can be made about extrapolating corrections to other configurations at the same stage of ionization. If the corrections to say, the $F^k(n\ell n\ell)$ integrals for a configuration $n\ell^w$ are given by (5.8), the functions $\{a_{ii}(r',r'')\}$ might be fairly insensitive to w as long as z =(Z-N+1) remains the same. Then the differences between the ab-initio and empirical F^k's might be nearly the same for all w.

5.2 K I Isoelectronic Sequence

A substantial amount of analysis has been done on the first several members of the K^{0+} isoelectronic sequence because of their theoretical simplicity and experimental accessibility[72-85]. The first few ions are dominated by the spectrum of a single electron outside a closed core of eighteen electrons (isoelectronic with Ar^{0+}). Beginning with Ti^{4+}, the promotion of the 3p-electron from the closed $3p^6$ shell to another $n\ell$ orbital becomes favorable at energies low enough to noticeably perturb the single electron spectrum[78-84]. Levels assigned to the $3p^5 3d^2$ and $3p^5 3d4s$ configurations have been identified for Ti^{3+} through Fe^{7+} with the aid of Cowan's HX calculations,[79,81,82] suggesting that the relationship of the calculated to the observed energy levels might be studied and used to extend the analyses of other ions in the series, particularly Mn^{6+} and Fe^{7+}. Fe^{7+} is probably the highest stage of ionization of iron that can be reasonably generated with a sliding spark source, and its spectra are of astrophysical interest.

The calculations are described and compared with the known energy levels along the isoelectronic sequence in (5.2.1). These comparisons are combined with the ideas discussed in section (5.1) to formulate an adjustment strategy for the calculated parameters of V^{4+} and Cr^{5+} in (5.2.2). The adjustments are then extrapolated Ti^{3+}, Mn^{6+}, and Fe^{7+}. Then the parameters of the identified configurations for each of these ions are optimized by least squares. The revised corrections for these refined parameters are then extrapolated to the ions where the corresponding configurations have not been identified (where possible) in (5.2.3).

5.2.1 Experimental Energies and HXR Calculations

A representative sample of the configurations identified in the ions K^{0+} through Fe^{7+} was selected for the study, including sixteen even parity configurations (4s, 5s, 6s, 7s, 8s, 4d, 5d, 6d, 7d, 7i, 8i, and $3p^5 3d4p$) and fifteen odd configurations (4p, 5p, 6p, 7p, 4f, 5f, 6f, 7f, 8f, 9f, 10f, 6h, 7h, $3p^5 3d^2$, and $3p^5 3d4s$). No levels belonging to the $3p^5 3d4p$ configuration have been identified for any ion, but it is suspected that this configuration perturbs the 5g, 6g, and 7g levels as early as Cr^{5+}, because of the anomalously large orbit splitting of the 5g levels[79]. Analysis of the Mn^{6+} and Fe^{7+} ions has been difficult to date, particularly in the case of the excited even parity configurations; most of the classified lines terminate with the $3d\ ^2D$ levels. Perhaps the transitions between the $3p^5 3d4p$ configuration and the $3p^5 3d^2$, $3p^5 3d4s$ configurations begin to dominate the spectra of Mn^{6+} and Fe^{7+}, explaining why more of even parity configurations have not been identified. The spectra of these two ions have been recalculated with

adjusted parameters and presented in the appendix.

The experimentally observed and calculated energy levels are displayed in tables (5.2) through (5.9); the calculated levels are derived from the "raw" HXR parameters without any empirical scaling and including Cowan's correlation correction (E_c of equation (3.19)). When scaling factors are applied to the $\zeta_{n\ell}$'s, R^k's, F^k's and G^k's, however, the calculated levels reproduce earlier work of Cowan[14,81,82,84]. The energies are compared relative to the $3p^6$ ground state of the parent ion (the calculated $3p^6$ average energy is set equal to the experimentally determined ionization energy) with zero taken at the observed ground state energy. For purposes of comparison, the elementary finite nuclear mass correction has been applied to the calculated levels for all displayed tables. Although this correction is only a few cm^{-1}, the inverse of this correction was applied to the observed levels before any adjustments were made.

The experimentally derived ionization energies, in order from K^{0+} to Fe^{7+}, are: 35009.77 (K I)[72,73], 95751.87 (CaII)[74], 199677.37 (ScIII)[75,76], 348973.7 (TiIV)[77], 526532.0 (V V)[78], 731020 (CrVI)[79], 962000 (MnVII)[83], 1218400 (FeVIII)[84]. An overall constant discrepancy between the observed and calculated levels is possible for any ion due to an error in the experimental ionization energy, but the the ionization energies are quite accurate ($\leq$ 6 cm^{-1}) through Cr^{5+} for the purpose of comparing with the calculations. The ground state of the parent ion is a convenient reference point for isoelectronic comparison because it is a non-degenerate, closed shell $^1S_0$ configuration, and its energy should vary smoothly with Z.

TABLE (5.2A)

K 0+ ODD LEVELS
HXR CALCULATIONS COMPARED WITH EXPERIMENTAL OBSERVATIONS
UNCORRECTED HXR PARAMETERS WITH CONFIGURATION INTERACTION
PARENTAGE -- DD(2S+1)L = 3D2(2S+1)L
DD(2S+1)L = 3D2(2S+1)L DS(2S+1)L = (3P5(2P)3D(2D))(2S+1)L

IRREP	CALC	EXP	INCR	J/MU	TOTAL	-- EIGENVECTOR COMPOSITION PCT
2P 1/2	11865.	12985.	-1119.9	.5	100.	100. 2P (4P)
2P 3/2	11936.	13043.	-1107.3	1.5	100.	100. 2P (4P)
2P 1/2	24402.	24701.	-299.0	.5	100.	100. 2P (5P)
2P 3/2	24427.	24720.	-293.0	1.5	100.	100. 2P (5P)
2F 5/2	28129.	28128.	1.3	2.5	100.	100. 2F (4F)
2F 7/2	28129.	28128.	1.3	3.5	100.	100. 2F (4F)
2P 1/2	28872.	28999.	-127.6	.5	100.	100. 2P (6P)
2P 3/2	28883.	29008.	-124.5	1.5	100.	100. 2P (6P)
2F 5/2	30604.	30606.	-1.6	2.5	100.	100. 2F (5F)
2F 7/2	30604.	30606.	-1.6	3.5	100.	100. 2F (5F)
2P 1/2	31004.	31070.	-66.3	.5	100.	100. 2P (7P)
2P 3/2	31010.	31074.	-64.6	1.5	100.	100. 2P (7P)
2F 5/2	31951.	31953.	-2.5	2.5	100.	100. 2F (6F)
2F 7/2	31951.	31953.	-2.5	3.5	100.	100. 2F (6F)
2H 9/2	31961.	31961.	.8	4.5	100.	100. 2H (6H)
2H11/2	31961.	31961.	.8	5.5	100.	100. 2H (6H)
2F 5/2	32763.	32765.	-1.4	2.5	100.	100. 2F (7F)
2F 7/2	32763.	32765.	-1.4	3.5	100.	100. 2F (7F)
2F 5/2	33290.	33291.	-1.0	2.5	100.	100. 2F (8F)
2F 7/2	33290.	33291.	-1.0	3.5	100.	100. 2F (8F)
2F 5/2	33651.	33652.	-.8	2.5	100.	100. 2F (9F)
2F 7/2	33651.	33652.	-.8	3.5	100.	100. 2F (9F)
2F 5/2	33910.	33910.	-.4	2.5	100.	100. 2F (10F)
2F 7/2	33910.	33910.	-.4	3.5	100.	100. 2F (10F)

NO. EXPERIMENTAL LEVELS = 24.

ABSOLUTE MEAN DEVIATION = 134.25

RMS DEVIATION = 335.16

TABLE (5.2B)

K 0+ EVEN LEVELS
HXR CALCULATIONS COMPARED WITH EXPERIMENTAL OBSERVATIONS
UNCORRECTED HXR PARAMETERS WITH CONFIGURATION INTERACTION
PARENTAGE -- DD(2S+1)L = 3D2(2S+1)L
DD(2S+1)L = 3D2(2S+1)L DS(2S+1)L = (3P5(2P)3D(2D))(2S+1)L

IRREP	CALC	EXP	INCR	J/MU	TOTAL	-- EIGENVECTOR COMPOSITION PCT
2S 1/2	-1473.	0.	-1472.5	.5	100.	100. 2S (4S)
2D 3/2	20208.	21537.	-1328.6	1.5	99.	99. 2D (3D)
2D 5/2	20209.	21534.	-1325.9	2.5	99.	99. 2D (3D)
2S 1/2	20985.	21027.	-41.7	.5	100.	100. 2S (5S)
2D 3/2	27323.	27398.	-74.7	1.5	100.	100. 2D (4D)
2D 5/2	27324.	27397.	-72.7	2.5	100.	100. 2D (4D)
2S 1/2	27445.	27451.	-5.4	.5	100.	100. 2S (6S)
2D 3/2	30150.	30186.	-35.9	1.5	100.	100. 2D (5D)
2D 5/2	30150.	30185.	-34.7	2.5	100.	100. 2D (5D)
2S 1/2	30274.	30274.	-.5	.5	100.	100. 2S (7S)
2G 7/2	30620.	30620.	-.1	3.5	100.	100. 2G (5G)
2G 9/2	30620.	30620.	-.1	4.5	100.	100. 2G (5G)
2D 3/2	31680.	31696.	-16.1	1.5	100.	100. 2D (6D)
2D 5/2	31680.	31696.	-15.4	2.5	100.	100. 2D (6D)
2S 1/2	31765.	31765.	.4	.5	100.	100. 2S (8S)
2G 7/2	31961.	31961.	.0	3.5	100.	100. 2G (6G)
2G 9/2	31961.	31961.	.0	4.5	100.	100. 2G (6G)
2D 3/2	32591.	32598.	-7.3	1.5	100.	100. 2D (7D)
2D 5/2	32591.	32598.	-7.0	2.5	100.	100. 2D (7D)

NO. EXPERIMENTAL LEVELS = 19.
ABSOLUTE MEAN DEVIATION = 233.65
RMS DEVIATION = 548.06

TABLE (5.3A)

CA1+ ODD LEVELS
HXR CALCULATIONS COMPARED WITH EXPERIMENTAL OBSERVATIONS
UNCORRECTED HXR PARAMETERS WITH CONFIGURATION INTERACTION
PARENTAGE -- DD(2S+1)L = 3D2(2S+1)L
DD(2S+1)L = 3D2(2S+1)L DS(2S+1)L = (3P5(2P)3D(2D))(2S+1)L

IRREP	CALC	EXP	INCR	J/MU	TOTAL	-- EIGENVECTOR COMPOSITION PCT
2P 1/2	23379.	25192.	-1812.3	.5	100.	100. 2P (4P)
2P 3/2	23645.	25414.	-1769.8	1.5	100.	100. 2P (4P)
2P 1/2	60241.	60533.	-291.6	.5	100.	100. 2P (5P)
2P 3/2	60339.	60611.	-272.6	1.5	100.	100. 2P (5P)
2F 5/2	67954.	68057.	-103.2	2.5	100.	100. 2F (4F)
2F 7/2	67954.	68057.	-103.0	3.5	100.	100. 2F (4F)
2P 1/2	74386.	74485.	-99.3	.5	100.	100. 2P (6P)
2P 3/2	74432.	74522.	-90.1	1.5	100.	100. 2P (6P)
2F 5/2	77959.	78034.	-75.9	2.5	100.	100. 2F (5F)
2F 7/2	77959.	78034.	-75.7	3.5	100.	100. 2F (5F)
2P 1/2	81453.	81498.	-45.2	.5	100.	100. 2P (7P)
2P 3/2	81478.	81517.	-38.8	1.5	100.	100. 2P (7P)
2F 5/2	83410.	83458.	-48.4	2.5	100.	100. 2F (6F)
2F 7/2	83410.	83458.	-48.3	3.5	100.	100. 2F (6F)
2H 9/2	83557.	83553.	4.5	4.5	100.	100. 2H (6H)
2H11/2	83557.	83553.	4.5	5.5	100.	100. 2H (6H)
2F 5/2	86696.	86727.	-31.5	2.5	100.	100. 2F (7F)
2F 7/2	86696.	86727.	-31.4	3.5	100.	100. 2F (7F)
2H 9/2	86792.	86790.	2.5	4.5	100.	100. 2H (7H)
2H11/2	86792.	86790.	2.5	5.5	100.	100. 2H (7H)
2F 5/2	88825.	88847.	-21.8	2.5	100.	100. 2F (8F)
2F 7/2	88826.	88847.	-21.8	3.5	100.	100. 2F (8F)
2F 5/2	90284.	90300.	-15.6	2.5	100.	100. 2F (9F)
2F 7/2	90284.	90300.	-15.6	3.5	100.	100. 2F (9F)

NO. EXPERIMENTAL LEVELS = 24.

ABSOLUTE MEAN DEVIATION = 209.41

RMS DEVIATION = 525.93

TABLE (5.3B)

CA1+ EVEN LEVELS
HXR CALCULATIONS COMPARED WITH EXPERIMENTAL OBSERVATIONS
UNCORRECTED HXR PARAMETERS WITH CONFIGURATION INTERACTION
PARENTAGE -- DD(2S+1)L = 3D2(2S+1)L
DD(2S+1)L = 3D2(2S+1)L DS(2S+1)L = (3P5(2P)3D(2D))(2S+1)L

IRREP	CALC	EXP	INCR	J/MU	TOTAL	-- EIGENVECTOR COMPOSITION PCT
2S 1/2	-2452.	0.	-2451.8	.5	99.	99. 2S (4S)
2D 3/2	13334.	13650.	-315.9	1.5	99.	99. 2D (3D)
2D 5/2	13446.	13711.	-265.0	2.5	99.	99. 2D (3D)
2S 1/2	52262.	52167.	94.7	.5	100.	100. 2S (5S)
2D 3/2	57025.	56839.	185.6	1.5	100.	100. 2D (4D)
2D 5/2	57049.	56858.	190.7	2.5	100.	100. 2D (4D)
2S 1/2	70747.	70678.	69.5	.5	100.	100. 2S (6S)
2D 3/2	72834.	72722.	111.5	1.5	100.	100. 2D (5D)
2D 5/2	72844.	72731.	113.3	2.5	100.	100. 2D (5D)
2G 7/2	78173.	78165.	8.7	3.5	100.	100. 2G (5G)
2G 9/2	78173.	78165.	8.7	4.5	100.	100. 2G (5G)
2S 1/2	79490.	79448.	42.0	.5	100.	100. 2S (7S)
2D 3/2	80590.	80522.	68.0	1.5	100.	100. 2D (6D)
2D 5/2	80595.	80526.	68.9	2.5	100.	100. 2D (6D)
2G 7/2	83541.	83540.	.8	3.5	100.	100. 2G (6G)
2G 9/2	83541.	83540.	.8	4.5	100.	100. 2G (6G)
2S 1/2	84327.	84301.	25.8	.5	100.	100. 2S (8S)
2D 3/2	84978.	84934.	44.4	1.5	100.	100. 2D (7D)
2D 5/2	84981.	84936.	45.2	2.5	100.	100. 2D (7D)
2G 7/2	86780.	86781.	-1.1	3.5	100.	100. 2G (7G)
2G 9/2	86780.	86781.	-1.1	4.5	100.	100. 2G (7G)

NO. EXPERIMENTAL LEVELS = 21.
ABSOLUTE MEAN DEVIATION = 195.88
RMS DEVIATION = 548.03

TABLE (5.4A)

SC2+ ODD LEVELS
HXR CALCULATIONS COMPARED WITH EXPERIMENTAL OBSERVATIONS
UNCORRECTED HXR PARAMETERS WITH CONFIGURATION INTERACTION
PARENTAGE -- DD(2S+1)L = 3D2(2S+1)L
DD(2S+1)L = 3D2(2S+1)L DS(2S+1)L = (3P5(2P)3D(2D))(2S+1)L

IRREP	CALC	EXP	INCR	J/MU	TOTAL	-- EIGENVECTOR COMPOSITION PCT
2P 1/2	60218.	62104.	-1886.2	.5	100.	100. 2P (4P)
2P 3/2	60774.	62578.	-1804.2	1.5	100.	100. 2P (4P)
2P 1/2	128028.	128107.	-79.2	.5	100.	100. 2P (5P)
2P 3/2	128238.	128283.	-45.0	1.5	100.	100. 2P (5P)
2F 5/2	136533.	136874.	-340.8	2.5	100.	100. 2F (4F)
2F 7/2	136535.	136874.	-338.8	3.5	100.	100. 2F (4F)
2P 1/2	155526.	155490.	36.0	.5	100.	100. 2P (6P)
2P 3/2	155627.	155575.	51.9	1.5	100.	100. 2P (6P)
2F 5/2	159308.	159472.	-164.7	2.5	100.	100. 2F (5F)
2F 7/2	159310.	159472.	-162.4	3.5	100.	100. 2F (5F)
2P 1/2	169682.	169638.	44.3	.5	100.	100. 2P (7P)
2P 3/2	169739.	169686.	52.9	1.5	100.	100. 2P (7P)
2F 5/2	171707.	171788.	-81.0	2.5	100.	100. 2F (6F)
2F 7/2	171708.	171788.	-79.4	3.5	100.	100. 2F (6F)
2H 9/2	172255.	172225.	30.1	4.5	100.	100. 2H (6H)
2H11/2	172255.	172225.	30.1	5.5	100.	100. 2H (6H)
2F 5/2	179175.	179215.	-39.7	2.5	100.	100. 2F (7F)
2F 7/2	179176.	179215.	-38.5	3.5	100.	100. 2F (7F)
2H 9/2	179533.	179508.	24.7	4.5	100.	100. 2H (7H)
2H11/2	179533.	179508.	24.7	5.5	100.	100. 2H (7H)

NO. EXPERIMENTAL LEVELS = 20.

ABSOLUTE MEAN DEVIATION = 267.74

RMS DEVIATION = 597.22

TABLE (5.4B)

SC2+ EVEN LEVELS
HXR CALCULATIONS COMPARED WITH EXPERIMENTAL OBSERVATIONS
UNCORRECTED HXR PARAMETERS WITH CONFIGURATION INTERACTION
PARENTAGE -- DD(2S+1)L = 3D2(2S+1)L
DD(2S+1)L = 3D2(2S+1)L DS(2S+1)L = (3P5(2P)3D(2D))(2S+1)L

IRREP	CALC	EXP	INCR	J/MU	TOTAL	-- EIGENVECTOR COMPOSITION PCT
2D 3/2	-76.	0.	-75.8	1.5	100.	100. 2D (3D)
2D 5/2	215.	198.	17.8	2.5	100.	100. 2D (3D)
2S 1/2	22461.	25539.	-3078.5	.5	99.	99. 2S (4S)
2D 3/2	112171.	112258.	-86.8	1.5	99.	99. 2D (4D)
2D 5/2	112225.	112303.	-78.4	2.5	99.	99. 2D (4D)
2S 1/2	115112.	114862.	250.0	.5	100.	100. 2S (5S)
2D 3/2	148300.	148130.	170.0	1.5	100.	100. 2D (5D)
2D 5/2	148325.	148150.	174.5	2.5	100.	100. 2D (5D)
2S 1/2	149375.	149194.	180.5	.5	100.	100. 2S (6S)
2G 7/2	160088.	160072.	15.7	3.5	100.	100. 2G (5G)
2G 9/2	160088.	160072.	15.7	4.5	100.	100. 2G (5G)
2D 3/2	165734.	165593.	141.0	1.5	100.	100. 2D (6D)
2D 5/2	165747.	165603.	143.5	2.5	100.	100. 2D (6D)
2S 1/2	166273.	166157.	116.2	.5	100.	100. 2S (7S)
2G 7/2	172179.	172177.	1.7	3.5	100.	100. 2G (6G)
2G 9/2	172179.	172177.	1.7	4.5	100.	100. 2G (6G)
2D 3/2	175565.	175457.	108.2	1.5	100.	100. 2D (7D)
2D 5/2	175573.	175464.	109.8	2.5	100.	100. 2D (7D)
2S 1/2	175877.	175796.	80.9	.5	100.	100. 2S (8S)
2G 7/2	179481.	179477.	4.0	3.5	100.	100. 2G (7G)
2G 9/2	179481.	179477.	4.0	4.5	100.	100. 2G (7G)

NO. EXPERIMENTAL LEVELS = 21.

ABSOLUTE MEAN DEVIATION = 231.19

RMS DEVIATION = 680.90

TABLE (5.5A)

TI3+ ODD LEVELS
HXR CALCULATIONS COMPARED WITH EXPERIMENTAL OBSERVATIONS
UNCORRECTED HXR PARAMETERS WITH CONFIGURATION INTERACTION
PARENTAGE -- DD(2S+1)L = 3D2(2S+1)L
DD(2S+1)L = 3D2(2S+1)L DS(2S+1)L = (3P5(2P)3D(2D))(2S+1)L

IRREP	CALC	EXP	INCR	J/MU	TOTAL	-- EIGENVECTOR COMPOSITION PCT	
2P 1/2	126089.	127921.	-1832.8	.5	99.	99. 2P (4P)	
2P 3/2	127037.	128740.	-1702.9	1.5	99.	99. 2P (4P)	
2P 1/2	230724.	230609.	115.3	.5	100.	100. 2P (5P)	
2P 3/2	231093.	230924.	168.2	1.5	100.	100. 2P (5P)	
2F 5/2	235435.	236135.	-700.4	2.5	99.	99. 2F (4F)	
2F 7/2	235451.	236142.	-691.8	3.5	99.	99. 2F (4F)	
2P 1/2	274870.	274726.	143.3	.5	100.	100. 2P (6P)	
2P 3/2	275051.	274881.	169.4	1.5	100.	100. 2P (6P)	
2F 5/2	275588.	275847.	-259.2	2.5	95.	90. 2F (5F)	6. 2F (DD(1G))
2F 7/2	275660.	275862.	-202.0	3.5	92.	92. 2F (5F)	
4F 5/2	280760.	274840.	5920.0	2.5	96.	73. 4F (DD(3F))	18. 2D (DD(1D))
						5. 2D (DD(3F))	
2P 1/2	298146.	298000.	146.4	.5	100.	100. 2P (7P)	
2P 3/2	298259.	298088.	170.6	1.5	99.	99. 2P (7P)	
2H11/2	300176.	300159.	17.2	5.5	100.	100. 2H (6H)	
2H 9/2	300176.	300159.	17.4	4.5	100.	100. 2H (6H)	
2H11/2	313115.	313111.	4.0	5.5	100.	100. 2H (7H)	
2H 9/2	313115.	313111.	4.0	4.5	100.	100. 2H (7H)	

NO. EXPERIMENTAL LEVELS = 17.

ABSOLUTE MEAN DEVIATION = 721.46

RMS DEVIATION = 1581.59

TABLE (5.5B)

TI3+ EVENLEVELS
HXR CALCULATIONS COMPARED WITH EXPERIMENTAL OBSERVATIONS
UNCORRECTED HXR PARAMETERS WITH CONFIGURATION INTERACTION
PARENTAGE -- DD(2S+1)L = 3D2(2S+1)L
DD(2S+1)L = 3D2(2S+1)L DS(2S+1)L = (3P5(2P)3D(2D))(2S+1)L

IRREP	CALC	EXP	INCR	J/MU	TOTAL	-- EIGENVECTOR COMPOSITION PCT
2D 3/2	-110.	0.	-109.6	1.5	100.	100. 2D (3D)
2D 5/2	406.	382.	23.7	2.5	100.	100. 2D (3D)
2S 1/2	76823.	80389.	-3565.6	.5	99.	99. 2S (4S)
2D 3/2	196578.	196804.	-226.0	1.5	99.	99. 2D (4D)
2D 5/2	196683.	196890.	-207.2	2.5	99.	99. 2D (4D)
2S 1/2	212767.	212407.	359.7	.5	100.	100. 2S (5S)
2D 3/2	259185.	258838.	346.4	1.5	100.	100. 2D (5D)
2D 5/2	259234.	258877.	356.7	2.5	100.	100. 2D (5D)
2S 1/2	266106.	265847.	258.6	.5	100.	100. 2S (6S)
2G 7/2	278468.	278511.	-43.1	3.5	100.	100. 2G (5G)
2G 9/2	278468.	278511.	-43.2	4.5	100.	100. 2G (5G)
2D 3/2	289443.	289186.	256.6	1.5	100.	100. 2D (6D)
2D 5/2	289469.	289207.	262.5	2.5	100.	100. 2D (6D)
2S 1/2	293160.	293000.	160.1	.5	100.	100. 2S (7S)
2G 7/2	299999.	300046.	-46.7	3.5	100.	100. 2G (6G)
2G 9/2	300000.	300046.	-46.6	4.5	100.	100. 2G (6G)
2D 3/2	306572.	306396.	176.2	1.5	100.	100. 2D (7D)
2D 5/2	306588.	306408.	179.7	2.5	100.	100. 2D (7D)
2S 1/2	308811.	308710.	101.8	.5	100.	100. 2S (8S)
2G 7/2	313001.	313034.	-32.8	3.5	100.	100. 2G (7G)
2G 9/2	313002.	313034.	-32.5	4.5	100.	100. 2G (7G)
2I 11/2	313139.	313131.	7.8	5.5	100.	100. 2I (7I)
2I 11/2	321537.	321531.	5.4	5.5	100.	100. 2I (8I)

NO. EXPERIMENTAL LEVELS = 23.

ABSOLUTE MEAN DEVIATION = 297.75

RMS DEVIATION = 766.36

TABLE (5.6A)

V 4+ ODD LEVELS
HXR CALCULATIONS COMPARED WITH EXPERIMENTAL OBSERVATIONS
UNCORRECTED HXR PARAMETERS WITH CONFIGURATION INTERACTION
PARENTAGE -- DD(2S+1)L = 3D2(2S+1)L
DD(2S+1)L = 3D2(2S+1)L DS(2S+1)L = (3P5(2P)3D(2D))(2S+1)L

IRREP	CALC	EXP	INCR	J/MU	TOTAL	-- EIGENVECTOR COMPOSITION PCT
2P 1/2	204681.	206394.	-1713.2	.5	99.	99. 2P (4P)
2P 3/2	206136.	207660.	-1524.4	1.5	99.	99. 2P (4P)
2D 5/2	320647.	319106.	1541.2	2.5	95.	35. 2D (DD(1D)) 25. 4F (DD(3F)) 16. 2F (DD(1G)) 11. 2F (DD(3F)) 8. 2D (DD(3F))
2F 7/2	322840.	320732.	2108.9	3.5	92.	49. 2F (DD(1G)) 38. 2F (DD(3F)) 6. 2F (DD(1D))
2F 7/2	334677.	332198.	2479.2	3.5	97.	75. 2F (DD(1D)) 8. 2G (DD(3F)) 8. 2F (4F) 5. 2F (DD(3F))
2F 5/2	339572.	337013.	2559.6	2.5	97.	70. 2F (DD(1D)) 22. 2F (4F) 5. 2F (DD(3F))
2F 7/2	349228.	349252.	-24.0	3.5	96.	85. 2F (4F) 12. 2F (DD(1D))
2F 5/2	350244.	349676.	568.2	2.5	97.	71. 2F (4F) 26. 2F (DD(1D))
2P 1/2	351845.	351501.	344.3	.5	99.	99. 2P (5P)
2P 3/2	352434.	352018.	415.2	1.5	99.	99. 2P (5P)
2F 5/2	406150.	417699.	-11548.8	2.5	95.	66. 2F (5F) 17. 2F (DD(3F)) 13. 2F (DD(1G))
2F 7/2	406893.	418188.	-11295.0	3.5	96.	70. 2F (5F) 15. 2F (DD(3F)) 11. 2F (DD(1G))
2P 1/2	415685.	415420.	264.9	.5	99.	99. 2P (6P)
2P 3/2	415982.	415676.	305.9	1.5	100.	100. 2P (6P)
2F 5/2	429134.	396135.	32998.4	2.5	94.	33. 2F (5F) 26. 2F (DD(3F)) 24. 2F (DD(1G)) 12. 2F (6F)
2F 7/2	430629.	397994.	32635.2	3.5	94.	28. 2F (5F) 26. 2F (DD(3F)) 25. 2F (DD(1G)) 15. 2F (6F)
2P 1/2	449708.	449587.	121.7	.5	99.	99. 2P (7P)
2P 3/2	449902.	449773.	129.4	1.5	99.	99. 2P (7P)
2H 9/2	450265.	450248.	16.9	4.5	100.	100. 2H (6H)
2H11/2	450265.	450248.	17.4	5.5	100.	100. 2H (6H)
2F 5/2	451968.	449371.	2597.4	2.5	91.	85. 2F (6F) 5. 2F (DD(1G))
2F 7/2	452307.	449422.	2884.5	3.5	94.	83. 2F (6F) 6. 2F (DD(1G)) 5. 2F (DD(3F))

TABLE (5.6A) CONTINUED

V 4+ ODD LEVELS
HXR CALCULATIONS COMPARED WITH EXPERIMENTAL OBSERVATIONS
UNCORRECTED HXR PARAMETERS WITH CONFIGURATION INTERACTION
PARENTAGE -- DD(2S+1)L = 3D2(2S+1)L
DD(2S+1)L = 3D2(2S+1)L DS(2S+1)L = (3P5(2P)3D(2D))(2S+1)L

IRREP	CALC	EXP	INCR	J/MU	TOTAL	-- EIGENVECTOR COMPOSITION PCT
2P 1/2	455313.	438018.	17294.9	.5	89.	63. 2P (DS(3P)) 26. 2P (DD(3P))
2P 3/2	457702.	439443.	18259.6	1.5	92.	58. 2P (DS(3P)) 29. 2P (DD(3P)) 6. 2P (DD(1D))
2H 9/2	470486.	470489.	-3.1	4.5	100.	100. 2H (7H)
2H11/2	470486.	470489.	-2.6	5.5	100.	100. 2H (7H)
2F 5/2	470765.	469702.	1063.2	2.5	91.	91. 2F (7F)
2F 7/2	470819.	469716.	1102.7	3.5	92.	92. 2F (7F)
2D 5/2	474895.	444154.	30741.6	2.5	96.	64. 2D (DD(3F)) 15. 2D (DD(1D)) 10. 2D (DD(3P)) 6. 2D (DS(3D))
2D 3/2	475274.	444621.	30653.0	1.5	85.	61. 2D (DD(3F)) 15. 2D (DD(1D)) 9. 2D (DD(3P))
2F 7/2	475908.	475531.	377.4	3.5	93.	93. 2F (DS(3F))
2F 5/2	479219.	478566.	653.0	2.5	92.	92. 2F (DS(3F))
2F 7/2	483690.	483038.	651.6	3.5	96.	96. 2F (8F)
2F 5/2	483710.	483019.	690.7	2.5	95.	95. 2F (8F)
2F 7/2	492455.	492202.	253.2	3.5	95.	84. 2F (9F) 11. 4D (DS(3D))
2F 5/2	492529.	492144.	384.4	2.5	97.	97. 2F (9F)
2F 5/2	500294.	496296.	3998.3	2.5	94.	62. 2F (DS(1F)) 18. 2F (10F) 8. 2D (DS(1D)) 5. 4D (DS(3D))
2F 7/2	501306.	497556	3750.0	3.5	94.	78. 2F (DS(1F)) 9. 2F (10F) 8. 4D (DS(3D))
2D 3/2	505494.	500117.	5376.7	1.5	96.	91. 2D (DS(3D)) 5. 2D (DD(3F))
2D 5/2	505874.	500502.	5371.5	2.5	97.	76. 2D (DS(3D)) 8. 2D (DS(1D)) 7. 2F (DS(1F)) 5. 2D (DD(3F))

NO. EXPERIMENTAL LEVELS = 40.

ABSOLUTE MEAN DEVIATION = 5718.03

RMS DEVIATION = 11252.31

TABLE (5.6B)

V 4+ EVEN LEVELS
HXR CALCULATIONS COMPARED WITH EXPERIMENTAL OBSERVATIONS
UNCORRECTED HXR PARAMETERS WITH CONFIGURATION INTERACTION
PARENTAGE -- DD(2S+1)L = 3D2(2S+1)L
DD(2S+1)L = 3D2(2S+1)L DS(2S+1)L = (3P5(2P)3D(2D))(2S+1)L

IRREP	CALC	EXP	INCR	J/MU	TOTAL	-- EIGENVECTOR COMPOSITION PCT
2D 3/2	-190.	0.	-189.6	1.5	100.	100. 2D (3D)
2D 5/2	615.	625.	-9.7	2.5	100.	100. 2D (3D)
2S 1/2	144216.	148143.	-3927.8	5	99.	99. 2S (4S)
2D 3/2	293726.	293903.	-176.5	1.5	99.	99. 2D (4D)
2D 5/2	293908.	294047.	-139.8	2.5	99.	99. 2D (4D)
2S 1/2	328697.	328217.	479.8	.5	100.	100. 2S (5S)
2D 3/2	388573.	387977.	595.6	1.5	99.	99. 2D (5D)
2D 5/2	388659.	388044.	614.9	2.5	99.	99. 2D (5D)
2S 1/2	404214.	403855.	358.7	.5	100.	100. 2S (6S)
2G 7/2	416265.	416360.	-95.1	3.5	100.	100. 2G (5G)
2G 9/2	416267.	416362.	-95.2	4.5	100.	100. 2G (5G)
2D 3/2	434701.	434304.	397.0	1.5	99.	99. 2D (6D)
2D 5/2	434749.	434341.	407.9	2.5	99.	99. 2D (6D)
2S 1/2	443303.	443075	228.2	.5	100.	100. 2S (7S)
2G 7/2	449959.	450025.	-65.3	3.5	100.	100. 2G (6G)
2G 9/2	449960.	450025.	-65.1	4.5	100.	100. 2G (6G)
2D 3/2	460948.	460697.	250.7	1.5	100.	100. 2D (7D)
2D 5/2	460977.	460720.	257.8	2.5	100.	100. 2D (7D)
2S 1/2	466214.	466066.	148.5	.5	100.	100. 2S (8S)
2G 7/2	470297.	470333.	-36.4	3.5	100.	100. 2G (7G)
2G 9/2	470297.	470334.	-36.5	4.5	100.	100. 2G (7G)
2I11/2	470537.	470524.	12.6	5.5	100.	100. 2I (7I)
2I11/2	483658.	483651.	7.0	5.5	100.	100. 2I (8I)

NO. EXPERIMENTAL LEVELS = 23.

ABSOLUTE MEAN DEVIATION = 373.73

RMS DEVIATION = 863.85

TABLE (5.7A)

CR5+ ODD LEVELS
HXR CALCULATIONS COMPARED WITH EXPERIMENTAL OBSERVATIONS
UNCORRECTED HXR PARAMETERS WITH CONFIGURATION INTERACTION
PARENTAGE -- DD(2S+1)L = 3D2(2S+1)L
DD(2S+1)L = 3D2(2S+1)L DS(2S+1)L = (3P5(2P)3D(2D))(2S+1)L

IRREP	CALC	EXP	INCR	J/MU	TOTAL	-- EIGENVECTOR COMPOSITION PCT
2P 1/2	294971.	296573.	-1602.6	.5	99.	99. 2P (4P)
2P 3/2	297057.	298397.	-1340.2	1.5	99.	99. 2P (4P)
2F 5/2	358498.	356962.	1535.6	2.5	90.	49. 2F (DD(1G)) 40. 2F (DD(3F))
2F 7/2	361097.	359165.	1932.4	3.5	90.	48. 2F (DD(1G)) 42. 2F (DD(3F))
2F 7/2	374058.	371618.	2440.1	3.5	95.	73. 2F (DD(1D)) 22. 2G (DD(3F))
2F 5/2	382104.	378677.	3426.7	2.5	95.	95. 2F (DD(1D))
2F 5/2	451960.	440135.	11825.2	2.5	97.	38. 2F (4F) 34. 2F (DD(3F)) 25. 2F (DD(1G))
2F 7/2	454021.	442940.	11080.2	3.5	97.	42. 2F (4F) 31. 2F (DD(3F)) 24. 2F (DD(1G))
2P 1/2	489471.	487589.	1881.5	.5	97.	97. 2P (5P)
2P 3/2	490371.	488562.	1809.1	1.5	97.	97. 2P (5P)
2F 5/2	491417.	481956.	9460.8	2.5	97.	61. 2F (4F) 18. 2F (DD(1G)) 18. 2F (DD(3F))
2F 7/2	492957.	482517.	10440.0	3.5	97.	57. 2F (4F) 21. 2F (DD(1G)) 19. 2F (DD(3F))
2P 1/2	516195.	493247.	22947.8	.5	94.	70. 2P (DD(3P)) 13. 2P (DD(1D)) 11. 2P (DD(1S))
2P 3/2	518135.	494911.	23223.9	1.5	95.	71. 2P (DD(3P)) 15. 2P (DD(1D)) 9. 2P (DD(1S))
2D 5/2	528368.	496958.	31409.9	2.5	99.	71. 2D (DD(3F)) 17. 2D (DD(1D)) 11. 2D (DD(3P))
2D 3/2	528685.	497495.	31190.0	1.5	99.	71. 2D (DD(3F)) 17. 2D (DD(1D)) 11. 2D (DD(3P))
2F 5/2	570904.	568957.	1946.7	2.5	97.	97. 2F (5F)
2F 7/2	571023.	568993.	2029.8	3.5	97.	97. 2F (5F)
2P 1/2	574064.	578566.	-4502.4	.5	98.	53. 2P (DS(3P)) 45. 2P (6P)
2P 3/2	575927.	575742.	185.0	1.5	99.	73. 2P (6P) 26. 2P (DS(3P))
2P 1/2	579724.	574135.	5589.2	.5	97.	54. 2P (6P) 43. 2P (DS(3P))
2P 3/2	582034.	580697.	1336.9	1.5	96.	69. 2P (DS(3P)) 27. 2P (6P)
4F 7/2	583144.	584371.	-1226.7	3.5	97.	97. 4F (DS(3F))

TABLE (5.7A) CONTINUED

CR5+ ODD LEVELS
HXR CALCULATIONS COMPARED WITH EXPERIMENTAL OBSERVATIONS
UNCORRECTED HXR PARAMETERS WITH CONFIGURATION INTERACTION
PARENTAGE -- DD(2S+1)L = 3D2(2S+1)L
DD(2S+1)L = 3D2(2S+1)L DS(2S+1)L = (3P5(2P)3D(2D))(2S+1)L

IRREP	CALC	EXP	INCR	J/MU	TOTAL	-- EIGENVECTOR COMPOSITION PCT
4F 5/2	585198.	586273.	-1074.6	2.5	96.	96. 4F (DS(3F))
2F 7/2	591424.	591137.	287.0	3.5	96.	96. 2F (DS(3F))
2F 5/2	595635.	594926.	709.4	2.5	94.	94. 2F (DS(3F))
4D 7/2	610554.	607615.	2939.0	3.5	99.	86. 4D (DS(3D)) 14. 2F (DS(1F))
4D 5/2	611946.	608631.	3314.9	2.5	97.	82. 4D (DS(3D)) 9. 2D (DS(1D)) 6. 2F (DS(1F))
4D 3/2	612687.	609166.	3520.9	1.5	98.	85. 4D (DS(3D)) 13. 2D (DS(1D))
2D 5/2	615192.	614385.	807.0	2.5	94.	56. 2D (DS(1D)) 22. 2F (DS(1F)) 17. 2D (DS(3D))
2D 3/2	616617.	611568.	5049.3	1.5	98.	85. 2D (DS(1D)) 13. 4D (DS(3D))
2F 5/2	617714.	610497.	7216.7	2.5	98.	41. 2F (DS(1F)) 23. 2D (DS(1D)) 21. 2F (6F) 12. 4D (DS(3D))
2F 7/2	618361.	618849.	-487.6	3.5	98.	55. 2F (6F) 36. 2F (DS(1F)) 8. 4D (DS(3D))
2F 5/2	620063.	618583.	1480.2	2.5	90.	75. 2F (6F) 15. 2F (DS(1F))
2F 7/2	620987.	616079.	4907.7	3.5	96.	47. 2F (DS(1F)) 44. 2F (6F) 5. 4D (DS(3D))
2H 9/2	621173.	621163.	9.8	4.5	100.	100. 2H (6H)
2H11/2	621174.	621163.	10.9	5.5	100.	100. 2H (6H)
2D 3/2	623294.	618491.	4802.8	1.5	98.	98. 2D (DS(3D))
2D 5/2	624005.	619419.	4586.4	2.5	96.	75. 2D (DS(3D)) 15. 2F (DS(1F)) 6. 2D (DS(1D))
2F 5/2	649076.	648521.	555.0	2.5	99.	99. 2F (7F)
2F 7/2	649098.	648533.	564.6	3.5	99.	99. 2F (7F)
2H 9/2	650297.	650311.	-14.0	4.5	100.	100. 2H (7H)
2H11/2	650297.	650311.	-13.5	5.5	100.	100. 2H (7H)
2F 5/2	668317.	667973.	344.2	2.5	100.	100. 2F (8F)
2F 7/2	668329.	667973.	355.9	3.5	100.	100. 2F (8F)
2F 5/2	681525.	681307.	217.9	2.5	100.	100. 2F (9F)
2F 7/2	681532.	681307.	225.2	3.5	100.	100. 2F (9F)

TABLE (5.7A) CONTINUED

CR5+ ODD LEVELS
HXR CALCULATIONS COMPARED WITH EXPERIMENTAL OBSERVATIONS
UNCORRECTED HXR PARAMETERS WITH CONFIGURATION INTERACTION
PARENTAGE -- DD(2S+1)L = 3D2(2S+1)L
DD(2S+1)L = 3D2(2S+1)L DS(2S+1)L = (3P5(2P)3D(2D))(2S+1)L

IRREP	CALC	EXP	INCR	J/MU	TOTAL	-- EIGENVECTOR COMPOSITION PCT
2F 5/2	690973.	690781.	191.8	2.5	100.	100. 2F (10F)
2F 7/2	690978.	690781.	197.1	3.5	100.	100. 2F (10F)

NO. EXPERIMENTAL LEVELS = 49.

ABSOLUTE MEAN DEVIATION = 4658.09

RMS DEVIATION = 8768.95

TABLE (5.7B)

CR5+ EVEN LEVELS
HXR CALCULATIONS COMPARED WITH EXPERIMENTAL OBSERVATIONS
UNCORRECTED HXR PARAMETERS WITH CONFIGURATION INTERACTION
PARENTAGE -- DD(2S+1)L = 3D2(2S+1)L
DD(2S+1)L = 3D2(2S+1)L DS(2S+1)L = (3P5(2P)3D(2D))(2S+1)L

IRREP	CALC	EXP	INCR	J/MU	TOTAL	-- EIGENVECTOR COMPOSITION PCT
2D 3/2	-305.	0.	-305.3	1.5	100.	100. 2D (3D)
2D 5/2	869.	940.	-71.4	2.5	100.	100. 2D (3D)
2S 1/2	223636.	227858.	-4221.6	.5	99.	99. 2S (4S)
2D 3/2	402639.	402662.	-22.7	1.5	99.	99. 2D (4D)
2D 5/2	402927.	402889.	38.3	2.5	99.	99. 2D (4D)
2S 1/2	461848.	461253.	594.7	.5	100.	100. 2S (5S)
2D 3/2	535227.	534382.	845.3	1.5	99.	99. 2D (5D)
2D 5/2	535366.	534490.	876.4	2.5	99.	99. 2D (5D)
2S 1/2	562527.	562064.	462.6	.5	100.	100. 2S (6S)
2G 7/2	572142.	572272.	-130.6	3.5	100.	100. 2G (5G)
2G 9/2	572145.	572274.	-129.6	4.5	100.	100. 2G (5G)
2G 7/2	620718.	620696.	21.5	3.5	100.	100. 2G (6G)
2G 9/2	620719.	620701.	19.0	4.5	100.	100. 2G (6G)

NO. EXPERIMENTAL LEVELS = 13.

ABSOLUTE MEAN DEVIATION = 595.30

RMS DEVIATION = 1240.56

TABLE (5.8A)

MN6+ ODD LEVELS
HXR CALCULATIONS COMPARED WITH EXPERIMENTAL OBSERVATIONS
UNCORRECTED HXR PARAMETERS WITH CONFIGURATION INTERACTION
PARENTAGE --- DD(2S+1)L = 3D2(2S+1)L
DD(2S+1)L = 3D2(2S+1)L DS(2S+1)L = (3P5(2P)3D(2D))(2S+1)L

IRREP	CALC	EXP	INCR	J/MU	TOTAL	-- EIGENVECTOR COMPOSITION PCT
2P 1/2	394929.	397650.	-2720.9	.5	95.	81. 2P (4P) 14. 2P (DD(1D))
2P 3/2	399435.	400120.	-685.0	1.5	98.	58. 2P (4P) 27. 2D (DD(1D)) 7. 2D (DD(3F)) 6. 4F (DD(3F))
2F 5/2	508605.	489880.	18724.9	2.5	98.	51. 2F (DD(3F)) 42. 2F (DD(1G)) 5. 2F (4F)
2F 7/2	513180.	494300.	18880.1	3.5	98.	48. 2F (DD(3F)) 44. 2F (DD(1G)) 6. 2F (4F)
2D 5/2	579254.	547370.	31884.3	2.5	99.	71. 2D (DD(3F)) 17. 2D (DD(1D)) 12. 2D (DD(3P))
2D 3/2	579542.	547930.	31612.0	1.5	100.	71. 2D (DD(3F)) 17. 2D (DD(1D)) 11. 2D (DD(3P))
2F 5/2	619832.	615960.	3871.9	2.5	95.	95. 2F (4F)
2F 7/2	620149.	616100.	4049.0	3.5	94.	94. 2F (4F)
4P 3/2	691387.	696420.	-5032.7	1.5	98.	98. 4P (DS(3P))
2P 1/2	701607.	700870.	736.6	.5	97.	97. 2P (DS(3P))
2P 3/2	706373.	705170.	1202.5	1.5	95.	95. 2P (DS(3P))
4F 7/2	709483.	709720.	-237.0	3.5	96.	96. 4F (DS(3F))
4F 5/2	711971.	712350.	-378.6	2.5	94.	94. 4F (DS(3F))
2F 7/2	718319.	717430.	889.1	3.5	95.	95. 2F (DS(3F))
2F 5/2	723408.	722100.	1307.6	2.5	92.	92. 2F (DS(3F))
4D 7/2	738958.	735510.	3448.0	3.5	100.	72. 4D (DS(3D)) 19. 2F (DS(1F)) 9. 2F (5F)
2F 5/2	740665.	739770.	895.4	2.5	93.	41. 2F (5F) 38. 4D (DS(3D)) 14. 2F (DS(1F))
2F 5/2	741433.	737020.	4413.5	2.5	97.	46. 2F (5F) 40. 4D (DS(3D)) 11. 2D (DS(1D))
2F 7/2	741540.	739940.	1600.4	3.5	99.	86. 2F (5F) 13. 4D (DS(3D))
2F 7/2	750610.	746450.	4160.4	3.5	91.	77. 2F (DS(1F)) 13. 4D (DS(3D))
2D 3/2	753474.	748170.	5304.1	1.5	98.	98. 2D (DS(3D))
2D 5/2	754570.	749430.	5140.4	2.5	97.	73. 2D (DS(3D)) 18. 2F (DS(1F)) 6. 2D (DS(1D))
2F 5/2	808971.	807760.	1211.2	2.5	100.	100. 2F (6F)

TABLE (5.8A) CONTINUED

MN6+ ODD LEVELS
HXR CALCULATIONS COMPARED WITH EXPERIMENTAL OBSERVATIONS
UNCORRECTED HXR PARAMETERS WITH CONFIGURATION INTERACTION
PARENTAGE -- DD(2S+1)L = 3D2(2S+1)L
DD(2S+1)L = 3D2(2S+1)L DS(2S+1)L = (3P5(2P)3D(2D))(2S+1)L

IRREP	CALC	EXP	INCR	J/MU	TOTAL	-- EIGENVECTOR COMPOSITION PCT
2F 7/2	809001.	807760.	1241.2	3.5	100.	100. 2F (6F)
2F 5/2	849733.	848850.	882.8	2.5	100.	100. 2F (7F)
2F 7/2	849749.	848850.	898.6	3.5	100.	100. 2F (7F)
2F 5/2	876201.	875530.	671.0	2.5	100.	100. 2F (8F)
2F 7/2	876211.	875530.	680.7	3.5	100.	100. 2F (8F)
2F 5/2	894328.	893740.	588.3	2.5	100.	100. 2F (9F)
2F 7/2	894335.	893740.	594.8	3.5	100.	100. 2F (9F)

NO. EXPERIMENTAL LEVELS = 30.

ABSOLUTE MEAN DEVIATION = 5131.44

RMS DEVIATION = 9840.54

TABLE (5.8B)

MN6+ EVEN LEVELS
HXR CALCULATIONS COMPARED WITH EXPERIMENTAL OBSERVATIONS
UNCORRECTED HXR PARAMETERS WITH CONFIGURATION INTERACTION
PARENTAGE -- DD(2S+1)L = 3D2(2S 1)L
DD(2S+1)L = 3D2(2S+1)L DS(2S+1)L = (3P5(2P)3D(2D))(2S+1)L

IRREP	CALC	EXP	INCR	J/MU	TOTAL	-- EIGENVECTOR COMPOSITION PCT
2D 3/2	-188.	0.	-188.3	1.5	100.	100. 2D (3D)
2D 5/2	1448.	1350.	98.2	2.5	100.	100. 2D (3D)
2S 1/2	314857.	318734.	-3877.2	.5	99.	99. 2S (4S)
2S 1/2	611957.	613934.	-1976.8	.5	100.	100. 2S (5S)
2S 1/2	740679.	752144.	-11464.5	.5	100.	100. 2S (6S)

NO. EXPERIMENTAL LEVELS = 5.

ABSOLUTE MEAN DEVIATION = 3521.02

RMS DEVIATION = 5484.90

TABLE (5.9A)

FE7+ ODD LEVELS
HXR CALCULATIONS COMPARED WITH EXPERIMENTAL OBSERVATIONS
UNCORRECTED HXR PARAMETERS WITH CONFIGURATION INTERACTION
PARENTAGE -- DD(2S+1)L = 3D2(2S+1)L
DD(2S+1)L = 3D2(2S+1)L DS(2S+1)L = (3P5(2P)3D(2D))(2S+1)L

IRREP	CALC	EXP	INCR	J/MU	TOTAL	-- EIGENVECTOR COMPOSITION PCT
2F 5/2	555363.	535926.	19436.7	2.5	97.	52. 2F (DD(3F)) 44. 2F (DD(1G))
2F 7/2	561515.	541777.	19737.5	3.5	96.	50. 2F (DD(3F)) 47. 2F (DD(1G))
2P 1/2	616022.	591973.	24048.7	.5	98.	71. 2P (DD(3P)) 13. 2P (DD(1D)) 13. 2P (DD(1S))
2P 3/2	619291.	595166.	24125.2	1.5	98.	73. 2P (DD(3P)) 15. 2P (DD(1D)) 9. 2P (DD(1S))
2D 5/2	626672.	596430.	32242.3	2.5	100.	71. 2D (DD(3F)) 17. 2D (DD(1D)) 12. 2D (DD(3P))
2D 3/2	628885.	597072.	31813.2	1.5	100.	71. 2D (DD(3F)) 17. 2D (DD(1D)) 11. 2D (DD(3P))
2F 5/2	767037.	763789.	3248.3	2.5	98.	98. 2F (4F)
2F 7/2	767246.	763821.	3425.2	3.5	98.	98. 2F (4F)
4P 3/2	826741.	833000.	-6259.5	1.5	97.	97. 4P (DS(3P))
2P 1/2	836235.	837750.	484.5	.5	93.	93. 2P (DS(3P))
2P 3/2	843971.	842930.	1040.9	1.5	92.	92. 2P (DS(3P))
4F 7/2	846363.	847250.	-886.6	3.5	95.	95. 4F (DS(3F))
4F 5/2	849321.	849990.	-669.3	2.5	93.	93. 4F (DS(3F))
2F 7/2	855775.	855190.	584.9	3.5	95.	95. 2F (DS(3F))
2F 5/2	861893.	860710.	1183.0	2.5	89.	89. 2F (DS(3F))
4D 7/2	878283.	874770.	3513.5	3.5	100.	80. 4D (DS(3D)) 19. 2F (DS(1F))
4D 5/2	880681.	876810.	3870.8	2.5	93.	73. 4D (DS(3D)) 11. 2F (DS(1F)) 9. 2D (DS(1D))
2F 7/2	891431.	887320.	4111.1	3.5	93.	76. 2F (DS(1F)) 17. 4D (DS(3D))
2D 3/2	894490.	889110.	5379.7	1.5	97.	97. 2D (DS(3D))
2D 5/2	896041.	890810.	5230.9	2.5	96.	71. 2D (DS(3D)) 19. 2F (DS(1F)) 7. 2D (DS(1D))
2F 5/2	929042.	927025.	2016.8	2.5	99.	99. 2F (5F)
2F 7/2	929121.	927053.	2067.9	3.5	99.	99. 2F (5F)
2F 5/2	1017688.	1016530.	1157.9	2.5	100.	100. 2F (6F)
2F 7/2	1017721.	1016570.	1150.5	3.5	100.	100. 2F (6F)

TABLE (5.9A) CONTINUED

FE7+ ODD LEVELS
HXR CALCULATIONS COMPARED WITH EXPERIMENTAL OBSERVATIONS
UNCORRECTED HXR PARAMETERS WITH CONFIGURATION INTERACTION
PARENTAGE -- DD(2S+1)L = 3D2(2S+1)L
DD(2S+1)L = 3D2(2S+1)L DS(2S+1)L = (3P5(2P)3D(2D))(2S+1)L

IRREP	CALC	EXP	INCR	J/MU	TOTAL	-- EIGENVECTOR COMPOSITION PCT
2F 5/2	1071311.	1069870.	1441.1	2.5	100.	100. 2F (7F)
2F 7/2	1071330.	1070030.	1300.1	3.5	100.	100. 2F (7F)

NO. EXPERIMENTAL LEVELS = 26.

ABSOLUTE MEAN DEVIATION = 7708.70

RMS DEVIATION = 12649.77

TABLE (5.9B)

FE7+ EVEN LEVELS
HXR CALCULATIONS COMPARED WITH EXPERIMENTAL OBSERVATIONS
UNCORRECTED HXR PARAMETERS WITH CONFIGURATION INTERACTION
PARENTAGE -- DD(2S+1)L = 3D2(2S+1)L
DD(2S+1)L = 3D2(2S+1)L DS(2S+1)L = (3P5(2P)3D(2D))(2S+1)L

IRREP	CALC	EXP	INCR	J/MU	TOTAL	-- EIGENVECTOR COMPOSITION PCT
2D 3/2	-415.	0.	-415.1	1.5	100.	100. 2D (3D)
2D 5/2	1791.	1838.	-46.5	2.5	100.	100. 2D (3D)

NO. EXPERIMENTAL LEVELS = 2.

ABSOLUTE MEAN DEVIATION = 230.82

RMS DEVIATION = 295.38

The Hamiltonian matrix reduces to block diagonal matrices of both parities, with angular momentum values ranging from J=1/2 to J=11/2. The basis vectors are LS coupled to final states $^{2\tilde{S}+1}\tilde{L}_J$ via the schemes $\{3p^5(^2P)3d^2(^{2\bar{S}+1}\bar{L})\}^{2\tilde{S}+1}\tilde{L}_J$, $\{[3p^5(^2P)3d(^2D)](^{2\bar{S}+1}\bar{L})4s(^2S)\}^{2\tilde{S}+1}\tilde{L}_J$, and $\{[3p^5(^2P)3d(^2D)](^{2\bar{S}+1}\bar{L})4p(^2P)\}^{2\tilde{S}+1}\tilde{L}_J$. The $^{2\bar{S}+1}\bar{L}$ parents are used to identify the basis set.

Isoelectronic Comparisons

Considerable configuration mixing occurs with the $3p^53d^2$ and $3p^53d4s$ configurations and some of the odd nℓ configurations from Cr^{5+} to Fe^{7+}. As mentioned in the previous section, ab-initio calculations tend to overestimate the magnitudes of configuration interaction parameters because of correlations absorbed into the average energy. For mild configuration mixing, the effect of including configuration interaction is a shift of the configuration average energy that varies weakly with Z. If the mixing configurations are nearly degenerate at some Z along the isoelectronic sequence, however, strong configuration interaction can occur, and the effect on the average energies is more dramatic. In this situation, the effective Hamiltonian is very sensitive to values of configuration interaction parameters, and any adjustments to ab-initio parameters must be made with this in mind.

The strength of the configuration interaction along the K^{0+} isoelectronic sequence can be determined by plotting the difference between the observed and calculated configuration average energies (relative to the $3p^6$ configuration) for the nℓ configurations. To accurately compare the calculated and observed configuration average

energies and possibly extrapolate their differences along the isoelectronic sequence, however, the correlation correction E_c of equation (3.19) added to the HXR calculation was removed. The difference between the observed and calculated average energies is the correlation energy, while the behavior of the correlation correction E_c as a Z is unknown. It is interesting to compare E_c to the average energy differences as a function of Z, and this was done graphically for selected levels. The correlation corrections for the even and odd parity configurations relative to the correlation energy of the parent $3p^6$ ion are presented in table (5.10).

The differences between the calculated and observed $n\ell$ configuration average energies are displayed in figures (5.1) through (5.7). Overall, the single configuration HXR term values (T^{calc}) are not as large as their experimental counterparts, implying that the valence electron is more tightly bound than the calculation suggests. For most configurations the differences are smooth and appear to be asymptotically linear in Z as expected. To emphasize this observation, the differences were fitted to a function $\Delta_c^{n\ell}(Z)$,

$$\Delta_c^{n\ell}(Z) = A^{n\ell}Z + B^{n\ell} + \frac{C^{n\ell}}{Z-18} \qquad (5.23)$$

and the function $\Delta_c^{n\ell}(Z)$ is plotted with the differences in each figure ($A^{n\ell}$, $B^{n\ell}$, and $C^{n\ell}$ are the adjustable parameters).

The strongly perturbed configurations, of course, do not fit well to a curve of this type; there are large deviations from a curve of this type when strong configuration interaction occurs. It is desirable to find a $\Delta_c^{n\ell}(Z)$ that best represents the differences in the average

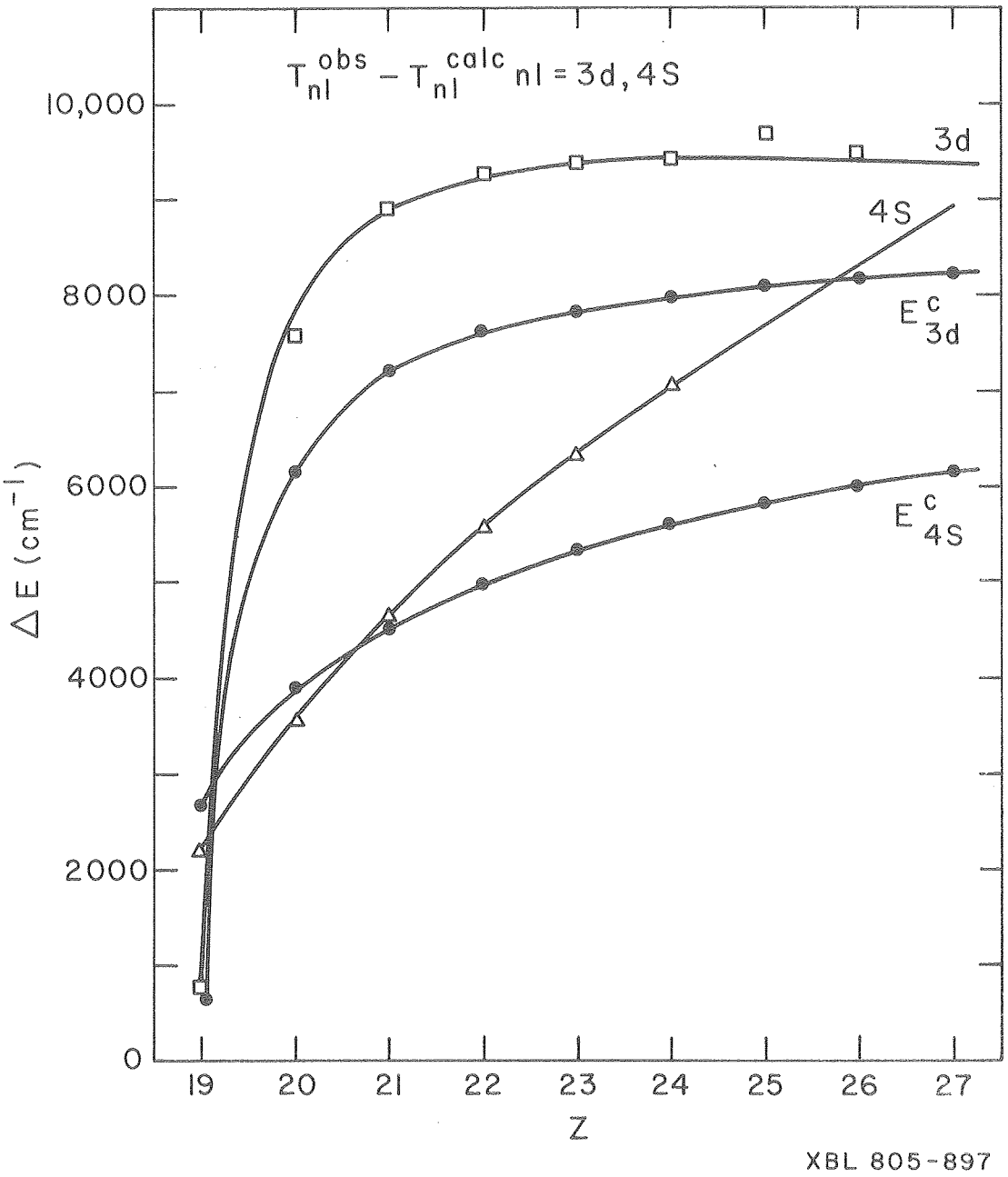

Figure (5.1)

Differences between the calculated and observed average term energies, plotted as functions of Z. The 3d and 4s configurations are shown along with their respective correlation corrections.

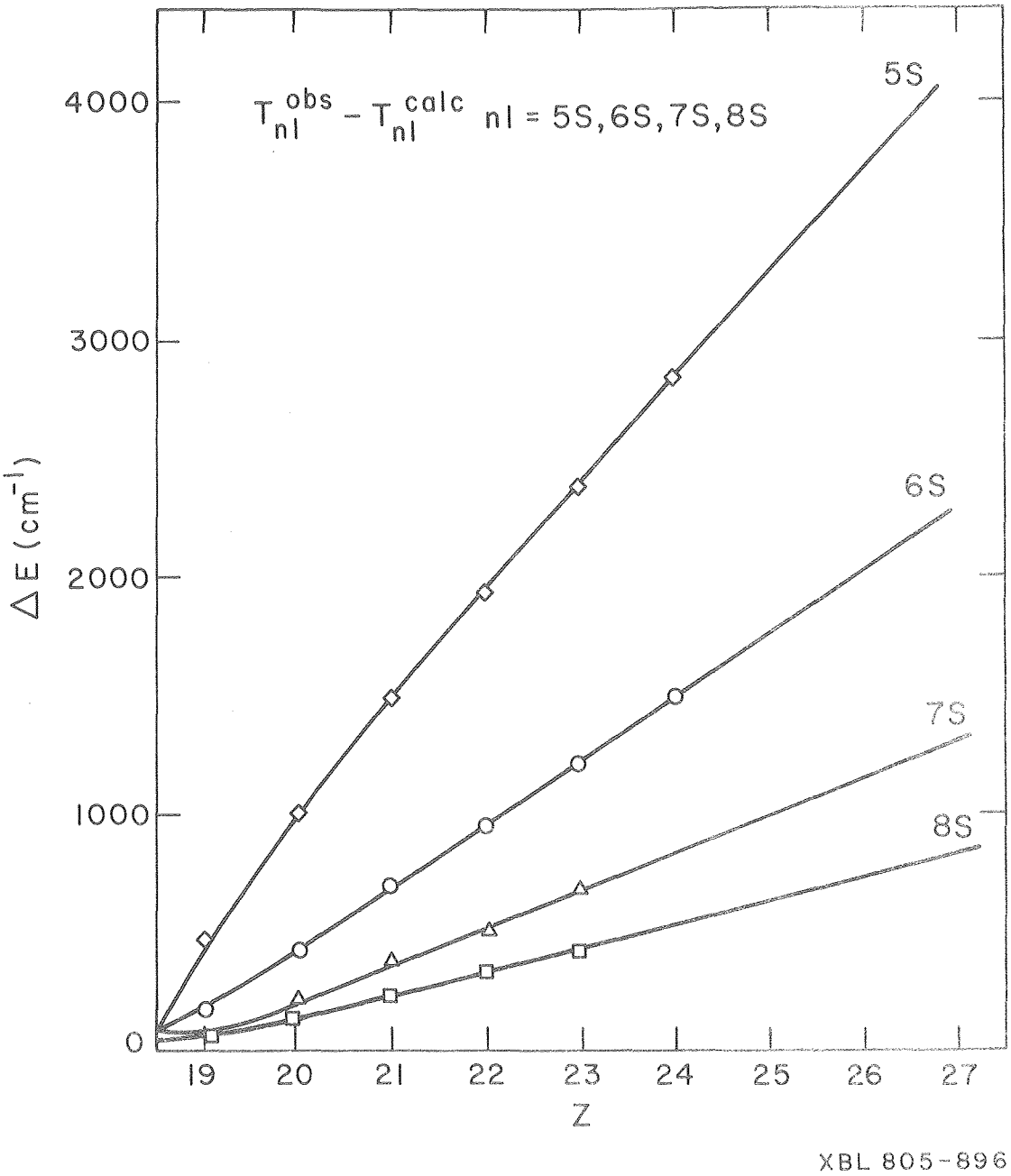

Figure (5.2)

Differences between the calculated and observed average term energies plotted as functions of Z. The 5s 6s, 7s, and 8s configurations are shown.

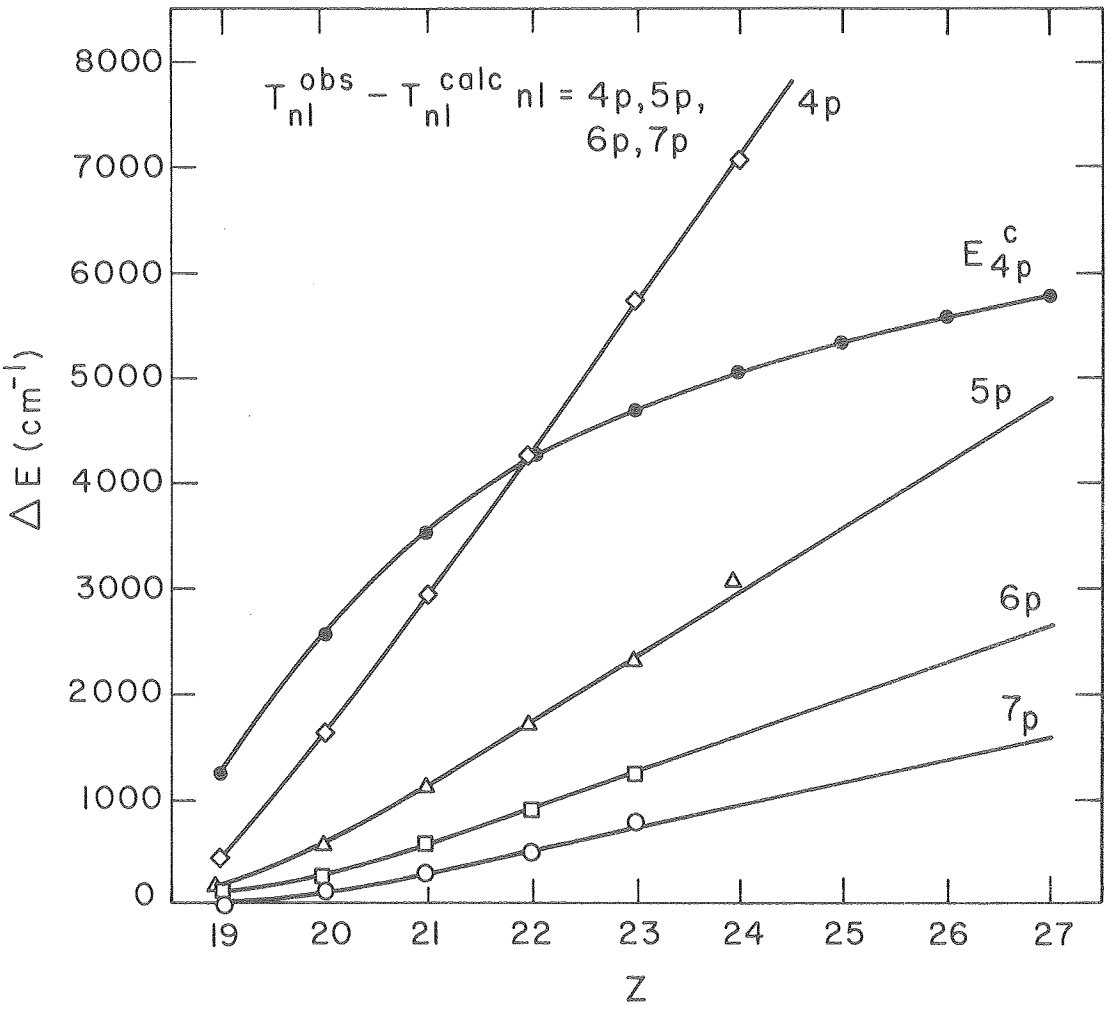

Figure (5.3)

Differences between the calculated and observed average term energies plotted as functions of Z. The 4p 5p, 6p, and 7p configurations are shown, along with the correlation correction E_{4p}^{c}.

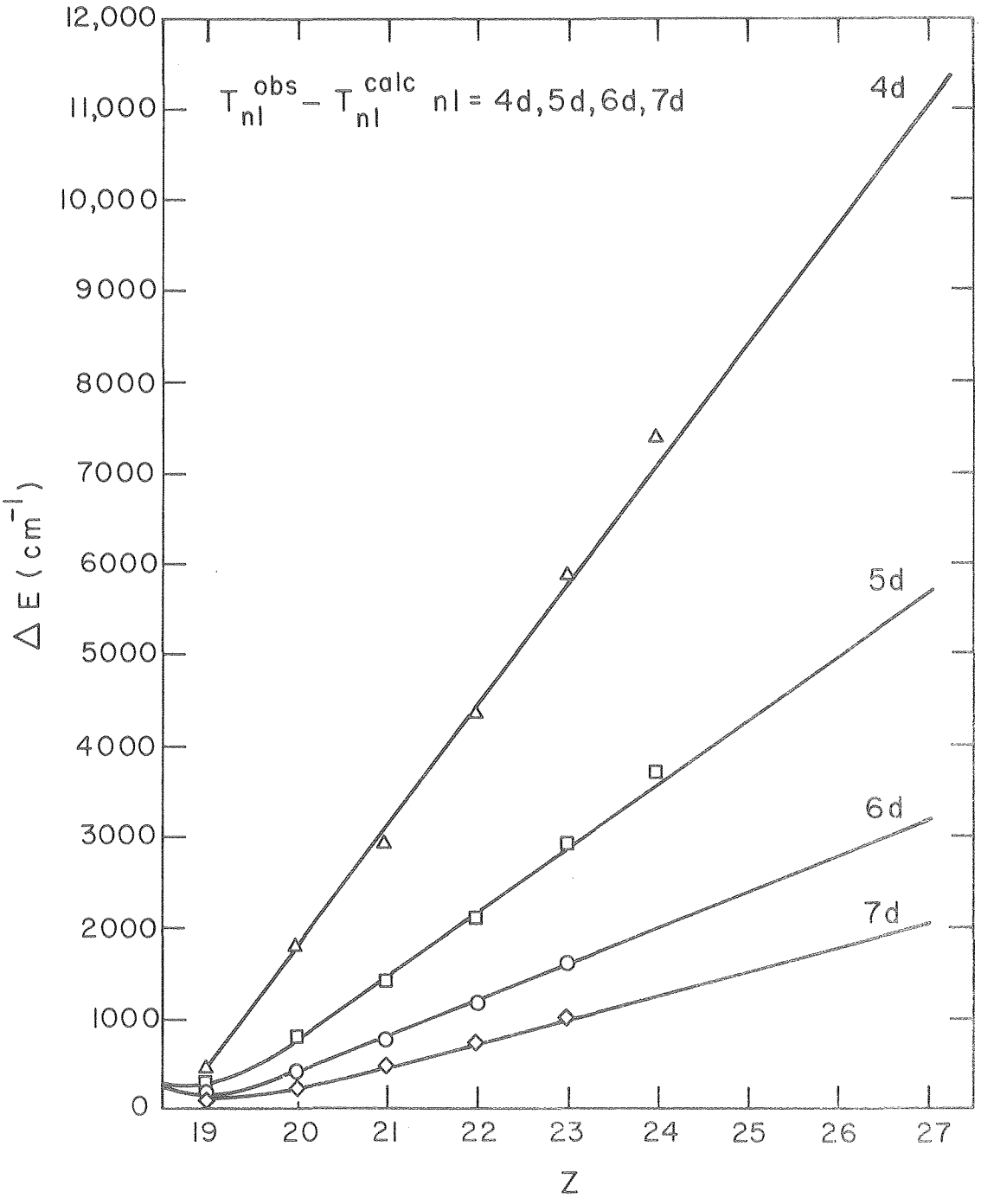

Figure (5.4)

Differences between the calculated and observed average term energies plotted as functions of Z. The 4d 5d, 6d, and 7d configurations are shown.

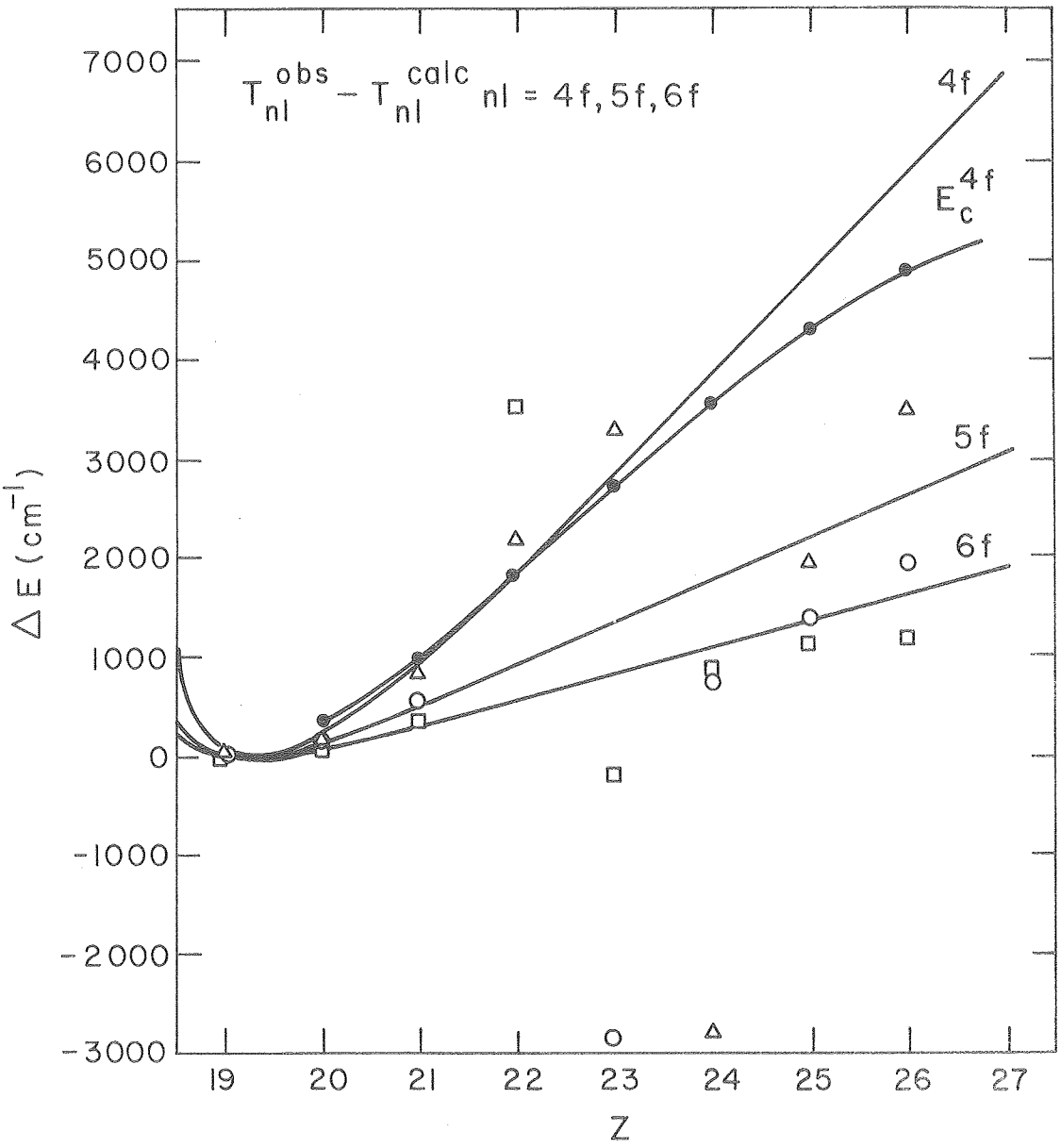

XBL 805-893

Figure (5.5)

Differences between the calculated and observed average term energies plotted as functions of Z. The 4f 5f, and 6f configurations are shown along with the correlation correction for the 4f configuration. Strong configuration interaction is evident beginning with Z=22.

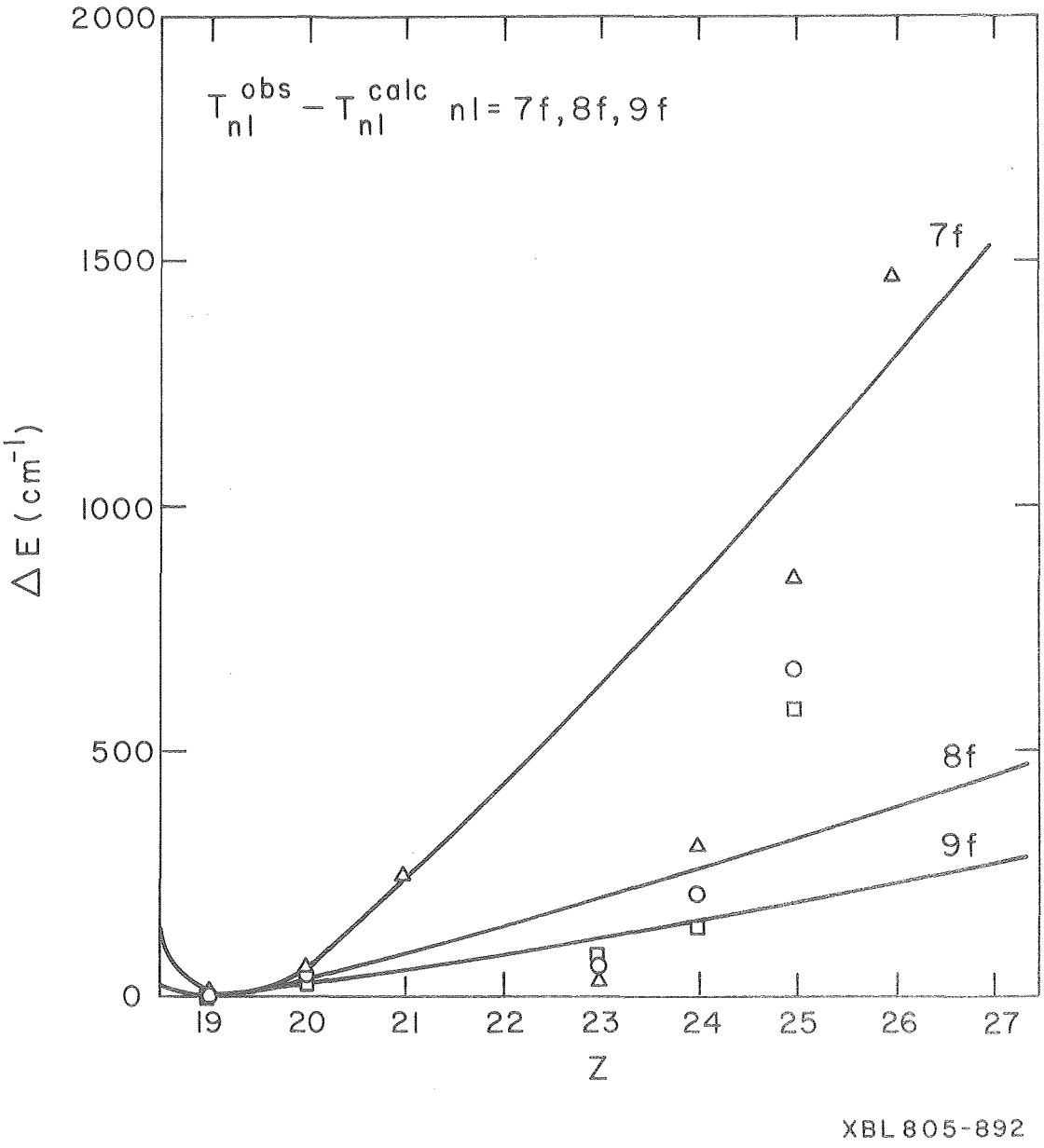

Figure (5.6)

Differences between the calculated and observed average term energies plotted as functions of Z. The 7f, 8f, and 9f, configurations are shown. Although the differences are smaller than for the 4f, 5f, and 6f configurations, the strong configuration interaction is again evident beginning with Z=22.

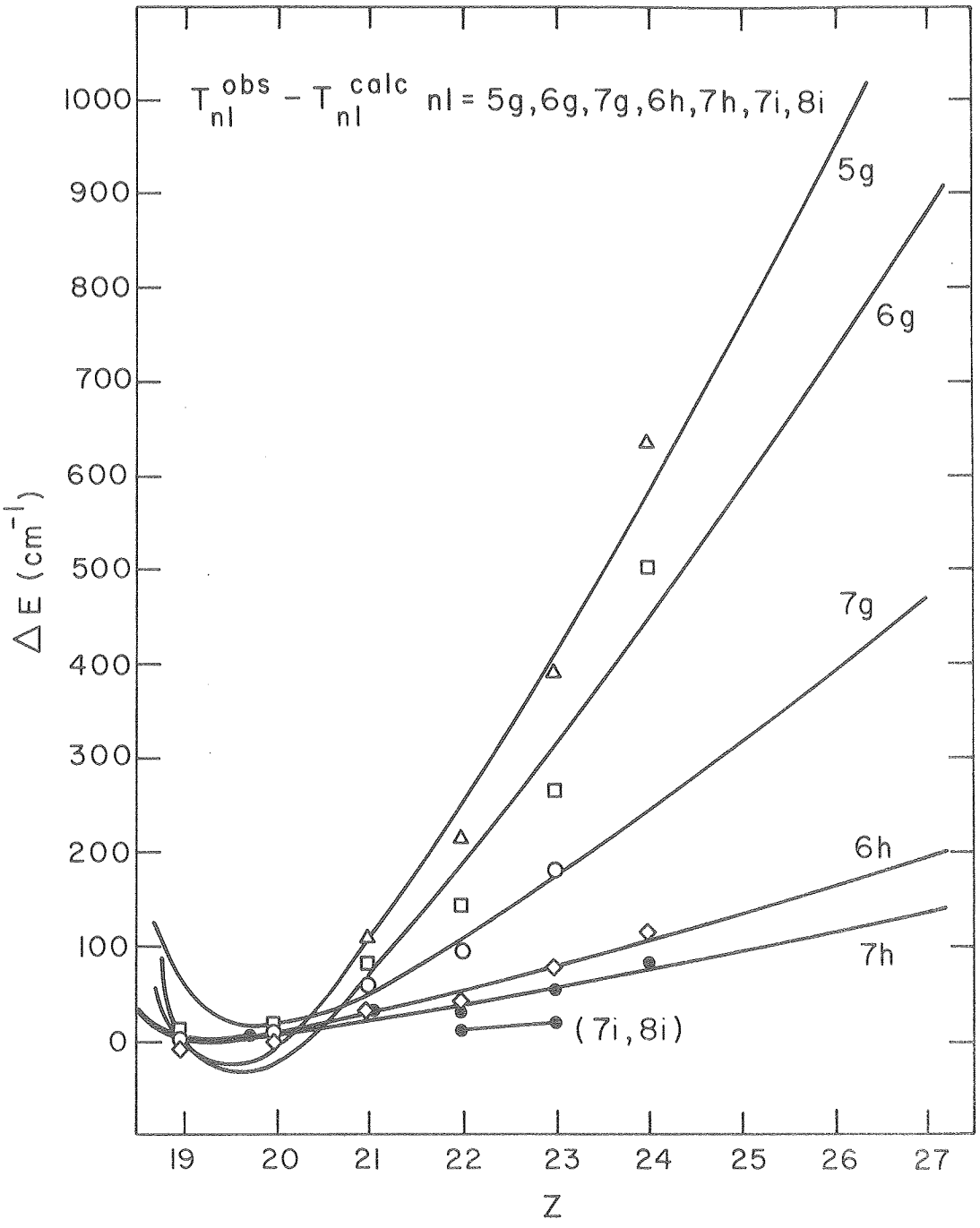

XBL 805-891

Figure (5.7)

Differences between the calculated and observed average term energies plotted as functions of Z. The 5g, 6g, 7g, 6h, 7h, 7I, and 8i, configurations are shown.

Table (5.10)
Relative Correlation Energies (cm^{-1})

Conf\Z	19	20	21	22	23	24	25	26
				Odd Parity n l Configurations				
4p	1228	2637	3557	4195	4673	5047	5350	5602
5p	351	663	909	1117	1305	1467	1632	1778
6p	142	286	399	499	589	670	744	812
7p	74	151	215	271	324	370	413	453
4f	19	291	949	1832	2746	3572	4278	4860
5f	13	180	503	835	1098	1293	1450	1592
6f	9	112	292	454	572	657	732	803
7f	5	74	183	274	338	3867	429	473
8f	4	50	122	179	217	248	275	304
9f	2	36	86	123	148	169	189	209
10f	2	26	61	88	106	121	135	142
6h	0	1	7	24	57	104	166	239
7h	0	1	8	24	55	95	145	201
$3p^5 3d^3$	1826	3617	6921	7404	7693	7890	8037	8153
$3p^5 3d4s$	2662	4207	4747	5125	5423	5667	5873	6051
				Even Parity nℓ Configurations				
4s	2715	3889	4549	4995	5332	5599	5818	6006
5s	480	801	1068	1297	1499	1678	1838	1984
6s	177	318	440	546	641	724	798	865
7s	84	160	228	289	342	391	432	472
8s	47	93	135	172	206	237	263	289
3d	690	6158	7238	7609	7829	7983	8101	8196
4d	405	1027	1787	2653	3401	4013	4512	4926
5d	234	421	679	917	1112	1277	1429	1573
6d	142	218	346	455	546	626	739	768
7d	91	129	202	262	314	360	402	442
5g	0	20	100	259	486	759	1059	1371
6g	0	18	80	189	327	476	622	760
7g	0	13	57	129	216	305	387	462
7i	0	0	0	1	4	10	16	19
8i	0	0	0	2	5	12	20	32
$3p^5 3d4p$	1737	3145	3872	4396	48090	5143	5423	5661

energies that are not associated with strong configuration interactions. To accomplish this, the Hamiltonian matrices were diagonalized with all the configuration interaction parameters multiplied by .5 (the factor .5 was used because the correlation correction E_c was retained), and the resulting changes in the energy levels from the single configuration approximation were used in weighting the fits to $\Delta_c^{n\ell}(Z)$. The result shows that for most configurations, the configuration mixing appears to be mild, and the differences fall on smooth curves. There are notable exceptions, particularly the nf configurations.

The differences between the observed and calculated term values appear to decrease with increasing n and ℓ, with the largest differences occuring for n = 3,4. The differences for the 3d and 4s terms are shown in figure (5.1). The 4s configuration is the ground configuration for K^{0+} and Ca^{1+}, while the 3d configuration is lowest for Sc^{2+} to Fe^{7+}. Thus figure (5.1) displays the discrepancy between the experimentally determined ionization energy and the values computed by differencing single HXR configurations. The deviation from the smooth curve for the 3d configuration for Z=26 and Z=27 is perhaps an indication of a possible error in the experimentally determined ionization energies; the ionization energies for Mn^{6+} and Fe^{7+} are determined from the Rydberg formula applied to the perturbed nf series[83,84]. The differences for the 4p, 4d, and 4f configurations displayed in figures (5.3), (5.4), and (5.5), are also quite large, but the 4p seems to become asymptotically linear very quickly, while the 4f configuration shows the effects of strong configuration interaction.

The observed ns, np, nd, nh, and ni configurations displayed in figures (5.2), (5.3), (5.4), and (5.7) do not show the effects of strong configuration interaction, but perhaps many of these levels have not been identified for ions where strong configuration interaction occurs. The large discrepancies in the even parity Mn^{6+} levels have been ignored as probable misidentifications. The uncorrected HXR calculation predicts no significant configuration interaction, and similar identifications from earlier work on Fe^{7+} have also been discounted[84].

The nf configurations displayed in figures (5.5) and (5.6), however, show very definite configuration interaction. At low Z the differences for the 4f, 5f, and 6f configurations rise above the smooth curves, indicating the depression of the energies (increases in the term values) from higher lying perturbing levels. At higher Z, the differences fall below the smooth curve, indicating the positions of the perturbing levels have fallen below the plotted configurations. The data for the 7f, 8f, and 9f configurations displayed in figure (5.6), however, are insufficient to show any real trends. The more mildly perturbed 4d, 5d, 5g, 6g, and 7g levels displayed in figures (5.2) and (5.7) show indications of configuration interaction by the scatter about the $\Delta_c^{n\ell}(Z)$ curves. The strength of these perturbations cannot be estimated accurately enough to properly weight the fits to $\Delta_c^{n\ell}(Z)$, so that definite trends do not emerge.

The correlation correction E_c for the 3d, 4s, 4p, and 4f configurations is also shown, and adding E_c is definitely an improvement. The unusual trend of the 3d configuration is followed quite well, with the sharp rise for the low Z values indicating the collapse of the 3d to the

ground state configuration. The asymptotic slope of the 3d difference is relatively small, and perhaps even negative. This indicates that the differences in the first order corrections to the hydrogenic average energies of the $3p^6 3d$ and $3p^6$ configurations is nearly constant at large Z, with perhaps a slightly larger linear component for the $3p^6$ correction. The best agreement of E_c with the observed differences, however, seems to be a low Z, indicating perhaps that the correlation correction gets poorer with increasing electron density. Note that E_c is an overestimate of the difference for 4s and 4p configurations at the low Z values.

5.2.2 Least Squares Adjustments to V^{4+} and Cr^{5+}

The odd parity levels of V^{4+} and Cr^{5+} are determined from 91 parameters, while the even parity configurations are determined from 77 parameters. In each case, the number of parameters is roughly twice the number of observed energy levels, so some method of reducing the number of free parameters with constraints had to be devised. To some extent, the final decisions on this matter were made by trial and error, but the constraints used follow the general guidelines described in (5.1). Because there was no information about the levels belonging to the even parity $3p^5 3d4p$ configuration, the odd parity parameters were adjusted first. The adjustments made to the $3p^5 3d4s$ parameters and the configuration interaction parameters were used as rough estimates for their counterparts associated with the $3p^5 3d4p$ configuration before the remaining even parity parameters were adjusted.

Odd Parity Parameters

The methods used to adjust the V^{4+} and Cr^{5+} parameters were nearly identical, so the overall scheme is outlined first and the few exceptions are described. Over half the parameters are related to configuration interaction (CI) between the $3p^5 3d^2$ and $3p^5 3d4s$ configurations and the $n\ell$ configurations (ℓ=p,f,h), so a means of constraining them had to be devised. The simplest technique is to scale them all by a single new free parameter, but this proved unsatisfactory, so the next simplest idea was used; they were scaled in two groups. A number of other constraints were used while the CI parameters were adjusted in order to stabilize the least squares optimization, because many energy levels are overdetermined in this situation. When the CI parameters were scaled to satisfactory values, these additional constraints were relaxed by trial and error and the optimization continued as long as convergence could be reached and reasonable values of the parameters were obtained.

Using an overall scale parameter for a large number of CI parameters is consistent with the constraint (5.14a), but strictly speaking the argument for leading to (5.14a) can only be made for integrals over the same set of radial wavefunctions. Because mild configuration interaction can be absorbed into the configuration average energy, however, an overall scale parameter can be used to adjust the most sensitive CI parameters, and a trade-off will exist between the less sensitive CI parameters and the average energies. The best method of scaling CI parameters appeared to be scaling the two groups

$$\overline{R}^k(n_a\ell_a n_b\ell_b n_c f n_d\ell_d) = \Theta_{nf} R^k(n_a\ell_a n_b\ell_b n_c f n_d\ell_d) \qquad (5.25a)$$

$$\bar{R}^k(n_a\ell_a n_b\ell_b n_c\ell_c n_d\ell_d) = \Theta_{oth} R^k(n_a\ell_a n_b\ell_b n_c\ell_c n_d\ell_d) \qquad (5.25b)$$

where the first group is all CI parameters involving an nf configuration, and the second group contains all the remaining CI parameters. The motivation for this choice was the relatively stronger configuration interaction of the nf configurations relative to the other odd parity $n\ell$ configurations. For V^{4+}, $\Theta_{nf} = .8783$ and $\Theta_{oth} = .1003$, while for Cr^{5+}, $\Theta_{nf} = .8821$ and $\Theta_{oth} = .3812$.

Most of the remaining single configuration parameters were independently adjusted, but exceptions are noted: The fine structure of the $n\ell$ configurations is small for $\ell>2$, so the ζ_{nl} parameters for ℓ=f,g,h,i were left at their HXR values. The ζ_{np} were all adjusted by a single scale parameter while the CI parameters were scaled, and then the V^{4+} values were optimized independently. This constraint had to be maintained for Cr^{5+} because configuration interaction caused the ζ_{5p} and ζ_{6p} parameters to have unrealistically large values, and the 7p configuration of Cr^{5+} is not observed. Initially the 7p average energy was adjusted by the value of the function whose smooth curve is plotted in figure (5.3) and labeled 7p. Later, a new value was determined by linear extrapolation from the adjusted 7p average energies of Ti^{3+} and V^{4+}. The 10f configuration is not observed for V^{4+}, and the Rydberg formula was also used to obtain an estimate of its average energy from the 7f, 8f, and 9f average energies.

The remaining constraints were applied to the parameters of the $3p^5 3d^2$ and $3p^5 3d4s$ configurations. While the CI parameters were optimized, the number of free parameters for these configurations were

reduced via the following constraints:

(1) $3p^5 3d^2$ parameters:

$$\overline{F}^4(3d,3d) = \frac{F^4(3d,3d)}{F^2(3d,3d)} \overline{F}^2(3d,3d) \qquad (5.26a)$$

$$\overline{G}^3(3p,3d) = \frac{G^3(3p,3d)}{G^1(3p,3d)} \overline{G}^1(3p,3d) \qquad (5.26b)$$

(2) $3p^5 3d4s$ parameters:

$$\overline{G}^1(3p,3d) = \frac{G^1(3p,3d)}{F^2(3p,3d)} \overline{F}^2(3p,3d) \qquad (5.27a)$$

$$\overline{G}^3(3p,3d) = \frac{G^3(3p,3d)}{G^1(3p,3d)} \overline{G}^1(3p,3d) \qquad (5.27b)$$

$$\overline{\xi}_{3d} = \frac{\xi_{3d}}{\xi_{3p}} \overline{\xi}_{3p} \qquad (5.27c)$$

After the scaling of the CI parameters was completed, all the constraints on the $3p^5 3d^2$ configuration parameters were removed, but the constraints (5.27b) and (5.27c) were retained for the $3p^5 3d4s$ configuration. The need for these constraints was traced in part to an error in the published energy level assignments, but the data was still insufficient for both V^{4+} and Cr^{5+} to accurately determine all of the $3p^5 3d4s$ parameters. After the extrapolations to the neighboring ions in the isoelectronic sequence, however, the constraint (5.27c) was lifted and the parameters were re-optimized.

The behavior of the $\overline{G}^1(3p,3d)$, $\overline{G}^3(3p,3d)$, and $\overline{\xi}_{3d}$ parameters for the $3p^5 3d4s$ configuration was erratic over the course of the

optimization, until correction of a level misassignment. The $(^3D)^2D_{3/2,5/2}$ levels had been assigned with the J=3/2 level lying higher in energy for both V^{4+} and Cr^{5+}. Upon closer inspection of Ekberg's work on Cr^{5+}, however, his assignments were cited as those from an earlier work of Cowan's[82], but Cowan had assigned the pair with the 3/2 level lower than the 5/2 level. Ekberg's published linelist also confirmed that the table values were listed in error. The same pair of levels has also been identified for Mn^{6+} and Fe^{7+} with the 3/2 level lying lower[83,84]. Apparently Van Deurzen made his assignment of the V^{4+} pair by analogy with Ekberg's published values, unaware of the error.

Even Parity Parameters

Only the nℓ single configuration parameters can be adjusted by least squares minimization because there are no observed levels for the $3p^5 3d4p$ configuration. The $3p^5 3d4s$ configuration levels are probably most sensitive to the 3p-3d interaction, and this should be the case for the $3p^5 3d4p$ configuration as well. By this reasoning, the difference between the ab-initio and adjusted values of the $3p^5 3d4s$ configuration average energy was used also as an approximate correction to the $3p^5 3d4p$ average energy. Also, since the configuration interaction seems to be mild between this configuration and the even parity nℓ configurations, all the CI parameters were scaled by the Θ_{oth} constant determined from the odd parity configurations of the appropriate ion. As a final consideration, the $F^k(3p3d)$ and $G^k(3p3d)$ parameters were adjusted by the same differences that were found for their counterparts in the $3p^5 3d4s$ configuration for the V^{4+} and the Cr^{5+} ions.

The remaining $n\ell$ single configuration parameters were adjusted by treating them as free parameters in the least squares minimization where possible. The $\zeta_{n\ell}$ parameters for $\ell>2$ were left alone because the fine structure splitting of these levels is so small. The parameters belonging to the 6d, 7d, 7s, 8s, 7g, 7i, and 8i configurations of Cr^{5+} could not be optimized either, because these levels are not observed. Instead, the 6d, 7d, 7s, 8s, and 7g configuration average energies were adjusted by the values of $\Delta_c^{n\ell}$, and then later refined by extrapolation from Ti^{3+} and V^{4+}, as described in (5.2.3).

Corrections to the 7i and 8i configurations were ignored, as the purpose of calculating these configurations was to test the relative precisions of the calculations and the measurements. These levels have nearly the hydrogenic values with z=Z-N+1, and should show very little discrepancy in the calculated and observed values.

The results of all optimizations are presented in tables (5.11) and (5.12), including energies and eigenvector compositions for unobserved levels. The comparison between the calculated and observed energy levels is satisfactory, given the simple method used to adjust the CI parameters. Closer agreement between the calculated and observed levels could be obtained by adjusting individual CI parameters, but many of the possible solutions that would give better agreement might not reliably extrapolate as functions of Z. Extrapolations of these corrections, however, to the ab-initio parameters of neighboring ions should in most cases give predictions with comparable accuracy. However, because of the strong configuration mixing involving some of the configurations, extrapolation in these cases cannot be relied upon because of the simple

TABLE (5.11A)

V 4+ ODD LEVELS
CALCULATIONS COMPARED WITH EXPERIMENTAL OBSERVATIONS
EXTRAPOLATED AND OPTIMIZED PARAMETERS
PARENTAGE -- DD(2S+1)L = 3D2(2S+1)L
DD(2S+1)L = 3D2(2S+1)L DS(2S+1)L = (3P5(2P)3D(2D))(2S+1)L

IRREP	CALC	EXP	INCR	J/MU	TOTAL	-- EIGENVECTOR COMPOSITION PCT
2P 1/2	206394.	206394.	0.	.5	100.	100. 2P (4P)
2P 3/2	207660.	207660.	0.	1.5	100.	100. 2P (4P)
4D 1/2	291514.	---	---	.5	100.	82. 4D (DD(3F)) 18. 4D (DD(3P))
4D 3/2	292008.	---	---	1.5	99.	81. 4D (DD(3F)) 19. 4D (DD(3P))
4D 5/2	292846.	---	---	2.5	99.	78. 4D (DD(3F)) 21. 4D (DD(3P))
4D 7/2	294078.	---	---	3.5	99.	75. 4D (DD(3F)) 24. 4D (DD(3P))
4G11/2	305899.	---	---	5.5	100.	100. 4G (DD(3F))
4G 9/2	307044.	---	---	4.5	95.	95. 4G (DD(3F))
4G 7/2	308339.	---	---	3.5	98.	92. 4G (DD(3F)) 5. 4F (DD(3F))
4G 5/2	309663.	---	---	2.5	95.	90. 4G (DD(3F)) 5. 4F (DD(3F))
4P 5/2	312761.	---	---	2.5	99.	99. 4P (DD(3P))
4P 3/2	314528.	---	---	1.5	98.	98. 4P (DD(3P))
4P 1/2	315779.	---	---	.5	99.	99. 4P (DD(3P))
4F 3/2	316604.	---	---	1.5	98.	70. 4F (DD(3F)) 21. 2D (DD(1D)) 7. 2D (DD(3F))
4F 5/2	316834.	---	---	2.5	94.	40. 4F (DD(3F)) 38. 2D (DD(1D)) 10. 2D (DD(3F)) 5. 4G (DD(3F))
4F 9/2	317147.	---	---	4.5	93.	93. 4F (DD(3F))
4F 7/2	317761.	---	---	3.5	91.	86. 4F (DD(3F)) 5. 4G (DD(3F))
4F 5/2	319114.	319106.	7.6	2.5	92.	37. 4F (DD(3F)) 26. 2F (DD(1G)) 20. 2F (DD(3F)) 9. 2D (DD(1D))
2D 5/2	319531.	---	---	2.5	94.	30. 2D (DD(1D)) 21. 2F (DD(1G)) 18. 2F (DD(3F)) 17. 4F (DD(3F)) 7. 2D (DD(3F))
2D 3/2	320425.	---	---	1.5	96.	48. 2D (DD(1D)) 29. 4F (DD(3F)) 11. 2D (DD(3F)) 8. 2P (DD(1D))
2F 7/2	320731.	320732.	-.7	3.5	96.	41. 2F (DD(1G)) 35. 2F (DD(3F)) 14. 2F (DD(1D)) 6. 4F (DD(3F))
2P 1/2	325619.	---	---	.5	99.	68. 2P (DD(1D)) 23. 2P (DD(3P)) 9. 2P (DD(1S))
2G 7/2	328387.	---	---	3.5	93.	87. 2G (DD(3F)) 6. 2F (DD(1D))

TABLE (5.11A) CONTINUED

V 4+ ODD LEVELS
CALCULATIONS COMPARED WITH EXPERIMENTAL OBSERVATIONS
EXTRAPOLATED AND OPTIMIZED PARAMETERS
PARENTAGE -- DD(2S+1)L = 3D2(2S+1)L
DD(2S+1)L = 3D2(2S+1)L DS(2S+1)L = (3P5(2P)3D(2D))(2S+1)L

IRREP	CALC	EXP	INCR	J/MU	TOTAL	-- EIGENVECTOR COMPOSITION PCT
2P 3/2	328426.	---	---	1.5	95.	53. 2P (DD(1D)) 21. 2P (DD(3P)) 11. 2P (DD(1S)) 10. 2D (DD(1D))
2H11/2	330531.	---	---	5.5	100.	100. 2H (DD(1G))
2G 9/2	331218.	---	---	4.5	90.	90. 2G (DD(3F))
2F 7/2	332191.	332198.	-7.6	3.5	92.	74. 2F (DD(1D)) 11. 2F (DD(3F)) 6. 2F (DD(1G))
2H 9/2	335697.	---	---	4.5	98.	98. 2H (DD(1G))
2F 5/2	337000.	337013.	-12.5	2.5	96.	81. 2F (DD(1D)) 9. 2F (4F) 6. 2F (DD(3F))
4D 7/2	344192.	---	---	3.5	99.	74. 4D (DD(3P)) 25. 4D (DD(3F))
4D 5/2	345234.	---	---	2.5	95.	74. 4D (DD(3P)) 21. 4D (DD(3F))
4D 3/2	346473.	---	---	1.5	94.	76. 4D (DD(3P)) 18. 4D (DD(3F))
4D 1/2	347655.	---	---	.5	100.	82. 4D (DD(3P)) 18. 4D (DD(3F))
2F 7/2	349279.	349252.	26.2	3.5	94.	89. 2F (4F) 5. 2F (DD(1D))
2F 5/2	349647.	349676.	-28.8	2.5	95.	84. 2F (4F) 11. 2F (DD(1D))
2P 1/2	351501.	351501.	0.	.5	100.	100. 2P (5P)
2P 3/2	352018.	352018.	0.	1.5	100.	100. 2P (5P)
2D 3/2	355711.	---	---	1.5	92.	84. 2D (DD(3P)) 8. 2D (DD(3F))
2D 5/2	357834.	---	---	2.5	92.	84. 2D (DD(3P)) 8. 2D (DD(3F))
2G 9/2	362405.	---	---	4.5	95.	95. 2G (DD(1G))
2G 7/2	363062.	---	---	3.5	96.	96. 2G (DD(1G))
4S 3/2	364354.	---	---	1.5	99.	99. 4S (DD(3P))
2S 1/2	364389.	---	---	.5	99.	99. 2S (DD(3P))
2P 3/2	379159.	---	---	1.5	98.	77. 2P (DD(1S)) 21. 2P (DD(1D))
2P 1/2	384402.	---	---	.5	96.	78. 2P (DD(1S)) 18. 2P (DD(1D))
2F 5/2	396249.	396135.	113.6	2.5	92.	35. 2F (5F) 30. 2F (DD(3F)) 27. 2F (DD(1G))
2F 7/2	397887.	397994.	-106.2	3.5	93.	41. 2F (5F) 26. 2F (DD(3F)) 26. 2F (DD(1G))
2P 1/2	415420.	415420.	0.	.5	100.	100. 2P (6P)

TABLE (5.11A) CONTINUED

V 4+ ODD LEVELS
CALCULATIONS COMPARED WITH EXPERIMENTAL OBSERVATIONS
EXTRAPOLATED AND OPTIMIZED PARAMETERS
PARENTAGE -- DD(2S+1)L = 3D2(2S+1)L
DD(2S+1)L = 3D2(2S+1)L DS(2S+1)L = (3P5(2P)3D(2D))(2S+1)L

IRREP	CALC	EXP	INCR	J/MU	TOTAL	-- EIGENVECTOR COMPOSITION PCT
2P 3/2	415676.	415676.	0.	1.5	100.	100. 2P (6P)
2F 5/2	417436.	417699.	-263.4	2.5	95.	64. 2F (5F) 16. 2F (DD(1G)) 15. 2F (DD(3F))
2F 7/2	418486.	418188.	298.7	3.5	94.	58. 2F (5F) 19. 2F (DD(1G)) 17. 2F (DD(3F))
2P 1/2	438067.	438018.	48.3	.5	97.	71. 2P (DD(3P)) 13. 2P (DD(1D)) 13. 2P (DD(1S))
2P 3/2	439384.	439443.	-58.4	1.5	98.	73. 2P (DD(3P)) 15. 2P (DD(1D)) 10. 2P (DD(1S))
2D 5/2	444171.	444154.	17.8	2.5	99.	70. 2D (DD(3F)) 18. 2D (DD(1D)) 11. 2D (DD(3P))
2D 3/2	444590.	444621.	-30.6	1.5	99.	71. 2D (DD(3F)) 18. 2D (DD(1D)) 11. 2D (DD(3P))
2F 5/2	449338.	449371.	-33.1	2.5	95.	95. 2F (6F)
2F 7/2	449453.	449422.	30.2	3.5	95.	95. 2F (6F)
2P 1/2	449587.	449587.	-.0	.5	100.	100. 2P (7P)
2P 3/2	449773.	449773.	.0	1.5	100.	100. 2P (7P)
2H 9/2	450248.	450248.	-.3	4.5	100.	100. 2H (6H)
2H11/2	450248.	450248.	.2	5.5	100.	100. 2H (6H)
4P 1/2	453682.	---	---	.5	99.	99. 4P (DS(3P))
4P 3/2	454992.	---	---	1.5	99.	99. 4P (DS(3P))
4P 5/2	457384.	---	---	2.5	99.	99. 4P (DS(3P))
2P 1/2	463392.	---	---	.5	97.	97. 2P (DS(3P))
2P 3/2	466139.	---	---	1.5	96.	96. 2P (DS(3P))
4F 9/2	466377.	---	---	4.5	100.	100. 4F (DS(3F))
4F 7/2	467918.	---	---	3.5	97.	97. 4F (DS(3F))
4F 5/2	469424.	---	---	2.5	97.	84. 4F (DS(3F)) 13. 2F (7F)
2F 5/2	469703.	469702.	1.0	2.5	98.	86. 2F (7F) 13. 4F (DS(3F))
2F 7/2	469715.	469716.	-1.5	3.5	98.	98. 2F (7F)
2H 9/2	470489.	470489.	-.0	4.5	100.	100. 2H (7H)

TABLE (5.11A) CONTINUED

V 4+ ODD LEVELS
CALCULATIONS COMPARED WITH EXPERIMENTAL OBSERVATIONS
EXTRAPOLATED AND OPTIMIZED PARAMETERS
PARENTAGE -- DD(2S+1)L = 3D2(2S+1)L
DD(2S+1)L = 3D2(2S+1)L DS(2S+1)L = (3P5(2P)3D(2D))(2S+1)L

IRREP	CALC	EXP	INCR	J/MU	TOTAL	-- EIGENVECTOR COMPOSITION PCT
2H11/2	470489.	470489.	.5	5.5	100.	100. 2H (7H)
4F 3/2	470873.	---	---	1.5	98.	98. 4F (DS(3F))
2F 7/2	475532.	475531.	.7	3.5	97.	97. 2F (DS(3F))
2F 5/2	478565.	478566.	-.7	2.5	95.	95. 2F (DS(3F))
2F 5/2	483023.	483019.	4.4	2.5	99.	99. 2F (8F)
2F 7/2	483033.	483038.	-4.7	3.5	99.	99. 2F (8F)
4D 7/2	489560.	---	---	3.5	99.	90. 4D (DS(3D)) 9. 2F (DS(1F))
4D 5/2	490491.	---	---	2.5	94.	86. 4D (DS(3D)) 8. 2D (DS(1D))
4D 3/2	490981.	---	---	1.5	98.	89. 4D (DS(3D)) 10. 2D (DS(1D))
4D 1/2	491359.	---	---	.5	99.	99. 4D (DS(3D))
2F 5/2	492143.	492144.	-1.7	2.5	98.	98. 2F (9F)
2F 7/2	492203.	492202.	1.6	3.5	98.	98. 2F (9F)
2D 5/2	493704.	---	---	2.5	97.	76. 2D (DS(1D)) 9. 2D (DS(3D)) 7. 2F (DS(1F)) 5. 4D (DS(3D))
2D 3/2	494155.	---	---	1.5	98.	88. 2D (DS(1D)) 10. 4D (DS(3D))
2F 5/2	496294.	496296.	-1.7	2.5	96.	68. 2F (DS(1F)) 12. 2D (DS(3D)) 9. 2D (DS(1D)) 6. 4D (DS(3D))
2F 7/2	497557.	497556.	1.2	3.5	97.	79. 2F (DS(1F)) 10. 2F (10F) 7. 4D (DS(3D))
2F 5/2	498791.	---	---	2.5	97.	97. 2F (10F)
2F 7/2	498932.	---	---	3.5	98.	89. 2F (10F) 9. 2F (DS(1F))
2D 3/2	500117.	500117.	-.4	1.5	99.	99. 2D (DS(3D))
2D 5/2	500503.	500502.	1.0	2.5	94.	75. 2D (DS(3D)) 19. 2F (DS(1F))
2P 3/2	604984.	---	---	1.5	100.	100. 2P (DS(1P))
2P 1/2	604997.	---	---	.5	100.	100. 2P (DS(1P))

NO. EXPERIMENTAL LEVELS = 40.

ABSOLUTE MEAN DEVIATION = 27.63

RMS DEVIATION = 69.57

TABLE (5.11B)

V 4+ EVEN LEVELS
CALCULATIONS COMPARED WITH EXPERIMENTAL OBSERVATIONS
EXTRAPOLATED AND OPTIMIZED PARAMETERS
PARENTAGE -- DD(2S+1)L = 3D2(2S+1)L
DD(2S+1)L = 3D2(2S+1)L DS(2S+1)L = (3P5(2P)3D(2D))(2S+1)L

IRREP	CALC	EXP	INCR	J/MU	TOTAL	-- EIGENVECTOR COMPOSITION PCT
2D 3/2	0.	0.	0.	1.5	100.	100. 2D (3D)
2D 5/2	625.	625.	0.	2.5	100.	100. 2D (3D)
2S 1/2	148143.	148143.	0.	.5	100.	100. 2S (4S)
2D 3/2	293903.	293903.	0.	1.5	100.	100. 2D (4D)
2D 5/2	294047.	294047.	0.	2.5	100.	100. 2D (4D)
2S 1/2	328217.	328217.	0.	.5	100.	100. 2S (5S)
2D 3/2	387977.	387977.	0.	1.5	100.	100. 2D (5D)
2D 5/2	388044.	388044.	0.	2.5	100.	100. 2D (5D)
2S 1/2	403855.	403855.	0.	.5	100.	100. 2S (6S)
2G 7/2	416360.	416360.	.1	3.5	100.	100. 2G (5G)
2G 9/2	416362.	416362.	-.1	4.5	100.	100. 2G (5G)
2D 3/2	434304.	434304.	0.	1.5	100.	100. 2D (6D)
2D 5/2	434341.	434341.	0.	2.5	100.	100. 2D (6D)
2S 1/2	443075.	443075.	0.	.5	100.	100. 2S (7S)
2G 7/2	450024.	450025.	-.1	3.5	100.	100. 2G (6G)
2G 9/2	450025.	450025.	.1	4.5	100.	100. 2G (6G)
2D 3/2	460697.	460697.	0.	1.5	100.	100. 2D (7D)
2D 5/2	460720.	460720.	0.	2.5	100.	100. 2D (7D)
2S 1/2	466066.	466066.	0.	.5	100.	100. 2S (8S)
2G 7/2	470333.	470333.	.0	3.5	100.	100. 2G (7G)
2G 9/2	470334.	470334.	0.	4.5	100.	100. 2G (7G)
2I11/2	470524.	470524.	0.	5.5	100.	100. 2I (7I)
2I11/2	483651.	483651.	0.	5.5	100.	100. 2I (8I)
4D 1/2	509745.	---	---	.5	96.	89. 4D (DP(3P)) 7. 4D (DP(3F))
4D 3/2	510510.	---	---	1.5	97.	88. 4D (DP(3P)) 9. 4D (DP(3F))
4D 5/2	511709.	---	---	2.5	97.	86. 4D (DP(3P)) 11. 4D (DP(3F))
4P 1/2	513123.	---	---	.5	98.	98. 4P (DP(3P))

TABLE (5.11B) CONTINUED

V 4+ EVEN LEVELS
CALCULATIONS COMPARED WITH EXPERIMENTAL OBSERVATIONS
EXTRAPOLATED AND OPTIMIZED PARAMETERS
PARENTAGE -- DD(2S+1)L = 3D2(2S+1)L
DD(2S+1)L = 3D2(2S+1)L DS(2S+1)L = (3P5(2P)3D(2D))(2S+1)L

IRREP	CALC	EXP	INCR	J/MU	TOTAL	-- EIGENVECTOR COMPOSITION PCT
4D 7/2	513296.	---	---	3.5	99.	82. 4D (DP(3P)) 16. 4D (DP(3F))
4P 3/2	513807.	---	---	1.5	91.	91. 4P (DP(3P))
4P 5/2	515255.	---	---	2.5	96.	96. 4P (DP(3P))
2P 1/2	515411.	---	---	.5	95.	95. 2P (DP(3P))
2P 3/2	516251.	---	---	1.5	88.	79. 2P (DP(3P)) 10. 4S (DP(3P))
4S 3/2	518527.	---	---	1.5	95.	85. 4S (DP(3P)) 10. 2P (DP(3P))
2D 3/2	522561.	---	---	1.5	91.	85. 2D (DP(3P)) 6. 2P (DP(3P))
2D 5/2	522941.	---	---	2.5	93.	81. 2D (DP(3P)) 6. 2D (DP(3F)) 6. 2D (DP(3D))
4G11/2	524260.	---	---	5.5	100.	100. 4G (DP(3F))
4G 9/2	524786.	---	---	4.5	97.	79. 4G (DP(3F)) 18. 4F (DP(3F))
4D 7/2	524929.	---	---	3.5	94.	36. 4D (DP(3F)) 32. 4F (DP(3F)) 12. 2F (DP(3F)) 9. 4D (DP(3P)) 6. 4D (DP(3D))
2F 7/2	525707.	---	---	3.5	92.	68. 2F (DP(3F)) 18. 4G (DP(3F)) 6. 4D (DP(3F))
2S 1/2	526033.	---	---	.5	97.	97. 2S (DP(3P))
4G 7/2	526044.	---	---	3.5	92.	70. 4G (DP(3F)) 14. 4D (DP(3F)) 8. 2F (DP(3F))
4F 9/2	526130.	---	---	4.5	96.	79. 4F (DP(3F)) 18. 4G (DP(3F))
4D 5/2	526152.	---	---	2.5	96.	46. 4D (DP(3F)) 28. 4F (DP(3F)) 9. 4D (DP(3D)) 8. 4D (DP(3P)) 5. 4G (DP(3F))
4G 5/2	527130.	---	---	2.5	97.	92. 4G (DP(3F)) 5. 4D (DP(3F))
4D 3/2	527440.	---	---	1.5	97.	56. 4D (DP(3F)) 20. 4F (DP(3F)) 12. 4D (DP(3D)) 8. 4D (DP(3P))
2F 5/2	528389.	---	---	2.5	91.	62. 2F (DP(3F)) 21. 4F (DP(3F)) 8. 4D (DP(3F))
4F 7/2	528419.	---	---	3.5	88.	64. 4F (DP(3F)) 17. 4D (DP(3F)) 7. 2F (DP(3F))
4D 1/2	528610.	---	---	.5	98.	74. 4D (DP(3F)) 15. 4D (DP(3D)) 9. 4D (DP(3P))

TABLE (5.11B) CONTINUED

V 4+ EVEN LEVELS
CALCULATIONS COMPARED WITH EXPERIMENTAL OBSERVATIONS
EXTRAPOLATED AND OPTIMIZED PARAMETERS
PARENTAGE -- DD(2S+1)L = 3D2(2S+1)L
DD(2S+1)L = 3D2(2S+1)L DS(2S+1)L = (3P5(2P)3D(2D))(2S+1)L

IRREP	CALC	EXP	INCR	J/MU	TOTAL	-- EIGENVECTOR COMPOSITION PCT
4F 5/2	529974.	---	---	2.5	88.	45. 4F (DP(3F)) 28. 2F (DP(3F)) 15. 4D (DP(3F))
4F 3/2	530103.	---	---	1.5	92.	74. 4F (DP(3F)) 18. 4D (DP(3F))
2G 9/2	533645.	---	---	4.5	97.	97. 2G (DP(3F))
2G 7/2	535852.	---	---	3.5	93.	93. 2G (DP(3F))
2D 5/2	536181.	---	---	2.5	85.	35. 2D (DP(1D)) 33. 2D (DP(3F)) 17. 2D (DP(1F))
2D 3/2	537000.	---	---	1.5	94.	46. 2D (DP(1D)) 29. 2D (DP(3F)) 13. 2D (DP(1F)) 6. 2D (DP(3D))
4D 7/2	546207.	---	---	3.5	94.	79. 4D (DP(3D)) 10. 4D (DP(3F)) 5. 2F (DP(1F))
4D 5/2	546829.	---	---	2.5	91.	66. 4D (DP(3D)) 10. 4D (DP(3F)) 5. 4F (DP(3D)) 5. 2D (DP(3D)) 5. 2F (DP(1F))
4D 3/2	547814.	---	---	1.5	87.	75. 4D (DP(3D)) 13. 4D (DP(3F))
2F 5/2	548238.	---	---	2.5	96.	35. 2F (DP(1D)) 18. 2D (DP(3F)) 18. 2D (DP(3D)) 13. 2F (DP(1F)) 6. 4F (DP(3D)) 6. 2D (DP(1D))
4D 1/2	548573.	---	---	.5	99.	82. 4D (DP(3D)) 17. 4D (DP(3F))
2F 5/2	548883.	---	---	2.5	94.	20. 2F (DP(1D)) 20. 2D (DP(3F)) 19. 2D (DP(3D)) 15. 4D (DP(3D)) 14. 2F (DP(1F)) 6. 2D (DP(1D))
2F 7/2	549546.	---	---	3.5	90.	36. 2F (DP(1D)) 31. 4F (DP(3D)) 15. 2F (DP(1F)) 8. 4D (DP(3D))
4F 9/2	549756.	---	---	4.5	97.	83. 4F (DP(3D)) 14. 2G (DP(1F))
4F 3/2	550138.	---	---	1.5	95.	75. 4F (DP(3D)) 11. 2D (DP(3F)) 9. 2D (DP(3D))
4F 7/2	550672.	---	---	3.5	89.	47. 4F (DP(3D)) 25. 2F (DP(1F)) 17. 2F (DP(1D))
4F 5/2	550687.	---	---	2.5	90.	84. 4F (DP(3D)) 7. 2F (DP(1F))
2D 3/2	550855.	---	---	1.5	94.	34. 2D (DP(3D)) 27. 2D (DP(3F)) 19. 4F (DP(3D)) 9. 4D (DP(3D)) 5. 2D (DP(1F))
2G 7/2	553592.	---	---	3.5	96.	67. 2G (DP(1F)) 16. 2F (DP(3D)) 13. 4F (DP(3D))

TABLE (5.11B) CONTINUED

V 4+ EVEN LEVELS
CALCULATIONS COMPARED WITH EXPERIMENTAL OBSERVATIONS
EXTRAPOLATED AND OPTIMIZED PARAMETERS
PARENTAGE -- DD(2S+1)L = 3D2(2S+1)L
DD(2S+1)L = 3D2(2S+1)L DS(2S+1)L = (3P5(2P)3D(2D))(2S+1)L

IRREP	CALC	EXP	INCR	J/MU	TOTAL	-- EIGENVECTOR COMPOSITION PCT
2F 5/2	554177.	---	---	2.5	95.	40. 2F (DP(1F)) 35. 2F (DP(3D)) 19. 2F (DP(1D))
2G 9/2	555077.	---	---	4.5	98.	86. 2G (DP(1F)) 13. 4F (DP(3D))
2F 7/2	555152.	---	---	3.5	96.	28. 2F (DP(1F)) 26. 2F (DP(1D)) 26. 2F (DP(3D)) 16. 2G (DP(1F))
4P 5/2	555201.	---	---	2.5	91.	91. 4P (DP(3D))
4P 3/2	555570.	---	---	1.5	92.	57. 4P (DP(3D)) 35. 2P (DP(1D))
2P 1/2	556042.	---	---	.5	99.	52. 2P (DP(1D)) 36. 4P (DP(3D)) 11. 2P (DP(3D))
4P 1/2	556995.	---	---	.5	99.	63. 4P (DP(3D)) 25. 2P (DP(1D)) 11. 2P (DP(3D))
2P 3/2	557331.	---	---	1.5	97.	47. 2P (DP(1D)) 41. 4P (DP(3D)) 9. 2P (DP(3D))
2D 3/2	558137.	---	---	1.5	93.	33. 2D (DP(1D)) 29. 2D (DP(1F)) 20. 2P (DP(3D)) 12. 2P (DP(1D))
2D 5/2	558601.	---	---	2.5	94.	42. 2D (DP(1F)) 37. 2D (DP(1D)) 10. 2D (DP(3D)) 5. 4P (DP(3D))
2F 7/2	560411.	---	---	3.5	97.	50. 2F (DP(3D)) 25. 2F (DP(1F)) 16. 2F (DP(1D)) 6. 2G (DP(1F))
2F 5/2	560769.	---	---	2.5	95.	58. 2F (DP(3D)) 19. 2F (DP(1F)) 18. 2F (DP(1D))
2P 3/2	560884.	---	---	1.5	94.	65. 2P (DP(3D)) 12. 2D (DP(1F)) 10. 2D (DP(1D)) 7. 2D (DP(3F))
2P 1/2	561836.	---	---	.5	97.	75. 2P (DP(3D)) 22. 2P (DP(1D))
2D 3/2	576066.	---	---	1.5	99.	40. 2D (DP(3D)) 33. 2D (DP(1F)) 14. 2D (DP(3F)) 6. 2D (DP(1D)) 6. 2D (DP(3P))
2D 5/2	577399.	---	---	2.5	99.	38. 2D (DP(3D)) 31. 2D (DP(1F)) 16. 2D (DP(3F)) 7. 2D (DP(3P)) 7. 2D (DP(1D))
2P 1/2	661382.	---	---	.5	99.	99. 2P (DP(1P))
2P 3/2	661935.	---	---	1.5	98.	98. 2P (DP(1P))
2D 3/2	664892.	---	---	1.5	97.	97. 2D (DP(1P))
2D 5/2	665683.	---	---	2.5	99.	99. 2D (DP(1P))

TABLE (5.11B) CONTINUED

V 4+ EVEN LEVELS
CALCULATIONS COMPARED WITH EXPERIMENTAL OBSERVATIONS
EXTRAPOLATED AND OPTIMIZED PARAMETERS
PARENTAGE -- DD(2S+1)L = 3D2(2S+1)L
DD(2S+1)L = 3D2(2S+1)L DS(2S+1)L = (3P5(2P)3D(2D))(2S+1)L

IRREP	CALC	EXP	INCR	J/MU	TOTAL	-- EIGENVECTOR COMPOSITION PCT
2S 1/2	667226.	---	---	.5	99.	99. 2S (DP(1P))

NO. EXPERIMENTAL LEVELS = 23.

ABSOLUTE MEAN DEVIATION = .02

RMS DEVIATION = .04

TABLE (5.12A)

CR5+ ODD LEVELS
CALCULATIONS COMPARED WITH EXPERIMENTAL OBSERVATIONS
EXTRAPOLATED AND OPTIMIZED PARAMETERS
PARENTAGE -- DD(2S+1)L = 3D2(2S+1)L
DD(2S+1)L = 3D2(2S+1)L DS(2S+1)L = (3P5(2P)3D(2D))(2S+1)L

IRREP	CALC	EXP	INCR	J/MU	TOTAL	-- EIGENVECTOR COMPOSITION PCT
2P 1/2	296573.	296573.	0.	.5	100.	100. 2P (4P)
2P 3/2	298397.	298397.	-.0	1.5	100.	100. 2P (4P)
4D 1/2	322022.	---	---	.5	100.	83. 4D (DD(3F)) 17. 4D (DD(3P))
4D 3/2	322661.	---	---	1.5	99.	81. 4D (DD(3F)) 18. 4D (DD(3P))
4D 5/2	323748.	---	---	2.5	99.	78. 4D (DD(3F)) 20. 4D (DD(3P))
4D 7/2	325362.	---	---	3.5	98.	75. 4D (DD(3F)) 24. 4D (DD(3P))
4G11/2	338991.	---	---	5.5	100.	100. 4G (DD(3F))
4G 9/2	340492.	---	---	4.5	95.	95. 4G (DD(3F))
4G 7/2	342193.	---	---	3.5	98.	92. 4G (DD(3F)) 6. 4F (DD(3F))
4G 5/2	343930.	---	---	2.5	95.	89. 4G (DD(3F)) 6. 4F (DD(3F))
4P 5/2	348273.	---	---	2.5	99.	99. 4P (DD(3P))
4P 3/2	350572.	---	---	1.5	98.	98. 4P (DD(3P))
4F 3/2	352133.	---	---	1.5	98.	74. 4F (DD(3F)) 18. 2D (DD(1D)) 6. 2D (DD(3F))
4P 1/2	352208.	---	---	.5	99.	99. 4P (DD(3P))
4F 5/2	352669.	---	---	2.5	97.	50. 4F (DD(3F)) 32. 2D (DD(1D)) 9. 2D (DD(3F)) 6. 4G (DD(3F))
4F 9/2	352765.	---	---	4.5	93.	93. 4F (DD(3F))
4F 7/2	353669.	---	---	3.5	94.	88. 4F (DD(3F)) 6. 4G (DD(3F))
4F 5/2	355880.	---	---	2.5	94.	43. 4F (DD(3F)) 42. 2D (DD(1D)) 10. 2D (DD(3F))
2F 5/2	356954.	356962.	-7.7	2.5	90.	49. 2F (DD(1G)) 41. 2F (DD(3F))
2D 3/2	357436.	---	---	1.5	96.	51. 2D (DD(1D)) 25. 4F (DD(3F)) 12. 2D (DD(3F)) 8. 2P (DD(1D))
2F 7/2	359167.	359165.	1.5	3.5	93.	44. 2F (DD(1G)) 39. 2F (DD(3F)) 10. 2F (DD(1D))
2P 1/2	364507.	---	---	.5	99.	70. 2P (DD(1D)) 21. 2P (DD(3P)) 8. 2P (DD(1S))
2P 3/2	368343.	---	---	1.5	95.	56. 2P (DD(1D)) 20. 2P (DD(3P)) 10. 2P (DD(1S)) 9. 2D (DD(1D))
2G 7/2	369321.	---	---	3.5	94.	71. 2G (DD(3F)) 22. 2F (DD(1D))

TABLE (5.12A) CONTINUED

CR5+ ODD LEVELS
CALCULATIONS COMPARED WITH EXPERIMENTAL OBSERVATIONS
EXTRAPOLATED AND OPTIMIZED PARAMETERS
PARENTAGE -- DD(2S+1)L = 3D2(2S+1)L
DD(2S+1)L = 3D2(2S+1)L DS(2S+1)L = (3P5(2P)3D(2D))(2S+1)L

IRREP	CALC	EXP	INCR	J/MU	TOTAL	-- EIGENVECTOR COMPOSITION PCT
2H11/2	370572.	---	---	5.5	100.	100. 2H (DD(1G))
2F 7/2	371656.	371618.	38.5	3.5	94.	67. 2F (DD(1D)) 20. 2G (DD(3F)) 8. 2F (DD(3F))
2G 9/2	373010.	---	---	4.5	93.	87. 2G (DD(3F)) 6. 2G (DD(1G))
2H 9/2	377329.	---	---	4.5	96.	96. 2H (DD(1G))
2F 5/2	378649.	378677.	-28.5	2.5	93.	93. 2F (DD(1D))
4D 7/2	385662.	---	---	3.5	99.	74. 4D (DD(3P)) 25. 4D (DD(3F))
4D 5/2	387109.	---	---	2.5	96.	75. 4D (DD(3P)) 20. 4D (DD(3F))
4D 3/2	388780.	---	---	1.5	95.	77. 4D (DD(3P)) 18. 4D (DD(3F))
4D 1/2	390280.	---	---	.5	100.	83. 4D (DD(3P)) 17. 4D (DD(3F))
2D 3/2	402048.	---	---	1.5	92.	84. 2D (DD(3P)) 7. 2D (DD(3F))
2D 5/2	404751.	---	---	2.5	92.	84. 2D (DD(3P)) 9. 2D (DD(3F))
2G 9/2	408268.	---	---	4.5	98.	93. 2G (DD(1G)) 5. 2G (DD(3F))
2G 7/2	408907.	---	---	3.5	95.	95. 2G (DD(1G))
4S 3/2	410178.	---	---	1.5	99.	99. 4S (DD(3P))
2S 1/2	410238.	---	---	.5	99.	99. 2S (DD(3P))
2P 3/2	427799.	---	---	1.5	98.	79. 2P (DD(1S)) 19. 2P (DD(1D))
2P 1/2	434893.	---	---	.5	96.	80. 2P (DD(1S)) 16. 2P (DD(1D))
2F 5/2	440102.	440135.	-33.1	2.5	97.	42. 2F (DD(3F)) 34. 2F (DD(1G)) 21. 2F (4F)
2F 7/2	442949.	442940.	8.4	3.5	97.	38. 2F (DD(3F)) 35. 2F (DD(1G)) 24. 2F (4F)
2F 5/2	481772.	481956.	-183.8	2.5	99.	78. 2F (4F) 11. 2F (DD(1G)) 10. 2F (DD(3F))
2F 7/2	482716.	482517.	198.7	3.5	99.	75. 2F (4F) 13. 2F (DD(1G)) 11. 2F (DD(3F))
2P 1/2	487645.	487589.	55.4	.5	97.	86. 2P (5P) 10. 2P (DD(3P))
2P 3/2	488507.	488562.	-54.9	1.5	98.	90. 2P (5P) 8. 2P (DD(3P))
2P 1/2	493286.	493247.	38.5	.5	100.	64. 2P (DD(3P)) 14. 2P (5P) 11. 2P (DD(1S)) 11. 2P (DD(1D))

TABLE (5.12A) CONTINUED

CR5+ ODD LEVELS
CALCULATIONS COMPARED WITH EXPERIMENTAL OBSERVATIONS
EXTRAPOLATED AND OPTIMIZED PARAMETERS
PARENTAGE -- DD(2S+1)L = 3D2(2S+1)L
DD(2S+1)L = 3D2(2S+1)L DS(2S+1)L = (3P5(2P)3D(2D))(2S+1)L

IRREP	CALC	EXP	INCR	J/MU	TOTAL	-- EIGENVECTOR COMPOSITION PCT
2P 3/2	494874.	494911.	-37.1	1.5	99.	68. 2P (DD(3P)) 13. 2P (DD(1D)) 10. 2P (5P) 8. 2P (DD(1S))
2D 5/2	496952.	496958.	-5.7	2.5	100.	70. 2D (DD(3F)) 17. 2D (DD(1D)) 12. 2D (DD(3P))
2D 3/2	497505.	497495.	9.7	1.5	100.	71. 2D (DD(3F)) 18. 2D (DD(1D)) 11. 2D (DD(3P))
2F 5/2	568939.	568957.	-18.4	2.5	98.	98. 2F (5F)
2F 7/2	569011.	568993.	18.4	3.5	98.	98. 2F (5F)
4P 1/2	569285.	---	---	.5	99.	99. 4P (DS(3P))
4P 3/2	570505.	---	---	1.5	99.	99. 4P (DS(3P))
4P 5/2	572733.	---	---	2.5	99.	99. 4P (DS(3P))
2P 1/2	574706.	574135.	571.3	.5	100.	92. 2P (6P) 7. 2P (DS(3P))
2P 3/2	575196.	575742.	-546.4	1.5	97.	97. 2P (6P)
2P 1/2	578478.	578566.	-88.5	.5	99.	92. 2P (DS(3P)) 8. 2P (6P)
2P 3/2	580962.	580697.	264.7	1.5	95.	95. 2P (DS(3P))
4F 9/2	582665.	---	---	4.5	100.	100. 4F (DS(3F))
4F 7/2	584404.	584371.	32.8	3.5	98.	98. 4F (DS(3F))
4F 5/2	586066.	586273.	-206.7	2.5	97.	97. 4F (DS(3F))
4F 3/2	587507.	---	---	1.5	98.	98. 4F (DS(3F))
2F 7/2	591032.	591137.	-104.9	3.5	95.	95. 2F (DS(3F))
2F 5/2	594813.	594926.	-113.3	2.5	95.	95. 2F (DS(3F))
4D 7/2	607607.	607615.	-7.6	3.5	100.	92. 4D (DS(3D)) 8. 2F (DS(1F))
4D 5/2	608650.	608631.	19.3	2.5	95.	84. 4D (DS(3D)) 11. 2D (DS(1D))
4D 3/2	609267.	609166.	101.0	1.5	98.	86. 4D (DS(3D)) 12. 2D (DS(1D))
4D 1/2	609713.	---	---	.5	100.	100. 4D (DS(3D))
2D 5/2	610445.	610497.	-52.2	2.5	93.	63. 2D (DS(1D)) 22. 2D (DS(3D)) 8. 4D (DS(3D))
2D 3/2	611649.	611568.	80.8	1.5	99.	79. 2D (DS(1D)) 13. 4D (DS(3D)) 7. 2D (DS(3D))

TABLE (5.12A) CONTINUED

CR5+ ODD LEVELS
CALCULATIONS COMPARED WITH EXPERIMENTAL OBSERVATIONS
EXTRAPOLATED AND OPTIMIZED PARAMETERS
PARENTAGE -- DD(2S+1)L = 3D2(2S+1)L
DD(2S+1)L = 3D2(2S+1)L DS(2S+1)L = (3P5(2P)3D(2D))(2S+1)L

IRREP	CALC	EXP	INCR	J/MU	TOTAL	-- EIGENVECTOR COMPOSITION PCT
2F 5/2	614516.	614385.	130.7	2.5	92.	78. 2F (DS(1F)) 7. 2D (DS(1D)) 6. 4D (DS(3D))
2F 7/2	615996.	616079.	-82.8	3.5	96.	78. 2F (DS(1F)) 11. 2F (6F) 7. 4D (DS(3D))
2D 3/2	618514.	618491.	23.1	1.5	99.	91. 2D (DS(3D)) 8. 2D (DS(1D))
2F 5/2	618585.	618583.	2.3	2.5	95.	78. 2F (6F) 17. 2D (DS(3D))
2F 7/2	618879.	618849.	29.7	3.5	98.	89. 2F (6F) 10. 2F (DS(1F))
2D 5/2	619308.	619419.	-111.0	2.5	99.	56. 2D (DS(3D)) 17. 2F (6F) 14. 2F (DS(1F)) 12. 2D (DS(1D))
2H 9/2	621163.	621163.	-.3	4.5	100.	100. 2H (6H)
2H11/2	621164.	621163.	.8	5.5	100.	100. 2H (6H)
2P 1/2	623485.	---	---	.5	100.	100. 2P (7P)
2P 3/2	623698.	---	---	1.5	100.	100. 2P (7P)
2F 5/2	648520.	648521.	-.9	2.5	100.	100. 2F (7F)
2F 7/2	648534.	648533.	.9	3.5	100.	100. 2F (7F)
2H 9/2	650310.	650311.	-.3	4.5	100.	100. 2H (7H)
2H11/2	650311.	650311.	.2	5.5	100.	100. 2H (7H)
2F 5/2	667969.	667973.	-4.1	2.5	100.	100. 2F (8F)
2F 7/2	667977.	667973.	4.1	3.5	100.	100. 2F (8F)
2F 5/2	681304.	681307.	-2.6	2.5	100.	100. 2F (9F)
2F 7/2	681310.	681307.	2.6	3.5	100.	100. 2F (9F)
2F 5/2	690779.	690781.	-1.9	2.5	100.	100. 2F (10F)
2F 7/2	690783.	690781.	1.9	3.5	100.	100. 2F (10F)
2P 3/2	730638.	---	---	1.5	100.	100. 2P (DS(1P))
2P 1/2	730699.	---	---	.5	100.	100. 2P (DS(1P))

NO. EXPERIMENTAL LEVELS = 49.

ABSOLUTE MEAN DEVIATION = 67.92

RMS DEVIATION = 136.63

TABLE (5.12B)

CR5+ EVEN LEVELS
CALCULATIONS COMPARED WITH EXPERIMENTAL OBSERVATIONS
EXTRAPOLATED AND OPTIMIZED PARAMETERS
PARENTAGE -- DD(2S+1)L = 3D2(2S+1)L
DD(2S+1)L = 3D2(2S+1)L DS(2S+1)L = (3P5(2P)3D(2D))(2S+1)L

IRREP	CALC	EXP	INCR	J/MU	TOTAL	-- EIGENVECTOR COMPOSITION PCT
2D 3/2	0.	0.	0.	1.5	100.	100. 2D (3D)
2D 5/2	940.	940.	0.	2.5	100.	100. 2D (3D)
2S 1/2	227858.	227858.	0.	.5	100.	100. 2S (4S)
2D 3/2	402662.	402662.	0.	1.5	100.	100. 2D (4D)
2D 5/2	402889.	402889.	0.	2.5	100.	100. 2D (4D)
2S 1/2	461253.	461253.	0.	.5	100.	100. 2S (5S)
2D 3/2	534382.	534382.	0.	1.5	100.	100. 2D (5D)
2D 5/2	534490.	534490.	0.	2.5	100.	100. 2D (5D)
2S 1/2	562064.	562064.	0.	.5	100.	100. 2S (6S)
2G 7/2	572272.	572272.	-.5	3.5	100.	100. 2G (5G)
2G 9/2	572275.	572274.	.5	4.5	100.	100. 2G (5G)
2D 3/2	599609.	---	---	1.5	100.	100. 2D (6D)
2D 5/2	599664.	---	---	2.5	100.	100. 2D (6D)
2S 1/2	615165.	---	---	.5	100.	100. 2S (7S)
2G 7/2	620698.	620696.	1.2	3.5	100.	100. 2G (6G)
2G 9/2	620699.	620701.	-1.2	4.5	100.	100. 2G (6G)
4D 1/2	634595.	---	---	.5	95.	88. 4D (DP(3P)) 8. 4D (DP(3F))
4D 3/2	635664.	---	---	1.5	97.	87. 4D (DP(3P)) 9. 4D (DP(3F))
4D 5/2	637311.	---	---	2.5	96.	83. 4D (DP(3P)) 12. 4D (DP(3F))
2D 3/2	637379.	---	---	1.5	99.	99. 2D (7D)
2D 5/2	637420.	---	---	2.5	98.	98. 2D (7D)
4P 1/2	638785.	---	---	.5	98.	98. 4P (DP(3P))
4D 7/2	639406.	---	---	3.5	98.	78. 4D (DP(3P)) 20. 4D (DP(3F))
4P 3/2	639747.	---	---	1.5	95.	90. 4P (DP(3P)) 5. 4S (DP(3P))
2P 1/2	641661.	---	---	.5	93.	93. 2P (DP(3P))
4P 5/2	641692.	---	---	2.5	95.	95. 4P (DP(3P))
2P 3/2	642608.	---	---	1.5	91.	73. 2P (DP(3P)) 12. 4S (DP(3P)) 6. 4P (DP(3P))

TABLE (5.12B) CONTINUED

CR5+ EVEN LEVELS
CALCULATIONS COMPARED WITH EXPERIMENTAL OBSERVATIONS
EXTRAPOLATED AND OPTIMIZED PARAMETERS
PARENTAGE -- DD(2S+1)L = 3D2(2S+1)L
DD(2S+1)L = 3D2(2S+1)L DS(2S+1)L = (3P5(2P)3D(2D))(2S+1)L

IRREP	CALC	EXP	INCR	J/MU	TOTAL	-- EIGENVECTOR COMPOSITION PCT
4S 3/2	645486.	---	---	1.5	93.	81. 4S (DP(3P)) 11. 2P (DP(3P))
2S 1/2	646600.	---	---	.5	100.	100. 2S (8S)
2D 3/2	650068.	---	---	1.5	89.	81. 2D (DP(3P)) 9. 2P (DP(3P))
2G 7/2	650069.	---	---	3.5	100.	100. 2G (7G)
2G 9/2	650070.	---	---	4.5	100.	100. 2G (7G)
2D 5/2	650250.	---	---	2.5	88.	74. 2D (DP(3P)) 7. 2D (DP(3D)) 7. 2D (DP(3F))
2I11/2	650384.	---	---	5.5	100.	100. 2I (7I)
4G11/2	651070.	---	---	5.5	100.	100. 4G (DP(3F))
4D 7/2	651460.	---	---	3.5	95.	33. 4D (DP(3F)) 33. 4F (DP(3F)) 12. 4D (DP(3P)) 11. 2F (DP(3F)) 6. 4D (DP(3D))
4G 9/2	651472.	---	---	4.5	96.	73. 4G (DP(3F)) 24. 4F (DP(3F))
2F 7/2	652519.	---	---	3.5	87.	65. 2F (DP(3F)) 22. 4G (DP(3F))
4D 5/2	652921.	---	---	2.5	88.	42. 4D (DP(3F)) 27. 4F (DP(3F)) 10. 4D (DP(3D)) 9. 4D (DP(3P))
4G 7/2	653135.	---	---	3.5	89.	65. 4G (DP(3F)) 13. 4D (DP(3F)) 12. 2F (DP(3F))
4F 9/2	653145.	---	---	4.5	95.	73. 4F (DP(3F)) 23. 4G (DP(3F))
2S 1/2	654120.	---	---	.5	95.	95. 2S (DP(3P))
4D 3/2	654558.	---	---	1.5	94.	52. 4D (DP(3F)) 20. 4F (DP(3F)) 13. 4D (DP(3D)) 9. 4D (DP(3P))
4G 5/2	654567.	---	---	2.5	92.	92. 4G (DP(3F))
4F 7/2	656040.	---	---	3.5	85.	61. 4F (DP(3F)) 18. 4D (DP(3F)) 6. 2F (DP(3F))
2F 5/2	656043.	---	---	2.5	88.	59. 2F (DP(3F)) 23. 4F (DP(3F)) 7. 4D (DP(3F))
4D 1/2	656179.	---	---	.5	96.	69. 4D (DP(3F)) 17. 4D (DP(3D)) 10. 4D (DP(3P))
4F 5/2	658075.	---	---	2.5	82.	40. 4F (DP(3F)) 25. 2F (DP(3F)) 17. 4D (DP(3F))
4F 3/2	658258.	---	---	1.5	89.	70. 4F (DP(3F)) 19. 4D (DP(3F))

TABLE (5.12B) CONTINUED

CR5+ EVEN LEVELS
CALCULATIONS COMPARED WITH EXPERIMENTAL OBSERVATIONS
EXTRAPOLATED AND OPTIMIZED PARAMETERS
PARENTAGE -- DD(2S+1)L = 3D2(2S+1)L
DD(2S+1)L = 3D2(2S+1)L DS(2S+1)L = (3P5(2P)3D(2D))(2S+1)L

IRREP	CALC	EXP	INCR	J/MU	TOTAL	-- EIGENVECTOR COMPOSITION PCT
2G 9/2	661760.	---	---	4.5	96.	96. 2G (DP(3F))
2D 5/2	664050.	---	---	2.5	87.	33. 2D (DP(1D)) 27. 2D (DP(3F)) 17. 2D (DP(1F)) 9. 2F (DP(3F))
2G 7/2	664590.	---	---	3.5	91.	91. 2G (DP(3F))
2D 3/2	664853.	---	---	1.5	95.	46. 2D (DP(1D)) 24. 2D (DP(3F)) 13. 2D (DP(1F)) 7. 2D (DP(3D)) 5. 4F (DP(3F))
2I11/2	669278.	---	---	5.5	100.	100. 2I (8I)
4D 7/2	674752.	---	---	3.5	98.	74. 4D (DP(3D)) 11. 4D (DP(3F)) 7. 2F (DP(1F)) 6. 4F (DP(3D))
4D 5/2	675461.	---	---	2.5	90.	57. 4D (DP(3D)) 10. 4D (DP(3F)) 9. 2F (DP(1F)) 8. 4F (DP(3D)) 6. 2F (DP(1D))
4D 3/2	676895.	---	---	1.5	88.	69. 4D (DP(3D)) 14. 4D (DP(3F)) 5. 4F (DP(3D))
2F 5/2	677176.	---	---	2.5	88.	43. 2F (DP(1D)) 17. 2F (DP(1F)) 11. 2D (DP(3F)) 10. 2D (DP(3D)) 7. 4D (DP(3D))
4D 1/2	678022.	---	---	.5	98.	78. 4D (DP(3D)) 19. 4D (DP(3F))
2D 5/2	678297.	---	---	2.5	92.	29. 2D (DP(3F)) 26. 2D (DP(3D)) 13. 4D (DP(3D)) 9. 2F (DP(1F)) 8. 2F (DP(1D)) 7. 2D (DP(1D))
2F 7/2	678856.	---	---	3.5	89.	31. 2F (DP(1D)) 31. 4F (DP(3D)) 11. 2F (DP(1F)) 10. 4D (DP(3D)) 6. 2G (DP(1F))
4F 9/2	678876.	---	---	4.5	97.	77. 4F (DP(3D)) 20. 2G (DP(1F))
4F 3/2	679513.	---	---	1.5	90.	84. 4F (DP(3D)) 7. 2D (DP(3F))
4F 7/2	680048.	---	---	3.5	96.	35. 4F (DP(3D)) 29. 2F (DP(1F)) 18. 2F (DP(1D)) 9. 2G (DP(1F)) 5. 2F (DP(3D))
4F 5/2	680235.	---	---	2.5	88.	81. 4F (DP(3D)) 7. 2F (DP(1F))
2D 3/2	680930.	---	---	1.5	91.	38. 2D (DP(3D)) 29. 2D (DP(3F)) 10. 4D (DP(3D)) 8. 4F (DP(3D)) 7. 2D (DP(1F))
2G 7/2	683065.	---	---	3.5	96.	66. 2G (DP(1F)) 21. 4F (DP(3D)) 10. 2F (DP(3D))

TABLE (5.12B) CONTINUED

CR5+ EVEN LEVELS
CALCULATIONS COMPARED WITH EXPERIMENTAL OBSERVATIONS
EXTRAPOLATED AND OPTIMIZED PARAMETERS
PARENTAGE -- DD(2S+1)L = 3D2(2S+1)L
DD(2S+1)L = 3D2(2S+1)L DS(2S+1)L = (3P5(2P)3D(2D))(2S+1)L

IRREP	CALC	EXP	INCR	J/MU	TOTAL	-- EIGENVECTOR COMPOSITION PCT
2F 5/2	684016.	---	---	2.5	92.	37. 2F (DP(1F)) 33. 2F (DP(3D)) 22. 2F (DP(1D))
2G 9/2	685173.	---	---	4.5	97.	79. 2G (DP(1F)) 19. 4F (DP(3D))
4P 5/2	685219.	---	---	2.5	92.	87. 4P (DP(3D)) 6. 2D (DP(1D))
2F 7/2	685403.	---	---	3.5	93.	31. 2F (DP(1D)) 28. 2F (DP(3D)) 26. 2F (DP(1F)) 8. 2G (DP(1F))
4P 3/2	685722.	---	---	1.5	88.	50. 4P (DP(3D)) 38. 2P (DP(1D))
2P 1/2	686320.	---	---	.5	98.	53. 2P (DP(1D)) 32. 4P (DP(3D)) 12. 2P (DP(3D))
4P 1/2	687551.	---	---	.5	99.	66. 4P (DP(3D)) 22. 2P (DP(1D)) 12. 2P (DP(3D))
4P 3/2	687978.	---	---	1.5	94.	41. 4P (DP(3D)) 32. 2P (DP(1D)) 15. 2P (DP(3D)) 6. 2D (DP(1F))
2D 3/2	688566.	---	---	1.5	91.	27. 2D (DP(1D)) 24. 2P (DP(1D)) 22. 2D (DP(1F)) 18. 2P (DP(3D))
2D 5/2	689278.	---	---	2.5	92.	41. 2D (DP(1F)) 34. 2D (DP(1D)) 10. 2D (DP(3D)) 7. 4P (DP(3D))
2F 7/2	691312.	---	---	3.5	96.	50. 2F (DP(3D)) 23. 2F (DP(1F)) 15. 2F (DP(1D)) 7. 2G (DP(1F))
2F 5/2	691712.	---	---	2.5	94.	59. 2F (DP(3D)) 18. 2F (DP(1D)) 18. 2F (DP(1F))
2P 3/2	692241.	---	---	1.5	95.	60. 2P (DP(3D)) 14. 2D (DP(1F)) 11. 2D (DP(1D)) 10. 2D (DP(3F))
2P 1/2	693264.	---	---	.5	96.	73. 2P (DP(3D)) 23. 2P (DP(1D))
2D 3/2	709580.	---	---	1.5	99.	39. 2D (DP(3D)) 31. 2D (DP(1F)) 15. 2D (DP(3F)) 7. 2D (DP(3P)) 7. 2D (DP(1D))
2D 5/2	711522.	---	---	2.5	98.	37. 2D (DP(3D)) 29. 2D (DP(1F)) 18. 2D (DP(3F)) 8. 2D (DP(3P)) 7. 2D (DP(1D))
2P 1/2	795932.	---	---	.5	99.	99. 2P (DP(1P))
2P 3/2	796751.	---	---	1.5	97.	97. 2P (DP(1P))
2D 3/2	800361.	---	---	1.5	96.	96. 2D (DP(1P))
2D 5/2	801531.	---	---	2.5	99.	99. 2D (DP(1P))

TABLE (5.12B) CONTINUED

CR5+ EVEN LEVELS
CALCULATIONS COMPARED WITH EXPERIMENTAL OBSERVATIONS
EXTRAPOLATED AND OPTIMIZED PARAMETERS
PARENTAGE -- DD(2S+1)L = 3D2(2S+1)L
DD(2S+1)L = 3D2(2S+1)L DS(2S+1)L = (3P5(2P)3D(2D))(2S+1)L

IRREP	CALC	EXP	INCR	J/MU	TOTAL	-- EIGENVECTOR COMPOSITION PCT
2S 1/2	803731.	---	---	.5	99.	99. 2S (DP(1P))

NO. EXPERIMENTAL LEVELS = 13.

ABSOLUTE MEAN DEVIATION = .27

RMS DEVIATION = .52

Table (5.13a)

Least Squares Corrections to Parameters: Odd Parity Configurations

Parameter	V^{4+} new	V^{4+} old	Cr^{5+} new	Cr^{5+} old	(z = Z-18) approx. new-old
Eav 4p	207266.	212661.	298253.	304493.	-952.30z-485.1
ξ 4p	844.	974.	1217.	1404.	$(-1.4580/z+3.970/z^2)\xi$(old)
Eav 5p	351856.	354102.	489021.	492968.	-1119.50z+2963.8
ξ 5p	345.	384.	490.	565.	$(-2.2268/z+8.583/z^2)\xi$(old)
Eav 6p	415600.	416840.	575273.	578267.	-856.50z+2721.5
ξ 6p	170.	191.	247.	285.	$(-2.0501/z+7.521/z^2)\xi$(old)
Eav 7p	449717.	450510.	623649.	624556.	-114.00z-223.0
ξ 7p	124.	109.	142.	164.	$(-8.0960/z+43.794/z^2)\xi$(old)
Eav 4f	351223.	352718.	472463.	479453.	-5462.16z+25815.7
ξ 4f	3.	3.	6.	6.	no change
Eav 5f	409831.	415105.	567180.	569641.	2812.76z-19337.9
ξ 5f	2.	2.	4.	4.	no change
Eav 6f	447672.	449176.	617771.	619005.	224.88z-2628.6
ξ 6f	1.	1.	2.	2.	no change
Eav 7f	468913.	469745.	648092.	652315.	-3393.67z+16139.0
ξ 7f	1.	1.	1.	1.	no change
Eav 8f	482592.	483098.	667713.	668193.	26.23z-637.5
ξ 8f	0.	0.	1.	1.	no change
Eav 9f	491925.	492248.	681137.	681451.	10.33z-376.1
ξ 9f	9.	0.	1.	1.	no change
Eav 10f	498572.	498787.	690664.	690924.	-46.53z+18.0
ξ 10f	9.	0.	1.	1.	no change
Eav 6h	450253.	450327.	621170.	621284.	-39.88z+125.2
ξ 6h	0.	0.	0.	0.	no change
Eav 7h	470494.	470546.	650318.	650399.	-29.36z+94.9
ξ 7h	0.	0.	0.	0.	no change
Eav $3p^5 3d^2$	338614.	350849.	378710.	390514.	438.81z-14427.3
F^2(3d3d)	91146.	91359.	111345.	103733.	3679.
F^4(3d3d)	43814.	57685.	50828.	65733.	-14473.
ξ 3p	5062.	5061.	6613.	6426.	$(.6663/z-2.923/z^2)\xi$(old)
ξ 3d	306.	322.	382.	466.	$(-5.2715/z+25.201/z^2)\xi$(old)
F^2(3p3d)	83464.	95189.	99841.	105385.	-8619.
G^1(3p3d)	94477.	117200.	107438.	128426.	-21860.
G^3(3p3d)	48579.	72269.	66867.	79905.	-18406.
Eav $3p^5 3d4s$	486431.	493848.	603883.	611357.	-69.19z-7082.7
ξ 3p	4919.	5216.	4906.	6720.	$(-.9854/z-0./z^2)\xi$(old)
ξ 3d	356.	361.	219.	514.	$(-.9863/z-0./z^2)\xi$(old)
F^2(3p3d)	85528.	99383.	92520.	109168.	-15285.

Table (5.13a)

Least Squares Corrections to Parameters: Odd Parity Configurations

Parameter	V^{4+} new	V^{4+} old	Cr^{5+} new	Cr^{5+} old	(z = Z-18) approx. new-old
$G^1(3p\,3d)$	109293.	121400.	116678.	131878.	-14076.
$G^3(3p\,3d)$	67951.	75478.	73142.	82671.	-8793.
$G^1(3p\,4s)$	9648.	9853.	13087.	11242.	1033.
$G^2(3d\,4s)$	12546.	11917.	5973.	12755.	-3415.
$R^1(3p\,4p\,3d\,3d)$	1003.	9732.	4937.	12952.	-8372.
$R^3(3p\,4p\,3d\,3d)$	1032.	10014.	4707.	12349.	-8312.
$R^1(3p\,4p\,3d\,4s)$	4829.	46866.	20247.	53118.	-37454.
$R^1(3p\,4p\,4s\,3d)$	958.	9297.	5308.	10554.	-6792.
$R^1(3p\,5p\,3d\,3d)$	517.	5019.	2490.	6532.	-4272.
$R^3(3p\,5p\,3d\,3d)$	494.	4797.	1609.	5893.	-4293.
$R^1(3p\,5p\,3d\,4s)$	1976.	19179.	8091.	21228.	-15170.
$R^1(3p\,5p\,4s\,3d)$	541.	5246.	2279.	5978.	-4203.
$R^1(3p\,6p\,3d\,3d)$	331.	3215.	1585.	4159.	-2728.
$R^3(3p\,6p\,3d\,3d)$	307.	2979.	1392.	3653.	-2466.
$R^1(3p\,6p\,3d\,4s)$	1206.	11704.	4905.	12868.	-9230.
$R^1(3p\,6p\,4s\,3d)$	363.	3520.	1532.	4020.	-2822.
$R^1(3p\,7p\,3d\,3d)$	237.	2303.	1133.	2973.	-1953.
$R^3(3p\,7p\,3d\,3d)$	216.	2098.	980.	2571.	-1736.
$R^1(3p\,7p\,3d\,4s)$	848.	8234.	3441.	9027.	-6486.
$R^1(3p\,7p\,4s\,3d)$	267.	2589.	1129.	2962.	-2078.
$R^1(3p\,4f\,3d\,3d)$	-23223.	-26440.	-31478.	-35684.	3711.
$R^3(3p\,4f\,3d\,3d)$	-12020.	-13685.	-16867.	-19121.	1959.
$R^3(3p\,4f\,3d\,4s)$	6792.	7733.	8305.	9415.	-1025.
$R^1(3p\,4f\,4s\,3d)$	1197.	1363.	874.	991.	-141.
$R^1(3p\,5f\,3d\,3d)$	-19266.	-21935.	-25146.	-28505.	3014.
$R^3(3p\,5f\,3d\,3d)$	-10388.	-11827.	-14042.	-15918.	1658.
$R^3(3p\,5f\,3d\,4s)$	4550.	5180.	4858.	5507.	-640.
$R^1(3p\,5f\,4s\,3d)$	619.	705.	109.	123.	-50.
$R^1(3p\,6f\,3d\,3d)$	-15199.	-17305.	-19405.	-21997.	2349.
$R^3(3p\,6f\,3d\,3d)$	-8356.	-9514.	-11048.	-12524.	1317.
$R^3(3p\,6f\,3d\,4s)$	3149.	3585.	3060.	3469.	-423.
$R^1(3p\,6f\,4s\,3d)$	328.	374.	-160.	-182.	-12.
$R^1(3p\,7f\,3d\,3d)$	-12178.	-13865.	-15373.	-17427.	1871.
$R^3(3p\,7f\,3d\,3d)$	-6769.	-7706.	-8847.	-10029.	1060.
$R^3(3p\,7f\,3d\,4s)$	2318.	2639.	2112.	2394.	-302.
$R^1(3p\,7f\,4s\,3d)$	186.	212.	-241.	-273.	3.
$R^1(3p\,8f\,3d\,3d)$	-9987.	-11370.	-12531.	-14206.	1529.

Table (5.13a)

Least Squares Corrections to Parameters: Odd Parity Configurations

Parameter	V^{4+} new	V^{4+} old	Cr^{5+} new	Cr^{5+} old	(z = Z-18) approx. new-old
R^3(3p8f3d3d)	-5588.	-6362.	-7259.	-8229.	872.
R^3(3p8f3d4s)	1794.	2042.	1562.	1770.	-229.
R^1(3p8f4s3d)	113.	128.	-255.	-290.	9.
R^1(3p9f3d3d)	-8365.	-9524.	-10477.	-11858.	1270.
R^3(3p9f3d3d)	-4701.	-5353.	-6085.	-6898.	732.
R^3(3p9f3d4s)	1442.	1642.	1214.	1377.	-181.
R^1(3p9f4s3d)	71.	81.	-246.	-279.	12.
R^1(3p10f3d3d)	-7133.	-8121.	-8901.	-10090.	1089.
R^3(3p10f3d3d)	-4021.	-4579.	-5193.	-5887.	625.
R^3(3p10f3d4s)	1193.	1359.	980.	1111.	-148.
R^1(3p10f4s3d)	47.	54.	-230.	-260.	12.
R^3(3p6h3d3d)	-103.	-194.	-118.	-309.	141.
R^3(3p7h3d3d)	-118.	-222.	-135.	-354.	161.
R^2(3p3d3p4s)	3520.	6624.	3511.	9212.	-4403.
R^1(3p3d4s3p)	5725.	10774.	4935.	12947.	-6530.
R^2(3d3d3d4s)	2717.	5112.	3500.	9182.	-4039.

Table (5.13b)

Least Squares Corrections to Parameters: Even Parity Configurations

Parameter	V^{4+} new	V^{4+} old	Cr^{5+} new	Cr^{5+} old	(z = Z-18) approx. new-old
Eav 3d	391.	9743.	796.	9979.	277.05z-12420.8+8215./z
ξ 3d	250.	322.	376.	469.	$(-1.5853/z+2.362/z^2)\xi$(old)
Eav 4d	294020.	299880.	403300.	410187.	-1273.50z+671.8
ξ 4d	58.	66.	89.	105.	$(-2.2479/z+8.260/z^2)\xi$(old)
Eav 5d	388034.	390904.	534693.	538177.	-713.00z+761.0
ξ 5d	27.	30.	42.	48.	$(-1.4338/z+4.168/z^2)\xi$(old)
Eav 6d	434338.	435967.	599824.	601924.	-471.00z+726.0
ξ 6d	15.	16.	21.	26.	$(-4.8911/z+22.198/z^2)\xi$(old)
Eav 7d	460721.	461734.	637582.	638504.	-20.58z+126.9
ξ 7d	9.	10.	12.	16.	$(-5.4588/z+25.604/z^2)\xi$(old)
Eav 4s	148197.	154487.	228717.	234916.	-794.10-2227.1
Eav 5s	328226.	330659.	461355.	464152.	-409.50z-355.2
Eav 6s	403862.	405054.	562118.	563554.	-253.00z+79.0
Eav 7s	443081.	443759.	615204.	616046.	-151.10z+81.1
Eav 8s	466072.	466496.	646647.	647183.	-96.40z+62.4
Eav 5g	416366.	416758.	572280.	572913.	-172.60z+437.2
ξ 5g	0.	0.	1.	1.	no change
Eav 6g	450030.	450294.	620706.	621208.	-138.10z+373.7
ξ 6g	0.	0.	0.	0.	no change
Eav 7g	470339.	470520.	650078.	650343.	-60.00z+127.0
ξ 7g	0.	0.	0.	0.	no change
Eav 7i	470533.	470546.	650401.	650401.	no change
ξ 7i	0.	0.	0.	0.	no change
Eav 8i	483661.	483668.	669298.	669298.	no change
ξ 8i	0.	0.	0.	0.	no change
Eav $3p^5 3d4p$	545165.	552594.	673957.	681456.	-69.70z-7080.3
ξ 3p	4194.	5224.	5623.	6728.	$(-.9836/z-.010/z^2)\xi$(old)
ξ 3d	291.	362.	431.	516.	$(-.9827/z-.012/z^2)\xi$(old)
ξ 4p	788.	981.	1178.	1409.	$(-.9820/z-.019/z^2)\xi$(old)
$F^2(3p3d)$	85785.	99588.	92492.	109316.	-15313.
$F^2(3p4p)$	26337.	26337.	30860.	30860.	no change
$F^2(3d4p)$	27420.	27420.	31361.	31361.	no change
$G^1(3p3d)$	109640.	121606.	115792.	132017.	-14095.
$G^3(3p3d)$	68198.	75641.	72611.	82786.	-8809.
$G^0(3p4p)$	8021.	8021.	9213.	9213.	no change
$G^2(3p4p)$	8844.	8844.	10349.	10349.	no change
$G^1(3d4p)$	9671.	9671.	10882.	10882.	no change
$G^3(3d4p)$	9273.	9273.	10554.	10554.	no change

Table (5.13b)

Least Squares Corrections to Parameters: Even Parity Configurations

Parameter	V^{4+} new	V^{4+} old	Cr^{5+} new	Cr^{5+} old	(z = Z-18) approx. new-old
R^0(3p3p3p4p)	379.	3756.	1557.	4085.	-2952.
R^2(3p3p3p4p)	1743.	17257.	7149.	18755.	-13560.
R^1(3p3d3d4p)	1030.	10195.	5201.	13644.	-8804.
R^3(3p3d3d4p)	1052.	10419.	4896.	12843.	-8657.
R^0(3p3d4p3d)	123.	1220.	589.	1544.	-1026.
R^2(3p3d4p3d)	1532.	15169.	6806.	17854.	-12342.
R^1(3p4d3d4p)	3743.	37055.	16871.	44259.	-30350.
R^3(3p4d3d4p)	1406.	13923.	6516.	17094.	-11547.
R^0(3p4d4p3d)	870.	8610.	3758.	9858.	-6920.
R^2(3p4d4p3d)	870.	8615.	3914.	10269.	-7050.
R^1(3p5d3d4p)	1912.	18934.	8082.	21201.	-15070.
R^3(3p5d3d4p)	878.	8688.	3900.	10231.	-7071.
R^0(3p5d4p3d)	534.	5282.	2270.	5956.	-4217.
R^2(3p5d4p3d)	563.	5576.	2477.	6498.	-4517.
R^1(3p6d3d4p)	1242.	12300.	5106.	13396.	-9673.
R^3(3p6d3d4p)	612.	6060.	2663.	6986.	-4885.
R^0(3p6d4p3d)	372.	3687.	1571.	4122.	-2932.
R^2(3p6d4p3d)	400.	3965.	1739.	4562.	-3193.
R^1(3p7d3d4p)	898.	8894.	3640.	9548.	-6952.
R^3(3p7d3d4p)	459.	4541.	1973.	5176.	-3643.
R^0(3p7d4p3d)	280.	2770.	1176.	3084.	-2200.
R^2(3p7d4p3d)	304.	3005.	1309.	3435.	-2414.
R^1(3p4s3d4p)	4743.	46961.	20263.	53155.	-37555.
R^2(3p4s4p3d)	925.	9156.	3999.	10491.	-7362.
R^1(3p5s3d4p)	1229.	12166.	5428.	14240.	-9874.
R^2(3p5s4p3d)	470.	4649.	2075.	5443.	-3774.
R^1(3p6s3d4p)	703.	6963.	3120.	8184.	-5662.
R^2(3p6s4p3d)	302.	2993.	1347.	3533.	-2439.
R^1(3p7s3d4p)	481.	4761.	2138.	5608.	-3875.
R^2(3p7s4p3d)	218.	2154.	973.	2554.	-1758.
R^1(3p8s3d4p)	359.	3554.	1598.	4193.	-2895.
R^2(3p8s4p3d)	167.	1652.	749.	1965.	-1351.
R^3(3p5g3d4p)	-214.	-2118.	-1155.	-3030.	1890.
R^2(3p5g4p3d)	-37.	-368.	-192.	-504.	321.
R^3(3p6g3d4p)	-198.	-1965.	-1048.	-2750.	1734.
R^2(3p6g4p3d)	-35.	-349.	-177.	-465.	301.
R^3(3p7g3d4p)	-171.	-1691.	-890.	-2334.	1482.
R^2(3p7g4p3d)	-31.	-303.	-151.	-397.	259.

method used to adjust the CI parameters. Also, because of relativistic effects that become increasingly more important with increasing Z, it would not be reliable to extrapolate any of these corrections beyond the neighboring ions in the sequence.

5.2.3 Extrapolations and Predictions

The old and new parameter values for V^{4+} and Cr^{5+} are presented in table (5.13), along with a function that estimates their differences as a function of z=Z-18. The corrections to the average energies were fit to a linear function of z, as there are only two ions with corrections. To this same order in the 1/Z expansion, the corrections to the Slater integrals are constant, so an average of the corrections to both ions was found for each parameter. The spin-orbit parameters, however, were fit to

$$\overline{\xi}_{n\ell} = \left(1 - \frac{A^{n\ell}}{(Z-18)} - \frac{B^{n\ell}}{(Z-18)^2}\right)\xi_{n\ell}$$

which is an approximate expansion of (5.18b). The $3p^5 3d4s$ spin-orbit parameters, ξ_{3p} and ξ_{3d}, have a somewhat erratic behavior, so the average ratio $\overline{\xi}_{n\ell}/\xi_{n\ell}$ for V^{4+} and Cr^{5+} was used to determine the $A^{n\ell}$ term in these cases, and the $B^{n\ell}$ term was omitted.

Applying these formulas with Z=22, 25, and 26, the corrections were extrapolated to Ti^{3+}, Mn^{6+} and Fe^{7+}. Then the average energies of all identified configurations for these ion were optimized by least squares. In addition, the parameters of the $3p^5 3d4s$ configuration were adjusted for Mn^{6+} and Fe^{7+} with the constraint (5.27b). The corrections to the average energies of the even parity $n\ell$ configurations of Ti^{3+} were

combined with the corrections to V^{4+} and Cr^{5+} and extrapolated to the 7s, 8s, 6d, and 7d configurations of Cr^{5+} and all the even configurations of Mn^{6+} and Fe^{7+}. Similarly, the corrections to the average energies of the np configurations were also extrapolated to Mn^{6+} and Fe^{7+}, and also the 7p configuration of Cr^{5+}. All the extrapolations were again made with the linear approximation, except for the 3d configuration; because of its curvature, the function Δ_c^{3d} was used instead. The nf configurations were too badly perturbed to extrapolate with any confidence, so the predictions for the 6f, 7f, 8f, 9f, and 10f, configurations cannot be taken very seriously. The functions used to extrapolate all the parameters appear in table (5.13).

The old and new parameters for Ti^{3+}, Mn^{6+}, and Fe^{7+} are displayed in table (5.14), while the predicted energy levels and eigenvector compositions for all three ions are presented and compared with the identified levels in tables (5.15) through (5.17). Agreement with the levels belonging to the $3p^5 3d^2$ and $3p^5 3d4s$ configurations of Mn^{6+} and Fe^{7+} was improved, even before any additional optimizations of these configurations. After the additional least squares adjustments, the agreement for the $3p^5 3d4s$ configuration is comparable with V^{4+} and Cr^{5+}. It is hoped that predictions for the spectra of the transition array with these two configurations and the $3p^5 3d4p$ are improved over the initial HXR estimates.

The small discrepancy in the agreement between the observed and calculated average energies of the 3d configuration for Mn^{6+} and Fe^{7+} reflects the accuracy of the extrapolation of ζ_{3d} and also perhaps the accuracy of the experimentally derived ionization energies. The

Table (5.14a)

Optimized and Extrapolated Parameter Corrections: Odd Parity

Parameter	Ti^{3+} new	Ti^{3+} old	Mn^{6+} new	Mn^{6+} old	Fe^{7+} new	Fe^{7+} old
Eav 4p	128493.	132675.	400961.	407690.	514019.	522124.
ζ 4p	559.	633.	1690.	1936.	2274.	2584.
Eav 5p	230838.	232546.	643690.	648563.	814663.	820655.
ζ 5p	240.	245.	679.	793.	919.	1074.
Eav 6p	274867.	275732.	754413.	759335.	955654.	959785.
ζ 6p	115.	120.	348.	404.	476.	553.
Eav 7p	298079.	298578.	818896.	819917.	1035413.	1036548.
ζ 7p	116.	68.	173.	235.	217.	323.
Eav 4f	236897.	238290.	611350.	617630.	759968.	766921.
ζ 4f	1.	1.	11.	11.	19.	19.
Eav 5f	278168.	278073.	738739.	740986.	925684.	928611.
ζ 5f	1.	1.	6.	6.	11.	11.
Eav 6f	298026.	299756.	807094.	808500.	1015957.	1017397.
ζ 6f	0.	0.	4.	4.	6.	6.
Eav 7f	315400.	312835.	848491.	849353.	1069628.	1071017.
ζ 7f	0.	0.	2.	2.	4.	4.
Eav 8f	320790.	321323.	875313.	875848.	1105334.	1105762.
ζ 8f	0.	0.	2.	2.	3.	3.
Eav 9f	326804.	327138.	893598.	893985.	1129234.	1129528.
ζ 9f	0.	0.	1.	1.	2.	2.
Eav 10f	331129.	331298.	906951.	906929.	1146125.	1146479.
ζ 10f	0.	0.	1.	1.	1.	1.
Eav 6h	300169.	300203.	812099.	812282.	1022791.	1022985.
ζ 6h	0.	0.	0.	0.	1.	1.
Eav 7h	313120.	313142.	851771.	851910.	1074605.	1074745.
ζ 7h	0.	0.	0.	0.	0.	0.
Eav $3p^5 3d2$	294293.	310221.	415730.	429505.	454675.	468161.
$F^2(3d3d)$	81789.	78111.	119250.	115572.	130733.	127054.
$F^4(3d3d)$	34599.	49073.	58963.	73436.	66436.	80910.
ζ 3p	3733.	3794.	8452.	8162.	10607.	10223.
ζ 3d	263.	209.	493.	648.	641.	872.
$F^2(3p3d)$	75460.	84079.	106425.	115043.	115735.	124354.
$G^1(3p3d)$	82618.	104478.	118392.	138765.	128356.	148529.
$G^3(3p3d)$	45324.	63730.	69465.	86999.	76334.	93737.
Eav $3p^5 3d4s$	380066.	387425.	731998.	739721.	871404.	878971.
ζ 3p	2995.	3974.	8409.	8162.	10160.	10650.
ζ 3d	181.	240.	205.	648.	345.	943.
$F^2(3p3d)$	73654.	88939.	100879.	118546.	107268.	127651.

Table (5.14a)

Optimized and Extrapolated Parameter Corrections: Odd Parity

Parameter	Ti^{3+} new	Ti^{3+} old	Mn^{6+} new	Mn^{6+} old	Fe^{7+} new	Fe^{7+} old
G^1(3p 3d)	95776.	109852.	128749.	141695.	138287.	151070.
G^3(3p 3d)	58836.	67629.	81373.	89451.	87984.	95954.
G^1(3p 4s)	9416.	8384.	4806.	12577.	5476.	13871.
G^2(3d 4s)	7797.	11213.	17612.	13662.	19481.	14607.
R^1(3p 4p 3d 3d)	-2186.	6186.	7563.	15935.	10370.	18742.
R^3(3p 4p 3d 3d)	-812.	7500.	6241.	14553.	8345.	16657.
R^1(3p 4 3p 3 3d 4s)	2633.	40087.	21551.	59005.	27175.	64629.
R^1(3p 4p 4s 3d)	1164.	7956.	4958.	11751.	6110.	12903.
R^1(3p 5p 3d 3d)	-911.	3361.	3668.	7940.	4999.	9271.
R^3(3p 5p 3d 3d)	-677.	3616.	2635.	6929.	3626.	7919.
R^1(3p 5 3p 3 3d 4s)	1705.	16874.	7933.	23102.	9681.	24851.
R^1(3p 5p 4s 3d)	263.	4465.	2473.	6675.	3144.	7346.
R^1(3p 6p 3d 3d)	-547.	2181.	2310.	5038.	3142.	5870.
R^3(3p 6p 3d 3d)	-215.	2252.	1822.	4289.	2430.	4896.
R^1(3p 6p 3d 4s)	1144.	10374.	4684.	13914.	5645.	14876.
R^1(3p 6p 4s 3d)	165.	2988.	1673.	4495.	2130.	4952.
R^1(3p 7p 3d 3d)	-382.	1570.	1645.	3598.	2235.	4188.
R^3(3p 7p 3d 3d)	-149.	1587.	1280.	3016.	1704.	3441.
R^1(3p 7p 3d 4s)	831.	7317.	3246.	9732.	3884.	10370.
R^1(3p 7p 4s 3d)	115.	2192.	1238.	3316.	1578.	3656.
R^1(3p 4f 3d 3d)	-13988.	-17699.	-41305.	-45017.	-50519.	-54230.
R^3(3p 4f 3d 3d)	-6730.	-8689.	-22763.	-24723.	-28377.	-30336.
R^3(3p 4f 3d 4s)	4688.	5714.	9713.	10739.	10724.	11749.
R^1(3p 4f 4s 3d)	1294.	1435.	234.	375.	-564.	-423.
R^1(3p 5f 3d 3d)	-12181.	-15195.	-31689.	-34703.	-37512.	-40526.
R^3(3p 5f 3d 3d)	-6117.	-7775.	-18219.	-19877.	-22005.	-23663.
R^3(3p 5f 3d 4s)	3651.	4290.	4734.	5374.	4263.	4903.
R^1(3p 5f 4s 3d)	957.	1007.	-701.	-651.	-1599.	-1549.
R^1(3p 6f 3d 3d)	-9944.	-12293.	-23994.	-26343.	-28059.	-30408.
R^3(3p 6f 3d 3d)	-5099.	-6416.	-14066.	-15383.	-16786.	-18103.
R^3(3p 6f 3d 4s)	2786.	3209.	2575.	2997.	1863.	2286.
R^1(3p 6f 4s 3d)	701.	714.	-884.	-872.	-1656.	-1644.
R^1(3p 7f 3d 3d)	-8139.	-10009.	-18853.	-20724.	-21943.	-23813.
R^3(3p 7f 3d 3d)	-4224.	-5283.	-11170.	-12230.	-13265.	-14325.
R^3(3p 7f 3d 4s)	2184.	2486.	1576.	1878.	880.	1182.
R^1(3p 7f 4s 3d)	534.	531.	-856.	-859.	-1503.	-1506.
R^1(3p 8f 3d 3d)	-6763.	-8292.	-15306.	-16835.	-17772.	-19301.

Table (5.14a)

Optimized and Extrapolated Parameter Corrections: Odd Parity

Parameter	Ti^{3+} new	Ti^{3+} old	Mn^{6+} new	Mn^{6+} old	Fe^{7+} new	Fe^{7+} old
R^3(3p8f3d3d)	-3536.	-4408.	-9127.	-9999.	-10812.	-11684.
R^3(3p8f3d4s)	1763.	1991.	1054.	1283.	425.	654.
R^1(3p8f4s3d)	423.	414.	-778.	-787.	-1323.	-1332.
R^1(3p9f3d3d)	-5720.	-6990.	-12756.	-14026.	-14789.	-16059.
R^3(3p9f3d3d)	-3001.	-3733.	-7633.	-8365.	-9029.	-9761.
R^3(3p9f3d4s)	1459.	1640.	753.	934.	195.	376.
R^1(3p9f4s3d)	345.	333.	-694.	-705.	-1159.	-1171.
R^1(3p10f3d3d)	-4898.	-5987.	-10832.	-11921.	-12549.	-13638.
R^3(3p10f3d3d)	-2583.	-3208.	-6505.	-7131.	-7687.	-8312.
R^3(3p10f3d4s)	1233.	1381.	566.	714.	72.	220.
R^1(3p10f4s3d)	288.	276.	-617.	-629.	-1019.	-1031.
R^3(3p6h3d3d)	34.	-107.	-311.	-452.	-479.	-620.
R^3(3p7h3d3d)	39.	-123.	-354.	-515.	-543.	-705.
R^2(3p3d3p4s)	-547.	3856.	7255.	11657.	9585.	13988.
R^1(3p3d4s3p)	1986.	8517.	8512.	15043.	10542.	17073.
R^2(3d3d3d4s)	-3420.	619.	8901.	12940.	12419.	16458.

Table (5.14b)

Optimized and Extrapolated Parameter Corrections: Even Parity

Parameter	Ti^{3+} new	Ti^{3+} old	Mn^{6+} new	Mn^{6+} old	Fe^{7+} new	Fe^{7+} old
Eav 3d	263.	9454.	810.	10118.	1102.	10280.
ξ 3d	155.	206.	538.	654.	740.	882.
Eav 4d	196867.	201207.	523377.	531620.	654566.	664082.
ξ 4d	36.	38.	133.	157.	190.	224.
Eav 5d	258869.	260954.	697261.	702139.	877639.	882582.
ξ 5d	16.	17.	63.	72.	91.	103.
Eav 6d	289207.	290365.	785008.	787579.	989512.	992554.
ξ 6d	11.	9.	29.	39.	41.	55.
Eav 7d	306411.	307117.	835278.	836696.	1054380.	1056018.
ξ 7d	7.	6.	17.	23.	24.	33.
Eav 4s	80410.	85938.	319504.	326688.	421957.	429633.
Eav 5s	212410.	214388.	611040.	614262.	777142.	780783.
Eav 6s	265850.	266780.	739920.	741612.	937410.	938974.
Eav 7s	293003.	293517.	808654.	809660.	1023161.	1024332.
Eav 8s	308713.	309025.	849700.	850348.	1074941.	1075701.
Eav 5g	278514.	278731.	745565.	746395.	935826.	936864.
ξ 5g	0.	0.	1.	1.	2.	2.
Eav 6g	300050.	300193.	811474.	812136.	1021897.	1022738.
ξ 6g	0.	0.	1.	1.	2.	2.
Eav 7g	313038.	313135.	851453.	851801.	1074127.	1074560.
ξ 7g	0.	0.	1.	1.	1.	1.
Eav 7i	313134.	313143.	851913.	851913.	1074745.	1074745.
ξ 7i	0.	0.	0.	0.	0.	0.
Eav 8i	321535.	321542.	877635.	877635.	1108348.	1108349.
ξ 8i	0.	0.	0.	0.	0.	0.
Eav $3p^5 3d4p$	427464.	434480.	813654.	821574.	964319.	971956.
ξ 3p	3000.	3982.	7327.	8527.	9345.	10657.
ξ 3d	182.	242.	608.	708.	828.	944.
ξ 4p	484.	642.	1667.	1940.	2268.	2586.
$F^2(3p3d)$	73928.	89241.	103344.	118657.	112423.	127737.
$F^2(3p4p)$	21597.	21597.	35226.	35226.	39473.	39473.
$F^2(3d4p)$	23331.	23331.	35190.	35190.	38935.	38935.
$G^1(3p3d)$	96086.	110182.	127697.	141792.	137045.	151141.
$G^3(3p3d)$	59067.	67876.	80727.	89536.	87209.	96018.
$G^0(3p4p)$	6756.	6756.	10358.	10358.	11468.	11468.
$G^2(3p4p)$	7252.	7252.	11790.	11790.	13185.	13185.
$G^1(3d4p)$	8463.	8463.	12083.	12083.	13269.	13269.
$G^3(3d4p)$	7966.	7966.	11808.	11808.	13039.	13039.

Table (5.14b)

Optimized and Extrapolated Parameter Corrections: Even Parity

Parameter	Ti^{3+} new	Ti^{3+} old	Mn^{6+} new	Mn^{6+} old	Fe^{7+} new	Fe^{7+} old
R^0(3p3p3p4p)	452.	3404.	1449.	4401.	1756.	4708.
R^2(3p3p3p4p)	2077.	15637.	6616.	20175.	7985.	21544.
R^1(3p3d3d4p)	-2560.	6245.	7964.	16768.	10860.	19664.
R^3(3p3d3d4p)	-905.	7752.	6444.	15101.	8583.	17240.
R^0(3pa3d)	-167.	859.	816.	1842.	1096.	2122.
R^2(3pa3d)	-101.	12242.	8038.	20380.	10451.	22793.
R^1(3p4d3d4p)	-1316.	29034.	20509.	50859.	26659.	57009.
R^3(3p4d3d4p)	-1042.	10505.	8512.	20059.	11311.	22858.
R^0(3p4d4p3d)	389.	7309.	4136.	11057.	5297.	12217.
R^2(3p4d4p3d)	-213.	6836.	4769.	11819.	6239.	13289.
R^1(3p5d3d4p)	891.	15961.	7926.	22997.	9399.	24469.
R^3(3p5d3d4p)	-199.	6872.	4498.	11569.	5683.	12754.
R^0(3p5d4p3d)	335.	4552.	2372.	6589.	2977.	7194.
R^2(3p5d4p3d)	14.	4531.	2814.	7331.	3582.	8099.
R^1(3p6d3d4p)	1034.	10707.	4506.	14179.	5083.	14757.
R^3(3p6d3d4p)	28.	4913.	2870.	7755.	3527.	8412.
R^0(3p6d4p3d)	277.	3210.	1597.	4530.	1989.	4921.
R^2(3p6d4p3d)	77.	3270.	1899.	5093.	2384.	5578.
R^1(3p7d3d4p)	927.	7879.	3025.	9977.	3307.	10259.
R^3(3p7d3d4p)	91.	3734.	2047.	5690.	2474.	6117.
R^0(3p7d4p3d)	227.	2426.	1181.	3380.	1465.	3665.
R^2(3p7d4p3d)	87.	2501.	1401.	3814.	1745.	4159.
R^1(3p4s3d4p)	2729.	40284.	21456.	59011.	27062.	64617.
R^2(3p4s4p3d)	337.	7698.	4371.	11732.	5542.	12903.
R^1(3p5s3d4p)	124.	9999.	6367.	16242.	8310.	18185.
R^2(3p5s4p3d)	29.	3803.	2421.	6195.	3141.	6915.
R^1(3p6s3d4p)	29.	5691.	3701.	9363.	4846.	10508.
R^2(3p6s4p3d)	-16.	2423.	1610.	4048.	2105.	4543.
R^1(3p7s3d4p)	3.	3878.	2550.	6425.	3344.	7219.
R^2(3p7s4p3d)	-25.	1733.	1178.	2936.	1547.	3305.
R^1(3p8s3d4p)	-7.	2888.	1914.	4809.	2512.	5406.
R^2(3p8s4p3d)	-27.	1324.	914.	2265.	1203.	2554.
R^3(3p5g3d4p)	573.	-1317.	-2128.	-4018.	-3164.	-5053.
R^2(3p5g4p3d)	82.	-239.	-321.	-642.	-456.	-777.
R^3(3p6g3d4p)	486.	-1248.	-1832.	-3566.	-2651.	-4385.
R^2(3p6g4p3d)	68.	-233.	-274.	-575.	-374.	-674.
R^3(3p7g3d4p)	393.	-1089.	-1499.	-2981.	-2130.	-3612.
R^2(3p7g4p3d)	54.	-205.	-221.	-480.	-291.	-550.

TABLE (5.15A)

TI3+ ODD LEVELS
CALCULATIONS COMPARED WITH EXPERIMENTAL OBSERVATIONS
EXTRAPOLATED AND OPTIMIZED PARAMETERS
PARENTAGE -- DD(2S+1)L = 3D2(2S+1)L
DD(2S+1)L = 3D2(2S+1)L DS(2S+1)L = (3P5(2P)3D(2D))(2S+1)L

IRREP	CALC	EXP	INCR	J/MU	TOTAL	-- EIGENVECTOR COMPOSITION PCT
2P 1/2	127911.	127921.	-10.3	.5	100.	100. 2P (4P)
2P 3/2	128750.	128740.	10.3	1.5	100.	100. 2P (4P)
2P 1/2	230587.	230609.	-21.9	.5	100.	100. 2P (5P)
2P 3/2	230946.	230924.	21.9	1.5	100.	100. 2P (5P)
2F 5/2	236132.	236135.	-3.3	2.5	99.	99. 2F (4F)
2F 7/2	236146.	236142.	3.4	3.5	99.	99. 2F (4F)
4D 1/2	252379.	---	---	.5	100.	82. 4D (DD(3F)) 18. 4D (DD(3P))
4D 3/2	252781.	---	---	1.5	100.	81. 4D (DD(3F)) 19. 4D (DD(3P))
4D 5/2	253460.	---	---	2.5	99.	79. 4D (DD(3F)) 21. 4D (DD(3P))
4D 7/2	254445.	---	---	3.5	99.	76. 4D (DD(3F)) 23. 4D (DD(3P))
4G11/2	265393.	---	---	5.5	100.	100. 4G (DD(3F))
4G 9/2	266266.	---	---	4.5	97.	97. 4G (DD(3F))
4G 7/2	267226.	---	---	3.5	95.	95. 4G (DD(3F))
4G 5/2	268193.	---	---	2.5	94.	94. 4G (DD(3F))
4P 5/2	272109.	---	---	2.5	99.	99. 4P (DD(3P))
4P 3/2	273422.	---	---	1.5	99.	99. 4P (DD(3P))
4P 1/2	274341.	---	---	.5	99.	99. 4P (DD(3P))
2P 1/2	274744.	274726.	17.7	.5	100.	100. 2P (6P)
4F 3/2	274750.	---	---	1.5	98.	71. 4F (DD(3F)) 21. 2D (DD(1D)) 6. 2D (DD(3F))
4F 5/2	274770.	274840.	-70.3	2.5	89.	34. 4F (DD(3F)) 32. 2D (DD(1D)) 9. 2F (5F) 8. 2D (DD(3F)) 6. 2F (DD(1G))
2P 3/2	274917.	274881.	35.5	1.5	99.	99. 2P (6P)
4F 9/2	275334.	---	---	4.5	95.	95. 4F (DD(3F))
4F 7/2	275559.	---	---	3.5	87.	62. 4F (DD(3F)) 18. 2F (5F) 8. 2F (DD(1G))
2F 5/2	275736.	275847.	-111.2	2.5	92.	43. 2F (5F) 21. 4F (DD(3F)) 18. 2F (DD(1G)) 10. 2F (DD(3F))

TABLE (5.15A) CONTINUED

TI3+ ODD LEVELS
CALCULATIONS COMPARED WITH EXPERIMENTAL OBSERVATIONS
EXTRAPOLATED AND OPTIMIZED PARAMETERS
PARENTAGE -- DD(2S+1)L = 3D2(2S+1)L
DD(2S+1)L = 3D2(2S+1)L DS(2S+1)L = (3P5(2P)3D(2D))(2S+1)L

IRREP	CALC	EXP	INCR	J/MU	TOTAL	-- EIGENVECTOR COMPOSITION PCT
2F 7/2	276095.	275862.	232.7	3.5	95.	49. 2F (5F) 31. 4F (DD(3F)) 9. 2F (DD(1G)) 5. 2F (DD(1D))
2D 5/2	276881.	---	---	2.5	94.	44. 2D (DD(1D)) 41. 4F (DD(3F)) 10. 2D (DD(3F))
2D 3/2	277752.	---	---	1.5	97.	51. 2D (DD(1D)) 28. 4F (DD(3F)) 12. 2D (DD(3F)) 6. 2P (DD(1D))
2F 5/2	279321.	---	---	2.5	98.	44. 2F (5F) 30. 2F (DD(3F)) 23. 2F (DD(1G))
2F 7/2	280211.	---	---	3.5	93.	35. 2F (DD(3F)) 30. 2F (5F) 28. 2F (DD(1G))
2P 1/2	282885.	---	---	.5	99.	68. 2P (DD(1D)) 22. 2P (DD(3P)) 9. 2P (DD(1S))
2P 3/2	284761.	---	---	1.5	97.	57. 2P (DD(1D)) 21. 2P (DD(3P)) 12. 2P (DD(1S)) 7. 2D (DD(1D))
2G 7/2	285922.	---	---	3.5	90.	90. 2G (DD(3F))
2H11/2	287677.	---	---	5.5	100.	100. 2H (DD(1G))
2G 9/2	288012.	---	---	4.5	92.	92. 2G (DD(3F))
2F 7/2	289257.	---	---	3.5	88.	81. 2F (DD(1D)) 6. 2F (DD(3F))
2H 9/2	291545.	---	---	4.5	98.	98. 2H (DD(1G))
2F 5/2	292945.	---	---	2.5	92.	82. 2F (DD(1D)) 10. 2F (6F)
2F 7/2	297828.	---	---	3.5	96.	96. 2F (6F)
2P 1/2	297957.	298000.	-42.7	.5	100.	100. 2P (7P)
2F 5/2	298085.	---	---	2.5	99.	89. 2F (6F) 10. 2F (DD(1D))
2P 3/2	298131.	298088.	42.7	1.5	100.	100. 2P (7P)
2H 9/2	300166.	300159.	6.8	4.5	100.	100. 2H (6H)
2H11/2	300166.	300159.	6.8	5.5	100.	100. 2H (6H)
4D 7/2	300317.	---	---	3.5	99.	76. 4D (DD(3P)) 24. 4D (DD(3F))
4D 5/2	301160.	---	---	2.5	97.	76. 4D (DD(3P)) 21. 4D (DD(3F))
4D 3/2	302074.	---	---	1.5	97.	78. 4D (DD(3P)) 19. 4D (DD(3F))
4D 1/2	302853.	---	---	.5	100.	82. 4D (DD(3P)) 18. 4D (DD(3F))
2D 3/2	310985.	---	---	1.5	94.	86. 2D (DD(3P)) 8. 2D (DD(3F))

TABLE (5.15A) CONTINUED

TI3+ ODD LEVELS
CALCULATIONS COMPARED WITH EXPERIMENTAL OBSERVATIONS
EXTRAPOLATED AND OPTIMIZED PARAMETERS
PARENTAGE -- DD(2S+1)L = 3D2(2S+1)L
DD(2S+1)L = 3D2(2S+1)L DS(2S+1)L = (3P5(2P)3D(2D))(2S+1)L

IRREP	CALC	EXP	INCR	J/MU	TOTAL	-- EIGENVECTOR COMPOSITION PCT
2D 5/2	312555.	---	---	2.5	94.	85. 2D (DD(3P)) 9. 2D (DD(3F))
2H 9/2	313116.	313111.	5.5	4.5	100.	100. 2H (7H)
2H11/2	313116.	313111.	5.5	5.5	100.	100. 2H (7H)
2F 7/2	314932.	---	---	3.5	96.	96. 2F (7F)
2F 5/2	314947.	---	---	2.5	97.	97. 2F (7F)
2G 9/2	315891.	---	---	4.5	95.	95. 2G (DD(1G))
2G 7/2	316434.	---	---	3.5	95.	95. 2G (DD(1G))
4S 3/2	318456.	---	---	1.5	100.	100. 4S (DD(3P))
2S 1/2	318473.	---	---	.5	100.	100. 2S (DD(3P))
2F 5/2	320438.	---	---	2.5	98.	98. 2F (8F)
2F 7/2	320457.	---	---	3.5	98.	98. 2F (8F)
2F 5/2	326489.	---	---	2.5	98.	98. 2F (9F)
2F 7/2	326508.	---	---	3.5	98.	98. 2F (9F)
2P 3/2	330074.	---	---	1.5	99.	78. 2P (DD(1S)) 21. 2P (DD(1D))
2F 5/2	330872.	---	---	2.5	98.	98. 2F (10F)
2F 7/2	330890.	---	---	3.5	98.	98. 2F (10F)
2P 1/2	333992.	---	---	.5	97.	79. 2P (DD(1S)) 18. 2P (DD(1D))
4P 1/2	352560.	---	---	.5	100.	100. 4P (DS(3P))
4P 3/2	353359.	---	---	1.5	99.	99. 4P (DS(3P))
2F 5/2	354408.	---	---	2.5	92.	46. 2F (DD(3F)) 46. 2F (DD(1G))
4P 5/2	354797.	---	---	2.5	99.	99. 4P (DS(3P))
2F 7/2	356525.	---	---	3.5	92.	47. 2F (DD(1G)) 45. 2F (DD(3F))
2P 1/2	359814.	---	---	.5	99.	99. 2P (DS(3P))
2P 3/2	361504.	---	---	1.5	98.	98. 2P (DS(3P))
4F 9/2	363281.	---	---	4.5	100.	100. 4F (DS(3F))
4F 7/2	364356.	---	---	3.5	99.	99. 4F (DS(3F))
4F 5/2	365348.	---	---	2.5	98.	98. 4F (DS(3F))

TABLE (5.15A) CONTINUED

TI3+ ODD LEVELS
CALCULATIONS COMPARED WITH EXPERIMENTAL OBSERVATIONS
EXTRAPOLATED AND OPTIMIZED PARAMETERS
PARENTAGE -- DD(2S+1)L = 3D2(2S+1)L
DD(2S+1)L = 3D2(2S+1)L DS(2S+1)L = (3P5(2P)3D(2D))(2S+1)L

IRREP	CALC	EXP	INCR	J/MU	TOTAL	-- EIGENVECTOR COMPOSITION PCT
4F 3/2	366182.	---	---	1.5	99.	99. 4F (DS(3F))
2F 7/2	370598.	---	---	3.5	97.	97. 2F (DS(3F))
2F 5/2	372754.	---	---	2.5	97.	97. 2F (DS(3F))
2P 1/2	381994.	---	---	.5	100.	74. 2P (DD(3P)) 13. 2P (DD(1D)) 12. 2P (DD(1S))
4D 7/2	383006.	---	---	3.5	95.	95. 4D (DS(3D))
2P 3/2	383072.	---	---	1.5	99.	75. 2P (DD(3P)) 15. 2P (DD(1D)) 10. 2P (DD(1S))
4D 5/2	383503.	---	---	2.5	96.	89. 4D (DS(3D)) 7. 2D (DS(1D))
4D 3/2	383845.	---	---	1.5	98.	90. 4D (DS(3D)) 8. 2D (DS(1D))
4D 1/2	384100.	---	---	.5	100.	100. 4D (DS(3D))
2D 5/2	385130.	---	---	2.5	96.	59. 2D (DD(3F)) 14. 2D (DD(1D)) 14. 2D (DS(3D)) 10. 2D (DD(3P))
2D 3/2	385173.	---	---	1.5	100.	49. 2D (DD(3F)) 19. 2D (DS(1D)) 12. 2D (DD(1D)) 8. 2D (DD(3P)) 7. 2D (DS(3D)) 5. 4D (DS(3D))
2D 5/2	385603.	---	---	2.5	97.	80. 2D (DS(1D)) 11. 2D (DS(3D)) 6. 4D (DS(3D))
2D 3/2	386288.	---	---	1.5	91.	69. 2D (DS(1D)) 11. 2D (DD(3F)) 11. 2D (DS(3D))
2F 5/2	388639.	---	---	2.5	89.	89. 2F (DS(1F))
2F 7/2	389328.	---	---	3.5	93.	93. 2F (DS(1F))
2D 3/2	392159.	---	---	1.5	92.	82. 2D (DS(3D)) 10. 2D (DD(3F))
2D 5/2	392315.	---	---	2.5	96.	73. 2D (DS(3D)) 9. 2D (DD(3F)) 8. 2D (DS(1D)) 6. 2F (DS(1F))
2P 3/2	484197.	---	---	1.5	100.	100. 2P (DS(1P))
2P 1/2	484220.	---	---	.5	100.	100. 2P (DS(1P))

NO. EXPERIMENTAL LEVELS = 17.

ABSOLUTE MEAN DEVIATION = 38.16

RMS DEVIATION = 67.75

TABLE (5.15B)

TI3+ EVENLEVELS
CALCULATIONS COMPARED WITH EXPERIMENTAL OBSERVATIONS
EXTRAPOLATED AND OPTIMIZED PARAMETERS
PARENTAGE -- DD(2S+1)L = 3D2(2S+1)L
DD(2S+1)L = 3D2(2S+1)L DS(2S+1)L = (3P5(2P)3D(2D))(2S+1)L

IRREP	CALC	EXP	INCR	J/MU	TOTAL	-- EIGENVECTOR COMPOSITION PCT
2D 3/2	-2.	0.	-2.2	1.5	100.	100. 2D (3D)
2D 5/2	384.	382.	2.2	2.5	100.	100. 2D (3D)
2S 1/2	80389.	80389.	0.	.5	100.	100. 2S (4S)
2D 3/2	196802.	196804.	-2.0	1.5	100.	100. 2D (4D)
2D 5/2	196892.	196890.	2.0	2.5	100.	100. 2D (4D)
2S 1/2	212407.	212407.	0.	.5	100.	100. 2S (5S)
2D 3/2	258838.	258838.	-.3	1.5	100.	100. 2D (5D)
2D 5/2	258877.	258877.	.3	2.5	100.	100. 2D (5D)
2S 1/2	265847.	265847.	0.	.5	100.	100. 2S (6S)
2G 7/2	278511.	278511.	.1	3.5	100.	100. 2G (5G)
2G 9/2	278511.	278511.	-.1	4.5	100.	100. 2G (5G)
2D 3/2	289183.	289186.	-3.2	1.5	100.	100. 2D (6D)
2D 5/2	289210.	289207.	3.2	2.5	100.	100. 2D (6D)
2S 1/2	293000.	293000.	0.	.5	100.	100. 2S (7S)
2G 7/2	300046.	300046.	-.1	3.5	100.	100. 2G (6G)
2G 9/2	300046.	300046.	.1	4.5	100.	100. 2G (6G)
2D 3/2	306393.	306396.	-2.4	1.5	100.	100. 2D (7D)
2D 5/2	306411.	306408.	2.4	2.5	100.	100. 2D (7D)
2S 1/2	308710.	308710.	0.	.5	100.	100. 2S (8S)
2G 7/2	313034.	313034.	-.1	3.5	100.	100. 2G (7G)
2G 9/2	313034.	313034.	.1	4.5	100.	100. 2G (7G)
2I11/2	313131.	313131.	0.	5.5	100.	100. 2I (7I)
2I11/2	321531.	321531.	0.	5.5	100.	100. 2I (8I)
4D 1/2	397455.	---	---	.5	97.	90. 4D (DP(3P)) 7. 4D (DP(3F))
4D 3/2	397970.	---	---	1.5	97.	89. 4D (DP(3P)) 8. 4D (DP(3F))
4D 5/2	398790.	---	---	2.5	98.	88. 4D (DP(3P)) 10. 4D (DP(3F))
4D 7/2	399909.	---	---	3.5	99.	85. 4D (DP(3P)) 14. 4D (DP(3F))

TABLE (5.15B) CONTINUED

TI3+ EVENLEVELS
CALCULATIONS COMPARED WITH EXPERIMENTAL OBSERVATIONS
EXTRAPOLATED AND OPTIMIZED PARAMETERS
PARENTAGE -- DD(2S+1)L = 3D2(2S+1)L
DD(2S+1)L = 3D2(2S+1)L DS(2S+1)L = (3P5(2P)3D(2D))(2S+1)L

IRREP	CALC	EXP	INCR	J/MU	TOTAL	-- EIGENVECTOR COMPOSITION PCT
4P 1/2	400142.	---	---	.5	99.	99. 4P (DP(3P))
4P 3/2	400602.	---	---	1.5	93.	93. 4P (DP(3P))
4P 5/2	401615.	---	---	2.5	97.	97. 4P (DP(3P))
2P 1/2	401844.	---	---	.5	96.	96. 2P (DP(3P))
2P 3/2	402549.	---	---	1.5	91.	84. 2P (DP(3P)) 7. 4S (DP(3P))
4S 3/2	404369.	---	---	1.5	96.	89. 4S (DP(3P)) 7. 2P (DP(3P))
2D 3/2	407821.	---	---	1.5	87.	87. 2D (DP(3P))
2D 5/2	408159.	---	---	2.5	95.	83. 2D (DP(3P)) 6. 2D (DP(3F)) 6. 2D (DP(3D))
4G11/2	409504.	---	---	5.5	100.	100. 4G (DP(3F))
4G 9/2	410050.	---	---	4.5	98.	86. 4G (DP(3F)) 12. 4F (DP(3F))
4D 7/2	410345.	---	---	3.5	94.	32. 4D (DP(3F)) 31. 4F (DP(3F)) 16. 2F (DP(3F)) 8. 4G (DP(3F)) 7. 4D (DP(3P))
2S 1/2	410752.	---	---	.5	98.	98. 2S (DP(3P))
2F 7/2	410800.	---	---	3.5	93.	68. 2F (DP(3F)) 16. 4G (DP(3F)) 9. 4D (DP(3F))
4G 7/2	410979.	---	---	3.5	88.	71. 4G (DP(3F)) 17. 4D (DP(3F))
4F 9/2	411133.	---	---	4.5	97.	85. 4F (DP(3F)) 12. 4G (DP(3F))
4D 5/2	411294.	---	---	2.5	97.	45. 4D (DP(3F)) 27. 4F (DP(3F)) 11. 4G (DP(3F)) 8. 4D (DP(3D)) 7. 4D (DP(3P))
4G 5/2	411766.	---	---	2.5	96.	87. 4G (DP(3F)) 9. 4D (DP(3F))
4D 3/2	412257.	---	---	1.5	98.	59. 4D (DP(3F)) 20. 4F (DP(3F)) 11. 4D (DP(3D)) 8. 4D (DP(3P))
2F 5/2	412797.	---	---	2.5	92.	66. 2F (DP(3F)) 19. 4F (DP(3F)) 8. 4D (DP(3F))
4F 7/2	412856.	---	---	3.5	90.	66. 4F (DP(3F)) 17. 4D (DP(3F)) 7. 2F (DP(3F))
4D 1/2	413070.	---	---	.5	99.	76. 4D (DP(3F)) 14. 4D (DP(3D)) 9. 4D (DP(3P))
4F 5/2	413979.	---	---	2.5	91.	49. 4F (DP(3F)) 27. 2F (DP(3F)) 15. 4D (DP(3F))

TABLE (5.15B) CONTINUED

TI3+ EVENLEVELS
CALCULATIONS COMPARED WITH EXPERIMENTAL OBSERVATIONS
EXTRAPOLATED AND OPTIMIZED PARAMETERS
PARENTAGE -- DD(2S+1)L = 3D2(2S+1)L
DD(2S+1)L = 3D2(2S+1)L DS(2S+1)L = (3P5(2P)3D(2D))(2S+1)L

IRREP	CALC	EXP	INCR	J/MU	TOTAL	-- EIGENVECTOR COMPOSITION PCT
4F 3/2	414102.	---	---	1.5	93.	76. 4F (DP(3F)) 17. 4D (DP(3F))
2G 9/2	417529.	---	---	4.5	98.	98. 2G (DP(3F))
2G 7/2	419126.	---	---	3.5	95.	95. 2G (DP(3F))
2D 5/2	419914.	---	---	2.5	88.	37. 2D (DP(1D)) 35. 2D (DP(3F)) 17. 2D (DP(1F))
2D 3/2	420554.	---	---	1.5	95.	46. 2D (DP(1D)) 31. 2D (DP(3F)) 13. 2D (DP(1F)) 5. 2D (DP(3D))
4D 7/2	428487.	---	---	3.5	92.	82. 4D (DP(3D)) 10. 4D (DP(3F))
4D 5/2	428995.	---	---	2.5	81.	72. 4D (DP(3D)) 10. 4D (DP(3F))
4D 3/2	429674.	---	---	1.5	90.	78. 4D (DP(3D)) 12. 4D (DP(3F))
4D 1/2	430184.	---	---	.5	99.	84. 4D (DP(3D)) 15. 4D (DP(3F))
2F 5/2	430203.	---	---	2.5	97.	32. 2F (DP(1D)) 20. 2D (DP(3F)) 20. 2D (DP(3D)) 12. 2F (DP(1F)) 7. 4F (DP(3D)) 6. 2D (DP(1D))
2F 5/2	430580.	---	---	2.5	89.	25. 2F (DP(1D)) 19. 2D (DP(3D)) 18. 2D (DP(3F)) 16. 2F (DP(1F)) 12. 4D (DP(3D))
2F 7/2	431073.	---	---	3.5	93.	39. 2F (DP(1D)) 31. 4F (DP(3D)) 17. 2F (DP(1F)) 6. 4D (DP(3D))
4F 9/2	431297.	---	---	4.5	97.	88. 4F (DP(3D)) 9. 2G (DP(1F))
4F 3/2	431612.	---	---	1.5	95.	69. 4F (DP(3D)) 14. 2D (DP(3F)) 12. 2D (DP(3D))
4F 5/2	431961.	---	---	2.5	91.	85. 4F (DP(3D)) 6. 2F (DP(1F))
4F 7/2	431987.	---	---	3.5	94.	55. 4F (DP(3D)) 21. 2F (DP(1F)) 18. 2F (DP(1D))
2D 3/2	431995.	---	---	1.5	90.	33. 2D (DP(3D)) 26. 4F (DP(3D)) 25. 2D (DP(3F)) 7. 4D (DP(3D))
2G 7/2	434672.	---	---	3.5	90.	59. 2G (DP(1F)) 23. 2F (DP(3D)) 8. 4F (DP(3D))
2F 5/2	434972.	---	---	2.5	96.	42. 2F (DP(1F)) 36. 2F (DP(3D)) 18. 2F (DP(1D))
2G 9/2	435663.	---	---	4.5	99.	90. 2G (DP(1F)) 9. 4F (DP(3D))
2G 7/2	435695.	---	---	3.5	97.	30. 2G (DP(1F)) 28. 2F (DP(1F)) 21. 2F (DP(1D)) 19. 2F (DP(3D))

TABLE (5.15B) CONTINUED

TI3+ EVENLEVELS
CALCULATIONS COMPARED WITH EXPERIMENTAL OBSERVATIONS
EXTRAPOLATED AND OPTIMIZED PARAMETERS
PARENTAGE -- DD(2S+1)L = 3D2(2S+1)L
DD(2S+1)L = 3D2(2S+1)L DS(2S+1)L = (3P5(2P)3D(2D))(2S+1)L

IRREP	CALC	EXP	INCR	J/MU	TOTAL	-- EIGENVECTOR COMPOSITION PCT
4P 5/2	435922.	---	---	2.5	93.	93. 4P (DP(3D))
4P 3/2	436209.	---	---	1.5	93.	62. 4P (DP(3D)) 31. 2P (DP(1D))
2P 1/2	436549.	---	---	.5	99.	49. 2P (DP(1D)) 40. 4P (DP(3D)) 10. 2P (DP(3D))
4P 1/2	437243.	---	---	.5	100.	60. 4P (DP(3D)) 30. 2P (DP(1D)) 10. 2P (DP(3D))
2P 3/2	437493.	---	---	1.5	99.	54. 2P (DP(1D)) 36. 4P (DP(3D)) 8. 2P (DP(3D))
2D 3/2	438465.	---	---	1 -	93.	35. 2D (DP(1D)) 33. 2D (DP(1F)) 17. 2P (DP(3D)) 7. 2P (DP(1D))
2D 5/2	438691.	---	---	2.5	91.	44. 2D (DP(1F)) 38. 2D (DP(1D)) 9. 2D (DP(3D))
2F 7/2	440283.	---	---	3.5	93.	52. 2F (DP(3D)) 24. 2F (DP(1F)) 17. 2F (DP(1D))
2P 3/2	440538.	---	---	1.5	94.	69. 2P (DP(3D)) 10. 2D (DP(1F)) 8. 2D (DP(1D)) 6. 2P (DP(1D))
2F 5/2	440597.	---	---	2.5	96.	58. 2F (DP(3D)) 20. 2F (DP(1F)) 18. 2F (DP(1D))
2P 1/2	441311.	---	---	.5	98.	77. 2P (DP(3D)) 20. 2P (DP(1D))
2D 3/2	453764.	---	---	1.5	99.	40. 2D (DP(3D)) 33. 2D (DP(1F)) 14. 2D (DP(3F)) 7. 2D (DP(1D)) 6. 2D (DP(3P))
2D 5/2	454672.	---	---	2.5	99.	38. 2D (DP(3D)) 32. 2D (DP(1F)) 16. 2D (DP(3F)) 7. 2D (DP(3P)) 7. 2D (DP(1D))
2P 1/2	529776.	---	---	.5	99.	99. 2P (DP(1P))
2P 3/2	530113.	---	---	1.5	99.	99. 2P (DP(1P))
2D 3/2	532686.	---	---	1.5	98.	98. 2D (DP(1P))
2D 5/2	533175.	---	---	2.5	99.	99. 2D (DP(1P))
2S 1/2	534598.	---	---	.5	99.	99. 2S (DP(1P))

NO. EXPERIMENTAL LEVELS = 23.

ABSOLUTE MEAN DEVIATION = .91

RMS DEVIATION = 1.48

TABLE (5.16A)

MN6+ ODD LEVELS
CALCULATIONS COMPARED WITH EXPERIMENTAL OBSERVATIONS
EXTRAPOLATED AND OPTIMIZED PARAMETERS
PARENTAGE -- DD(2S+1)L = 3D2(2S+1)L
DD(2S+1)L = 3D2(2S+1)L DS(2S+1)L = (3P5(2P)3D(2D))(2S+1)L

IRREP	CALC	EXP	INCR	J/MU	TOTAL	-- EIGENVECTOR COMPOSITION PCT
4D 1/2	354226.	---	---	.5	100.	83. 4D (DD(3F)) 17. 4D (DD(3P))
4D 3/2	355013.	---	---	1.5	99.	81. 4D (DD(3F)) 18. 4D (DD(3P))
4D 5/2	356354.	---	---	2.5	98.	78. 4D (DD(3F)) 20. 4D (DD(3P))
4D 7/2	358365.	---	---	3.5	98.	73. 4D (DD(3F)) 24. 4D (DD(3P))
4G11/2	372437.	---	---	5.5	100.	100. 4G (DD(3F))
4G 9/2	374154.	---	---	4.5	99.	93. 4G (DD(3F)) 5. 4F (DD(3F))
4G 7/2	376202.	---	---	3.5	97.	89. 4G (DD(3F)) 8. 4F (DD(3F))
4G 5/2	378330.	---	---	2.5	92.	84. 4G (DD(3F)) 9. 4F (DD(3F))
4P 5/2	381838.	---	---	2.5	98.	98. 4P (DD(3P))
4P 3/2	384692.	---	---	1.5	97.	97. 4P (DD(3P))
4F 3/2	386641.	---	---	1.5	97.	70. 4F (DD(3F)) 20. 2D (DD(1D)) 7. 2D (DD(3F))
4P 1/2	386789.	---	---	.5	98.	98. 4P (DD(3P))
4F 5/2	387452.	---	---	2.5	97.	41. 4F (DD(3F)) 38. 2D (DD(1D)) 11. 2D (DD(3F)) 8. 4G (DD(3F))
4F 9/2	387505.	---	---	4.5	96.	91. 4F (DD(3F)) 5. 2G (DD(3F))
4F 7/2	388755.	---	---	3.5	90.	83. 4F (DD(3F)) 7. 4G (DD(3F))
4F 5/2	391357.	---	---	2.5	86.	48. 4F (DD(3F)) 32. 2D (DD(1D)) 7. 2D (DD(3F))
2F 5/2	392109.	---	---	2.5	96.	44. 2F (DD(1G)) 38. 2F (DD(3F)) 7. 4G (DD(3F)) 7. 2D (DD(1D))
2D 3/2	392913.	---	---	1.5	93.	44. 2D (DD(1D)) 28. 4F (DD(3F)) 11. 2P (DD(1D)) 10. 2D (DD(3F))
2F 7/2	394672.	---	---	3.5	95.	42. 2F (DD(1G)) 38. 2F (DD(3F)) 10. 2F (DD(1D)) 5. 4F (DD(3F))
2P 1/2	397152.	397650.	-498.1	.5	96.	65. 2P (4P) 25. 2P (DD(1D)) 6. 2P (DD(3P))
2F 3/2	400501.	400120.	380.5	1.5	90.	84. 2P (4P) 6. 2P (DD(1D))
2P 1/2	401406.	---	---	.5	95.	44. 2P (DD(1D)) 35. 2P (4P) 15. 2P (DD(3P))
2G 7/2	404709.	---	---	3.5	92.	71. 2G (DD(3F)) 21. 2F (DD(1D))

TABLE (5.16A) CONTINUED

MN6+ ODD LEVELS
CALCULATIONS COMPARED WITH EXPERIMENTAL OBSERVATIONS
EXTRAPOLATED AND OPTIMIZED PARAMETERS
PARENTAGE -- DD(2S+1)L = 3D2(2S+1)L
DD(2S+1)L = 3D2(2S+1)L DS(2S+1)L = (3P5(2P)3D(2D))(2S+1)L

IRREP	CALC	EXP	INCR	J/MU	TOTAL	-- EIGENVECTOR COMPOSITION PCT
2H11/2	405890.	---	---	5.5	100.	100. 2H (DD(1G))
2P 3/2	405920.	---	---	1.5	95.	45. 2P (DD(1D)) 18. 2P (DD(3P)) 14. 2P (4P) 10. 2D (DD(1D)) 8. 2P (DD(1S))
2F 7/2	407819.	---	---	3.5	98.	67. 2F (DD(1D)) 17. 2G (DD(3F)) 8. 2F (DD(3F)) 5. 2F (DD(1G))
2G 9/2	409388.	---	---	4.5	91.	85. 2G (DD(3F)) 6. 2G (DD(1G))
2H 9/2	414349.	---	---	4.5	94.	94. 2H (DD(1G))
2F 5/2	416950.	---	---	2.5	93.	93. 2F (DD(1D))
4D 7/2	422046.	---	---	3.5	98.	73. 4D (DD(3P)) 26. 4D (DD(3F))
4D 5/2	423637.	---	---	2.5	99.	73. 4D (DD(3P)) 21. 4D (DD(3F)) 5. 2D (DD(3P))
4D 3/2	425711.	---	---	1.5	99.	75. 4D (DD(3P)) 17. 4D (DD(3F)) 6. 2D (DD(3P))
4D 1/2	427831.	---	---	.5	99.	83. 4D (DD(3P)) 16. 4D (DD(3F))
2D 3/2	439219.	---	---	1.5	95.	82. 2D (DD(3P)) 7. 2D (DD(3F)) 6. 4D (DD(3P))
2D 5/2	442715.	---	---	2.5	90.	82. 2D (DD(3P)) 8. 2D (DD(3F))
2G 9/2	447104.	---	---	4.5	92.	92. 2G (DD(1G))
2G 7/2	447798.	---	---	3.5	95.	95. 2G (DD(1G))
4S 3/2	448373.	---	---	1.5	99.	99. 4S (DD(3P))
2S 1/2	448452.	---	---	.5	99.	99. 2S (DD(3P))
2P 3/2	468545.	---	---	1.5	98.	78. 2P (DD(1S)) 20. 2P (DD(1D))
2P 1/2	477527.	---	---	.5	95.	79. 2P (DD(1S)) 16. 2P (DD(1D))
2F 5/2	489817.	489880.	-62.9	2.5	95.	50. 2F (DD(3F)) 45. 2F (DD(1G))
2F 7/2	494645.	494300.	345.4	3.5	94.	47. 2F (DD(1G)) 47. 2F (DD(3F))
2P 1/2	541046.	---	---	.5	99.	73. 2P (DD(3P)) 14. 2P (DD(1S)) 13. 2P (DD(1D))
2P 3/2	543160.	---	---	1.5	99.	75. 2P (DD(3P)) 15. 2P (DD(1D)) 10. 2P (DD(1S))
2D 5/2	547212.	547370.	-158.3	2.5	100.	70. 2D (DD(3F)) 17. 2D (DD(1D)) 12. 2D (DD(3P))

TABLE (5.16A) CONTINUED

MN6+ ODD LEVELS
CALCULATIONS COMPARED WITH EXPERIMENTAL OBSERVATIONS
EXTRAPOLATED AND OPTIMIZED PARAMETERS
PARENTAGE -- DD(2S+1)L = 3D2(2S+1)L
DD(2S+1)L = 3D2(2S+1)L DS(2S+1)L = (3P5(2P)3D(2D))(2S+1)L

IRREP	CALC	EXP	INCR	J/MU	TOTAL	-- EIGENVECTOR COMPOSITION PCT
2D 3/2	547935.	547930.	5.4	1.5	100.	71. 2D (DD(3F)) 18. 2D (DD(1D)) 11. 2D (DD(3P))
2F 5/2	615914.	615960.	-46.0	2.5	96.	96. 2F (4F)
2F 7/2	616136.	616100.	36.2	3.5	96.	96. 2F (4F)
2P 1/2	642961.	---	---	.5	100.	100. 2P (5P)
2P 3/2	643985.	---	---	1.5	100.	100. 2P (5P)
4P 1/2	693227.	---	---	.5	99.	99. 4P (DS(3P))
4P 3/2	695053.	693420.	-1367.1	1.5	97.	97. 4P (DS(3P))
4P 5/2	698506.	---	---	2.5	98.	98. 4P (DS(3P))
2P 1/2	701987.	700870.	1116.8	.5	98.	98. 2P (DS(3P))
2P 3/2	705897.	705170.	726.8	1.5	96.	96. 2P (DS(3P))
4F 9/2	707599.	---	---	4.5	100.	100. 4F (DS(3F))
4F 7/2	710064.	709720.	343.5	3.5	98.	90. 4F (DS(3F)) 8. 2F (DS(3F))
4F 5/2	712861.	712350.	511.4	2.5	96.	89. 4F (DS(3F)) 6. 2F (DS(3F))
4F 3/2	715702.	---	---	1.5	95.	95. 4F (DS(3F))
2F 7/2	716984.	717430.	-445.8	3.5	98.	90. 2F (DS(3F)) 7. 4F (DS(3F))
2F 5/2	721412.	722100.	-688.0	2.5	91.	85. 2F (DS(3F)) 6. 4F (DS(3F))
4D 7/2	735283.	735510.	-226.7	3.5	97.	81. 4D (DS(3D)) 16. 2F (DS(1F))
4D 5/2	737295.	737020.	275.5	2.5	93.	66. 4D (DS(3D)) 9. 2D (DS(3D)) 9. 2D (DS(1D)) 9. 2F (DS(1F))
4D 3/2	738508.	---	---	1.5	92.	61. 4D (DS(3D)) 31. 2D (DS(1D))
4D 1/2	739549.	---	---	.5	99.	99. 4D (DS(3D))
2F 5/2	739741.	739770.	-29.1	2.5	94.	82. 2F (5F) 6. 2F (DS(1F)) 5. 2D (DS(1D))
2F 7/2	739948.	739940.	7.7	3.5	93.	93. 2F (5F)
2D 3/2	741019.	---	---	1.5	98.	50. 2D (DS(1D)) 36. 4D (DS(3D)) 11. 2D (DS(3D))
2D 5/2	741830.	---	---	2.5	96.	77. 2D (DS(1D)) 7. 4D (DS(3D)) 6. 2F (5F) 6. 2F (DS(1F))

TABLE (5.16A) CONTINUED

MN6+ ODD LEVELS
CALCULATIONS COMPARED WITH EXPERIMENTAL OBSERVATIONS
EXTRAPOLATED AND OPTIMIZED PARAMETERS
PARENTAGE -- DD(2S+1)L = 3D2(2S+1)L
DD(2S+1)L = 3D2(2S+1)L DS(2S+1)L = (3P5(2P)3D(2D))(2S+1)L

IRREP	CALC	EXP	INCR	J/MU	TOTAL	-- EIGENVECTOR COMPOSITION PCT
2D 5/2	742876.	---	---	2.5	96.	44. 2D (DS(3D)) 25. 2F (DS(1F)) 19. 4D (DS(3D)) 8. 2F (5F)
2F 7/2	746649.	746450.	199.0	3.5	92.	80. 2F (DS(1F)) 13. 4D (DS(3D))
2D 3/2	748362.	748170.	192.3	1.5	98.	83. 2D (DS(3D)) 15. 2D (DS(1D))
2F 5/2	749300.	749430.	-129.7	2.5	92.	50. 2F (DS(1F)) 42. 2D (DS(3D))
2P 1/2	756039.	---	---	.5	100.	100. 2P (6P)
2P 3/2	756559.	---	---	1.5	100.	100. 2P (6P)
2F 5/2	807748.	807760.	-12.5	2.5	100.	100. 2F (6F)
2F 7/2	807772.	807760.	12.2	3.5	100.	100. 2F (6F)
2H 9/2	812090.	---	---	4.5	100.	100. 2H (6H)
2H11/2	812092.	---	---	5.5	100.	100. 2H (6H)
2P 1/2	818670.	---	---	.5	100.	100. 2P (7P)
2P 3/2	818928.	---	---	1.5	100.	100. 2P (7P)
2F 5/2	848843.	848850.	-6.9	2.5	100.	100. 2F (7F)
2F 7/2	848857.	848850.	6.7	3.5	100.	100. 2F (7F)
2H 9/2	851762.	---	---	4.5	100.	100. 2H (7H)
2H11/2	851763.	---	---	5.5	100.	100. 2H (7H)
2P 1/2	872176.	---	---	.5	100.	100. 2P (DS(1P))
2P 3/2	872258.	---	---	1.5	100.	100. 2P (DS(1P))
2F 5/2	875526.	875530.	-4.3	2.5	100.	100. 2F (8F)
2F 7/2	875534.	875530.	4.2	3.5	100.	100. 2F (8F)
2F 5/2	893737.	893740.	-2.9	2.5	100.	100. 2F (9F)
2F 7/2	893743.	893740.	2.8	3.5	100.	100. 2F (9F)
2F 5/2	907046.	---	---	2.5	100.	100. 2F (10F)
2F 7/2	907050.	---	---	3.5	100.	100. 2F (10F)

TABLE (5.16A) CONTINUED

MN6+ ODD LEVELS
CALCULATIONS COMPARED WITH EXPERIMENTAL OBSERVATIONS
EXTRAPOLATED AND OPTIMIZED PARAMETERS
PARENTAGE -- DD(2S+1)L = 3D2(2S+1)L
DD(2S+1)L = 3D2(2S+1)L DS(2S+1)L = (3P5(2P)3D(2D))(2S+1)L

NO. EXPERIMENTAL LEVELS =	30.
ABSOLUTE MEAN DEVIATION =	261.49
RMS DEVIATION =	426.72

TABLE (5.16B)

MN6+ EVEN LEVELS
CALCULATIONS COMPARED WITH EXPERIMENTAL OBSERVATIONS
EXTRAPOLATED AND OPTIMIZED PARAMETERS
PARENTAGE -- DD(2S+1)L = 3D2(2S+1)L
DD(2S+1)L = 3D2(2S+1)L DS(2S+1)L = (3P5(2P)3D(2D))(2S+1)L

IRREP	CALC	EXP	INCR	J/MU	TOTAL	-- EIGENVECTOR COMPOSITION PCT
2D 3/2	-185.	0.	-184.7	1.5	100.	100. 2D (3D)
2D 5/2	1159.	1350.	-190.8	2.5	100.	100. 2D (3D)
2S 1/2	318636.	318734.	-97.7	.5	100.	100. 2S (4S)
2D 3/2	522536.	---	---	1.5	100.	100. 2D (4D)
2D 5/2	522873.	---	---	2.5	100.	100. 2D (4D)
2S 1/2	610900.	613934.	-3034.1	.5	100.	100. 2S (5S)
2D 3/2	696875.	---	---	1.5	100.	100. 2D (5D)
2D 5/2	697037.	---	---	2.5	100.	100. 2D (5D)
2S 1/2	739831.	752144.	-12312.6	.5	100.	100. 2S (6S)
2G 7/2	745551.	---	---	3.5	100.	100. 2G (5G)
2G 9/2	745557.	---	---	4.5	100.	100. 2G (5G)
4D 1/2	768832.	---	---	.5	94.	87. 4D (DP(3P)) 7. 4D (DP(3F))
4D 3/2	770288.	---	---	1.5	96.	87. 4D (DP(3P)) 9. 4D (DP(3F))
4D 5/2	772510.	---	---	2.5	97.	84. 4D (DP(3P)) 13. 4D (DP(3F))
4P 1/2	773817.	---	---	.5	97.	97. 4P (DP(3P))
4P 3/2	775129.	---	---	1.5	94.	88. 4P (DP(3P)) 6. 4S (DP(3P))
4D 7/2	775242.	---	---	3.5	98.	75. 4D (DP(3P)) 23. 4D (DP(3F))
2P 1/2	777394.	---	---	.5	92.	92. 2P (DP(3P))
4P 5/2	777672.	---	---	2.5	94.	94. 4P (DP(3P))
2P 3/2	778396.	---	---	1.5	94.	68. 2P (DP(3P)) 13. 4S (DP(3P)) 7. 4P (DP(3P)) 6. 2D (DP(3P))
4S 3/2	781967.	---	---	1.5	95.	78. 4S (DP(3P)) 11. 2P (DP(3P)) 6. 2D (DP(3P))
2D 3/2	784389.	---	---	1.5	96.	88. 2D (6D) 8. 2D (DP(3P))
2D 5/2	784542.	---	---	2.5	99.	93. 2D (6D) 6. 2D (DP(3P))
2D 5/2	787288.	---	---	2.5	83.	64. 2D (DP(3P)) 7. 2D (DP(3D)) 7. 2D (DP(3F)) 6. 2D (6D)
2D 3/2	787366.	---	---	1.5	89.	69. 2D (DP(3P)) 10. 2D (6D) 10. 2P (DP(3P))

TABLE (5.16B) CONTINUED

MN6+ EVEN LEVELS
CALCULATIONS COMPARED WITH EXPERIMENTAL OBSERVATIONS
EXTRAPOLATED AND OPTIMIZED PARAMETERS
PARENTAGE -- DD(2S+1)L = 3D2(2S+1)L
DD(2S+1)L = 3D2(2S+1)L DS(2S+1)L = (3P5(2P)3D(2D))(2S+1)L

IRREP	CALC	EXP	INCR	J/MU	TOTAL	-- EIGENVECTOR COMPOSITION PCT
4G11/2	787969.	---	---	5.5	100.	100. 4G (DP(3F))
4F 7/2	788010.	---	---	3.5	95.	33. 4F (DP(3F)) 31. 4D (DP(3F)) 13. 4D (DP(3P)) 11. 2F (DP(3F)) 6. 4D (DP(3D))
4G 9/2	788138.	---	---	4.5	95.	68. 4G (DP(3F)) 28. 4F (DP(3F))
2F 7/2	789366.	---	---	3.5	88.	60. 2F (DP(3F)) 28. 4G (DP(3F))
4D 5/2	789772.	---	---	2.5	83.	38. 4D (DP(3F)) 27. 4F (DP(3F)) 9. 4D (DP(3D)) 9. 4D (DP(3P))
4F 9/2	790295.	---	---	4.5	95.	68. 4F (DP(3F)) 26. 4G (DP(3F))
4G 7/2	790324.	---	---	3.5	88.	57. 4G (DP(3F)) 17. 2F (DP(3F)) 14. 4D (DP(3F))
2S 1/2	791623.	---	---	.5	93.	93. 2S (DP(3P))
4D 3/2	791866.	---	---	1.5	92.	49. 4D (DP(3F)) 21. 4F (DP(3F)) 13. 4D (DP(3D)) 8. 4D (DP(3P))
4G 5/2	792142.	---	---	2.5	91.	91. 4G (DP(3F))
2F 5/2	793831.	---	---	2.5	92.	56. 2F (DP(3F)) 23. 4F (DP(3F)) 7. 4D (DP(3F)) 6. 2D (DP(3P))
4F 7/2	793846.	---	---	3.5	88.	59. 4F (DP(3F)) 18. 4D (DP(3F)) 6. 4G (DP(3F)) 5. 2F (DP(3F))
4D 1/2	794078.	---	---	.5	95.	67. 4D (DP(3F)) 18. 4D (DP(3D)) 10. 4D (DP(3P))
4F 5/2	796416.	---	---	2.5	82.	36. 4F (DP(3F)) 22. 2F (DP(3F)) 18. 4D (DP(3F)) 6. 2D (DP(1D))
4F 3/2	796697.	---	---	1.5	87.	66. 4F (DP(3F)) 20. 4D (DP(3F))
2G 9/2	799924.	---	---	4.5	94.	94. 2G (DP(3F))
2D 5/2	802756.	---	---	2.5	90.	29. 2D (DP(1D)) 26. 2D (DP(3F)) 17. 2D (DP(1F)) 12. 2F (DP(3F)) 6. 4F (DP(3F))
2G 7/2	803516.	---	---	3.5	88.	88. 2G (DP(3F))
2D 3/2	803656.	---	---	1.5	94.	44. 2D (DP(1D)) 23. 2D (DP(3F)) 13. 2D (DP(1F)) 8. 4F (DP(3F)) 7. 2D (DP(3D))
2S 1/2	808629.	---	---	.5	100.	100. 2S (7S)
2G 7/2	811447.	---	---	3.5	100.	100. 2G (6G)

TABLE (5.16B) CONTINUED

MN6+ EVEN LEVELS
CALCULATIONS COMPARED WITH EXPERIMENTAL OBSERVATIONS
EXTRAPOLATED AND OPTIMIZED PARAMETERS
PARENTAGE -- DD(2S+1)L = 3D2(2S+1)L
DD(2S+1)L = 3D2(2S+1)L DS(2S+1)L = (3P5(2P)3D(2D))(2S+1)L

IRREP	CALC	EXP	INCR	J/MU	TOTAL	-- EIGENVECTOR COMPOSITION PCT
2G 9/2	811453.	---	---	4.5	100.	100. 2G (6G)
4D 7/2	814301.	---	---	3.5	98.	72. 4D (DP(3D)) 11. 4D (DP(3F)) 8. 2F (DP(1F)) 7. 4F (DP(3D))
4D 5/2	815046.	---	---	2.5	88.	52. 4D (DP(3D)) 11. 2F (DP(1F)) 10. 4D (DP(3F)) 9. 4F (DP(3D)) 7. 2F (DP(1D))
4D 3/2	816988.	---	---	1.5	97.	65. 4D (DP(3D)) 13. 4D (DP(3F)) 6. 2D (DP(3D)) 6. 4F (DP(3D)) 6. 2D (DP(1F))
2F 5/2	817115.	---	---	2.5	86.	36. 2F (DP(1D)) 17. 2D (DP(3F)) 15. 2D (DP(3D)) 11. 2F (DP(1F)) 6. 4D (DP(3D))
4D 1/2	818528.	---	---	.5	96.	76. 4D (DP(3D)) 20. 4D (DP(3F))
2D 5/2	818549.	---	---	2.5	91.	23. 2D (DP(3F)) 20. 2D (DP(3D)) 17. 4D (DP(3D)) 13. 2F (DP(1D)) 12. 2F (DP(1F)) 6. 2D (DP(1D))
4F 9/2	819127.	---	---	4.5	97.	73. 4F (DP(3D)) 24. 2G (DP(1F))
4F 7/2	819343.	---	---	3.5	86.	37. 4F (DP(3D)) 21. 2F (DP(1D)) 12. 2G (DP(1F)) 11. 4D (DP(3D)) 6. 2F (DP(3D))
4F 3/2	819901.	---	---	1.5	88.	80. 4F (DP(3D)) 8. 2D (DP(3F))
2F 7/2	820754.	---	---	3.5	94.	35. 2F (DP(1F)) 27. 2F (DP(1D)) 18. 4F (DP(3D)) 9. 2G (DP(1F)) 6. 2F (DP(3D))
4F 5/2	821011.	---	---	2.5	87.	78. 4F (DP(3D)) 9. 2F (DP(1F))
2D 3/2	821837.	---	---	1.5	88.	34. 2D (DP(3D)) 25. 2D (DP(3F)) 13. 4D (DP(3D)) 10. 4F (DP(3D)) 6. 2D (DP(1F))
2G 7/2	824001.	---	---	3.5	94.	59. 2G (DP(1F)) 28. 4F (DP(3D)) 7. 2F (DP(3D))
2F 5/2	825183.	---	---	2.5	90.	36. 2F (DP(1F)) 32. 2F (DP(3D)) 21. 2F (DP(1D))
4P 5/2	826407.	---	---	2.5	91.	83. 4P (DP(3D)) 7. 2D (DP(1D))
2G 9/2	826976.	---	---	4.5	96.	74. 2G (DP(1F)) 22. 4F (DP(3D))
4P 3/2	827055.	---	---	1.5	85.	45. 4P (DP(3D)) 40. 2P (DP(1D))

TABLE (5.16B) CONTINUED

MN6+ EVEN LEVELS
CALCULATIONS COMPARED WITH EXPERIMENTAL OBSERVATIONS
EXTRAPOLATED AND OPTIMIZED PARAMETERS
PARENTAGE -- DD(2S+1)L = 3D2(2S+1)L
DD(2S+1)L = 3D2(2S+1)L DS(2S+1)L = (3P5(2P)3D(2D))(2S+1)L

IRREP	CALC	EXP	INCR	J/MU	TOTAL	-- EIGENVECTOR COMPOSITION PCT
2F 7/2	827114.	---	---	3.5	90.	32. 2F (DP(1D)) 29. 2F (DP(3D)) 23. 2F (DP(1F)) 5. 2G (DP(1F))
2P 1/2	827807.	---	---	.5	97.	55. 2P (DP(1D)) 30. 4P (DP(3D)) 12. 2P (DP(3D))
4P 1/2	829343.	---	---	.5	99.	68. 4P (DP(3D)) 18. 2P (DP(1D)) 13. 2P (DP(3D))
2P 3/2	829698.	---	---	1.5	89.	31. 2P (DP(3D)) 22. 4P (DP(3D)) 18. 2D (DP(1F)) 17. 2D (DP(1D))
2P 3/2	830289.	---	---	1.5	93.	48. 2P (DP(1D)) 26. 4P (DP(3D)) 12. 2D (DP(1D)) 7. 2D (DP(1F))
2D 5/2	831314.	---	---	2.5	88.	36. 2D (DP(1F)) 32. 2D (DP(1D)) 12. 2D (DP(3D)) 8. 4P (DP(3D))
2F 7/2	833603.	---	---	3.5	95.	48. 2F (DP(3D)) 23. 2F (DP(1F)) 14. 2F (DP(1D)) 9. 2G (DP(1F))
2F 5/2	833959.	---	---	2.5	92.	57. 2F (DP(3D)) 17. 2F (DP(1D)) 17. 2F (DP(1F))
2D 3/2	834198.	---	---	1.5	92.	42. 2D (7D) 39. 2P (DP(3D)) 6. 2D (DP(3F)) 6. 2D (DP(1D))
2D 5/2	835181.	---	---	2.5	96.	96. 2D (7D)
2D 3/2	835793.	---	---	1.5	98.	55. 2D (7D) 19. 2P (DP(3D)) 12. 2D (DP(1F)) 6. 2D (DP(1D)) 6. 2D (DP(3F))
2P 1/2	835997.	---	---	.5	95.	70. 2P (DP(3D)) 25. 2P (DP(1D))
2S 1/2	849663.	---	---	.5	100.	100. 2S (8S)
2G 7/2	851448.	---	---	3.5	100.	100. 2G (7G)
2G 9/2	851451.	---	---	4.5	100.	100. 2G (7G)
2I11/2	851904.	---	---	5.5	100.	100. 2I (7I)
2D 3/2	853588.	---	---	1.5	97.	39. 2D (DP(3D)) 30. 2D (DP(1F)) 15. 2D (DP(3F)) 7. 2D (DP(3P)) 7. 2D (DP(1D))
2D 5/2	856168.	---	---	2.5	97.	36. 2D (DP(3D)) 28. 2D (DP(1F)) 18. 2D (DP(3F)) 8. 2D (DP(3P)) 7. 2D (DP(1D))
2I11/2	877627.	---	---	5.5	100.	100. 2I (8I)
2P 1/2	947629.	---	---	.5	98.	98. 2P (DP(1P))

TABLE (5.16B) CONTINUED

MN6+ EVEN LEVELS
CALCULATIONS COMPARED WITH EXPERIMENTAL OBSERVATIONS
EXTRAPOLATED AND OPTIMIZED PARAMETERS
PARENTAGE -- DD(2S+1)L = 3D2(2S+1)L
DD(2S+1)L = 3D2(2S+1)L DS(2S+1)L = (3P5(2P)3D(2D))(2S+1)L

IRREP	CALC	EXP	INCR	J/MU	TOTAL	-- EIGENVECTOR COMPOSITION PCT
2P 3/2	948777.	---	---	1.5	95.	95. 2P (DP(1P))
2D 3/2	952740.	---	---	1.5	94.	94. 2D (DP(1P))
2D 5/2	954364.	---	---	2.5	99.	99. 2D (DP(1P))
2S 1/2	956619.	---	---	.5	98.	98. 2S (DP(1P))

NO. EXPERIMENTAL LEVELS = 5.

ABSOLUTE MEAN DEVIATION = 3164.00

RMS DEVIATION = 5672.51

TABLE (5.17A)

FE7+ ODD LEVELS
CALCULATIONS COMPARED WITH EXPERIMENTAL OBSERVATIONS
EXTRAPOLATED AND OPTIMIZED PARAMETERS
PARENTAGE -- DD(2S+1)L = 3D2(2S+1)L
DD(2S+1)L = 3D2(2S+1)L DS(2S+1)L = (3P5(2P)3D(2D))(2S+1)L

IRREP	CALC	EXP	INCR	J/MU	TOTAL	-- EIGENVECTOR COMPOSITION PCT
4D 1/2	387014.	---	---	.5	100.	84. 4D (DD(3F)) 16. 4D (DD(3P))
4D 3/2	387990.	---	---	1.5	99.	81. 4D (DD(3F)) 18. 4D (DD(3P))
4D 5/2	389651.	---	---	2.5	98.	77. 4D (DD(3F)) 20. 4D (DD(3P))
4D 7/2	392163.	---	---	3.5	97.	72. 4D (DD(3F)) 25. 4D (DD(3P))
4G11/2	406913.	---	---	5.5	100.	100. 4G (DD(3F))
4G 9/2	408845.	---	---	4.5	98.	92. 4G (DD(3F)) 6. 4F (DD(3F))
4G 7/2	411263.	---	---	3.5	96.	86. 4G (DD(3F)) 10. 4F (DD(3F))
4G 5/2	413787.	---	---	2.5	95.	78. 4G (DD(3F)) 11. 4F (DD(3F)) 5. 2F (DD(3F))
4P 5/2	417179.	---	---	2.5	98.	98. 4P (DD(3P))
4P 3/2	420655.	---	---	1.5	96.	96. 4P (DD(3P))
4F 3/2	422496.	---	---	1.5	96.	68. 4F (DD(3F)) 21. 2D (DD(1D)) 8. 2D (DD(3F))
4P 1/2	423296.	---	---	.5	97.	97. 4P (DD(3P))
2D 5/2	423688.	---	---	2.5	97.	41. 2D (DD(1D)) 34. 4F (DD(3F)) 12. 2D (DD(3F)) 10. 4G (DD(3F))
4F 9/2	423710.	---	---	4.5	95.	89. 4F (DD(3F)) 7. 2G (DD(3F))
4F 7/2	425329.	---	---	3.5	94.	78. 4F (DD(3F)) 9. 4G (DD(3F)) 7. 2G (DD(3F))
4F 5/2	428435.	---	---	2.5	90.	46. 4F (DD(3F)) 24. 2D (DD(1D)) 11. 2F (DD(1G)) 9. 2F (DD(3F))
2F 5/2	429175.	---	---	2.5	97.	37. 2F (DD(1G)) 31. 2F (DD(3F)) 11. 4G (DD(3F)) 11. 2D (DD(1D)) 6. 4F (DD(3F))
2D 3/2	430193.	---	---	1.5	93.	42. 2D (DD(1D)) 30. 4F (DD(3F)) 12. 2P (DD(1D)) 9. 2D (DD(3F))
2F 7/2	432159.	---	---	3.5	94.	41. 2F (DD(1G)) 37. 2F (DD(3F)) 10. 2F (DD(1D)) 6. 4F (DD(3F))
2P 1/2	437336.	---	---	.5	98.	70. 2P (DD(1D)) 21. 2P (DD(3P)) 7. 2P (DD(1S))
2G 7/2	442679.	---	---	3.5	92.	59. 2G (DD(3F)) 33. 2F (DD(1D))
2H11/2	443597.	---	---	5.5	100.	100. 2H (DD(1G))

TABLE (5.17A) CONTINUED

FE7+ ODD LEVELS
CALCULATIONS COMPARED WITH EXPERIMENTAL OBSERVATIONS
EXTRAPOLATED AND OPTIMIZED PARAMETERS
PARENTAGE -- DD(2S+1)L = 3D2(2S+1)L
DD(2S+1)L = 3D2(2S+1)L DS(2S+1)L = (3P5(2P)3D(2D))(2S+1)L

IRREP	CALC	EXP	INCR	J/MU	TOTAL	-- EIGENVECTOR COMPOSITION PCT
2P 3/2	444253.	---	---	1.5	92.	49. 2P (DD(1D)) 19. 2P (DD(3P)) 15. 2D (DD(1D)) 10. 2P (DD(1S))
2F 7/2	446058.	---	---	3.5	97.	56. 2F (DD(1D)) 27. 2G (DD(3F)) 8. 2F (DD(3F)) 6. 2F (DD(1G))
2G 9/2	448757.	---	---	4.5	88.	81. 2G (DD(3F)) 7. 2G (DD(1G))
2H 9/2	454039.	---	---	4.5	98.	92. 2H (DD(1G)) 5. 2G (DD(3F))
2F 5/2	457388.	---	---	2.5	93.	93. 2F (DD(1D))
4D 7/2	461176.	---	---	3.5	98.	71. 4D (DD(3P)) 27. 4D (DD(3F))
4D 5/2	462931.	---	---	2.5	98.	71. 4D (DD(3P)) 20. 4D (DD(3F)) 6. 2D (DD(3P))
4D 3/2	465455.	---	---	1.5	98.	73. 4D (DD(3P)) 17. 4D (DD(3F)) 9. 2D (DD(3P))
4D 1/2	468305.	---	---	.5	99.	83. 4D (DD(3P)) 16. 4D (DD(3F))
2D 3/2	480347.	---	---	1.5	95.	80. 2D (DD(3P)) 8. 4D (DD(3P)) 7. 2D (DD(3F))
2D 5/2	484754.	---	---	2.5	95.	81. 2D (DD(3P)) 8. 2D (DD(3F)) 6. 4D (DD(3P))
2G 9/2	489320.	---	---	4.5	91.	91. 2G (DD(1G))
2G 7/2	489968.	---	---	3.5	94.	94. 2G (DD(1G))
4S 3/2	490102.	---	---	1.5	98.	98. 4S (DD(3P))
2S 1/2	490217.	---	---	.5	99.	99. 2S (DD(3P))
2P 1/2	510415.	---	---	.5	98.	98. 2P (4P)
2P 3/2	511604.	---	---	1.5	100.	57. 2P (DD(1S)) 29. 2P (4P) 14. 2P (DD(1D))
2P 3/2	514906.	---	---	1.5	98.	70. 2P (4P) 21. 2P (DD(1S)) 6. 2P (DD(1D))
2P 1/2	523955.	---	---	.5	99.	77. 2P (DD(1S)) 16. 2P (DD(1D)) 6. 2P (DD(3P))
2F 5/2	536181.	535926.	255.3	2.5	97.	51. 2F (DD(3F)) 46. 2F (DD(1G))
2F 7/2	542516.	541777.	739.2	3.5	96.	49. 2F (DD(1G)) 48. 2F (DD(3F))
2P 1/2	590976.	591973.	-997.1	.5	99.	72. 2P (DD(3P)) 15. 2P (DD(1S)) 12. 2P (DD(1D))

TABLE (5.17A) CONTINUED

FE7+ ODD LEVELS
CALCULATIONS COMPARED WITH EXPERIMENTAL OBSERVATIONS
EXTRAPOLATED AND OPTIMIZED PARAMETERS
PARENTAGE -- DD(2S+1)L = 3D2(2S+1)L
DD(2S+1)L = 3D2(2S+1)L DS(2S+1)L = (3P5(2P)3D(2D))(2S+1)L

IRREP	CALC	EXP	INCR	J/MU	TOTAL	-- EIGENVECTOR COMPOSITION PCT
2P 3/2	593618.	595166.	-1548.3	1.5	98.	74. 2P (DD(3P)) 15. 2P (DD(1D)) 10. 2P (DD(1S))
2D 5/2	597093.	596430.	662.5	2.5	100.	70. 2D (DD(3F)) 17. 2D (DD(1D)) 12. 2D (DD(3P))
2D 3/2	597945.	597072.	873.3	1.5	100.	71. 2D (DD(3F)) 18. 2D (DD(1D)) 11. 2D (DD(3P))
2F 5/2	763711.	763789.	-77.9	2.5	98.	98. 2F (4F)
2F 7/2	763884.	763821.	62.8	3.5	98.	98. 2F (4F)
2P 1/2	813521.	---	---	.5	99.	99. 2P (5P)
2P 3/2	814928.	---	---	1.5	99.	99. 2P (5P)
4P 1/2	829166.	---	---	.5	99.	99. 4P (DS(3P))
4P 3/2	831387.	833000.	-1612.9	1.5	97.	97. 4P (DS(3P))
4P 5/2	835614.	---	---	2.5	97.	97. 4P (DS(3P))
2P 1/2	839127.	837750.	1377.3	.5	97.	97. 2P (DS(3P))
2P 3/2	843877.	842930.	947.5	1.5	95.	95. 2P (DS(3P))
4F 9/2	844687.	---	---	4.5	100.	100. 4F (DS(3F))
4F 7/2	847454.	847250.	203.8	3.5	98.	89. 4F (DS(3F)) 8. 2F (DS(3F))
4F 5/2	850638.	849990.	648.2	2.5	94.	88. 4F (DS(3F)) 7. 2F (DS(3F))
4F 3/2	854021.	---	---	1.5	93.	93. 4F (DS(3F))
2F 7/2	855176.	855190.	-13.6	3.5	97.	90. 2F (DS(3F)) 7. 4F (DS(3F))
2F 5/2	860243.	860710.	-467.2	2.5	88.	82. 2F (DS(3F)) 6. 4F (DS(3F))
4D 7/2	874439.	874770.	-331.1	3.5	98.	82. 4D (DS(3D)) 17. 2F (DS(1F))
4D 5/2	876867.	876810.	56.9	2.5	93.	65. 4D (DS(3D)) 11. 2D (DS(3D)) 9. 2D (DS(1D)) 9. 2F (DS(1F))
4D 3/2	878204.	---	---	1.5	96.	58. 4D (DS(3D)) 32. 2D (DS(1D)) 6. 4F (DS(3F))
4D 1/2	879355.	---	---	.5	99.	99. 4D (DS(3D))
2D 3/2	881161.	---	---	1.5	97.	47. 2D (DS(1D)) 38. 4D (DS(3D)) 12. 2D (DS(3D))
2D 5/2	881712.	---	---	2.5	96.	62. 2D (DS(1D)) 20. 2F (DS(1F)) 14. 2D (DS(3D))

TABLE (5.17A) CONTINUED

FE7+ ODD LEVELS
CALCULATIONS COMPARED WITH EXPERIMENTAL OBSERVATIONS
EXTRAPOLATED AND OPTIMIZED PARAMETERS
PARENTAGE -- DD(2S+1)L = 3D2(2S+1)L
DD(2S+1)L = 3D2(2S+1)L DS(2S+1)L = (3P5(2P)3D(2D))(2S+1)L

IRREP	CALC	EXP	INCR	J/MU	TOTAL	-- EIGENVECTOR COMPOSITION PCT
2D 5/2	883095.	---	---	2.5	98.	33. 2D (DS(3D)) 29. 4D (DS(3D)) 21. 2D (DS(1D)) 15. 2F (DS(1F))
2F 7/2	887538.	887320.	218.2	3.5	96.	81. 2F (DS(1F)) 15. 4D (DS(3D))
2D 3/2	889398.	889110.	288.0	1.5	97.	82. 2D (DS(3D)) 16. 2D (DS(1D))
2F 5/2	890796.	890810.	-14.4	2.5	97.	50. 2F (DS(1F)) 41. 2D (DS(3D)) 6. 2F (DS(3F))
2F 5/2	927006.	927025.	-19.1	2.5	99.	99. 2F (5F)
2F 7/2	927071.	927053.	18.2	3.5	99.	99. 2F (5F)
2P 1/2	955065.	---	---	.5	100.	100. 2P (6P)
2P 3/2	955774.	---	---	1.5	100.	100. 2P (6P)
2F 5/2	1016535.	1016530.	4.6	2.5	100.	100. 2F (6F)
2F 7/2	1016565.	1016570.	-5.4	3.5	100.	100. 2F (6F)
2P 1/2	1022094.	---	---	.5	97.	97. 2P (DS(1P))
2P 3/2	1022196.	---	---	1.5	97.	97. 2P (DS(1P))
2H 9/2	1022779.	---	---	4.5	100.	100. 2H (6H)
2H11/2	1022783.	---	---	5.5	100.	100. 2H (6H)
2P 1/2	1035516.	---	---	.5	98.	98. 2P (7P)
2P 3/2	1035843.	---	---	1.5	98.	98. 2P (7P)
2F 5/2	1069941.	1069870.	70.8	2.5	100.	100. 2F (7F)
2F 7/2	1069959.	1070030.	-71.3	3.5	100.	100. 2F (7F)
2H 9/2	1074593.	---	---	4.5	100.	100. 2H (7H)
2H11/2	1074595.	---	---	5.5	100.	100. 2H (7H)
2F 5/2	1105521.	---	---	2.5	100.	100. 2F (8F)
2F 7/2	1105533.	---	---	3.5	100.	100. 2F (8F)
2F 5/2	1129355.	---	---	2.5	100.	100. 2F (9F)
2F 7/2	1129363.	---	---	3.5	100.	100. 2F (9F)
2F 5/2	1146207.	---	---	2.5	100.	100. 2F (10F)
2F 7/2	1146213.	---	---	3.5	100.	100. 2F (10F)

TABLE (5.17A) CONTINUED

FE7+ ODD LEVELS
CALCULATIONS COMPARED WITH EXPERIMENTAL OBSERVATIONS
EXTRAPOLATED AND OPTIMIZED PARAMETERS
PARENTAGE -- DD(2S+1)L = 3D2(2S+1)L
DD(2S+1)L = 3D2(2S+1)L DS(2S+1)L = (3P5(2P)3D(2D))(2S+1)L

NO. EXPERIMENTAL LEVELS =	26.
ABSOLUTE MEAN DEVIATION =	445.58
RMS DEVIATION =	666.38

TABLE (5.17B)

FE7+ EVEN LEVELS
CALCULATIONS COMPARED WITH EXPERIMENTAL OBSERVATIONS
EXTRAPOLATED AND OPTIMIZED PARAMETERS
PARENTAGE -- DD(2S+1)L = 3D2(2S+1)L
DD(2S+1)L = 3D2(2S+1)L DS(2S+1)L = (3P5(2P)3D(2D))(2S+1)L

IRREP	CALC	EXP	INCR	J/MU	TOTAL	-- EIGENVECTOR COMPOSITION PCT
2D 3/2	-254.	0.	-253.8	1.5	100.	100. 2D (3D)
2D 5/2	1596.	1838.	-241.9	2.5	100.	100. 2D (3D)
2S 1/2	419796.	---	---	.5	100.	100. 2S (4S)
2D 3/2	653279.	---	---	1.5	100.	100. 2D (4D)
2D 5/2	653763.	---	---	2.5	100.	100. 2D (4D)
2S 1/2	776901.	---	---	.5	100.	100. 2S (5S)
2D 3/2	876960.	---	---	1.5	100.	100. 2D (5D)
2D 5/2	877198.	---	---	2.5	100.	100. 2D (5D)
4D 1/2	914337.	---	---	.5	94.	87. 4D (DP(3P)) 7. 4D (DP(3F))
4D 3/2	916261.	---	---	1.5	95.	87. 4D (DP(3P)) 9. 4D (DP(3F))
4D 5/2	919169.	---	---	2.5	96.	83. 4D (DP(3P)) 13. 4D (DP(3F))
4P 1/2	920187.	---	---	.5	95.	95. 4P (DP(3P))
4P 3/2	921935.	---	---	1.5	93.	86. 4P (DP(3P)) 7. 4S (DP(3P))
4D 7/2	922608.	---	---	3.5	97.	71. 4D (DP(3P)) 26. 4D (DP(3F))
2P 1/2	924549.	---	---	.5	90.	90. 2P (DP(3P))
4P 5/2	925156.	---	---	2.5	92.	92. 4P (DP(3P))
2P 3/2	925575.	---	---	1.5	93.	64. 2P (DP(3P)) 14. 4S (DP(3P)) 9. 4P (DP(3P)) 6. 2D (DP(3P))
4S 3/2	929990.	---	---	1.5	95.	75. 4S (DP(3P)) 11. 2P (DP(3P)) 8. 2D (DP(3P))
2D 5/2	935354.	---	---	2.5	86.	62. 2D (DP(3P)) 7. 2D (DP(3D)) 6. 2F (DP(3F)) 6. 4D (DP(3F)) 5. 2D (DP(3F))
2D 3/2	935618.	---	---	1.5	86.	71. 2D (DP(3P)) 15. 2P (DP(3P))
4F 7/2	935718.	---	---	3.5	95.	34. 4F (DP(3F)) 28. 4D (DP(3F)) 15. 4D (DP(3P)) 12. 2F (DP(3F)) 6. 4D (DP(3D))
2G 7/2	935792.	---	---	3.5	100.	100. 2G (5G)
2G 9/2	935799.	---	---	4.5	96.	96. 2G (5G)
4G 9/2	935932.	---	---	4.5	95.	61. 4G (DP(3F)) 30. 4F (DP(3F)) 5. 2G (DP(3F))

TABLE (5.17B) CONTINUED

FE7+ EVEN LEVELS
CALCULATIONS COMPARED WITH EXPERIMENTAL OBSERVATIONS
EXTRAPOLATED AND OPTIMIZED PARAMETERS
PARENTAGE -- DD(2S+1)L = 3D2(2S+1)L
DD(2S+1)L = 3D2(2S+1)L DS(2S+1)L = (3P5(2P)3D(2D))(2S+1)L

IRREP	CALC	EXP	INCR	J/MU	TOTAL	-- EIGENVECTOR COMPOSITION PCT
4G11/2	936133.	---	---	5.5	100.	100. 4G (DP(3F))
2S 1/2	936905.	---	---	.5	99.	91. 2S (6S) 8. 2S (DP(3P))
2F 7/2	937296.	---	---	3.5	87.	55. 2F (DP(3F)) 32. 4G (DP(3F))
4D 5/2	937758.	---	---	2.5	80.	33. 4D (DP(3F)) 25. 4F (DP(3F)) 9. 4D (DP(3P)) 8. 4D (DP(3D)) 6. 2D (DP(3P))
4F 9/2	938679.	---	---	4.5	94.	65. 4F (DP(3F)) 29. 4G (DP(3F))
4G 7/2	938745.	---	---	3.5	86.	50. 4G (DP(3F)) 21. 2F (DP(3F)) 14. 4D (DP(3F))
4D 3/2	940362.	---	---	1.5	88.	45. 4D (DP(3F)) 21. 4F (DP(3F)) 14. 4D (DP(3D)) 8. 4D (DP(3P))
4G 5/2	940986.	---	---	2.5	89.	89. 4G (DP(3F))
2S 1/2	941048.	---	---	.5	89.	81. 2S (DP(3P)) 9. 2S (6S)
2F 5/2	942841.	---	---	2.5	91.	54. 2F (DP(3F)) 23. 4F (DP(3F)) 8. 2D (DP(3P)) 6. 4D (DP(3F))
4F 7/2	942919.	---	---	3.5	86.	57. 4F (DP(3F)) 18. 4D (DP(3F)) 6. 4G (DP(3F)) 5. 4D (DP(3P))
4D 1/2	943332.	---	---	.5	90.	62. 4D (DP(3F)) 18. 4D (DP(3D)) 10. 4D (DP(3P))
4F 5/2	946019.	---	---	2.5	82.	31. 4F (DP(3F)) 21. 4D (DP(3F)) 17. 2F (DP(3F)) 8. 2D (DP(1D)) 5. 2D (DP(3P))
4F 3/2	946525.	---	---	1.5	84.	62. 4F (DP(3F)) 22. 4D (DP(3F))
2G 9/2	949300.	---	---	4.5	93.	93. 2G (DP(3F))
2D 5/2	952665.	---	---	2.5	91.	25. 2D (DP(3F)) 24. 2D (DP(1D)) 18. 2F (DP(3F)) 16. 2D (DP(1F)) 9. 4F (DP(3F))
2D 3/2	953565.	---	---	1.5	93.	41. 2D (DP(1D)) 22. 2D (DP(3F)) 12. 2D (DP(1F)) 11. 4F (DP(3F)) 7. 2D (DP(3D))
2G 7/2	953696.	---	---	3.5	85.	85. 2G (DP(3F))
4D 7/2	964637.	---	---	3.5	97.	69. 4D (DP(3D)) 11. 4D (DP(3F)) 9. 2F (DP(1F)) 8. 4F (DP(3D))

TABLE (5.17B) CONTINUED

FE7+ EVEN LEVELS
CALCULATIONS COMPARED WITH EXPERIMENTAL OBSERVATIONS
EXTRAPOLATED AND OPTIMIZED PARAMETERS
PARENTAGE -- DD(2S+1)L = 3D2(2S+1)L
DD(2S+1)L = 3D2(2S+1)L DS(2S+1)L = (3P5(2P)3D(2D))(2S+1)L

IRREP	CALC	EXP	INCR	J/MU	TOTAL	-- EIGENVECTOR COMPOSITION PCT
4D 5/2	965371.	---	---	2.5	86.	47. 4D (DP(3D)) 12. 2F (DP(1F)) 10. 4F (DP(3D)) 9. 4D (DP(3F)) 8. 2F (DP(1D))
2F 5/2	967887.	---	---	2.5	83.	31. 2F (DP(1D)) 21. 2D (DP(3F)) 18. 2D (DP(3D)) 7. 2F (DP(1F)) 5. 4D (DP(3D))
4D 3/2	967959.	---	---	1.5	96.	61. 4D (DP(3D)) 13. 4D (DP(3F)) 8. 2D (DP(3D)) 8. 2D (DP(1F)) 7. 4F (DP(3D))
4D 5/2	969791.	---	---	2.5	90.	20. 4D (DP(3D)) 19. 2D (DP(3F)) 17. 2F (DP(1D)) 15. 2D (DP(3D)) 14. 2F (DP(1F)) 6. 2D (DP(1D))
4D 1/2	970013.	---	---	.5	94.	74. 4D (DP(3D)) 21. 4D (DP(3F))
4F 9/2	970114.	---	---	4.5	97.	68. 4F (DP(3D)) 29. 2G (DP(1F))
4F 7/2	970580.	---	---	3.5	90.	37. 4F (DP(3D)) 21. 2G (DP(1F)) 11. 2F (DP(3D)) 11. 4D (DP(3D)) 11. 2F (DP(1D))
4F 3/2	971123.	---	---	1.5	92.	77. 4F (DP(3D)) 9. 2D (DP(3F)) 5. 2D (DP(3D))
2F 7/2	972473.	---	---	3.5	94.	37. 2F (DP(1F)) 35. 2F (DP(1D)) 7. 2G (DP(1F)) 5. 2F (DP(3D)) 5. 4F (DP(3D)) 5. 2F (DP(3F))
4F 5/2	972724.	---	---	2.5	85.	75. 4F (DP(3D)) 10. 2F (DP(1F))
2D 3/2	973741.	---	---	1.5	91.	29. 2D (DP(3D)) 21. 2D (DP(3F)) 16. 4D (DP(3D)) 11. 4F (DP(3D)) 7. 4P (DP(3D)) 6. 2D (DP(1F))
2G 7/2	975862.	---	---	3.5	91.	50. 2G (DP(1F)) 35. 4F (DP(3D)) 5. 2F (DP(1F))
2F 5/2	977230.	---	---	2.5	92.	35. 2F (DP(1F)) 30. 2F (DP(3D)) 21. 2F (DP(1D)) 5. 4F (DP(3D))
4P 5/2	978454.	---	---	2.5	94.	80. 4P (DP(3D)) 9. 2D (DP(1D)) 5. 2D (DP(1F))
2P 3/2	979331.	---	---	1.5	96.	41. 2P (DP(1D)) 38. 4P (DP(3D)) 6. 2D (DP(3F)) 5. 2P (DP(3D)) 5. 2D (DP(3D))
2G 9/2	979871.	---	---	4.5	95.	69. 2G (DP(1F)) 26. 4F (DP(3D))
2F 7/2	979875.	---	---	3.5	90.	34. 2F (DP(1D)) 29. 2F (DP(3D)) 20. 2F (DP(1F)) 7. 4F (DP(3D))

TABLE (5.17B) CONTINUED

FE7+ EVEN LEVELS
CALCULATIONS COMPARED WITH EXPERIMENTAL OBSERVATIONS
EXTRAPOLATED AND OPTIMIZED PARAMETERS
PARENTAGE -- DD(2S+1)L = 3D2(2S+1)L
DD(2S+1)L = 3D2(2S+1)L DS(2S+1)L = (3P5(2P)3D(2D))(2S+1)L

IRREP	CALC	EXP	INCR	J/MU	TOTAL	-- EIGENVECTOR COMPOSITION PCT
2P 1/2	980230.	---	---	.5	95.	55. 2P (DP(1D)) 28. 4P (DP(3D)) 12. 2P (DP(3D))
2P 3/2	982013.	---	---	1.5	92.	36. 2P (DP(3D)) 25. 2D (DP(1D)) 21. 2D (DP(1F)) 9. 4P (DP(3D))
4P 1/2	982058.	---	---	.5	98.	69. 4P (DP(3D)) 15. 2P (DP(1D)) 14. 2P (DP(3D))
2P 3/2	983244.	---	---	1.5	92.	50. 2P (DP(1D)) 42. 4P (DP(3D))
2D 5/2	984379.	---	---	2.5	89.	31. 2D (DP(1F)) 30. 2D (DP(1D)) 13. 2D (DP(3D)) 9. 4P (DP(3D)) 5. 2F (DP(3D))
2F 7/2	986922.	---	---	3.5	93.	47. 2F (DP(3D)) 23. 2F (DP(1F)) 13. 2F (DP(1D)) 10. 2G (DP(1F))
2F 5/2	987176.	---	---	2.5	89.	56. 2F (DP(3D)) 17. 2F (DP(1D)) 16. 2F (DP(1F))
2D 3/2	987368.	---	---	1.5	93.	41. 2D (6D) 38. 2P (DP(3D)) 7. 2D (DP(3F)) 6. 2D (DP(1D))
2D 5/2	989201.	---	---	2.5	92.	92. 2D (6D)
2P 1/2	989811.	---	---	.5	93.	66. 2P (DP(3D)) 27. 2P (DP(1D))
2D 3/2	990294.	---	---	1.5	97.	51. 2D (6D) 17. 2P (DP(3D)) 16. 2D (DP(1F)) 6. 2D (DP(3F)) 6. 2D (DP(1D))
2D 3/2	1008533.	---	---	1.5	94.	38. 2D (DP(3D)) 29. 2D (DP(1F)) 15. 2D (DP(3F)) 7. 2D (DP(3P)) 6. 2D (DP(1D))
2D 5/2	1011876.	---	---	2.5	94.	35. 2D (DP(3D)) 27. 2D (DP(1F)) 18. 2D (DP(3F)) 8. 2D (DP(3P)) 7. 2D (DP(1D))
2G 7/2	1021892.	---	---	3.5	100.	100. 2G (6G)
2G 9/2	1021899.	---	---	4.5	100.	100. 2G (6G)
2S 1/2	1023045.	---	---	.5	100.	100. 2S (7S)
2D 3/2	1054527.	---	---	1.5	100.	100. 2D (7D)
2D 5/2	1054597.	---	---	2.5	99.	99. 2D (7D)
2G 7/2	1074117.	---	---	3.5	100.	100. 2G (7G)
2G 9/2	1074121.	---	---	4.5	100.	100. 2G (7G)

TABLE (5.17B) CONTINUED

FE7+ EVEN LEVELS
CALCULATIONS COMPARED WITH EXPERIMENTAL OBSERVATIONS
EXTRAPOLATED AND OPTIMIZED PARAMETERS
PARENTAGE -- DD(2S+1)L = 3D2(2S+1)L
DD(2S+1)L = 3D2(2S+1)L DS(2S+1)L = (3P5(2P)3D(2D))(2S+1)L

IRREP	CALC	EXP	INCR	J/MU	TOTAL	-- EIGENVECTOR COMPOSITION PCT	
2I11/2	1074734.	---	---	5.5	100.	100. 2I (7I)	
2S 1/2	1074792.	---	---	.5	100.	100. 2S (8S)	
2P 1/2	1107447.	---	---	.5	98.	98. 2P (DP(1P))	
2I11/2	1108337.	---	---	5.5	100.	100. 2I (8I)	
2P 3/2	1108974.	---	---	1.5	100.	92. 2P (DP(1P))	7. 2D (DP(1P))
2D 3/2	1113426.	---	---	1.5	99.	91. 2D (DP(1P))	7. 2P (DP(1P))
2D 5/2	1115584.	---	---	2.5	99.	99. 2D (DP(1P))	
2S 1/2	1118319.	---	---	.5	97.	97. 2S (DP(1P))	

NO. EXPERIMENTAL LEVELS = 2.

ABSOLUTE MEAN DEVIATION = 247.88

RMS DEVIATION = 247.95

relative energies, of course, are unaffected by an error in the ionization energy. The 5s and 6s configurations cited for Mn^{6+} are probably misidentifications because the discrepancies are so large, and the predictions for most of the even parity configurations for both Mn^{6+} and Fe^{7+} should be fairly good (less than 1000 cm^{-1}). The predicted intensities may be even more useful for identifying many expected transitions for these ions, but the long lists of relative intensities of the electric dipole transitions between pairs of levels are given in the appendix. These were calculated by Cowan's RCG code with the reduced matrix elements for the dipole operator obtained from the HXR calculation.

5.3 $(UX_6)^{2-}$ Complexes (X=F,Cl,Br,I)

Features of the spectra of certain crystals containing metal ions can be interpreted as electronic transitions of free ions perturbed by the presence of the crystal lattice. Bethe[86] first described the effect of a crystal lattice on an ion as a homogeneous electric field derived from a potential with the local symmetry at the ion's lattice site. The rare earth ions (i.e. ions with a single unfilled shell of f-electrons) have been treated by Wybourne[87]. This section discusses the electronic structure of U^{4+} ions in crystals with octahedral (actually O_h) site symmetry.

5.3.1 Effective Hamiltonians and Experimental Analyses

The effective Hamiltonian for an ion with an $(nf)^w$ configuration in the presence of a perturbing field with O_h symmetry takes the form

$$H_e = E_{av} + H_C + \zeta_{nf}\sqrt{14}\, W^{(11)0}(nf) + H_c(B_0^4, B_0^6) \qquad (5.28a)$$

where E_{av} is a constant energy, H_C is the traceless portion of the effective Coulomb interaction between the nf electrons,

$$H_C = \sum_{\bar{S}=0}^{1} \sum_{\bar{L}=0}^{6} \frac{1+(-1)^{\bar{S}+\bar{L}}}{2} E(\bar{S}\bar{L}) [\bar{S},\bar{L}]^{1/2} W^{C_{SL}(\overline{SLSL})00}_{(nf,nf;nf,nf)} \quad (5.28b)$$

$$E(\bar{S}\bar{L}) = f_2(\bar{L})F^2(nfnf) + f_4(\bar{L})F^4(nfnf) + f_6(\bar{L})F^6(nfnf) \quad (5.28c)$$

$$f_k(\bar{L}) = \left[49(-1)^{\bar{L}} \begin{Bmatrix} 3 & 3 & k \\ 3 & 3 & \bar{L} \end{Bmatrix} + \frac{7}{13} \right] \begin{Bmatrix} 3 & k & 3 \\ 0 & 0 & 0 \end{Bmatrix}^2 \quad (5.28d)$$

and H_c is the crystal field Hamiltonian:

$$H_c(B_0^4, B_0^6) = B_0^4 \left[\frac{28}{11}\right]^{1/2} \left(W_{00}^{04}(nf) + \sqrt{5/14} \left[W_{0-4}^{04}(nf) + W_{04}^{04}(nf) \right] \right) \quad (5.28e)$$

$$- B_0^6 \frac{10}{13} \left[\frac{14}{33}\right]^{1/2} \left(W_{00}^{06}(nf) - \sqrt{7/2} \left[W_{0-4}^{06}(nf) + W_{04}^{06}(nf) \right] \right)$$

The parameters B_0^4 and B_0^6 are derived empirically from the observed electronic transitions.

States of O_h Symmetry

The representations of D^J of $O^+(3)$ reduce to direct sums of irreducible representations of O_h upon restriction to this subgroup. The Hamiltonian matrix for a configuration f^{nl} becomes block diagonal with respect to a basis that carries the irreducible representations of the subgroup. The configuration f^2, with SLJ states $^1S_0$, $^3P_{0,1,2}$, $^1D_2$, $^3F_{4,3,2}$, $^1G_4$, $^3H_{6,5,4}$, $^1I_6$, decomposes into the irreducible representations of O_h,

$$^1S_0 \oplus {}^3P_0 \rightarrow (2)\,{}^1\Gamma_1 \quad (5.29a)$$

$$^3P_1 \rightarrow {}^3\Gamma_4 \qquad (5.29b)$$

$$^3P_2 \oplus {}^1D_2 \oplus {}^3F_2 \rightarrow (3)^2\Gamma_3 \oplus (3)^3\Gamma_5 \qquad (5.29c)$$

$$^3F_3 \rightarrow {}^1\Gamma_2 \oplus {}^3\Gamma_4 \oplus {}^3\Gamma_5 \qquad (5.29d)$$

$$^3F_4 \oplus {}^1G_4 \oplus {}^3H_4 \rightarrow (3)^1\Gamma_1 \oplus (3)^2\Gamma_3 \oplus (3)^3\Gamma_4 \oplus (3)^3\Gamma_5 \qquad (5.29e)$$

$$^3H_5 \rightarrow {}^2\Gamma_3 \oplus (2)^3\Gamma_4 \oplus {}^3\Gamma_5 \qquad (5.29f)$$

$$^3H_6 \oplus {}^1I_6 \rightarrow (2)^1\Gamma_1 \oplus (2)^1\Gamma_2 \oplus (2)^2\Gamma_3 \oplus (2)^3\Gamma_4 \oplus (4)^3\Gamma_5 \qquad (5.29g)$$

for a total of thirty-nine energy levels ($^d\Gamma_r$ denotes the representation Γ_r with dimension d). The irreducible representations of O_h can alternately be designated $A_1 = {}^1\Gamma_1$, $A_2 = {}^1\Gamma_2$, $E = {}^2\Gamma_3$, $T_1 = {}^3\Gamma_4$, and $T_2 = {}^3\Gamma_5$.

Experimental Analyses

Extensive analyses of the absorption spectra of crystals of Cs_2UCl_6 and Cs_2UBr_6 enabled Satten and co-workers[88-91] to identify twenty-one electronic energy levels relative to the ground state of each of the complexes $(UCl_6)^{2-}$ and $(UBr_6)^{2-}$. Aided by these efforts, Edelstein et al[92] were able to identify eleven relative levels of $(UI_6)^{2-}$ and twenty-one relative levels of $(UF_6)^{2-}$ from absorption spectra of $(NEt_4)_2UI_6$ and $(NEt_4)_2UF_6$ crystals.

Using empirically derived[93] constraints $F^4(5f5f) = .74F^2(5f5f)$ and $F^6(5f5f) = 0.55F^2(5f5f)$, Edelstein fitted the parameters of the effective Hamiltonian for each of the four complexes. The results of the least squares fits are given in table (5.18) and the relationship of the

Table (5.18)

$(UX_6)^{2-}$ Parameters (cm^{-1}) X = F, Cl, Br, I

Parameter	UF_6	UCl_6	UBr_6	UI_6
$F^2(5f5f)$	49699	43170	40867	38188
ζ_{5f}	1970	1774	1756	1724
B_0^4	10067	7463	6946	6338
B_0^6	22	992	999	941
$\sqrt{\langle\Delta^2\rangle}^a$	67	168	176	188
$\langle\|\Delta\|\rangle^b$	39	76	95	106

[a] rms deviation

[b] absolute mean deviation

calculated to observed levels is displayed in figure (5.8). The results are typical of the effective Hamiltonian (5.28ab). In other cases, additional parameterized effective operators have been added to the crystal field Hamiltonian to reduce the rms deviation (reduced chi-square) to about twenty-five cm^{-1} [94]. Two such corrections suggested by Judd are described and tested here on the tetravalent uranium hexahalide complexes[95,96].

5.3.2 Correlated Crystal Fields

One method suggested for improving the agreement between the effective Hamiltonian description and the observed electronic transitions is the inclusion of 2-electron operators in the crystal field Hamiltonian inspired by a variety of physical mechanisms[95-98]. The major obstacle

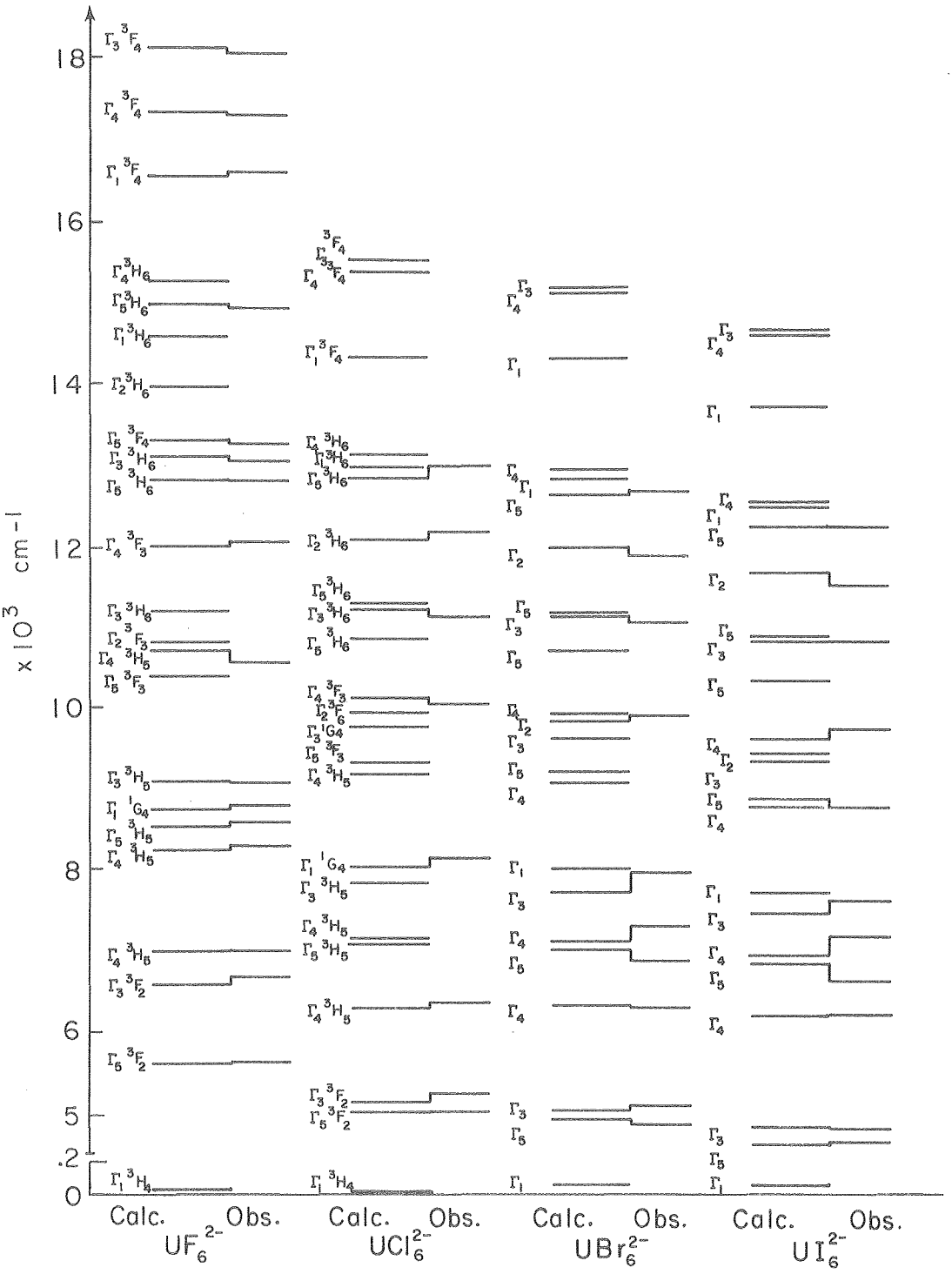

Figure (5.8)

XBL 766-3039

Comparison between the observed and calculated electronic transitions for the $(UX_6)^{2-}$ complexes. The calculated energies are derived from the effective Hamiltonian H_e given by equation (5.28).

in testing this hypothesis for f-electrons is the large number of additional parameters required for a purely empirical model; the lowest symmetry case requires 637 parameters, and even in octahedral symmetry 41 parameters are needed for empirical crystal field Hamiltonian[95,1]. Judd has proposed models of the correlated crystal field derived from physical assumptions that substantially reduce the number of additional parameters, and two of these models were tested for the $(UX_6)^{2-}$ complexes[95,96].

Electron Delocalization Model

The first model tested was derived from the assumption that the 5f electrons are not as closely localized to the ion center in a crystal lattice as say, the 4f electrons, and tend to drift over to the ligand atoms[95]. A 5f-electron wavefunction is replaced with a superposition of itself and a ligand localized function,

$$\psi^{r}_{b\mu}(x) = \theta_r \phi^{r}_{b\mu}(x) + \lambda_r \Lambda^{r}_{b\mu}(x) \tag{5.30}$$

where $\phi^{r}_{b\mu}$ carries an irreducible representation of O_h with respect to symmetry operations on the space coordinates ($D^3 \supset D^{r_1} + D^{r_2} + D^{r_3}$, $r_1 = A_2$, $r_2 = T_1$, $r_3 = T_2$):

$$\phi^{1}_{1\mu}(x) = \frac{1}{\sqrt{2}} \phi_{5f,2,\mu}(x) - \frac{1}{\sqrt{2}} \phi_{5f,-2,\mu}(x) \tag{5.31a}$$

$$\phi^{2}_{1\mu}(x) = \phi_{5f,0,\mu}(x) \tag{5.31b}$$

$$\phi^{2}_{2\mu}(x) = \sqrt{5/8}\, \phi_{5f,3,\mu}(x) + \sqrt{3/8}\, \phi_{5f,-1,\mu}(x) \tag{5.31c}$$

$$\phi^{2}_{3\mu}(x) = \sqrt{5/8}\, \phi_{5f,-3,\mu}(x) + \sqrt{3/8}\, \phi_{5f,1,\mu}(x) \tag{5.31d}$$

$$\phi^3_{1\mu}(x) = \frac{1}{\sqrt{2}}\phi_{5f,2,\mu}(x) + \frac{1}{\sqrt{2}}\phi_{5f,-2,\mu}(x) \qquad (5.31e)$$

$$\phi^3_{2\mu}(x) = \sqrt{3/8}\,\phi_{5f,3,\mu}(x) - \sqrt{5/8}\,\phi_{5f,-1,\mu}(x) \qquad (5.31f)$$

$$\phi^3_{3\mu}(x) = \sqrt{3/8}\,\phi_{5f,-3,\mu}(x) - \sqrt{5/8}\,\phi_{5f,1,\mu}(x) \qquad (5.31g)$$

Judd then argues that the Coulomb interaction between electrons is the largest contribution to the effective Hamiltonian and that the integrals involving the ligand wavefunctions, e.g.

$$\int dx_1 dx_2 \phi^{r_1*}_{b_1\mu_1}(x_1)\phi^{r_2*}_{b_2\mu_2}(x_2)\frac{2}{r_{12}}\phi^{r'_1}_{b'_1\mu'_1}(x_1)\phi^{r'_2}_{b'_2\mu'_2}(x_2) \qquad (5.32a)$$

can be neglected with respect to the integrals

$$\int dx_1 dx_2 \phi^{r_1*}_{b_1\mu_1}(x_1)\phi^{r_2*}_{b_2\mu_2}(x_2)\frac{2}{r_{12}}\phi^{r'_1}_{b'_1\mu'_1}(x_1)\phi^{r'_2}_{b'_2\mu'_2}(x_2) \qquad (5.32b)$$

owing to the fact that the 5f-electron has a small overlap with the ligand, and that the terms of the type represented by (5.32a) are largest for the monopole component ($\sim 2/r_2$) and contribute to the effective 1-electron crystal field Hamiltonian.

The end result is to replace $\phi^r_{b\mu}$ with $\Theta_r\phi^r_{b\mu}$ when evaluating the Coulomb operator. For m 5f-electrons, this can be accomplished by inserting the Coulomb operator between a pair of operators $P^m(\Theta_1,\Theta_2,\Theta_3)$ constructed from the 1-electron projection operators:

$$P^{w}(\theta_1,\theta_2,\theta_3) = \frac{1}{w!} \sum_{r_1,b_1} \cdots \sum_{r_w b_w} \tag{5.33}$$

$$\theta_{r_1} \cdots \theta_{r_w} e_{r_1 b_1 r_1 b_1}(1) \cdots e_{r_w b_w r_w b_w}(w)$$

The 1-electron projection operators can be rewritten in terms of the unit tensors,

$$e_{rbrb} = \left|\phi_b^r\right\rangle\left\langle\phi_b^r\right| = b_0\sqrt{14}\,\hat{w}^{00}(nf) + h_c(\beta,\gamma) \tag{5.34a}$$

where h_c is identical to the effective crystal field Hamiltonian H_c with $W_{0q}^{0k}(nf)$ replaced by $\hat{w}_{0q}^{0k}(nf)$, and

$$b_0 = \frac{\theta_1 + 3\theta_2 + 3\theta_3}{7} \tag{5.34b}$$

$$\beta = \frac{3}{4}(3\theta_2 - \theta_3 - 2\theta_1) \tag{5.34c}$$

$$\gamma = \frac{39}{280}(4\theta_1 + 5\theta_2 - 9\theta_3) \tag{5.34d}$$

Judd then argues that $\theta_1 = 1$ from molecular orbital theory, and that θ_2 and θ_3 must be nearly equal to 1, so that β and γ are small. $P^{w}(\theta_1,\theta_2,\theta_3)$ can be approximated by linear expansion in β and γ

$$(b_0)^{w} + (b_0)^{w-1} H_c(\beta,\gamma) \tag{5.35}$$

To this order, the effective Coulomb operator is replaced by

$$H_C \rightarrow (b_0)^{2w} H_C + (b_0)^{2w-1}\left[H_c(\beta,\gamma)H_C + H_C H_c(\beta,\gamma)\right] \tag{5.36}$$

For two electrons, the effective Coulomb operator is diagonal in the SLJM basis set, with matrix elements given by

$$\left\langle SLJM\left|H_C\right|S'L'J'M'\right\rangle = \delta_{SS'}\delta_{LL'}\delta_{JJ'}\delta_{MM'}\,E(SLJ) \tag{5.37}$$

the replacement (5.37) can be written in matrix form:

$$\left\langle SLJM\left|H_C\right|S'L'J'M'\right\rangle \rightarrow (b_0)^4 \left\langle SLJM\left|H_C\right|S'L'J'M'\right\rangle + \tag{5.38}$$

$$\Big[E(SL) + E(S'L')\Big]\left\langle SLJM\left|H_c(\beta,\gamma)\right|S'L'J'M'\right\rangle$$

Test of the Electron Delocalization Model

The correction to the effective Hamiltonian, given in matrix form by (5.38), was easily incorporated into a least squares fitting program. The renormalized Coulomb parameters $\bar{F}^k(nfnf) = (b_0)^4 F^k(nfnf)$, along with the constraints $F^4(5f5f) = .74F^2(5f5f)$ and $F^6(5f5f) = .55F^2(5f5f)$, lead to the correction matrix $H'(S,T)$, where

$$\left\langle SLJM\left|H'(S,T)\right|S'L'J'M'\right\rangle = \left\langle SLJM\left|H_c(S,T)\right|S'L'J'M'\right\rangle \cdot \tag{5.39a}$$

$$\Big[f^2(SL) + f^2(S'L') + .74\Big[f^2(SL) + f^4(S'L')\Big] + .55\Big[f^6(SL) + f^6(S'L')\Big]\Big]$$

$$S = (\beta/b_0)\bar{F}^2(5f5f) \tag{5.39b}$$

$$T = (\gamma/b_0)\bar{F}^2(5f5f) \tag{5.39c}$$

The matrices multiplied by the parameters S and T were constructed from the matrix elements multiplied by B_0^4, B_0^6, $F^2(5f5f)$, $F^4(5f5f)$, and $F^6(5f5f)$.

In the actual fitting, S, T, and $\bar{F}^2(5f5f)$ were treated as free parameters. Direct fitting treating Θ_2 and Θ_3 as free parameters ($\Theta_1 = 1$) was attempted with constraints $0 \leq \Theta_2 \leq 1$ and $0 \leq \Theta_3 \leq 1$, but the eigenvalues were not linear enough locally in these parameters to obtain convergence with the fitting algorithm used. The values of Θ_2,

θ_3, and b_0 were recovered with the equations

$$\theta_2 = \frac{1 + 2S/[11\bar{F}^2(5f5f)] - 100T/[429\bar{F}^2(5f5f)]}{1 - 4S/[11\bar{F}^2(5f5f)] + 280T/[143\bar{F}^2(5f5f)]} \qquad (5.40a)$$

$$\theta_3 = \frac{1 - 2S/[33\bar{F}^2(5f5f)] - 60T/[429\bar{F}^2(5f5f)]}{1 - 4S/[11\bar{F}^2(5f5f)] + 280T/[143\bar{F}^2(5f5f)]} \qquad (5.40b)$$

$$b_0 = \frac{1}{1 - 4S/[11\bar{F}^2(5f5f)] + 280T/[143\bar{F}^2(5f5f)]} \qquad (5.40c)$$

assuming that $\theta_1 = 1$. The parameters obtained by this method are presented and compared with the uncorrected model in table (5.19).

The uncorrected effective Hamiltonian was refitted to the data, taking some care to properly weight the observed levels, which might explain the small discrepancies with Edelstein's work (table (5.18)). From the reduced chi-squares, one can conclude that the correction has little or no correlation with the observed data. In most cases, the inclusion of the extra parameters tended to cause the deviations between the observed and calculated levels to become more uniformly distributed.

Judd suggested that the constraints on $F^4(5f5f)$ and $F^6(5f5f)$ might be too severe, so the fit was repeated with the constraint removed. The implementation was the same as before, but the ratios .74 and .55 were replaced with the computed ratios $F^4(5f5f)/F^2(5f5f)$ and $F^6(5f5f)/F^2(5f5f)$ computed from the previous iteration. The fitted parameters for this case along with the parameters for the effective Hamiltonian without the correction terms are presented in table (5.20). The results did not show any significant improvement except perhaps in the case of the iodide. The small number of observed levels made con-

Table (5.19)

Electron Delocalization Model Parameters ($F^4 = .74F^2$, $F^6 = .55F^2$)

Parameter	UI_6		UBr_6		UCl_6		UF_6	
ζ_{5f}	1742	1731	1767	1798	1804	1811	1973	1974
$\bar{F}^2$	38459	38396	40888	40457	41851	41732	49856	50443
B_0^4	6608	6331	6399	6030	7142	6748	10081	10272
B_0^6	849	880	1605	1560	1486	1703	41	125
S	0	-1741	0	3449	0	3492	0	1076
T	0	620	0	1089	0	1119	0	263
$b_0 \times 10^5$	100000	95411	100000	97875	100000	97839	100000	99755
$\theta_2 \times 10^5$	100000	94266	100000	98778	100000	98716	100000	100002
$\theta_3 \times 10^5$	100000	95027	100000	96263	100000	96242	100000	99408
E_{av}	11804	11984	12471	12419	12803	12746	14844	14894
$\langle \lvert\Delta\rvert \rangle$	106	105	201	189	169	160	36	39
D.F.	7	5	16	14	16	14	12	10
$\sqrt{\chi^2/\text{D.F.}}$	173	198	283	262	235	233	57	61

vergence of this case difficult, however, and it should not be taken too seriously. The details of calculated levels and the eigenvector compositions have been omitted, since there is little change from the previous results.

Table (5.20)

Electron Delocalization Model Parameters (Free F^4, F^6)

Parameter	UI_6		UBr_6		UCl_6		UF_6	
ζ_{5f}	1707	1717	1789	1785	1782	1789	1980	1983
$\bar{F}^2$	36417	36145	41098	40519	42712	42236	49582	50570
$\bar{F}^4$	32201	30834	37709	38052	37940	38375	35468	35062
$\bar{F}^6$	17888	17263	29078	28081	30304	29564	25233	25879
B_0^4	6839	6440	6572	6573	7215	7242	9969	1011
B_0^6	928	870	1124	1165	1353	1400	56	221
S	0	-3446	0	1361	0	921	0	692
T	0	144	0	293	0	460	0	1034
$b_0 \times 10^5$	100000	95925	100000	99806	100000	98676	100000	96614
$\theta_2 \times 10^5$	100000	94174	100000	100025	100000	99020	100000	96394
$\theta_3 \times 10^5$	100000	96319	100000	99300	100000	98095	100000	95075
E_{av}	12250	11920	12508	12491	12826	12807	14769	14827
$\langle \lvert\Delta\rvert \rangle$	98	94	141	140	102	100	31	32
D.F.	5	3	14	12	14	12	10	8
$\sqrt{\chi^2/\text{D.F.}}$	192	234	202	216	155	166	53	53

Spin Dependent Correlated Crystal Field Model

Judd[96] proposed another correlated crystal field model for the lanthanides based on the notion that a pair of electrons with parallel spins experience stronger "exchange" forces than a pair with antiparallel spins and would tend to be more localized on the metal ion than near the ligands. This means the parallel spin pair would feel the crystal

field forces more strongly than an antiparallel pair. For two electrons, this suggests a substitution

$$B_q^k \rightarrow B_q^k\left[1+c_k \frac{\vec{S}\cdot\vec{S}}{2}\right] \qquad (4.41)$$

as the crystal field operator commutes with the spin operators.

Although the effect may not be relevant to actinides because of their relatively stronger interaction with the crystal field, the model was tested because of its simplicity in the case of the uranium hexahalide complexes. The matrices for B_0^4 and B_0^6 were simply replicated, removing all matrix elements between the singlet (S = 0) basis vectors. These matrices were then multiplied by two new free parameters and fitted to the observed levels.

The results obtained with and without the extra parameters are presented in table (5.21). The iodide, however, is something of a pathological case. Because of difficulty in obtaining convergence, the constraints on $F^4(5f5f)$ and $F^6(5f5f)$ were used. Even then the B_0^6 parameter changed sign and the two new parameters were larger than expected. Overall there seems to be little or no improvement with the addition of the two new parameters, and in particular the iodide result cannot be taken very seriously. Again, the details of the calculated energies and eigenvector compositions have been omitted because the model had such little success.

Table (5.21)

Spin Dependent Crystal Field Model

Parameter	UI_6		UBr_6		UCl_6		UF_6	
ζ_{5f}	1707	1746	1770	1793	1783	1794	1980	1987
$\bar{F}^2$	36417	38998	41098	39788	42712	41680	49582	50038
$\bar{F}^4$	32201	29059†	37709	37235	37940	37987	35468	35223
$\bar{F}^6$	17888	22449†	29078	26039	30304	28219	25233	25802
B_0^4	6839	1721	6572	7354	7215	7768	9969	10271
B_0^6	928	-1496	1124	1658	1353	1749	56	284
$c_4 \times 10^4$	0	27970	0	-1260	0	-713	0	-305
$c_6 \times 10^4$	0	-14620	0	-4019	0	-2815	0	-9228
E_{av}	12250	12042	12508	12460	12826	12795	14769	14797
$\langle \lvert\Delta\rvert \rangle$	98	76	141	124	102	95	31	27
D.F.	5	5	14	12	14	12	10	8
$\sqrt{\chi^2/\text{D.F.}}$	192	163	202	202	155	157	53	49

†$F^4(5f5f) = .74F^2(5f5f)$; $F^6(5f5f) = .55F^2(5f5f)$.

VI. Concluding Comments

Although there were no new spectra actually analyzed during the course of this work, a logical next step is to use the predictions for Ti^{3+}, V^{4+}, Cr^{5+}, Mn^{6+}, and Fe^{7+} to attempt to extend the analyses for these ions. The author feels he has learned a great deal about semi-empirical theories, however, and hopes to continue investigations in this direction in the course of some experimental work also. This work is somewhat like a research notebook because many of the ideas are only partially developed, there is much material to build upon in the future. The ideas about systematic incorporation of correlations in semi-empirical theories discussed in chapter IV are perhaps the most interesting, because some practical new techniques for effective Hamiltonian descriptions of quantum mechanical systems can come out of them.

References

1. J. C. Slater, Phys. Rev. 34, 1293 (1929).

2. E. U. Condon and G. H. Shortley, The Theory of Atomic Spectra, Cambridge Univ. Press (1935).

3. R. D. Cowan, The Theory of Atomic Structure and Spectra, Univ. of Calif. Press (1980).

4. D. R. Hartree, Proc. Roy. Soc. (London) A141, 282 (1933).

5. V. Fock, Z. Physik 61, 126 (1930).

6. J. C. Slater, Phys. Rev. 35, 210 (1930).

7. B. Edlén, "Atomic Spectra," Encyclopedia of Physics Vol XXVII, Springer Verlag (1964).

8. G. Racah, Phys. Rev. 61, 186 (1942); Phys. Rev. 61, 537 (1942); Phys. Rev. 62, 438 (1942).

9. F. Herman and S. Skillman, Atomic Structure Calculations, Prentice Hall (1963).

10. R. D. Cowan, Phys Rev. 163, 54 (1967).

11. R. D. Cowan and D. C. Griffin, J. Opt. Soc. Am. 66, 1010 (1976).

12. R. D. Cowan, K. Rajnak, and P. Renard, Users Guide to Program RCN, Lawrence Livermore Laboratory report, UCID 17169.

13. R. D. Cowan, J. Opt. Soc. Am. 66, 808 (1968).

14. Cowan has recommended scaling of the ab-initio parameters by empirically determined constants for various ranges of Z, the nuclear charge, and N, the number of electrons. These factors are discussed in reference 3, chapter 16 section 2.

15. A. Hibbert, Repts. Prog. Phys. 11, 1 (1975).

16. J. von Neumann, Mathematical Foundations of Quantum Mechanics, Princeton Univ. Press (1955).

17. P. A. M. Dirac, Proc. Cam. Phil. Soc. (London) 26, 376 (1930); P. A. M. Dirac, Proc. Cam. Phil. Soc. (London) 27, 240 (1931).

18. J. E. Lennard-Jones, Proc. Cam. Phil. Soc. (London) 27, 489 (1931).

19. P. O. Löwdin, Phys. Rev. 97, 1474 (1959); Phys. Rev. 97, 1490 (1959); Phys. Rev. 97, 1509 (1959).

20. A. J. Coleman, Rev. Mod. Phys. 25, 668 (1963); J. Math. Phys. 13, 142 (1972).

21. In essence, an alternative labeling scheme has been proposed in a series of papers by R. M. Sternheimer, Phys. Rev. A15, 1817 (1977); Phys. Rev. A16, 459 (1977); Phys. Rev. A16, 1752 (1977); Phys. Rev. A19, 474 (1979).

22. J. C. Slater, The Quantum Theory of Atomic Structure, Vol. I, Mcgraw-Hill, (1960).

23. K. Rajnak and B. G. Wybourne, Phys. Rev. 132, 280 (1963).

24. K. Rajnak and B. G. Wybourne, Phys. Rev. 134, A596 (1964).

25. B. G. Wybourne, Phys. Rev. 137, A364 (1965).

26. J. C. Morrison and K. Rajnak, Phys. Rev. A4, 536 (1971).

27. J. C. Morrison, Phys. Rev. A6, 643 (1972).

28. H. A. Bethe and E. E. Salpeter, Quantum Mechanics of One- and Two-Electron Atoms, Springer-Verlag (1957).

29. B. R. Judd, Operator Techniques in Atomic Spectroscopy, McGraw-Hill (1963).

30. The convention used here is that of Edmonds, Angular Momentum and Quantum Mechanics, Princeton Univ. Press (1960).

31. C. Eckart, Revs. Modern Phys. 2, 305 (1930).

32. E. P. Wigner, "On the Matrices Which Reduce the Kronecker Products of S. R. Groups," manuscript (1940) first published in a collection of reprints by L. C. Biedenharn and H. Van Dam, eds. Quantum Theory of Angular Momentum, Academic Press (1965).

33. M. Blume and R. E. Watson, Proc. Roy. Soc. (London), A270, 127, (1962).

34. Nielsen and Koster, Spectroscopic Parameters for the p^n, u^n, and f^n Configurations, M.I.T. Press (1963).

35. H. Boerner, Representations of Groups, North Holland (1970).

36. M. Hammermesh, Group Theory and Its Applications to Physical Problems, Addison-Wesley (1962).

37. J. D. Louck, Am. J. Phys. 38, 3 (1970).

38. C. M. Vincent, Phys. Rev. 163, 1044 (1967).

39. B. R. Judd, Second Quantization and Atomic Spectroscopy, Johns Hopkins Press (1967).

40. B. R. Judd, "Group Theory in Atomic Spectroscopy," in Group Theory and Its Applications, E. M. Loebl Ed., Academic Press (1968).

41. J. C. Slater, Quantum Theory of Atomic Structure, Vol. II, McGraw-Hill (1960).

42. C. Froese-Fischer, The Hartree-Fock Method for Atoms: A Numerical Approach, John Wiley & Sons(1977).

43. C. Froese-Fischer, Comm. in Comp. Phys. 1, 151 (1951).

44. D. Griffin, PhD thesis: Self-Consistent Field Calculations of Excited Electronic Configurations, University Microfilms (1970).

45. D. C. Griffin, R. D. Cowan, and K. L. Andrew, Phys. Rev. A3, 1233 (1971).

46. J. C. Slater, Phys. Rev. 81, 385 (1951).

47. E. Clementi, J. Chem. Phys. 38, 2248 (1963); 39, 175 (1963); 42, 2783 (1965)

48. A list of references to these calculations can be found in either reference 3 or reference 10.

49. B. W. Shore and D. H. Menzel, Principles of Atomic Spectra, John Wiley (1968).

50. D. A. S. Fraser, Statistics: An Introduction, John Wiley, New York (1958).

51. B. R. Bevington, Data Reduction and Error Analysis for the Physical Sciences, McGraw Hill, New York (1969).

52. T. Kato, Perturbation Theory for Linear Operators, Springer Verlag, Berlin (1966).

53. R. Melhorn, PhD. Thesis Univ. Calif. Berkeley, 1968, also Lawrence Radiation Laboratory Report No. UCRL 18040.

54. B. Edlén, Physica Scripta, 19, 255 (1979).

55. C. W. Scherr, J. N. Silverman, and F. A. Matsen, Phys. Rev. 127, 830 (1962).

56. G. Golub, V. Pereyra, and J Bolsted, authors of VARPRO, Computer Science Department, Stanford University. See also G. Golub and V. Pereyra, SIAM J. Numer. Anal. 10, 1973.

57. A. A. Kirillov, Elements of the Theory of Representations, Springer-Verlag (1970).

58. R. Gilmore, Lie Groups, Lie Algebras, and Some of Their Applications, John Wiley (1974).

59. Similar constructions of Weyl tableau wavefunctions have been used by Harter and Patterson, but the conjugate representations are divided between the spin and space coordinates: W. G. Harter, Phys. Rev. A8 2819 (1973); W. G. Harter and C. W. Patterson, Phys. Rev. A13 (1976); W. G. Harter and C. W. Patterson, "A Unitary Calculus for Electronic Orbitals," Lecture Notes in Physics 49, Springer Verlag (1976).

60. O. Sinanoglu and K. A. Brueckner, Three Approaches to Electron Correlation in Atoms, Yale Univ. Press (1970), especially the paper cited in the next reference.

61. O. Sinanoglu, Proc. Roy. Soc. (London) A260, 379 (1961).

62. L. Brilloun, J. Phys. 3, 373 (1932).

63. D.R. Hartree, W. Hartree, and B. Swirles, Phil. Trans. Roy. Soc. Lond. A238, 7 (1938).

64. Y. Tal, Phys. Rev. A18, 1781 (1978).

65. M. Born, and W. Heisenberg, Z. Phys. 23, 388 (1924).

66. I. Waller, Z. Phys. 38, 635 (1926).

67. J. E. Mayer and M. G. Mayer, Phys Rev. 43, 605 (1933).

68. D. Layzer, Ann. Phys. 8, 271 (1959).

69. D. Layzer, Z. Horak, M. N. Lewis, and D. P. Thompson, Ann. Phys. 29, 101 (1964).

70. D. Layzer and J. Bahcall, Ann. Phys. 17, 177 (1962).

71. H. P. Doyle, "Relativistic Z-Dependent Corrections to Atomic Energy Levels" in Advances in Atomic and Molecular Physics 5, D. R. Bates and I. Estermann, eds., Academic Press (1969).

72. P. Risberg, Ark. Fys. 10, 583 (1956).

73. B. Edlén and P. Risberg, Ark. Fys. 10, 533 (1956).

74. G. Risberg, Ark. Fys. 37, 231 (1968).

75. J. E. Holmström, Phys. Scrip. 5, 249 (1972).

76. C. H. H. Van Deurzen, J. G. Conway, and S. P. Davis, J. Opt. Soc. Am. 63, 158 (1973).

77. J. W. Swenson and B. Edlén, Phys. Scrip. 9, 335 (1974).

78. C. H. H. Van Deurzen, J. Opt. Soc. Am. 67, 476 (1977).

79. J. O. Ekberg, Phys. Scrip. 8, 35 (1973).

80. J. Sugar and C. Corliss, J. Chem. Phys, Ref. Data 7, 1228 (1978).

81. R. D. Cowan and N. J. Peacock,, Astrophys. J. 142, 377 (1965).

82. R. D. Cowan, Astrophys. J. 147, 377 (1967).

83. J. Sugar and C. Corliss, J. Chem. Phys. Ref. Data 6, 1301 (1977).

84. J. Sugar and C. Corliss, J. Chem. Phys. Ref. Data 4, 411 (1975).

85. A. M. Crooker, private communication.

86. H. A. Bethe, Ann. Physik 3, 133 (1929).

87. B. G. Wybourne, Spectroscopic Properties of the Rare Earths, John Wiley (1965).

88. R. A. Satten and J. J. Margolis, J. Chem. Phys. 32, 573 (1960).

89. R. A. Satten, D. Young, and D. M. Gruen, J. Chem. Phys. 33, 1140 (1960).

90. R. A. Satten, C. L. Schrieber, and E. Y. Wong, J. Chem. Phys. 42, 162 (1965).

91. D. R. Johnston, R. A. Satten, C. L. Schrieber, and E. Y. Wong, J. Chem. Phys. 44, 3141 (1966).

92. W. Wagner, N. Edelstein, B. W. Whittaker, and D. Brown, Inorg. Chem. 16, 1021 (1977).

93. K. Rajnak, Phys. Rev. A14, 1979 (1976).

94. J. P. Hessler and W. T. Carnall, "Optical Properties of Actinide and Lanthanide Ions," in The Chemistry of Lanthanides and Actinides, N. Edelstein ed., A. C. S. Symposium Series, symposium held September 1979.

95. B. R. Judd, J. Chem. Phys. 66, 3163 (1977).

96. B. R. Judd, Phys. Rev. Lett. 39, 242 (1977).

97. S. S. Bishton and D. J. Newman, J. Phys. C 3, 1753 (1970).

98. D. J. Newman, Adv. Phys. 20, 197 (1971).

Appendix. Predicted Energies, Eigenvectors, and Spectra

(Microfiche available from author upon request.)